National Library of Canada
Canadian Theses Service
Ottawa, Canada
K1A 0N4

Bibliothèque nationale du Canada
Services des thèses canadiennes

CANADIAN THESES

THÈSES CANADIENNES

NOTICE

The quality of this microfiche is heavily dependent upon the quality of the original thesis submitted for microfilming. Every effort has been made to ensure the highest quality of reproduction possible.

If pages are missing, contact the university which granted the degree.

Some pages may have indistinct print especially if the original pages were typed with a poor typewriter ribbon or if the university sent us an inferior photocopy.

Previously copyrighted materials (journal articles, published tests, etc.) are not filmed.

Reproduction in full or in part of this film is governed by the Canadian Copyright Act, R.S.C. 1970, c. C-30.

AVIS

La qualité de cette microfiche dépend grandement de la qualité de la thèse soumise au microfilmage. Nous avons tout fait pour assurer une qualité supérieure de reproduction

S'il manque des pages, veuillez communiquer avec l'université qui a conféré le grade

La qualité d'impression de certaines pages peut laisser à désirer, surtout si les pages originales ont été dactylographiées à l'aide d'un ruban usé ou si l'université nous a fait parvenir une photocopie de qualité inférieure.

Les documents qui font déjà l'objet d'un droit d'auteur (articles de revue, examens publiés, etc.) ne sont pas microfilmés

La reproduction, même partielle, de ce microfilm est soumise à la Loi canadienne sur le droit d'auteur, SRC 1970, c. C-30.

THIS DISSERTATION HAS BEEN MICROFILMED EXACTLY AS RECEIVED

LA THÈSE A ÉTÉ MICROFILMÉE TELLE QUE NOUS L'AVONS REÇUE

NL-339 (r. 86/06)

Canada

Computer Simulation of the Effect of Building Thermal Mass on the Thermal Loads

Radu G. Zmeureanu

A Thesis

in

The Centre for Building Studies

Presented in Partial Fulfillment of the Requirements
for the Degree of Doctor of Philosophy at
Concordia University
Montréal, Québec, Canada

January 1987

ISBN 0-315-35550-6

ABSTRACT

Computer Simulation of the Effect of Building Thermal Mass on the Thermal Loads

Radu G. Zmeureanu, Ph.D.
Concordia University, 1987.

The better use of the thermal storage effect of the building mass is one of the possible ways to reduce the heating/cooling energy requirements in buildings.

In this research, the thermal behavior of the hollow core slab system in summer and of the attached unheated solarium in winter are analyzed, for an office space in Montreal.

Since the modification of the existing software or the implementation of new algorithms, as required by the present research is very difficult, if not impossible task, due to the internal structure of these programs and to the access to the code, a research oriented software was developed, as a simulation tool. The program computes the hourly variation of the sensible heating/cooling loads, the room air temperature and thermal comfort index for a given configuration of the space and for a design day.

The computer simulation of the thermal behavior of the hollow core slab design, on a particular warm day in July in Montreal, shows the thermal comfort can be realized during occupation, when the ventilation rate is increased only three times at night, to cool down the structure efficiently. The energy savings for cooling are between 20 and 50 W/m^2 with respect to an HVAC system. The maximum temperature difference between the air entering and the air leaving the hollow core slab

is between 3 and 7°C, during the occupation.

The computer simulation of the thermal behavior of the unheated solarium attached to an office space indicates that on a particular cold day in winter in Montreal, the heating loads of the space are reduced by 60 to 100 percent.

A probabilistic approach is used in the research to analyze the results from the computer simulation of the thermal behavior of buildings, taking into consideration the uncertainties in predicting the climate. Decision models under uncertainty are used to define alternatives implying attached solaria and hollow core slabs which perform well under all possible weather conditions.

ACKNOWLEDGEMENTS

I wish to express my profound thanks and gratitude to my thesis supervisor Dr. Paul Fazio for his guidance, encouragement, criticism and suggestions throughout this study.

The financial support of the National Research Council of Canada, grant no. D-67 and Fonds pour la Formation de Chercheurs et l'Aide a la Recherche (FCAR) (Equipe Fazio) is greatly appreciated.

Thanks are also due to: Angie de Benedictis for typing this thesis; Ian Mackintosh and Alan Munn for their permanent availability and expertise in the CABD laboratory.

I wish to express my deepest acknowledgements to my wife Marie-Dana and to my children Dana and Radu for their continuous support, patience and understanding.

TABLE OF CONTENTS

PAGE

LIST OF FIGURES

LIST OF TABLES

NOTATION

b_n, c_n, d_n - Conduction transfer function coefficients

C - heat exchange by convection

c - specific heat

CLDM - total cloud amount

d - width of the exterior shading devices

d_e - characteristic dimension

E - heat exchange by evaporation

e - emissivity factor

ER - heat extraction rate

ET - equation of time

FA - angle factor

FE - emissivity factor

FSB - surface-to-built environment view factor

FSG - surface-to-ground view factor

FSS - surface-to-sky view factor

H_a - hour angle

H - height of window

h_{ac} - thermal conductance of air cavity

h_{cv} - convective heat transfer coefficient

h_{cvf} - convective heat transfer coefficient within the hollow core slab

h_g - convective heat transfer coefficient on the inside surface of window

h_i - film coefficient on interior surface

h_o - film coefficient on exterior surface

h_R - radiative heat transfer coefficient

I_{cl} - thermal resistance of clothing

IDN - direct normal radiation

Id - diffuse radiation

IP - solar radiation incident on interior surface

IRBLD - radiation reflected by built environment

IREF - solar radiation distributed over the interior surfaces, after the first reflection

IRG - ground-reflected radiation

IT - solar radiation on outside surface

ITP - solar radiation transmitted through glazing

K - heat conduction through clothing

k - thermal conductivity

L - latitude

l - width of hollow core slab

LON - local longitude

LSM - local standard time meridian

LST - local standard time

M - metabolism

m - air flow rate

Nu - Nusselt's number

N_b, N_c, N_d, N_i - number of conduction transfer function terms

N_s - total number of heat transfer surfaces

N_v, N_w - number of weighting factors

pa - water vapour pressure

pi, gi - air temperature weighting factors

PMV - predicted mean vote

Pr - Prandtl's number

ps - saturated water vapour pressure

Q, q - heat flow

R - heat exchange by radiation

R_{ac} - thermal resistance of air cavity

Re - Reynold's number

r_e, r_o, r_l - fraction of internal heat gain from equipment, occupants and lighting that are assumed to be convective

RES - heat exchange by respiration

RFl - total radiation on horizontal surface

R_T - thermal resistance of wall

RWN - ratio between the U value of glazing at night and by day

S - surface area

SC - shading coefficient

SG - glazing area

SO - sunlit area of window

SR - sunlit ratio

T - temperature

t - time

T_{cl} - surface temperature of clothing

TDB - outdoor dry-bulb temperature

TEV - return air temperature

TG - inside surface temperature of window

TIS - inside surface temperature

TMRT - mean radiant temperature

TOS - outside surface temperature

TR - room air temperature

TRE - air temperature of adjacent room

TREF - reference air temperature

TS - supply air temperature.

TSA - sol-air temperature

U - overall heat transfer coefficient

v - air velocity

X_j, Y_j, R_j - conduction transfer function coefficients

x - distance

W_1 - external work

W - width of window

W_s - wind speed

α - absorptivity coefficient

$\alpha 1$ - inclination of overhang

β - solar altitude angle

Δt - time increment

$\Delta x, \Delta x1, \Delta y1$ - distance increment

δ - thickness

$\delta 1$ - solar declination

θ - angle of incidence

ν - kinematic viscosity

ν_i, w_i - heat gain weighting factors

ρ - density

ρ_B - reflectivity of built environment

ρ_g - reflectivity of ground

$\sum$ - tilt angle of surface from horizontal

σ - Stephan - Boltzman constant

τ - glass transmissivity

$\emptyset$ - solar azimuth angle

ϕ - relative humidity

ψ - wall azimuth angle

Ω - index of optimism

CHAPTER 1

INTRODUCTION

CHAPTER 1

INTRODUCTION

1.1 ENERGY CONSUMPTION IN BUILDINGS

The International Energy Agency [1] warned in a report made public in June 17, 1985 that Canada is one of the most inefficient users of energy resources in the West. About one third of the total energy consumed in Canada is used in buildings for heating, cooling, lighting and ventilation [2]. Yellot [3] and Faucher [4] indicated that the heating and cooling systems in office buildings require about 30-45 percent of the total energy consumption.

In the early eighties, about 12 percent of the total energy consumed in Canada was used for commercial and public administration buildings [5]. Annual energy consumption for office buildings in Canada and the United States varied between 1000 and 4000 MJ/(m^2yr). Between 1950 and 1973, the average energy consumption for office buildings in the United States rose to 5400 MJ/(m^2yr), due to the following reasons:

i) great popularity of glass facades (mainly single glazing),
ii) very intensive area lighting (up to 65 W/m^2), and
iii) use of oversized and inefficient HVAC systems.

A survey of seven low-energy-office buildings larger than 10,000 m^2 floor area, in various regions of Canada [5] shows relatively high energy consumption, between 800 to 1000 MJ/(m^2yr).

Wilson [6] found that the energy consumption for offices is about

1700 MJ/(m^2yr), independent of floor area. The floorspace of office buildings in Canada is estimated to be 30,000,000 m^2, then the annual energy consumption is about 51 GJ/yr. Large office buildings, with floor area greater than 2000 m^2, consume about 63 percent of the total energy consumption, that is, 32 GJ/yr.

Piette, Wall and Gardiner [7] analyzed the actual energy consumption of 88 office buildings in United States and Canada. The majority of office buildings (over 60 percent) use between 450 to 800 MJ/(m^2yr). The median intensity is 670 MJ/(m^2yr) for large office, and 540 MJ/(m^2yr) for small office. For comparison, the recommended ASHRAE standard values for large office buildings is 490 to 650 MJ/(m^2yr). On average, the large buildings use about as much energy per square meter as the average for the overall sample. There appears to be a larger range of energy intensities for small buildings than for larger ones.

This may be partially attributable to the greater weather dependency of small buildings, while the internal gains tend to dominate the conditioning requirements of large buildings.

Bourassa et al. [2] used the computer simulation to analyze the energy consumption of office buildings in Canada and found that the application of no cost measures produce savings of 44 to 50 percent. The application of minor cost measures produces savings of about 60 percent. They indicated that a consumption of 1200 MJ/(m^2yr) could reasonably be attained by office buildings of size and shape similar to those studied.

An obvious conclusion is that the better design and operation of office buildings will reduce the energy consumption, by making use of renewable energies. This will avoid the energy bills to follow the fluctuations of the gas/oil price on the international market.

The better use of the thermal storage effect of the building mass is one of the possible ways to reduce the heating/cooling energy requirements in buildings. Relatively little is known about the application of the effect of thermal mass to the office buildings, which differ from houses in sizes, form, internal loads, control, occupancy profiles and schedules.

The preliminary Solar Energy Program (SEP) Passive Solar Plan [8] has identified the integrated passive solar design for non-residential buildings as a priority area, where the strategies for heating, cooling, lighting and ventilation should be combined.

The International Energy Agency [9] has started to examine the use of passive solar concepts in commercial buildings (retail, office, public and educational), and will provide a practical handbook with guidelines for incorporating passive solar designs such as atria, daylighting, vertical louvers, special shading devices and passive cooling features which help to avoid air conditioning.

This research aims to study the effect of the thermal storage in the building mass, in order to reduce the heating/cooling energy requirements in office buildings, while the thermal comfort is maintained within acceptable limits.

This chapter presents a literature survey, the objectives of the research, and the outline of the thesis.

1.2 LITERATURE SURVEY

Some studies have used a "static approach", by analyzing the variation of the building mass when the indoor conditions were kept constant by the HVAC systems.

Catani [10] used the m-factor to alter the effective U-value of heavy weight walls. The West German Standard DIN - 4702 [11] uses the m-factor to take into consideration the thermal inertia of the building, in calculating the heating design load. Howard [12] indicated that the mass of walls and roofs can save from 5 to 25 percent of heating and cooling in commercial buildings with internal loads, economizer cycles and daylighting systems. Romanko and Rudoy [13] analyzed the effect of the thermal mass on the annual heating and cooling energy for apartment buildings in Chicago and Phoenix, using the NBSLD program. They obtained heating savings of about 30 to 50 percent for south facing apartments, when the total thermal mass varied between 200 and 650 KJ/(m^3°C), corresponding to light and heavyweight structures. When the thermal mass of the internal structure was modified, the peak cooling load showed a change of about 16 percent for east orientation. The same change in peak load occurs whether the exterior wall is light or heavy. The authors concluded that additional

studies are required to analyze the thermal storage effect particularly for south facing apartments, including temperature set-point schedules, comfort indices, location and distribution of thermal mass, free cooling.

Mitalas [14] utilized a computer program based on ASHRAE procedures to simulate the annual heating requirements of large office buildings in Ottawa, Winnipeg and Vancouver, when the interior mass varied between 150 and 700 kg/m^2. The mass of exterior walls was included in the interior mass, if the insulating layer was on the exterior side of the wall. Several thermostat set-point schedules for occupied and unoccupied periods were considered, with throttling range of 1.7°C. The results indicated that the increase of the building mass reduces the annual energy consumption for heating by 10 to 20 percent (North and West) and by 60 to 95 percent (South). The author concluded that the effect of the building mass is usually of much less significance than the other factors, such as the night set back temperature. However, for a particular case the impact could be significant and he recommended the use of BLAST or DOE programs, for more advance studies. Mackie [15] investigated the effect of the storage of energy in building mass on the cooling energy consumption, using a computer program based on the transfer function method. The results indicated a variation of 12 to 14 percent in load, design capacity and energy use of buildings, when the interior mass was varied from 50 to 800 kg/m^2 of floor area.

Other researchers analyzed the dynamic thermal behavior of the building when the convective cooling by nocturnal ventilation was utilized.

Givoni [16] analyzed the thermal behavior of a building ventilated at night. During the daytime, the cooled mass can serve as a heat sink to absorb the heat. He concluded that the nocturnal ventilation can lower the daytime room temperature by about 15 percent, as compared with buildings which are not ventilated at night. Hoffman et al. [17] simulated the heat storage effect in a concrete building, using the total thermal time constant (TTTC) method and the results indicated that the nocturnal ventilation provides an annual electricity savings of more than 98 kWh/m^2, compared with the conventional design.

Other works analyzed the effect of a better coupling between the building mass and the forced air, in order to increase the efficiency of the thermal mass.

Monette [18] analyzed the thermal effect of a composite concrete and steel floor system, as a combination of return air plenum and heat storage mass, on the energy requirements of a wood-frame rowhouse. He utilized the TRANSHEAT and HOTCAN programs, and obtained annual energy savings of about 6 to 25 percent. Allen et al. [19] utilized ENERPASS program to simulate the effect of a hollow core slab in a low energy passive solar house in Ottawa and obtained energy savings of about 13 percent.

Thermo-Deck System (Sweden) or Ekono-System (Finland) [20, 21] utilized a concrete hollow core slab as air duct and heat storage mass. In summer, the outdoor air is circulated through this slab before it is introduced to the room. Thus, at night the concrete slab is cooled, and by day it will act as a heat sink, reducing the room cooling load. The system achieved a cooling effect of about 50 W/m^2 using an air flow of 50-100 m^3/h for an area of 6 m^2. The refrigeration load was reduced by about 70 percent.

Barnaby et al. [22] used a modified version of the NBSLD program to simulate the thermal behavior of the hollow core slab in a building of 90,000 m^2 in Sacramento. The results indicated that this system provides energy savings of about 13 percent and a reduction of the peak cooling load of about 31 percent, with respect to the conventional design. Svenberg [23] indicated that the thermal storage capacity of the hollow core concrete slab is about 1200 KJ/m^2. Block et al. [24] designed a residence in Iowa using a concrete cored slab as a thermal storage mass. Based on the assumption that the indoor air temperature is 26°C and the slab temperature is 20°C, he estimated the thermal storage capacity as being 2000-3000 KJ/m^2.

Tamblyn [25] estimated that a hollow core slab is more useful in a 24 hour cycle than a flat slab. His studies indicated that a reduction of chiller demand by up to 25 percent could be obtained with temperature swing of 3°C during occupied hours.

Birrer [26] designed a six storey office building in Johannesburg using hollow concrete columns and slabs. The measurements indicate the floor temperature is between 22 and 23°C. The cooling load was reduced by 50 W/m^2.

Another possible way to reduce the heating energy consumption in office buildings is to use the heat storage effect of the common wall between the attached solarium and the office space.

In 1980 Public Works Canada and Energy, Mines and Resources Canada have organized a competition on low energy building design [27]. Most projects have included sunspaces and atria. However, among the weaknesses of these projects was the inability to estimate the thermal performance of these solar spaces. Three years later, a study was carried out by Jones [28] for NRC, to analyze several passive solar strategies for office buildings. He used the available version of the DOE program, which had no capability to simulate this problem, for analyzing the effect of an atrium. The results indicate that the addition of a heated atrium to the South face of the building will increase the energy consumption in winter by about 7 percent.

Sodha et al. [29] developed a computer program to analyze the thermal performance of a solarium, based on the harmonic methods, considering the incident solar radiation and the ambient temperature as periodic functions. The results of the simulation for Boulder, Colorado on January 13 indicate that 0.35 m concrete wall between the solarium and the living room will create an appropriate time lag of

about 12 hours, that is the heat stored during the peak hours of insolation will be released in the living space at night.

1.3 CONCLUSIONS FROM LITERATURE SURVEY

The following conclusions were drawn from the literature review:

i) Some works have analyzed the effect of the building enclosure, neglecting the interior mass.

ii) Usually, the effect of the variation of the building mass was analyzed for constant room air temperature.

iii) Computer programs with limited capabilities to analyze this effect were utilized, and consequently no important reductions of the energy consumption were observed.

iv) Very few papers have analyzed the effect of the "free cooling" or the special operation of HVAC system in order to make better use of the building storage mass.

v) There are no papers analyzing the thermal comfort related with different energy saving solutions.

vi) The building mass can be used for storing energy and account for significant energy savings, if appropriate design alternatives are used, which allow the room air temperature to fluctuate within the comfort limits.

vii) Although some buildings use the hollow core slabs or columns to reduce the energy consumption for cooling, there is no detailed analysis of the capabilities of this system. The available information contain general indices, such as the percentage of the energy savings or the average cooling effect, based on

metered or simulated energy consumption for a particular building and weather data.

viii) The use of solarium or greenspaces for housing was analyzed in detail, while their application to the office buildings was neglected. However, in the last years the architectural design has included the use of solaria and atria.

1.4 OBJECTIVE OF RESEARCH

The objective of this research is to analyze design solutions which use heat storage in the building mass, for reducing the energy consumption in office buildings in Montreal. These design solutions will use the hollow core slabs for reducing the cooling load in summer and the attached solaria for reducing the heating load in winter. The performances of these design solutions will be studied.

In order to achieve this objective, the following tasks will be performed:

i) Development of a research oriented computer program as an experimental tool.

ii) Validation of the computer program.

iii) Evaluation of the design alternatives using the computer program, for estimating the building thermal loads and the thermal comfort index.

iv) Analysis of the design alternatives taking into consideration the uncertainties in predicting the climate.

1.5 OUTLINE OF THE THESIS

In Chapter 2, a survey of existing building energy analysis programs with comments on their peculiarities is presented.

In Chapter 3, the research oriented software called CBS - MASS, developed during this research is presented. This computer program has a modularized structure to facilitate the implementation of new algorithms or the use of different algorithms for a given problem. The program is based on the heat balance method, and uses finite difference techniques to calculate the transient heat transfer through opaque walls. The actual weather data for Montreal, as provided by meteorological services or other particular weather data can be used. The main results are the hourly and daily values of space thermal loads, thermal comfort index, room air temperature and temperature distribution within walls.

In Chapters 4, the validation of CBS-MASS computer program is presented.

In Chapters 5 and 6, the thermal analysis of the design alternatives using hollow core slabs and solaria is performed for office buildings in Montreal, using the computer simulation.

In Chapter 7, the effect of the uncertainties in predicting the climate on the performance of these design alternatives is analyzed.

In Chapter 8, the original contributions of this research are emphasized.

In Chapter 9, the recommendations for further research are presented.

CHAPTER 2

SURVEY OF THE BUILDING ENERGY ANALYSIS PROGRAMS

CHAPTER 2

SURVEY OF THE BUILDING ENERGY ANALYSIS PROGRAMS

2.1 EXISTING ENERGY ANALYSIS PROGRAMS

The development of the building energy analysis software can be divided into two main periods in terms of interest and orientation of activities:

i) Between 1964 and 1980, and mainly after 1973, when a large number of computer programs were developed in response to the building owners search for more cost effective design and operation of buildings.

ii) Since 1980, the activities have been concentrated on the improvement and development of new algorithms, and the validation of the existing codes.

During the past few years, several building energy analysis programs for microcomputers have been released. These can be clasified as follows:

i) Detailed programs, which use algorithms from the detailed main-frame programs (e.g., CALPAS-3, ADM-2, PC-DOE which are based on DOE program).

ii) Simplified programs, which can use simplified algorithms and are faster than the previous ones (e.g., BESA and TRACKLOAD which use Modified Bin Method, HOTCAN for residential buildings).

iii) Correlations programs, which use correlations between the building parameters and thermal loads (e.g. SOLPAS). These

correlations were developed by performing a large number of runs of main-frame programs.

The building energy analysis methods can be classified as:

- Single Measure Methods, which use only one measure such as annual degree-days.
- Simplified Multiple-Measure Methods
- Detailed Simulation Methods, which are the most elaborate methods currently in use and perform energy calculations at each hour over the period of analysis.

The building energy analysis programs, which can be used in the research activity, are mainly based on the detailed simulation methods and perform energy calculations every hour over the period of the analysis. All these programs have similar steps, which correspond to their major blocks:

i) Space Load Simulation, where the instantaneous heat gains/losses and the space heating/cooling loads are calculated.

ii) Secondary System or Fan System Simulation, where the air parameters in the important points of the secondary system and the energy demands are calculated.

iii) Primary System or Central Plant Simulation, where the energy consumption of the building is calculated.

Some programs perform the economic analysis based on the life cycle cost or the payback period.

These programs use the Step-by-Step strategy, where the Space Loads Block is executed for every space and for every hour of the simulation period. This is followed by the execution of the Secondary System Block for every hour of the simulation. Then the Plant Block is executed. In this sequence, all the information flux has only this direction. The output of the Space Loads Block becomes the input for the Secondary System Block and so on, but the output never becomes the input for the previous block. A version of this strategy is used by the ESP-II program. It gives the possibility to recalculate the space loads (not the instantaneous heat gains/losses), the space air temperature and the system variables if the capacity of the central plant is smaller than the energy requirements.

Most programs provide the option to choose the simulation period, from one day to one year. When the DESIGN DAY option is selected by the user, the building loads and the energy use are calculated under specific weather conditions, to establish the peak load or the equipment size. It may be run first and the results analyzed before doing the full-year simulations.

2.2 SIMULATION OF THE THERMAL LOADS

The following discussion on the detailed programs is limited to the techniques used to calculate the space loads, since this part is of interest to the present research. These techniques can be classified into the following categories:

- Conduction Transfer Function
- Weighting Factors
- Thermal Network

Among the existing software for building energy analysis, BLAST, DOE and ESP-II programs play a distinct role by their degree of sophistication in simulation, their large use, their good support and their continuous improvement. Although these programs have been developed as design tools, especially for commercial buildings, they have become very attractive for people involved in building research due to their capabilities and their continuous improvement.

However, the training period for these programs is extremely time-consuming. For instance the user must spend about 32 man/hours learning the BLAST input/output data [30].

The BLAST (Building Load Analysis and System Thermodynamics) program [31, 32, 33, 34] uses the Conduction Transfer Function method to calculate the heat transfer through walls (Eq. 2.1).

$$q_{i,t} = \sum_{j=o}^{N_i} X_{i,j}\, TIS_{i,t-j} - \sum_{j=o}^{N_i} Y_{i,j}\, TOS_{i,t-j} + R_i\, q_{i,t-1} =$$

$$h_{cv_i} (TR_t - TIS_{i,t}) + \sum_{k=1}^{N_s} G_{i,k} (TIS_{k,t} - TIS_{i,t}) + R_{i,t} \qquad (2.1)$$

where,

q_i - heat flow (W/m^2)

X_i, Y_i - Conduction Transfer Function coefficients ($W/m^2\,°C$)

R_i - common ratio of the Conduction Transfer Function coefficients

TIS_i - inside surface temperature (°C)

TOS_i - outside surface temperature (°C)

TR - room air temperature (°C)

h_{cv_i} - convective inside surface coefficient (W/m^2 °C)

$$G_{i,k} = 4\, e_i\, FA_{i,k}\, (TR_t + 460)^3\, 0.1714\, 10^{-8} \qquad (2.2)$$

e_i - emmissivity factor

$FA_{i,k}$ - radiation view factor between the surfaces i and k

$$R_{i,t} = IP_{i,t} + \frac{(1-r_e)\, Q_E + (1-r_o)\, Q_0 + (1-r_l)\, Q_L}{\sum_{i=1}^{N_s} S_i} \qquad (2.3)$$

IP_i - solar incident radiation on inside surface i (W/m^2)

r_e, r_o, r_l - fraction of internal heat gain from equipment, occupants and lighting that are assumed to be convective

S_i - area of surface i (m^2).

Q_E, Q_0, Q_L - internal heat gains generated by equipment, occupants and lighting (W)

A heat balance equation is written for the room air (Eq. 2.4) to include all the convective heat flows which occur within the space:

$$\sum_{i=1}^{N_s} S_i\, (TIS_{i,t} - TR_t)\, h_{cv_i} + \dot{m}_{in} c\, (TDB_t - TR_t) +$$

$$+ \dot{m}_{s,t}\, c\, (TS_t - TR_t) + Q_E\, r_e + Q_0\, r_o + Q_L\, r_l = 0 \qquad (2.4)$$

where,

$\dot{m}_{in}$ - air flow rate due to infiltration (kg/s)

c - specific heat of air (J/kg°C)

TDB - outdoor dry-bulb temperature (°C)

$\dot{m}_s$ - supply air flow rate (kg/s)

The number of the Conduction Transfer Function coefficients (X_i, Y_i) used in the calculations depends upon the type of roof and wall. Heavy constructions require a large value, usually less than 20.

The calculation of these cofficients involves lengthy mathematical solutions of the transient heat diffusion equations [35, 36]. A computer program was developed by Mitalas and Arseneault [37] at the National Research Council of Canada to compute these coefficients.

The system of simultaneous linear equations (2.1) and (2.4) are solved each hour for the unknown variables:

- temperatures on the inside surfaces TIS_i (i=1,..,N),
- room air temperature TR

Since the matrix of this set of equations contains many coefficients which do not depend on time, this matrix is partially solved once and then the solution is completed in the hourly loop.

Sowell and Walton [38] have shown that through careful choice of solution algorithms, the heat balance method can be greatly improved in efficiency, so that although still slightly more costly than using

weighting factors, it may become the more attractive alternative on accuracy and flexibility grounds. Their results indicate that for the cases considered, the savings achieved by the use of the weighting factors method relative to the improved heat balance method range only between 13 and 29 percent.

For the first hour of simulation, the system of equations must use the previously values for TIS_i, TOS_i and q_i. Because the "history" of wall and air temperatures are unknown, the program will use default values. In order to eliminate the effect of these initial values and to obtain a "stabilized" solution, the system is solved four times for the first day of simulation period. The last solution, only, will be used as a good solution.

The supply air flow rate and room air temperature are used to calculate the heating or cooling loads, which must be introduced or evacuated by the HVAC system to keep the space temperature within the given limits.

An improved version of the space loads algorithms is included in TARP (Thermal Analysis Research Program) program, which was developed by Walton [39] as a research oriented program for the thermal analysis of buildings. TARP provides more detailed models for air movement and multi-room thermal analysis. The radiant interchange between the interior surfaces is based on the mean radiant temperature method of Carroll [40]. The next extensions to the program will include:

- moisture and contamination migration in multiroom buildings,
- earth contact heat transfer,

- comfort index,
- simultaneous simulation of the equipment performance with the building thermal response

The DOE and ESP-II programs [41, 42] use the weighting factors method, where the space loads and the space air temperature are calculated by a multi-step procedure, which eliminates the need for the simultaneous solution of a set of linear equations. In the first step, the space instantaneous heat gains/losses are calculated, assuming that the space air temperature is held fixed at some refence value TR, usually an average of cooling and heating set-point temperatures.

$$q_{i,t} = \sum_{n=0}^{N_b} b_n \, TSA_{t-n\Delta} - TR_t \sum_{n=0}^{N_c} C_n - \sum_{n=1}^{N_d} d_n \, q_{i,t-1} \qquad (2.5)$$

where,

TSA - sol-air temperature (°C)

b_n, c_n - Conduction Transfer Function coefficients ($W/m^2°C$)

d_n - Conduction Transfer Function coefficient

In order to eliminate the effect of the assumed thermal history of the wall, the DOE program computes the heat gains/losses four times for the first day of the simulation period. Hence, the heat gains/losses for the fourth day are used in the further steps.

In the DOE program, the combined inside film coefficient is included in the wall definition. This coefficient cannot be modified during the simulation.

Generally, the cooling/heating load differs from the instantaneous heat gain/loss because some of the energy from the heat gain can be absorbed by walls or furniture, and stored for later release to the air. The heat storage effect of the building enclosure and the furniture is taken into account in the room weighting factors, one set for each type of heat gain considered in calculations, such as solar, lighting, people, equipment, conduction or internal mass such as furniture.

$$Q_t = \sum_{i=0}^{N_v} v_i \, q_{t-i} + \sum_{i=1}^{N_w} w_i \, Q_{t-i} \qquad (2.6)$$

where

Q_t = cooling load for hour t, calculated for fixed space temperature (W/m^2)

q_{t-i} = heat gain at time (t-i) (W/m^2)

v_i, w_i = heat gain weighting factors, which represent the transfer functions relating the space cooling load to the instantaneous heat gain.

The weighting factor technique, developed by Mitalas and Stephenson [43, 44], represents a compromise between simpler methods such as steady-state calculation that ignores the ability of the building mass to store energy, and more complex methods such as complete energy-balance calculations.

The physical meaning of the weighting factors is how much of the energy entering a room is stored and how rapidly the stored energy is released during later hours. The user can select from the program

library a set of standard materials which best describes the building, and then the standard weighting factors will be automatically used. If the building structure is different from all those recorded in the library, the user can give the structure description (layers, thickness etc.) and the program will calculate the custom weighting factors. This last procedure is more accurate than the Standard Weighting Factor procedure, since it fits better the thermal properties of the walls under analysis, but it is time consuming. Hence, the use of the Custom Weighting Factors is suggested in the following cases [45]:

- passive solar buildings
- masonry buildings
- heavy construction buildings
- any building in which it is necessary to define the distribution of the solar radiation on the interior surfaces
- buildings located in sunny locations with large amount of solar energy entering the space

In the weighting factors method two main assumptions are made:

- thermal processes are linear, hence the superposition of effects is permitted
- system properties are not functions of time

For $N_v = 1$, $N_w = 1$ Equation 2.6 becomes:

$$Q_t = v_0 q_t + v_1 q_{t-1} + w_1 Q_{t-1} \qquad (2.7)$$

Thus, the cooling load for a given hour (Q_t) is related to the heat gain in that hour (q_t), to the heat gain at previous hour (q_{t-1}), and the cooling load at previous hour (Q_{t-1}).

At the end of the first step, the heating/cooling load from various sources are summed to provide total load of the space.

In the second step, the total cooling/heating load is used to calculate the actual heat extraction rate and the room air temperature, using the air temperature weighting factors. The extraction rate differs from the cooling load because of the HVAC system characteristics (coils capacity, plant capacity, controls etc.). The actual room air temperature is obtained using the following equation:

$$\sum_{i=1}^{N_p} p_i \, (ER_{t-i} - Q_{t-i}) = \sum_{i=0}^{N_g} g_i \, (TREF - TR_{t-i}) \qquad (2.8)$$

where

ER_{t-i} = heat extraction rate at time $(t-i)$ required to satisfy the thermostatic set point

Q_{t-i} = cooling load at time $(t-i)$

TREF = fixed space air temperature at which loads were calculated

TR_{t-i} = actual space air temperature at time $(t-i)$.

p_i, g_i = air temperature weighting factors

For $N_p = 1$, $N_g = 1$ Equation 2.8 becomes:

$$p_o \, (ER_t - Q_t) + p_1 \, (ER_{t-1} - Q_{t-1}) = g_o \, (TREF - TR_t) + g_1 (TREF - TR_{t-1}) \qquad (2.9)$$

The actual room air temperature is:

$$TR_t = TREF - \frac{1}{g_0}\left\{p_0\,(ER_t - Q_t) + p_1\,(ER_{t-1} - Q_{t-1}) - g_1\,(TREF - TR_{t-1})\right\} \qquad (2.10)$$

In the second step the throttling range of the thermostat and the limitation of the heating/cooling capacities are taken into account. If the cooling capacity cannot meet the peak cooling load, the room air temperature cannot be maintained within the imposed range. The user must check the input data and modify them, in order to respect the desired values of the space air temperature.

If the Standard Weighting Factors method is used, the computing time is 3-5 times less than that for the heat balance method [42]. If the Custom Weighting Factors are used, the computing time will be slightly bigger, these factors being calculated only once for the whole simulation period.

The experience with the BLAST and DOE programs has indicated that there are no substantial differences between the results, provided that the weighting factors are determined for the specific building under analysis [46, 47]. The convergence of the two methods increases with the number of weighting factors, and the maximum difference in space air temperature which is calculated with these two methods is about 0.5 F.

A comparison of BLAST and DOE programs has shown [48]:

i) Good agreement in the estimation of the annual heating load,

except for the Standard Weighting Factors (DOE) which show underestimates for mild heating climates.

ii) The DOE annual cooling loads (both Standard and Custom Weighting Factors) are higher (25-33%) than the BLAST predictions. The reason for this difference may be the different method to perform the shading calculations, or the absorption of solar radiation on interior surfaces, because in the case of a building without windows a good agreement was found.

A comparison of the estimated cooling loads against the measured data [49] has indicated the results of DOE program are closer to the measurements than the BLAST results. For this particular case, the DOE program will not overestimate the capacity of the HVAC system, because the heat storage effect in the building mass is better simulated.

The PASOLE program, developed by McFarland at Los Alamos Scientific Laboratory [50] is based on the thermal network method. PASOLE was designed specifically for detailed analysis of passive solar heated structures and includes algorithms for calculating solar sources in a general way. This program allows the user to describe the thermal network model by specifying nodes that represent finite regions of uniform temperature, connections between these nodes, and parameters associated with the nodes and connections. Each node i may be connected to any other node j by a thermal conductance $K_{ij} = U_k S_k$, where U_k is the overall heat transfer coefficient for connection k between nodes i and j, and S_k is the heat transfer area of connection k.

The rate of heat flow from node i to node j is:

$$Q_{ij} = K_{ij} (T_i - T_j) \tag{2.11}$$

Each node may have a heat capacitance $M = \rho cV$

The heat balance at any given node i at time t is:

$$\sum_{j=I}^{N} K_{ij} (T_i - T_j) + M_i \left(\frac{dT}{dt}\right)_i = E_i \tag{2.12}$$

Some nodes, such as outside air temperature node, have "fixed" or known temperature at a given time, whereas other nodes have "variable" or unknown temperature that must be determined. The system of linear equations, obtained for the N nodes with N unknown temperature, is then solved.

PASOLE is not a standard "user oriented" program, that is, to use the program for other than the specific models for which is developed, the user must have some knowledge of heat transfer principles and FORTRAN programming.

The DEROB program was developed by Arumi-Noe at the University of Texas to integrate with PASOLE program, and to avoid the limitations of the previous one [51]. The DEROB program uses the finite difference method and can handle generalized architectural shapes and radiative interactions. The first version of DEROB/PASOLE program had the capability to use up to 39 nodes, which reduces the accuracy of the simulation results. An increase up to 200 nodes was planned for the next version.

2.3 CONCLUSIONS

From the survey of the building energy analysis programs the following conclusions have been drawn:

i) Initially, the energy analysis programs were developed to analyze different HVAC systems working in a given building. The conduction transfer function and the weighting factor techniques were developed as a solution to simplify the calculation of the space loads. Hence, the computing time was reduced with respect to the numerical methods. The requirements change if the emphasis is on the building design and analysis, instead of the HVAC systems. Different design alternatives of the building envelope and interior elements (partitions, floors) must be analyzed, which require the calculation of the Conduction Transfer Functions each time. Consequently, the advantage of reducing the computing time is lost. Moreover, the weighting factors are precalculated only for three types of construction (light, medium and heavy), which does not cover all possible design alternatives.

ii) The modification of the existing programs or the implementation of new algorithms, as required by the present research is very difficult, if not an impossible task, due to the internal structure of these programs and to the access to the code. Hence, the development of a research oriented software is required, as a simulation tool for analyzing those design alternatives which use the thermal storage effect in the building structure such as

hollow core slab design.

iii) The development of a research oriented software in building energy analysis implies a modular structure and new or improved mathematical models. The modular structure will allow the researcher to build a code for a particular problem, using the available modules from library and by adding new modules.

CHAPTER 3

CBS-MASS PROGRAM

CHAPTER 3

CBS-MASS PROGRAM

The conclusions from the survey of the building energy analysis programs, presented in Chapter 2, have indicated that the modification of the existing programs or the implementation of new algorithms is a difficult task, due to the internal structure of these programs and to the access to the code. Also, the conduction transfer function technique, as used by programs such as BLAST or TARP, cannot simulate particular problems such as hollow core slab. Hence, a research oriented software called CBS-MASS was developed during this research.

In Chapter 3 the general structure of this program and the algorithms developed to simulate the heat transfer processes are presented.

3.1 PROGRAM STRUCTURE

A research oriented program called CBS-MASS (Centre for Building Studies - building MASS) was developed as a simulation tool to analyze the thermal behavior of the buildings [52].

The program computes the hourly variation of the sensible heating/cooling loads, the room air temperature and the thermal comfort index, for a given configuration of the space and for a design day. The design day was selected, instead of one-year simulation, to allow the reseacher to analyze several design alternatives in a short time.

Detailed algorithms are used to simulate the following processes which occur within the building and between the built environment and the building:

i) Transient heat conduction through the building elements (walls, roofs, floors, partitions).

ii) Sensible heat gains from people, lights and equipment, taking into account the relative split of these gains into radiative and convective

iii) Air infiltration

iv) Shortwave solar radiation on exterior and interior surfaces

v) Longwave radiation exchange between internal surfaces

vi) Shading of external opaque and transparent surfaces.

The program can estimate the effect of design alternatives involving:

- building orientation
- building geometry
- thermal properties of building materials
- occupancy
- shading
- night insulating shutters
- control of room air temperature
- supply air flow

On the Perkin-Elmer mini-computer, the CBS-MASS program requires 230 K memory and the computing time varies between 30 s to 5 minutes

depending on the number of walls in space, the number of identical days and on the control of room air temperatures. The general structure of CBS-MASS program is presented in Figure 3.1.

3.1.a Main Program

The main role is to create a framework, where the appropriate routines will be connected, and to control the information transfer between them. The principal tasks of the main program are the following (Fig. 3.2).

i) Read input data from the building file, which contains the geometrical and the thermophysical properties of the space, and from the operation file, which contains the data about occupation and control (block INPUT). These two files are created by the user using a pre-processor and can be stored for later use.

ii) Read weather data (block WEATHER). The user can use either the existing library, which contains data for Montreal in December, January, July and September provided by meteorological services [53], or his particular climatic data.

iii) Control the solar calculations on hourly basis (block SOLAR), which provides:

- solar radiation on exterior surfaces
- solar radiation through windows
- solar radiation on interior surfaces

iv) Simulate several identical days to eliminate the effect of the initial conditions, which were introduced to describe the

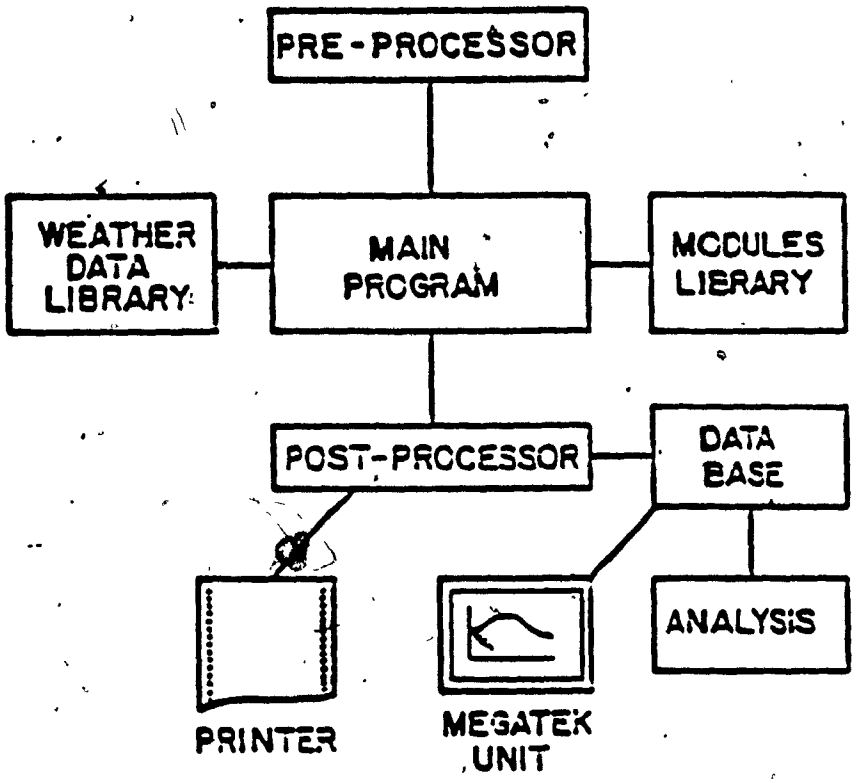

Fig. 3.1 General structure of the CBS-MASS program

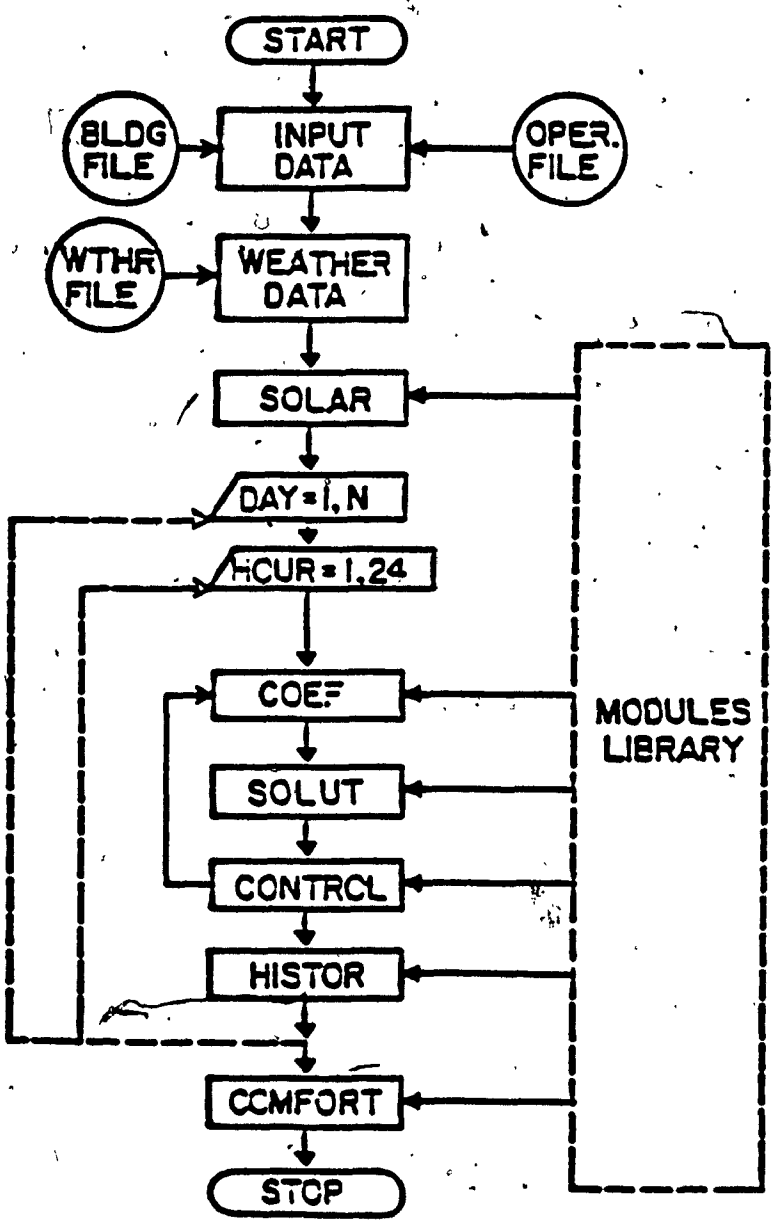

Fig. 3.2 Flowchart of the main program

thermal history of the building.

v) Assign values to the coefficients of the matrix A and vector B, based on the input data (block COEF). The simulation model of the thermal behavior of the building has the form of a system of simultaneous linear equations [A][T] = [B], where T is the vector of unknown temperatures. Some coefficients vary from hour to hour, while others remain constant.

vi) Solve the system of equations and obtain the unknown temperatures of the room air and of the walls (block SOLUT).

vii) Control the room air temperature (block CONTROL). The room air temperature as obtained in block SOLUT (step 1) is compared with the limits prescribed by the user, and if the conditions are not fulfilled the coefficients in block COEF are modified (step 2). The space thermal loads are calculated taking into consideration the restrictions (e.g. minimum and/or maximum room air temperature). Usually, the calculations for each hour follow steps 1 and 2. For simulations with no restrictions on the room air temperature, or with very high upper limit or very low lower limit, only the step 1 is performed.

viii) Save the thermal history of the space (block HISTOR).

ix) Calculate the thermal comfort index, based on Fanger's model [75] (block COMFORT).

To accomplish these tasks, the main program calls the appropriate modules from library.

3.1.b Program Library

The program library is composed of the weather data library and the modules library:

i) The weather data library, contains actual data for Montreal as provided by the meteorological services [53] and other particular climatic conditions, as defined by the user. The weather data library contains the following hourly values:

- total radiation on horizontal surfaces,
- total cloud amount,
- dry bulb temperature of outdoor air.

However, if the intensity of solar radiation on the exterior surfaces are available from different mathematical models or from measurements, then the program can use these values to simulate the thermal behavior of the building.

ii) The modules library, contains a set of routines for calculating the transient heat transfer through cavity walls, partitions and hollow core slab.

The modular structure creates a more flexible software [54, 55], which allows the researcher to:

- select from the library those algorithms more appropriate for a particular problem,
- compare the effect of different algorithms within the same general conditions (e.g., differences between the cooling loads calculated with the Conduction Transfer Function method and

those obtained using numerical methods, or variation of room air temperature for diffuse versus non-diffuse glazing).

- develop the library, by incorporating modules based on new developements in mathematical models or on the experimental results.

3.1.c Pre-processor

The pre-processor assists the user in creating a new building and/or operation file, and in modifying an existing building and/or operation file.

The following data are required to create a building file:

i) General building data

- number of elements such as exterior and interior walls, floors, partitions
- volume of space
- absorptivity of outside surface
- U-value of glazing
- ratio between U-value of glazing at night and U-value by day (when night insulating shutters are used).
- shading coefficient of window
- glazing type (diffuse or non-diffuse)
- air infiltration rate, as air changes per hour
- reflectance of ground
- reflectance of built environment

- surface to sky view factor
- surface to ground view factor
- surface to built environment view factor

ii) Data for each element

- type (exterior, interior, roof, hollow core slab etc.)
- orientation with respect to South
- tilt
- surface area
- absorptivity of inside surface
- for each layer
  - thickness
  - thermal conductivity
  - density
  - specific heat
- conductance of air cavity (for air cavity wall)
- if there is a window
  - window to wall ratio
  - type (single or double)
  - tilt
- hourly variation of the sunlit area on wall and window

The following data are required to create an operation file:

i) Selection of weather data file

- actual data for Montreal 1979.
- particular weather data, provided by user

ii) Hourly schedules

- occupancy

- internal gains (people, lights)

iii) If there is supply air by an HVAC system, then hourly schedules of:

- thermostat set point
- throttling range
- air mass flow rate

Also, the air supply efficiency and the operation of HVAC system during unoccupied hours (system shutdown, normal operation, fresh air supply) have to be specified by the researcher.

iv) Air temperature in adjacent rooms

- equal with air temperature in room under analysis
- given hourly variation

v) Thermal resistance of clothing

3.1.d Post-Processor

At the end of each simulation the main results are displayed on the screen:

- hourly variation of room air temperature, space thermal load and thermal comfort index
- average value of room air temperature and thermal confort index, over the occupation period
- daily total load

The user can decide to print and/or save the results, or to pass directly to another simulation and to change the design solution, if the results are not acceptable (e.g., thermal discomfort or high thermal loads). If the print option is selected, the user can choose

the information to be listed, among the following:

- main results,
- weather data,
- temperature distribution in walls,
- radiation on exterior and/or interior surfaces,
- radiative coefficients on internal surface.

If the save option is selected, the main results are stored in data base. They can be presented in graphical form on MEGATEK unit, where the effect of different design alternatives can be better visualized, and then hardcopies can be obtained. Also, the information stored in data base can be used for further analysis of the design alternatives.

3.2 HEAT BALANCE FOR ROOM AIR

The building energy analysis programs calculate only the sensible loads, while the latent loads are usually approximated by assuming a constant indoor relative humidity. This simplification is due to the lack of available data to be used in the mathematical models of the moisture migration across the walls, the absorption of moisture from hygroscopic materials, the condensation and the evaporation within buildings.

In order to analyze the complex thermal phenomena occuring within a space, a heat balance equation for the room air is considered, including all convective heat flows which occur.

$$Q_1 + Q_2 + Q_3 + Q_4 + Q_5 + Q_6 = 0 \qquad (3.1)$$

where

Q_1 = heat flow between the inside surface of the walls and the room air (W)

$$Q_1 = \sum_j S_j h_{cvj} (TIS_j - TR) \qquad (3.2)$$

S_j = net surface area of wall j (m^2)

h_{cvj} = convective heat transfer coefficient on the inside surface of wall ($W/m^2\,°C$)

TIS_j = inside surface temperature of wall j (°C)

TR = room air temperature (°C)

Q_2 = heat flow between the inside surface of window and the room air (W)

$$Q_2 = \sum_k SG_k h_g (TG_k - TR) \qquad (3.3)$$

SG_k = glazing area of window k (m^2)

h_g = convective heat transfer coefficient on the inside surface of the window ($W/m^2\,°C$)

TG_k = inside surface temperature of window k (°C)

Q_3 = heat gain/loss due to the supply air of HVAC system (W)

$$Q_3 = \eta \dot{m} c (TS - TR) \qquad (3.4)$$

η = efficiency of air distribution system

$$\eta = \frac{TS - TEV}{TS - TR} \qquad (3.5)$$

TS = supply air temperature (°C)

TEV = return air temperature (°C)

$\dot{m}$ = supply air flow rate (kg/s)

c = specific heat of air (J/kg°C)

Q_4 = convective heat gain due to lighting (W)
$Q_4 = r_1 Q_L$

r_1 = fraction of heat gain generated by lights assumed to be convective (default $r_1 = 0.5$)

Q_L = power of lights (W)

Q5 = heat gain/loss due to the air infiltration (W)

$$Q_5 = m_{IN}\, cp\, (TDB - TR) \qquad (3.7)$$

m_{IN} = air infiltration mass flow rate (kg/s)

TDB = outdoor dry bulb temperature (°C)

Q_6 = heat gain/loss due to the internal sources (people, equipment)

Equation 3.1 becomes:

$$\sum_j S_j\, h_{cvj}\, (T1S_j - TR) + \sum_k SG_k\, h_{gk}\, (TG_k - TR) +$$
$$+ n\, \dot{m}\, c\, (TS - TR) + r_1 Q_L + \dot{m}_{IN}\, c\, (TDB - TR) +$$
$$+ Q_6 = 0 \qquad (3.8)$$

An assumption generally accepted in building energy analysis programs and introduced in the present program is an uniform room air temperature, that is, no horizontal or vertical temperature gradients. For rooms with small or medium floor-to-ceiling height, where the temperature gradient is about 0.5 to 1.0 °C/m, this assumption provides good results.

3.3 HEAT TRANSFER THROUGH WALLS

The computer programs for the analysis of the energy consumption in buildings were developed as a tool to evaluate different design alternatives [56], and not to provide exact information about the thermal behavior of buildings.

The capabilities of these programs are obtained as a compromise between the best simulation of the thermal processes and the shortest comfuting time required by the analysis of all alternatives.

Although complex mathematical models for simulating these processes are available, several input data cannot be assessed with sufficient accuracy. Such examples are:

- as built thermal parameters of the building elements, including modification with age, construction and design defaults,
- intensity and direction of wind for particular location in urban area, where the built environment modifies the data measured by meteorological stations, usually near airports,
- variation of the inside and the outside air film coefficients as a function of position and time,
- radiation exchange between the built environment and the building,
- pattern of air movement within the room, as a result of air convection and HVAC system operation.

The CBS-MASS program uses one-dimensional analysis of the transient heat transfer through walls, as used by all building energy analysis programs. However, the user can take into consideration the two and three-dimensional heat transfer for a particular analysis, using one of the following two ways:

- Developing and incorporating in the modules library appropriate routines for the two and three-dimensional analysis. More complete input data have to be supplied by the user, describing the variation of some thermal parameters in terms of position and time, such as solar distribution on each wall, radiative and convective surface coefficients.

- Defining the temperature or the heat flow distribution within walls, using computer programs developed for two- or three-dimensional analysis [57]. An equivalent one-dimensional model can be obtained, and then be used for more complex analysis on the CBS-MASS program.

The one-dimensional heat transfer equation

$$\frac{\partial T}{\partial t} = \frac{k}{\rho c} \frac{\partial^2 T}{\partial x^2} \qquad (3.9)$$

has to be solved every hour, for each wall under variable boundary conditions.

Exterior wall (Fig. 3.3)

$$x = 0 \quad q_j = -k \frac{\partial T}{\partial x} = q_{R,j} + q_{cv,j} \tag{3.10}$$

$$q_{R,j} = \alpha \, IT_j \tag{3.11}$$

$$q_{cv,j} = h_o \, (TDB - TOS_j) \tag{3.12}$$

$$x = \delta \quad q_j = k \frac{\partial T}{\partial x} = q_{R,j} + q_{cv,j} \tag{3.13}$$

$$q_{R,j} = a \, Q_L + IP_j \, \alpha_j + h_{R,j} \, (TMRT_j - TIS_j) + IREF \tag{3.14}$$

$$q_{cv,j} = h_{cv} \, (TR - TIS_j) \tag{3.15}$$

Interior wall (Fig. 3.4)

$$x = o \quad q_j = -k \frac{\partial T}{\partial x} = q_{cv,j} + q_{R,j} \tag{3.16}$$

$$q_{cv,j} = h_{cv,j} \, (TRE - TOS_j) \tag{3.17}$$

$$q_{R,j} = h_{R,j} \, (TMRT_j - TOS_j) \tag{3.18}$$

where

IT_j - total solar radiation on outside surface j (W/m^2)

h_o - film coefficient on exterior surfaces (W/m^2)

α - absorptivity coefficient of the exterior or interior surfaces

k - thermal conductivity ($W/m°C$)

q_R - radiant heat flow (W/m^2)

q_{cv} - convective heat flow (W/m^2)

$$a = \frac{1 - r_1}{\Sigma S_i - S_{ceiling}}$$

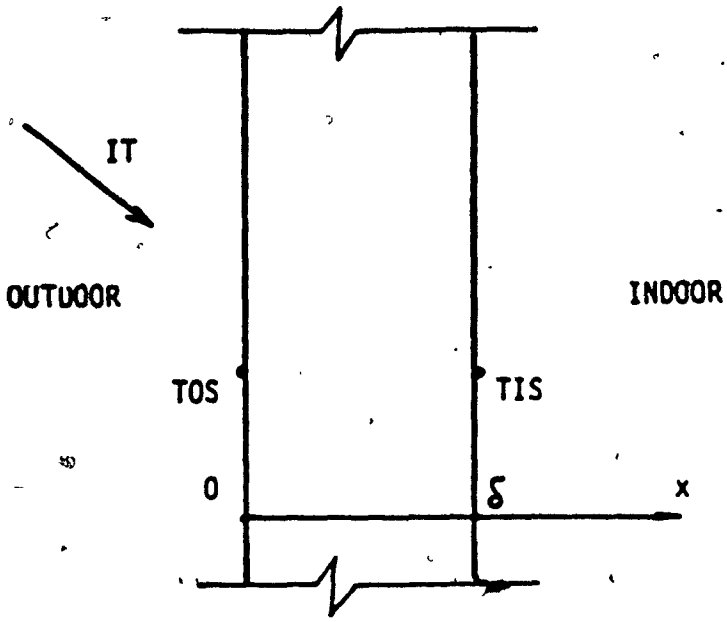

Fig. 3.3 Schema of exterior wall

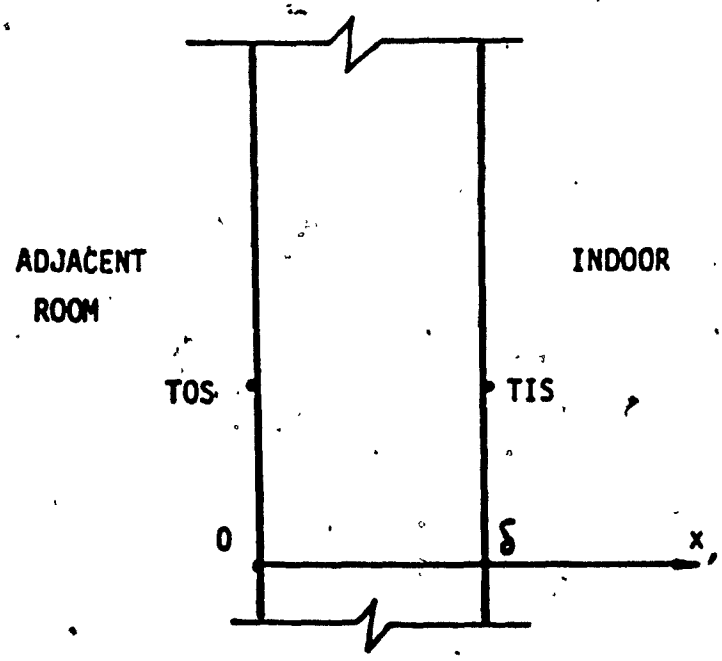

Fig. 3.4 Schema of interior wall

Q_L - internal heat gains from lighting (W)

IP - solar radiation received by the interior surfaces, before the first absorption (W/m^2)

IREF - solar radiation uniformly distributed over the interior surfaces, after the first reflection (W/m^2)

h_R - radiative heat transfer coefficient ($W/m^2 °C$)

$TMRT_j$ - mean radiant temperature as seen by surface j (°C)

h_{cv} - convective heat transfer coefficient ($W/m^2 °C$)

TRE - air temperature of adjacent room (°C)

The boundary conditions at $x = \delta$ for interior walls are defined by Equations 3.13-3.15.

Two options are available to assess the air temperature TRE in adjacent rooms:

- Equal to air temperature TR of the room under analysis. This assumption is valid if the air temperature is kept everywhere within small limits such as 20 $\pm$ 1°C. The air temperature TR and TRE are simultaneously computed every hour.
- Equal to a given hourly variation of the air temperature for each adjacent space, which has to be provided by the user. The effect of solar radiation on the interior surfaces of adjacent rooms is introduced by using the sol-air temperature instead of the room air temperature.

These options allow to analyze the effect of adjacent room and a better simulation of the heat storage in interior walls or floors.

The initial conditions which are required for solving the parabolic type of the partial differential equation (Eq. 3.9) concern the temperatures within walls and the room air temperature. Since the temperature history is unknown, the temperatures are assumed to be equal to 20°C. Several identical days are simulated to eliminate the effect of these initial conditions. The CBS-MASS program allows the user to select between 1 and 10 identical days. Additional comments on the required number of the identical days are presented in Chapter 4.

The solution of the transient heat transfer equation is obtained using finite difference technique, which is more flexible than response factor method, and can be applied to conventional problems or to those which are not soluble, containing for example the non-linear effects.

The CRANK-NICOLSON's implicit formula has been selected, which uses an average of approximations in the j and j+1 time steps, and is unconditionally stable for all computational time and space increments [58].

$$-\frac{\lambda}{2} T_{i-1}^{j+1} + (1+\lambda) T_i^{j+1} - \frac{\lambda}{2} T_{i+1}^{j+1} = \frac{\lambda}{2} T_{i-1}^{j} + (1-\lambda) T_i^{j} + \frac{\lambda}{2} T_{i+1}^{j} \qquad (3.19)$$

where

$$\lambda = \frac{\Delta t}{(\Delta x)^2} \frac{k}{\rho c} \qquad (3.20)$$

The corresponding computational molecula, much easier to be visualized and used, is given in Figure 3.5.

3.3.a Mathematical Model of the Air Cavity Wall.

The development of the set of equations for air cavity wall, using the CRANK-NICOLSON's formula is presented below. The standard structure, which is presented in Figure 3.6, has three nodes for each layer. Clark [59] found small difference in the temperature variation at the inside surface of a homogeneous concrete layer, when he used three and nine nodes for each layer.

The selection of the time step Δt used to analyze the variation in time is subjected to the following constraints:

- Large time step for quick answer.
- Small time step for high accuracy.
- Available weather data are based on hourly measurements.

Emery et al. [60] obtained difference of less than 10 percent when the time step was varied from one hour to two minutes in calculating the indoor air temperature. The present study (Figure 3.7) shows differences of less than 1°C for the room air temperature, when time steps of one hour and of 15 minutes are used. Hence, a time step of one hour is used by the CBS-MASS program.

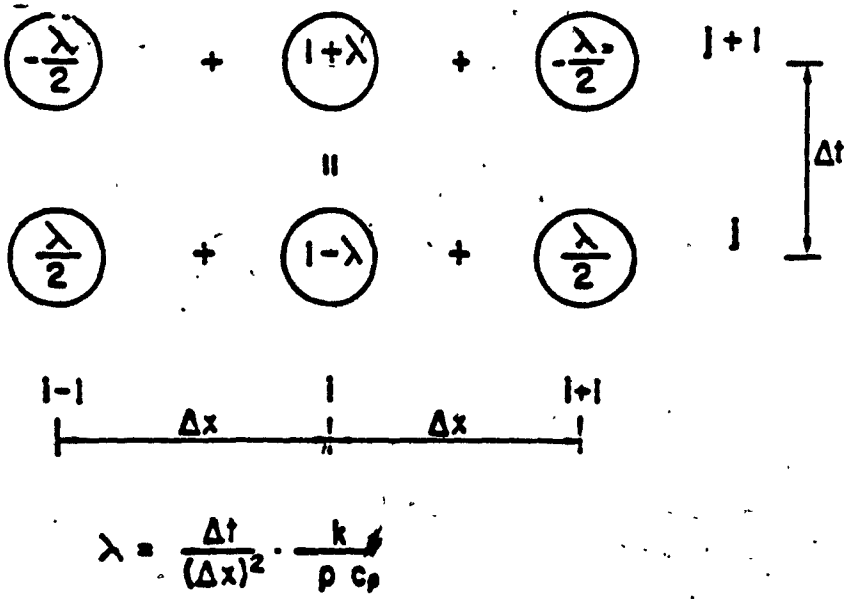

$$\lambda = \frac{\Delta t}{(\Delta x)^2} \cdot \frac{k}{\rho c_p}$$

Fig. 3.5 CRANK-NICOLSON's computational molecula for one-dimensional equation

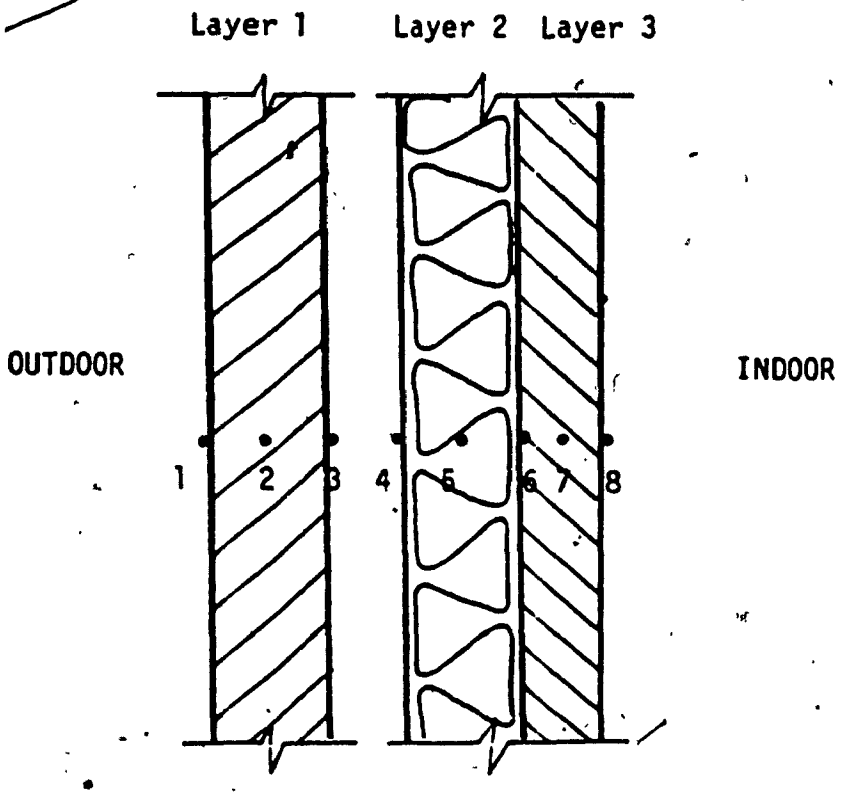

Fig. 3.6 Schema of air cavity wall

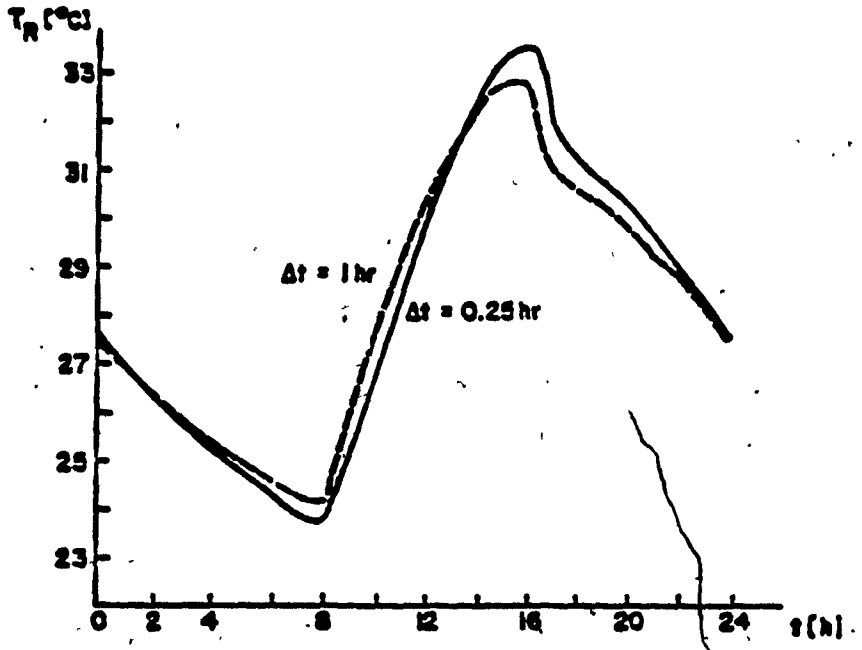

Fig. 3.7 Room temperature variation for different time steps

Node 1

$$-\frac{\lambda_1}{2} TX^{t+1} + (1+\lambda_1)\, T_1^{t+1} - \frac{\lambda_1}{2} T_2^{t+1} = \frac{\lambda_1}{2} TX^{t} + (1-\lambda_1)\, T_1^{t} + \frac{\lambda_1}{2} T_2^{t} \qquad (3.21)$$

The unknown temperature TX is obtained from the relation of the heat flow at the outside surface of the wall:

$$q = -k \left(\frac{\partial T}{\partial x}\right)_{x=0} = \frac{TX - T_2}{2\Delta x_1} k_1 \qquad (3.22)$$

where Δx_1, k_1 and λ_1 refer to layer 1.

Then

$$TX = T_2 + 2 \frac{\Delta x_1}{k_1} q \qquad (3.23)$$

Equation 3.21 becomes:

$$(1 + \lambda_1) T_1^{t+1} - \lambda_1 T_2^{t+1} - \lambda_1 \frac{\Delta x_1}{k_1} q^{t+1} = (1 - \lambda_1)\, T_1^{t} + \lambda_1 T_2^{t} + \lambda_1 \frac{\Delta x_1}{k_1} q^{t} \qquad (3.24)$$

Replacing the heat flow rate q by the Equations 3.10 - 3.12 it obtains:

$$(1 + \lambda_1 + \lambda_1 \frac{\Delta x_1}{k_1} h_o) T_1^{t+1} - \lambda_1 T_2^{t+1} = (1 - \lambda_1 - \lambda_1 \frac{\Delta x_1}{k_1} h_o)\, T_1^{t} + \lambda_1 T_2^{t} + \lambda_1 \frac{\Delta x_1}{k_1} h_o\, (TDB^{t} + TDB^{t+1}) + \lambda_1 \frac{\Delta x_1}{k_1} \alpha\, (IT^{t} + IT^{t+1}) \qquad (3.25)$$

where

$T_1 = TOS$

Node 2

$$-\frac{\lambda_1}{2} T_1^{t+1} + (1 + \lambda_1)\, T_2^{t+1} - \frac{\lambda_1}{2} T_3^{t+1} = \frac{\lambda_1}{2} T_1^t + (1 - \lambda_1)\, T_2^t + \frac{\lambda_1}{2} T_3^t \qquad (3.26)$$

Node 3

$$-\frac{\lambda_1}{2} T_2^{t+1} + (1 + \lambda_1)\, T_3^{t+1} - \frac{\lambda_1}{2} TY^{t+1} = \frac{\lambda_1}{2} T_2^t + (1 - \lambda_1)\, T_3^t + \frac{\lambda_1}{2} TY^t \qquad (3.27)$$

The unknown temperature TY is obtained from the relation of the heat flow rate within the air cavity:

$$q = -k \left(\frac{\partial T}{\partial x}\right) = k_1 \frac{T_2 - TY}{2\,\Delta x_1} = q_{3-4} = \frac{T_3 - T_4}{R_{ac}} \qquad (3.28)$$

then

$$TY = T_2 - 2 \frac{\Delta x_1}{k_1} \frac{1}{R_{ac}} (T_3 - T_4) \qquad (3.29)$$

where R_{ac} is the thermal resistance of air cavity ($m^2 °C/W$)

Equation 3.27 becomes:

$$-T_2^{t+1} \lambda_1 + T_3^{t+1} \left(1 + \lambda_1 + \lambda_1 \frac{\Delta x_1}{k_1} \frac{1}{R_{ac}}\right) - T_4^{t+1} \lambda_1 \frac{\Delta x_1}{k_1} \frac{1}{R_{ac}} =$$

$$T_2^t \lambda_1 + T_3^t \left(1 - \lambda_1 - \lambda_1 \frac{\Delta x_1}{k_1} \frac{1}{R_{ac}}\right) + T_4^t \lambda_1 \frac{\Delta x_1}{k_1} \frac{1}{R_{ac}} \qquad (3.30)$$

Node 4

$$-\frac{\lambda_2}{2} TZ^{t+1} + (1+\lambda_2)\, T_4^{t+1} - \frac{\lambda_2}{2} T_5^{t+1} = \frac{\lambda_2}{2} TZ^{t} + (1-\lambda_2)\, T_4^{t} + \frac{\lambda_2}{2} T_5^{t} \qquad (3.31)$$

In similar manner as for the node 3 one obtains:

$$-\lambda_2 \frac{\Delta x_2}{k_2} \frac{1}{R_{ac}} T_3^{t+1} + T_4^{t+1} \left(1+\lambda_2+\lambda_2 \frac{\Delta x_2}{k_2} \frac{1}{R_{ac}}\right) - \lambda_2 T_5^{t+1} =$$

$$\lambda_2 \frac{\Delta x_2}{k_2} \frac{1}{R_{ac}} T_3^{t} + T_4^{t} \left(1-\lambda_2 - \lambda_2 \frac{\Delta x_2}{k_2} \frac{1}{R_{ac}}\right) + \lambda_2 T_5^{t} \qquad (3.32)$$

Node 5

In similar manner as for node 2 one obtains

$$-\frac{\lambda_2}{2} T_4^{t+1} + (1+\lambda_2)\, T_5^{t+1} - \frac{\lambda_2}{2} T_6^{t+1} = \frac{\lambda_2}{2} T_4^{t} + (1-\lambda_2)\, T_5^{t} + \frac{\lambda_2}{2} T_6^{t} \qquad (3.33)$$

Node 6

A perfect contact at the interface between the layers 2 and 3 is assumed, that is no temperature and heat flow discontinuity in the vicinity of the contact (Fig. 3.8).

$$-k_2 \left(\frac{\partial T}{\partial x}\right) = -k_3 \left(\frac{\partial T}{\partial x}\right) \qquad (3.34)$$

$$-\frac{k_2}{\Delta x_2} T_5^{t+1} + T_6^{t+1} \left(\frac{k_2}{\Delta x_2} + \frac{k_3}{\Delta x_3}\right) - \frac{k_3}{\Delta x_3} T_7^{t+1} = 0 \qquad (3.35)$$

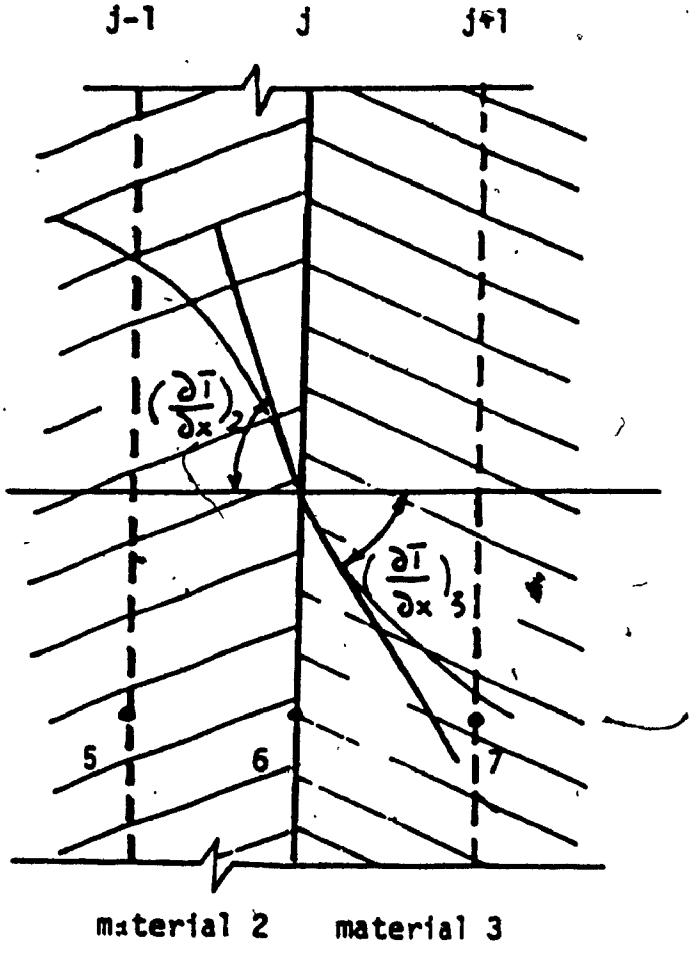

Fig. 3.8 Continuity at the interface contact

Node 7

In similar manner as for node 2 or 5 one obtains:

$$-\frac{\lambda_3}{2} T_6^{t+1} + (1+\lambda_3) T_7^{t+1} - \frac{\lambda_3}{2} T_8^{t+1} = \frac{\lambda_3}{2} T_6^{t+1} + (1-\lambda_3) T_7^t + \frac{\lambda_3}{2} T_8^t \qquad (3.36)$$

Node 8

$$-\frac{\lambda_3}{2} T_7^{t+1} + (1+\lambda_3) T_8^{t+1} - \frac{\lambda_3}{2} TW^{t+1} = \frac{\lambda_3}{2} T_7^t + (1-\lambda_3) T_8^t + \frac{\lambda_3}{2} TW^t \qquad (3.37)$$

where

$$TW = T_7 + 2\frac{\Delta x_3}{k_3} q \qquad (3.38)$$

$$T_8 = TIS$$

Replacing the heat flow rate q by Equations 3.13 - 3.15 one obtains:

$$-\lambda_3 T_7^{t+1} + T_8^{t+1}\left(1+\lambda_3+\lambda_3\frac{\Delta x_3}{k_3}(h_{cv}+h_R)\right) - \lambda_3\frac{\Delta x_3}{k_3} h_{cv}\, TR^{t+1} =$$

$$\lambda_3 T_7^t + T_8^t(1-\lambda_3) + \lambda_3\frac{\Delta x_3}{k_3} q^t + h_R\, TMRT^{t+1} + a\, Q_L^{t+1} +$$

$$+ IP^{t+1}\alpha + IREF^{t+1} \qquad (3.39)$$

A set of eight simultaneous linear equations [A][T] = [B] is obtained, to describe the transient heat transfer through the air cavity wall. These equations can be used with acceptable accuracy for

exterior massive walls, homogeneous or non-homogeneous, provided that the thermal resistance of air cavity has a very low value (e.g., 0.01 m²°C/W).

3.3.b Mathematical Model of the Interior Elements (Floors and Partitions)

The structure presented in Figure 3.9 is considered, with three nodes for each layer.

In similar manner as for air cavity wall, a set of simultaneous equations is obtained.

3.3.c Mathematical Model of the Hollow Core Slab

A plane air flow between two concrete plates is considered as a physical model of the hollow core slab (Fig. 3.10).

A two-dimensional model is used to calculate the transient heat transfer through the concrete plates, taking into consideration the temperature variation in the direction of the air flow.

$$\frac{\partial T}{\partial t} = \frac{k}{\rho c} \left(\frac{\partial^2 T}{\partial x^2} + \frac{\partial^2 T}{\partial y^2} \right) \qquad (3.40)$$

The CRANK-NICOLSONS's implicit formula, which is always stable for rectangular fields [58], is used to solve Equation 3.40. The corresponding computational molecula is given in Figure 3.11, where

$$r_1 = \left(\frac{\Delta y_1}{\Delta x_1} \right)^2 \qquad (3.41)$$

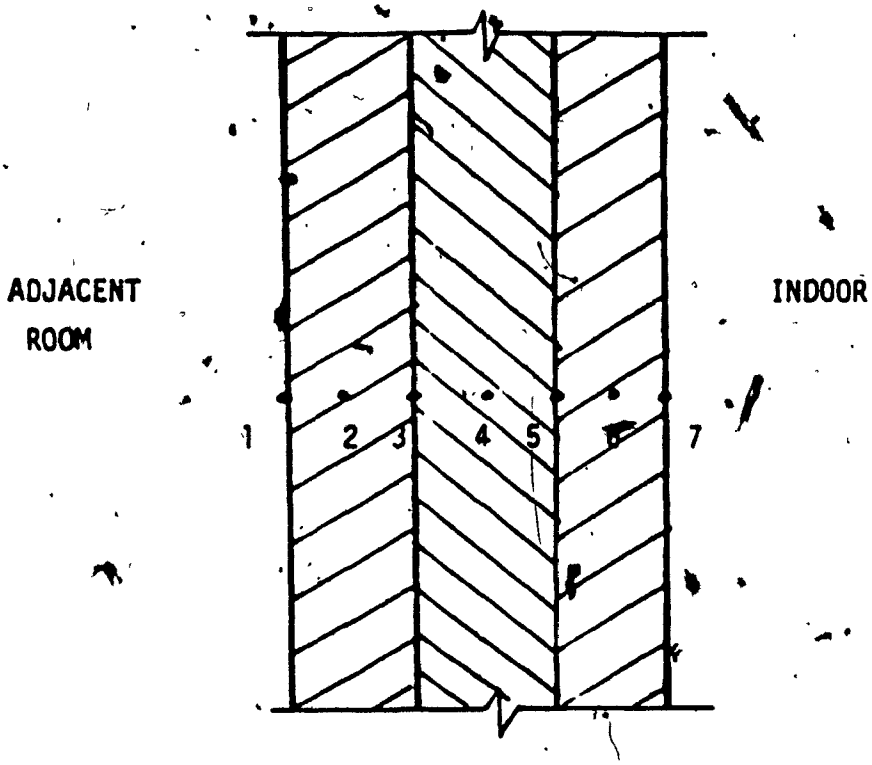

Fig. 3.9 Schema of interior element

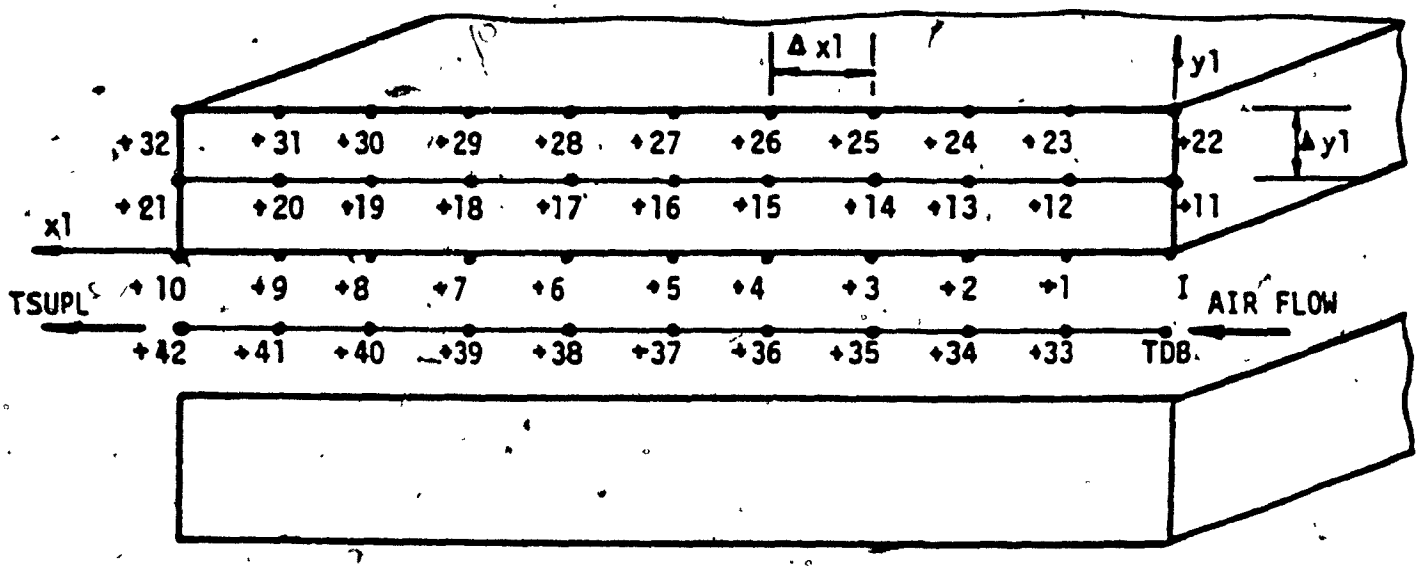

Fig. 3.10 Schema of hollow core slab

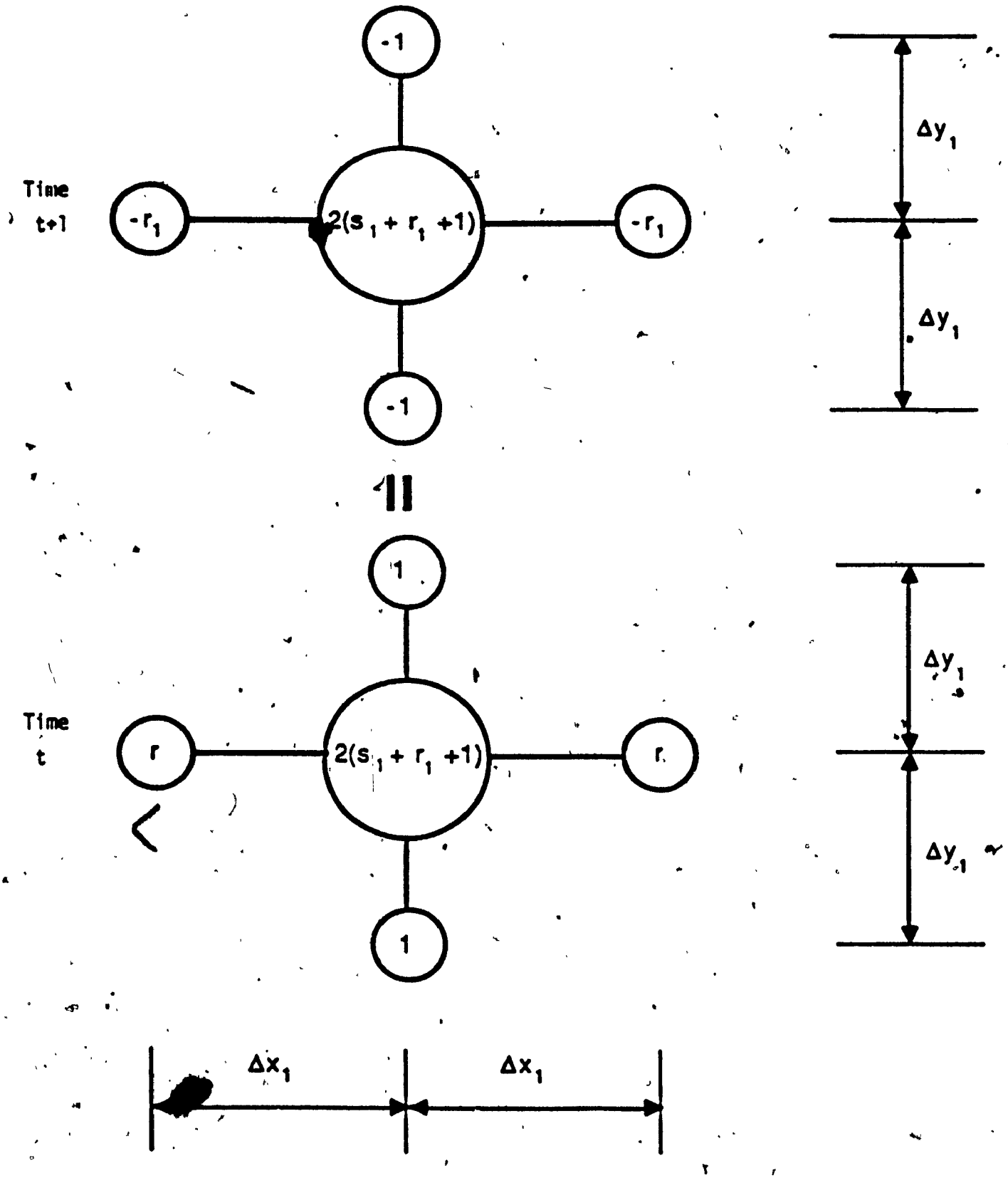

Fig. 3.11 CRANK-NICOLSON's computational molecula for two-dimensional equation

$$S_1 = \frac{\Delta y_1^2}{\Delta t} \frac{\rho c}{k} \tag{3.42}$$

Node I

$$- r_1 T(+1)^{t+1} - r_1 TX^{t+1} - T(+11)^{t+1} - TY^{t+1} + 2(r_1+s_1+1)\, T(I)^{t+1} =$$

$$r_1 T(+1)^{t} + r_1 TX^{t} + T(+11)^{t} + TY^{t} + 2(s_1-r_1-1)\, T(I)^{t} \tag{3.43}$$

The unknown temperature TX is obtained by using the assumption of no heat flow at the boundary x1 = 0.

$$q = - k \left(\frac{\partial T}{\partial x1}\right)_{x1=0} = k \frac{T(+1) - TX}{2\,\Delta x1} \tag{3.44}$$

Then TX = T(+1). (3.45)

The unknown TY is obtained by considering the heat flow at the boundary y1 = 0.

$$q = - k\left(\frac{\partial T}{\partial y1}\right)_{y1=0} = k \frac{TY - T(+11)}{2\,\Delta y1} = h_{cvf}\,(TDB - T(I)) \tag{3.46}$$

where h_{cvf} is convective heat flow coefficient within the hollow core slab ($W/m^2\,°C$)

$$TY = T(+11) + 2 \frac{\Delta y1\, h_{cvf}}{k} (TDB - T(I)) \tag{3.47}$$

Equation 3.43 becomes:

$$\left(s_1+r_1+1 + \frac{\Delta y1\, h_{cvf}}{k}\right) T(I)^{t+1} - r_1\, T(+1)^{t+1} - T(+11)^{t+1} =$$

$$\left(s_1-r_1-1 - \frac{\Delta y1\, h_{cvf}}{k}\right) T(I)^{t} + r_1\, T(+1)^{t} + T(+11)^{t} +$$

$$+ \frac{\Delta y1\, h_{cvf}}{k} (TDB^{t+1} + TDB^{t}) \tag{3.48}$$

Node +1

$$- r_1\, T(I)^{t+1} - r_1\, T(+2)^{t+1} - T(+12)^{t+1} - TY^{t+1} + 2(s_1+r_1+1)\, T(+1)^{t+1} =$$

$$r_1\, T(I)^{t} + r_1\, T(+2)^{t} + T(+12)^{t} + TY^{t} + 2(s_1-r_1-1)\, T(+1)^{t} \qquad (3.49)$$

The unknown TY is obtained by considering the heat flow at the boundary y1 = 0.

$$q = - k \left(\frac{\partial T}{\partial y1}\right)_{y1=0} = k\, \frac{TY - T(+12)}{2\, \Delta y1} = h_{cvf}\, (T(+33) - T(+1)) \qquad (3.50)$$

then

$$TY = T(+12) + 2\, \frac{\Delta y1\, h_{cvf}}{k}\, (T(+33) - T(+1)) \qquad (3.51)$$

Equation 3.49 becomes:

$$- \frac{r_1}{2}\, T(I)^{t+1} + (s_1 + r_1 + 1 + \frac{\Delta y1\, h_{cvf}}{k})\, T(+1)^{t+1} -$$

$$\frac{r_1}{2}\, T(+2)^{t+1} - T(+12)^{t+1} - \frac{\Delta y1\, h_{cvf}}{k}\, T(+33)^{t+1} =$$

$$\frac{r_1}{2}\, T(I)^{t+1} + (s_1 - r_1 - 1 - \frac{\Delta y1\, h_{cvf}}{k})\, T(+1)^{t} + \frac{r_1}{2}\, T(+2)^{t} +$$

$$+ T(+12)^{t} + \frac{\Delta y1\, h_{cvf}}{k}\, T(+33)^{t} \qquad (3.52)$$

Equations for the nodes +2 to +9 are obtained in a similar way.

Node +10

$$- r_1\, TX^{t+1} + 2(s_1+r_1+1)\, T(+10)^{t+1} - r_1\, T(+9)^{t+1} - T(+21)^{t+1} - TY^{t+1} =$$

$$r_1\, TX^{t} + 2(s_1-r_1-1)\, T(+10)^{t} + r_1\, T(+9)^{t} + T(+21)^{t} + TY^{t} \qquad (3.53)$$

Taking into consideration the boundary conditions at x1=L and y1=0, one obtains:

$$TX = T(+9) \tag{3.54}$$

$$TY = T(+21) + 2\frac{\Delta y1\ h_{cvf}}{k}\ (T(+42) - T(+10)) \tag{3.55}$$

Equation 3.53 becomes:

$$- r_1\ T(+9)^{t+1} + T(+10)^{t+1}\ (s_1+r_1+1 + \frac{\Delta y1\ h_{cvf}}{k}) - T(+21)^{t+1} -$$

$$- \frac{\Delta y1\ h_{cvf}}{k}\ T(+42)^{t+1} =$$

$$r_1\ T(+9)^{t} + T(+10)^{t}\ (s_1-r_1-1 - \frac{\Delta y1\ h_{cvf}}{k}) + T(+21)^{t} +$$

$$+ \frac{\Delta y1\ h_{cvf}}{k}\ T(+42)^{t} \tag{3.56}$$

Node +11

$$- 2\ r_1\ T(+12)^{t+1} + 2\ (s_1+r_1+1)\ T(+11)^{t+1} - T(I)^{t+1} - T(+22)^{t+1} =$$

$$2\ r_1\ T(+12)^{t} + 2\ (s_1-r_1-1)\ T(+11)^{t} + T(I)^{t} + T(+22)^{t} \tag{3.57}$$

Node +12

$$- r_1 T(+13)^{t+1} - r_1\ T(+11)^{t+1} - T(+23)^{t+1} - T(+1)^{t+1} + 2\ (s_1+r_1+1)\ T(+12)^{t+1} =$$

$$r_1 T(+13)^{t} + r_1 T(+11)^{t} + T(+23)^{t} + T(+1)^{t} + 2(s_1-r_1-1)\ T(+12)^{t} \tag{3.58}$$

Similar equations are obtained for the nodes +13 to +20.

Node +21

$$- 2\ r_1\ T(+20)^{t+1} + 2(s_1+r_1+1)\ T(+21)^{t+1} - T(+32)^{t+1} - T(+10)^{t+1} =$$

$$2\ r_1\ T(+20)^{t} + 2(s_1-r_1-1)\ T(+21)^{t} + T(+32)^{t} + T(+10)^{t} \tag{3.59}$$

Node +22

$$- T(+11)^{t+1} - r_1\, T(+23)^{t+1} - r_1\, TX^{t+1} - TY^{t+1} + 2(s_1+r_1+1)\, T(+22)^{t+1} = T(+11)^{t} + r_1\, T(+23)^{t} + r_1\, TX^{t} + TY^{t} + 2(s_1-r_1-1)\, T(+22)^{t} \qquad (3.60)$$

Considering the boundary conditions at x1=0 and y1=d, one obtains:

$$TX = T(+23) \qquad (3.61)$$

$$TY^{t+1} = T(+11)^{t+1} + 2\frac{\Delta y1\, h_{cv}}{k}\, TR^{t+1} - 2\frac{\Delta y1\, h_{cv}}{k}\, T(+22)^{t+1} + \frac{2\Delta y1}{k}\,(a\, Q_L + IP\, \alpha + IREF)^{t+1} + 2\frac{\Delta y1\, h_R}{k}\, TMRT^{t+1} - 2\frac{\Delta y1\, h_R}{k}\, T(+22)^{t+1} \qquad (3.62)$$

$$TY^{t} = T(+11)^{t} + 2\frac{\Delta y1}{k}\, q^{t} \qquad (3.63)$$

Equation 3.60 becomes:

$$- T(+11)^{t+1} + (s_1+r_1+1 + \frac{\Delta y1\, h_{cv}}{k} + \frac{\Delta y1\, h_R}{k})\, T(+22)^{t+1} - r_1\, T(+23)^{t+1} - \frac{\Delta y1\, h_{cv}}{k}\, TR^{t+1} = \frac{\Delta y1}{k}\,(a\, Q_L + IP\, \alpha + IREF)^{t+1} + \frac{\Delta y1\, h_R}{k}\, TMRT^{t+1} + T(+11)^{t} + (s_1-r_1-1)\, T(+22)^{t} + \frac{\Delta y1}{k}\, q^{t} + r_1\, T(+23)^{t} \qquad (3.64)$$

Node +23

$$- r_1\, T(+22)^{t+1} - r_1\, T(+24)^{t+1} + 2(s_1+r_1+1)\, T(+23)^{t+1} - T(+12)^{t+1} - TY^{t+1} = r_1\, T(+22)^{t} + r_1\, T(+24)^{t} + 2(s_1-r_1-1)\, T(+23)^{t} + T(+12)^{t} + TY^{t} \qquad (3.65)$$

The unknown TY is obtained from the boundary conditions at y1=d.

$$TY = T(+12) + 2\frac{\Delta y1\, h_{cv}}{k} TR - 2\frac{\Delta y1\, h_{cv}}{k} T(+23) +$$

$$+ 2\frac{\Delta y1}{k}(a\, Q_L + IP\, \alpha + IREF) + 2\frac{\Delta y1\, h_R}{k}(TMRT - T(+23)) \qquad (3.66)$$

Equation 3.65 becomes:

$$- T(+12)^{t+1} - \frac{r_1}{2} T(+22)^{t+1} + (s_1+r_1+1 + \frac{\Delta y1\, h_{cv}}{k} + \frac{\Delta y1\, h_R}{k}) T(+23)^{t+1} -$$

$$- \frac{r_1}{2} T(+24)^{t+1} - \frac{\Delta y1\, h_{cv}}{k} TR^{t+1} =$$

$$\frac{\Delta y1}{k}(a\, Q_L + IP\, \alpha + IREF)^{t+1} + \frac{\Delta y1\, h_R}{k} TMRT^{t+1} + T(+12)^t +$$

$$+ \frac{r_1}{2} T(+22)^t + (s_1-r_1-1)\, T(+23)^t + \frac{r_1}{2} T(+24)^t + \frac{\Delta y1}{k} q^t \qquad (3.67)$$

In similar way, the equations for nodes +24 to +31 are obtained:

Node +32

$$- T(+21)^{t+1} + T(+32)^{t+1} (s_1+r_1+1 + \frac{\Delta y1\, h_{cv}}{k} + \frac{\Delta y1\, h_R}{k}) - r_1\, T(+31)^{t+1} -$$

$$- \frac{\Delta y1\, h_{cv}}{k} TR^{t+1} =$$

$$\frac{\Delta y1}{k}(a\, Q_L + IP\, \alpha + IREF)^{t+1} + \frac{\Delta y1\, h_R}{k} TMRT^{t+1} + T(+21)^t +$$

$$+ (s_1-r_1-1)\, T(+32)^t + \frac{\Delta y1}{k} q^t + r_1\, T(+31)^t \qquad (3.68)$$

The average temperature of the nodes +22 to +32 is used as the temperature of the slab in the heat balance equation.

The temperature variation of the air circulating through the hollow core slab is determined using the heat balance for the control space ABCD. (Fig. 3.12)

$$(Q_I + Q_{II} - Q_{III})\, dt = m\, c\, d\Delta \tag{3.69}$$

$$\Delta = T_{f2} - T_{f1} \tag{3.70}$$

$$Q_I = 2\, h_{cvf} \left(\frac{T_{w1} + T_{w2}}{2} - T_a\right) \Delta x 1\, l \tag{3.71}$$

$$T_a = \frac{T_{f1} + T_{f2}}{2} = T_{f1} + \frac{\Delta}{2} \tag{3.72}$$

$$Q_I = 2\, h_{cvf}\, \Delta x 1 \left(\frac{T_{w1} + T_{w2}}{2} - T_{f1} - \frac{\Delta}{2}\right) l \tag{3.73}$$

$$Q_{II} = m\, c\, T_{f1} \tag{3.74}$$

$$Q_{III} = m\, c\, T_{f2} \tag{3.75}$$

where l is the width of the hollow core slab (m).

Equation 3.69 becomes:

$$\left(2\, h_{cvf}\, \Delta x 1\, l \left(\frac{T_{w1} + T_{w2}}{2} - T_{f1} - \frac{\Delta}{2}\right) - m\, c\, \Delta\right) dt = m\, c\, d\Delta \tag{3.76}$$

then

$$\Delta = T_{w1}\, \beta + T_{w_2}\, \beta - 2\, T_{f1}\, \beta \tag{3.77}$$

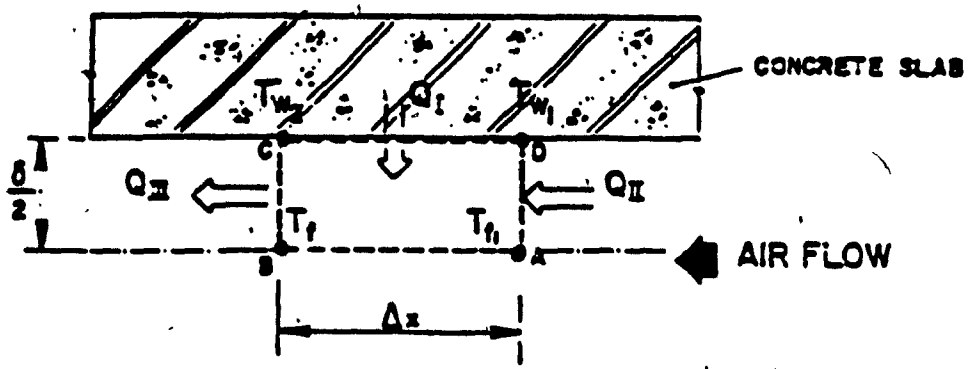

Fig. 3.12 Control volume for the heat balance of air within the hollow core slab.

where

$$\beta = \frac{Z}{Z_1}\left[1 - \exp(-Z_1)\right] \qquad (3.78)$$

$$Z_1 = 1 + Z \qquad (3.79)$$

$$Z = \frac{h_{cvf}\ \Delta x l\ l}{\dot{m}c} \qquad (3.80)$$

The variation of the air temperature is given by:

$$T_{f2} = T_{f1}\ (1-2\beta) + T_{w1}\beta + T_{w2}\beta \qquad (3.81)$$

The temperature of air entering the hollow core slab is equal to the outdoor air temperature. The heat transfer coefficient h_{cvf} between the concrete plate and the air flow is defined using the following formula [61] for forced convection:

$$Nu = 0.023\ Re^{0.8}\ Pr^{0.35} \qquad (3.82)$$

where

$$Nu = \frac{h_{cvf}\ d_e}{\lambda} \qquad (3.83)$$

$$Re = \frac{v\ d_e}{\nu} \qquad (3.84)$$

$$Pr = 0.72 \qquad (3.85)$$

v = air velocity (m/s)

ν = kinematic viscosity of air (m^2/s)

d_e = characteristic dimension (m), of a duct with width a and height b

$$d_e = 2\frac{ab}{a+b} = \frac{2}{\frac{1}{a}+\frac{1}{b}}$$

For duct with the width much larger the height one obtains $d_e = 2b$. One obtains:

$$h_{cvf} = 3.71 \frac{v^{0.8}}{d_e^{0.2}} \qquad (3.86)$$

A set of forty-four simultaneous linear equations is obtained to be utilized in the calculation of the heat transfer process within the hollow core slab. This set of equations must be used along with the equations corresponding to the exterior and interior walls, and to the heat balance of the room air.

3.3.d Convective Coefficient on Interior Surfaces

The building energy analysis programs such as DOE, BLAST or NBSLD use simplified models of convection in rooms, with constant convective coefficient for each surface, usually taken from ASHRAE Handbook [46]. Also, no thermal stratification and no air movements are considered. Gadgil et al. [62] developed a computerized analysis technique to study the natural and forced convective transfer problems, including stack effects in multi-storey atrium spaces, stratification in rooms, inlet and outlet effects of vents in mass storage walls. However, the program is too complex to be implemented in energy analysis programs and to be used in current practice.

The inlet and outlet location, the occupancy, the heat generating sources (computers, typewriters, people, lighting) create air movements, which increase the degree of complexity of the problem.

CBS-MASS program uses a constant value of the convective coefficient on inside surface of walls $h_{cv} = 3.00$ W/(m^2 °C), based on ASHRAE data [46].

3.3.e Radiative Heat Exchange Between Interior Surfaces.

The radiant heat flux from surface 1 to 2 can be expressed by the following relation:

$$q_R = \sigma \, FA \, FE \, (T_1^4 - T_2^4) \qquad (3.87)$$

where

σ = Stephan-Boltzman constant (5.67E-08).

FA = angle factor, accounting for the proportion of energy leaving one surface which reaches directly the other surface involved in exchange.

FE = emissivity factor, accounting for the departure from blackbody emissivities

$$FE = \frac{1}{\frac{1}{e_1} + \frac{1}{e_2} - 1} \qquad (3.88)$$

T_1, T_2 = surface temperature (°K)

Since a large computation time is required to solve the non-linear model, the energy analysis programs use the linear models.

i) $$q_R = h_R \, (T_1 - T_2) \qquad (3.89)$$

where h_R is the radiative coefficient, constant for the whole simulation period, for all surfaces or only for each surface.

ii) $$q_R = 4 \, \sigma \, e_1 \, FA \, TAVG^3 \, (T_1 - T_2) \qquad (3.90)$$

where TAVG is the average absolute temperature of surfaces 1 and 2.

In order to facilitate the computations, the TAVG temperature is assumed either constant (BLAST) or equal with the room air temperature (NBSLD). Carroll [63] discovered errors in heat flux when these simplification are made.

A second observation concerns the use of the emissivity coefficient e instead of the emissivity factor FE. This simplification is valid only when the surface 2 is large compared to the surface 1. In this case, the surface 2 will act as a cavity with little interference from the small surface and so it can be considered as a black body with emissivity e = 1, and FE = e_1.

In a real case, the surfaces within a space are comparable and then, the above assumption is not valid. Moreover, when surfaces with different emissivities are used, a radiation imbalance is obtained with differences of about 100 percent [64].

The angle factor is only exact if individual surfaces are isothermal, gray and uniformly irradiated by other surfaces [63]. Ordinary room surfaces can be assumed to be diffuse gray, but they are seldom isothermal or evenly irradiated.

The NBSLD program calculates the angle factor correctly, but requires rooms to be modeled as simple rectangular boxes. The program assumes that coplanar surfaces have the same angle factors of other surfaces. As a result, NBSLD is inexact in its predictions of the distribution of heat flux from a hot or cold surface and over-

estimates slightly the overall flux, if other emittances are less than one. But more seriously, if e_i and e_j are different, then some errors on heat balance occur.

The BLAST program avoids the geometrical complexity of the angle factor computations by approximating FA for surface j seen by surface i as follows:

$$FA_i = \frac{A_j}{\sum_{j \neq i}^{n} A_j} \qquad (3.91)$$

If two surfaces i and j have different areas, then the denominator will not be the same for them and $A_i F_{ij} \neq A_j F_{ji}$. This lack of reciprocity causes heat balance errors for all rooms which are not cube-shaped.

iii) Mean Radiant Temperature Model.

Walton [64] has proposed that the radiant interchange in a room can be adequately modeled by assuming a fictitious surface which has an area, emissivity and temperature giving about the same transfer as in the real case (Fig. 3.13). This concept simplifies the calculations, especially for rooms with complex geometry and several surfaces, avoiding the use of the angle factor FA.

The area of the fictitious surface is the sum of all other surfaces in the room:

$$AF_i = \sum_{j \neq i}^{n} A_j \qquad (3.92)$$

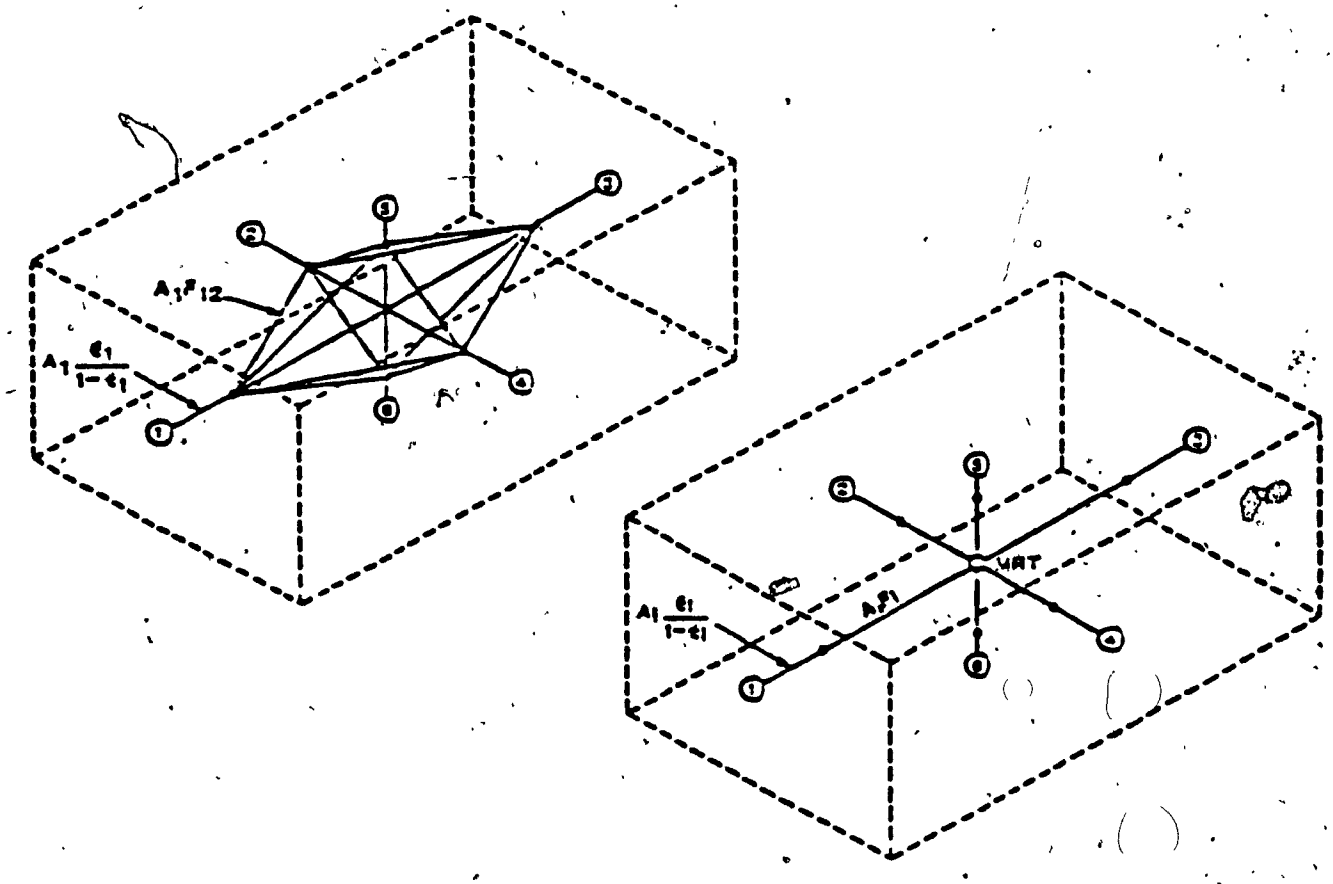

Fig. 3.13 Comparison of detailed (left) and MRT (right) representation of room radiant interchange[64].

The emissivity is an area weighted average of all other surface emissivities:

$$e_{f_i} = \frac{\sum_{j \neq i}^{n} A_j \, e_j}{\sum_{j \neq i}^{n} A_j} \tag{3.93}$$

The Mean Radiant Temperature TMRT is an area and emissivity weighted temperature:

$$TMRT_i = \frac{\sum_{j \neq i}^{n} A_j \, e_j \, TIS_j}{\sum_{j \neq i}^{n} A_j \, e_j} \tag{3.94}$$

The emissivity factor is given by:

$$FE_i = \frac{1}{\frac{1-e_i}{e_i} + 1 + \frac{A_i}{AF} \frac{1-e_f}{e_f}} \tag{3.95}$$

It was assumed that the surface "f" completely encloses the surface "i", and then a radiation interchange factor for two concentric cylinders or spheres was considered.

The net rate of radiant flux is given by:

$$q_{R_i} = h_{R_i} (TIS_i - TMRT_i) \tag{3.96}$$

where

$$h_{R_i} = 4 \sigma \, FE_i (TMRT_i)^3 \tag{3.97}$$

In 1984 [65], Walton proposed a new form of the emissivity factor:

$$FE_i = \frac{1}{1 - \frac{A_i \, FE_i}{\Sigma \, A_j \, FE_j}} \tag{3.98}$$

The radiative coefficient is obtained:

$$h_{R_i} = \frac{4\,\sigma\,TAVG_i^3}{\frac{1}{FE_i} + \frac{1-e_i}{e_i}} \qquad (3.99)$$

The radiative couplings between surfaces vary by about one percent for each 1°C variation in the Mean Radiant Temperature because of the non-linear effect. The radiant coefficient can be left as a constant by using a value of TAVG near the mean radiant temperature TMRT of the room for the total period of the simulation.

Walton [65] suggested the following four steps to estimate the radiant fluxes within 1 percent for surface temperatures between 0°C and 50°C:

Step 1. Initialize all h_R for 27°C.

$$h_{R_i} = \frac{6.13}{\frac{1}{FE_i} + \frac{1-e_i}{e_i}} \qquad (3.100)$$

Step 2. At each iteration adjust all h_{Ri}.

$$h_{Ri} = (0.865 + 0.005\,TIS_i)\,h_{Ri} \qquad (3.101)$$

Step 3. Evaluate:

$$TMRT_i = \frac{\sum h_{Ri}\,S_i\,TIS_i}{\sum h_{Ri}\,S_i} \qquad (3.102)$$

Step 4. Adjust all h_{Ri} again:

$$h_{Ri} = (0.865 + 0.005\,TMRT_i)\,h_{Ri} \qquad (3.103)$$

Some comparisons [64, 66] show good agreement with the non-linear model.

iv) Modified Thermal Balance Model [66]

This technique is somewhat similar to Walton's mean radiant temperature concept. The procedure is based on a surface-area average temperature for each surface within a space. The net rate of radiant heat gain/loss for surface i is expressed as:

$$q_{R_i} = h_{R_i} (TMRT_i - TIS_i) \tag{3.104}$$

where

h_{R_i} = radiative heat transfer coefficient of surface i ($W/m^2\,°C$)

$TMRT_i$ = average temperature of the surfaces seen by surface i (°C)

$$TMRT_i(t) = \frac{\sum_{m \neq i} A_m \, TIS_m(t-1) \, e_m}{\sum_{m \neq i} A_m \, e_m} \tag{3.105}$$

$$h_{R_i} = 4 \, e_i \, \sigma (TMRT_i)^3 \tag{3.106}$$

The heat balance is solved iteratively for surfaces in the room and the individual mean radiant temperatures are updated after each calculation.

First observation about this method concerns the use of the emissivity coefficient e_1 instead of the emissivity factor FE as discussed above. The second observation concerns the simplification of procedure, using the surface temperatures at previous time for

estimating the actual temperature of fictitious surface TMRT. This will provide a reduction of the computation time and the results show acceptable accuracy.

v) Proposed model.

In the CBS-MASS program a modified form of the Modified Thermal Balance approach was used.

$$q_{R_i} = h_{R_i}(TMRT_i - TIS_i) \tag{3.107}$$

$$h_{R_i} = A\ \sigma\ FE_i (TMRT_i)^3 \tag{3.108}$$

It considers that the fictitious surface "f" and the real surface "i" as two concentric spheres, where "f" completely encloses "i".

$$FE_i = \frac{1}{\frac{1}{e_i} + \frac{A_i}{A_f}\left(\frac{1}{e_{f_i}} - 1\right)} \tag{3.109}$$

$$e_{f_i} = \frac{\sum_{j \neq i} A_j\ e_j}{\sum_{j \neq i} A_j} \tag{3.110}$$

$$TMRT_i = \frac{\sum_{j \neq i} A_j\ TIS_j(t-1)\ e_j}{\sum_{j \neq i} A_j\ e_j} \tag{3.111}$$

The use of the mean radiant temperature concept, for simulating the radiative heat exchanges within a room, allows to analyze complex room configurations. The input data task is simplified, since no exact location of each element is required as for the angle factor method.

3.3.f Film Coefficient on Exterior Surfaces.

Kusuda [31] indicated the following relation:

$$h_o = A\, W_s^2 + B\, W_s + C \qquad (3.112)$$

where W_s is the wind speed (km/h) and A, B, C are coefficients depending on the outside surface roughness. Equation (3.112) gives for concrete surface h_o = 38.9 W/(m^2°C) (winter) and 24.5 W/(m^2°C) (summer), and for brick surface h_o = 41.0 W/(m^2°C) (winter) and 26.5 W/(m^2°C) (summer), for wind speed of 24.2 km/h in winter and 12.10 km/h in summer.

The Dutch Standard NEN 1068 recommends an average value h_o = 25 W/(m^2°C), which corresponds to a wind speed of 4 m/s.

ASHRAE Fundamentals [46] recommends h_o = 34 W/(m^2°C) for winter and 23 W/(m^2°C) for summer. These values were selected to be used in CBS-MASS program.

3.3.g Thermal Resistance of Air Cavity.

The heat transfer between surfaces separated by an airspace take place by convection and radiation. For calculations of the heat transfer in cavity walls the airspace is generally regarded as sealed.

The IHVE Guide Book [102] recommends that the thermal resistance of a 5 mm thick airspace, unventilated and with high emissivity surfaces, independent of the direction of heat flux, should be taken 0.11 m^2°C/W. When one or both surfaces have a low emissivity, a value of 0.18 m^2°C/W is recommended.

For a thicker airspace, 20 mm or more, the corresponding values are 0.18 and 0.35 m^2 °C/W except when the heat flow is downwards for which the suggested values are 0.21 and 1.06 m^2 °C/W respectively.

The measurements of Griffiths and Davis presented in reference [67] indicate that for 2.5 cm air cavity and mean temperature between 9.3°C and 37.6°C the thermal resistance is between 0.26 to 0.33 m^2 °C/W. The work of Rowley and Algren presented in reference [67] used hot plate and hot box to measure the thermal resistance of airspaces between materials commonly used in wall sections. For example, the thermal resistance of 2.5 cm air cavity and mean temperature of 21°C is 0.14m^2 °C/W. In the case of mean temperature 0°C, the corresponding value is 0.16 m^2 °C/W. ASHRAE Handbook of Fundamentals [46] gives the values of the thermal resistance for plane air spaces, based on the guarded hot plate method (ASTM C-177), the heat flow method (ASTM C-518), the guarded hot box method (ASTM C-236) and the calibrated hot box method (ASTM C-976). Thermal resistance of air cavity between 1.9 to 4.0 cm width, for mean temperature of 10°C is between 0.16 and 0.18 m^2 °C/W.

Kusuda [31] used the following relation to calculate the thermal resistance of the air cavity in walls and roof.

$$R_{ac} = \frac{1}{h_{cv} + \frac{1}{\frac{1}{e_1} + \frac{1}{e_2} - 1} h_R} \qquad (3.113)$$

For the case of 2.5 cm air cavity with 10°C temperature difference, the thermal resistance of the air cavity calculated by the above relation is 0.11 m^2°C/W. Achterbosch et al. [68] used in their building thermal model a constant value R_{ac} = 0.17 m^2°C/W.

When the airspace is ventilated, it is necessary to define an "effective" cavity resistance. The air movement within the air cavity is influenced by the wind intensity as shown in Figure 3.14 [67]. The thermal effect of ventilating a 75 mm airspace in a cavity roof structure has been calculated assuming a ventilation rate of 50 air changes per hour. The ventilation causes the resistance to fall from the value of 0.176 m^2°C/W (sealed air cavity) to an "effective" value of 0.144 m^2°C/W. Pratt [67] indicated that the ventilation of the cavity increases the U-value of the cavity roof deck by about 40 percent, and by 60 percent if the airspace has low emissivity.

The models presented above give the thermal resistance of 2.5 cm sealed air cavity values between 0.14 and 0.18 m^2°C/W, except the results of Griffiths and Davis. Hence, a default value of 0.17 m^2°C/W was selected to be used in CBS-MASS program. However, the user can modify and use his own estimation taking into account the ventilation of air cavity or emissivity.

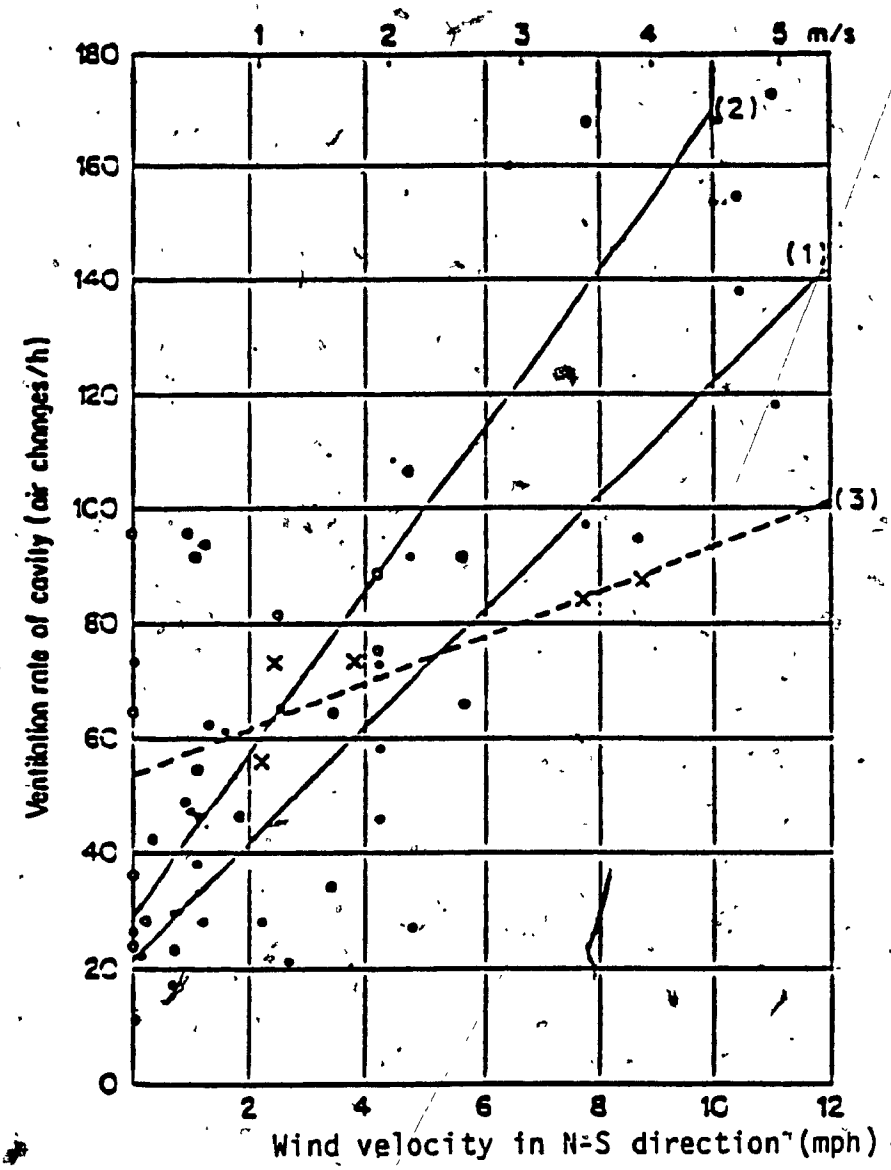

Fig. 3.14 Ventilation rate of cavity. • (1) Metal roof: 86 mm cavity. o (2) Metal roof-lap joints open: 86 mm cavity. x (3) Asbestos cement roof: 140 mm cavity [67]

3.3.h Solar Radiation on Exterior Surfaces.

The user has two options:

- to calculate the solar radiation on exterior surface, or
- to use the available data from other solar models or from experiments.

The program computes the hourly variation of the solar altitude β above the horizontal and solar azimuth ϕ measured from South [46], in order to define the sun's position on sky (Fig. 3.15):

$$\sin \beta = \cos L \cos \delta_1 \cos H_a + \sin L \sin \delta_1 \tag{3.114}$$

$$\cos \phi = \frac{(\sin \beta \sin L - \sin \delta_1)}{\cos \beta \cos L} \tag{3.115}$$

where

L - Local latitude

δ_1 - Solar declination

H_a - Hour Angle (degree)

$$H_a = 0.25 \text{ AST} \tag{3.116}$$

AST = Number of minutes from local solar noon

$$\text{AST} = \text{LST} + \text{ET} + 4 (\text{LSM} - \text{LON}) \tag{3.117}$$

LST - Local Standard Time (min)

ET - Equation of Time (min)

LSM - Local Standard Time Meridian (degree of arc)

LON - Local longitude (degrees of arc)

The angle of incidence θ, between the incoming solar rays and the normal to surface is given by:

$$\cos \theta = \cos \beta \cos \gamma \sin \Sigma + \sin \beta \cos \Sigma \tag{3.118}$$

where Σ is the tilt angle of the surface from the horizontal.

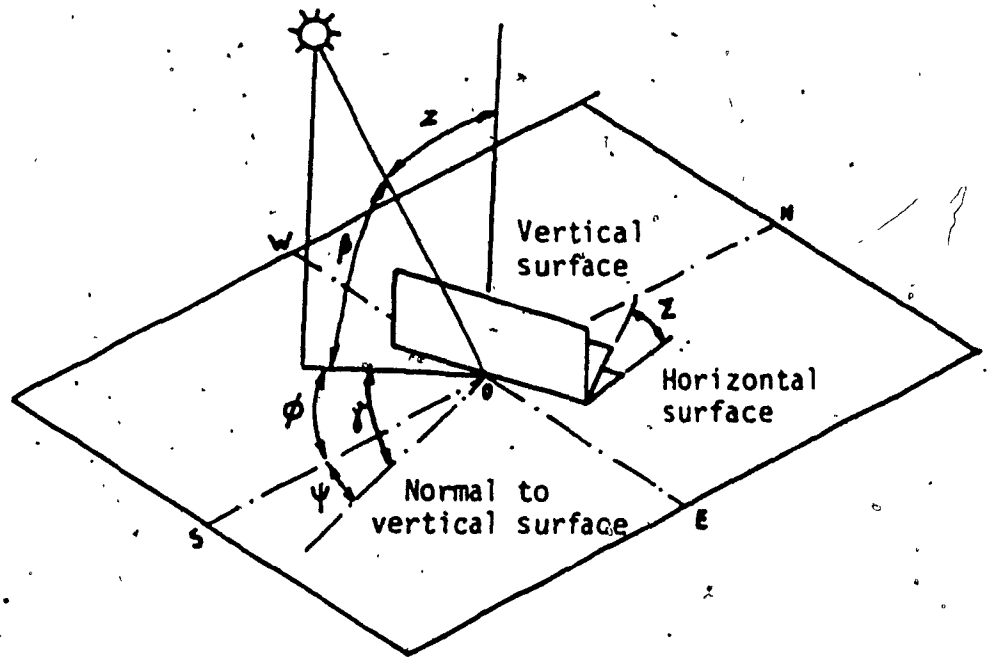

Fig. 3.15 Solar angles for vertical and horizontal surfaces [46].

To calculate the solar radiation on exterior surfaces the following hourly climatic data are required:

- direct normal radiation on clear day IDN [46].
- total cloud amount CLDM [53].
- total radiation on horizontal surface RFl [53].

The direct normal radiation for cloudy conditions is [41]:

$$IDNC = \left(1 - \frac{CLDM}{10}\right) IDN \qquad (3.119)$$

The diffuse radiation for cloudy conditions is [41].

$$Id = (RFl - IDNC \sin\beta)\, FSS \qquad (3.120)$$

where FSS is the surface to sky view factor, i.e., the fraction of shortwave radiation emitted by the sky that reaches the surface. The user can use the standard relation [46]:

$$FSS = \frac{1 + \cos\gamma}{2} \qquad (3.121)$$

which is valid only for isolated buildings or can provide an appropriate value, for the cases where obstacles are close to the building under analysis.

The ground-reflected radiation is:

$$IRG = \rho_g\, FSG\, RFl \qquad (3.122)$$

The surface-to-ground view factor FSG can be calculated with the following relation [46]:

$$FSG = \frac{1 - \cos\gamma}{2} \qquad (3.123)$$

or can be supplied by the user.

The solar radiation reflected by other surfaces and incident on the analyzed building is:

$$IRBLD = IDNC\ \rho_B\ FSB \qquad (3.124)$$

where the surface-to-building view factor FSB has to be supplied by the user.

For sunlit surfaces ($\theta < 90$) the total incident solar radiation is:

$$IT = IDNC \cos\theta\ SR + Id + IRG \qquad (3.125)$$

For shaded surfaces ($\theta > 90$) the total incident solar radiation is:

$$IT = IRBLD + Id \qquad (3.126)$$

3.3.i Solar Radiation on Interior Surfaces.

Usually, the energy analysis programs use the assumption of diffuse glazing, that is, the solar radiation penetrating through windows is uniformly distributed over the interior surfaces. BLAST-3.0 and TARP programs use an additional option, where the solar radiation falls only on floors.

In the CBS-MASS program two options are available:

- Option A, where the solar radiation transmitted through glazing ITP is uniformly distributed on the interior surfaces:

$$IP = \frac{ITP}{\sum S_i - SG} \qquad (3.127)$$

- Option B, where the user provides the hourly distribution of the solar radiation of each interior surface, as a percentage of the

radiation transmitted through the glazing.

The solar radiation penetrating through glazing is absorbed by the interior surfaces proportional with the absorptivity coefficients, and then a succession of reflections and absorptions of the remaining radiation occur.

In the CBS-MASS program, it was considered that after the first absorption by the surface, the reflected radiation is uniformly distributed over the other interior surfaces. This distributed radiation, which is completely absorbed by the receiving interior surfaces, is given by:

$$IREF = IP\ (1 - \alpha_j)\ \frac{S_j}{\sum S_i - S_j} \qquad (3.128)$$

where α_j is the absorptivity coefficient of surface j.

Hence, the solar radiation impinging on the interior surface k is obtained as a summation of the solar radiation before the first absorption IP and the distributed solar radiation IREF.

Figure 3.16 presents the variation of the room air temperature in terms of the distribution of solar radiation on internal surfaces, as estimated by CBS-MASS program. For this particular case (6 x 6 x 3.6m room, 50% glazing on South wall, occupancy between 9:00 a.m. and 5:00 p.m.), the maximum difference is about 2°C, but the effect on the thermal comfort index is important.

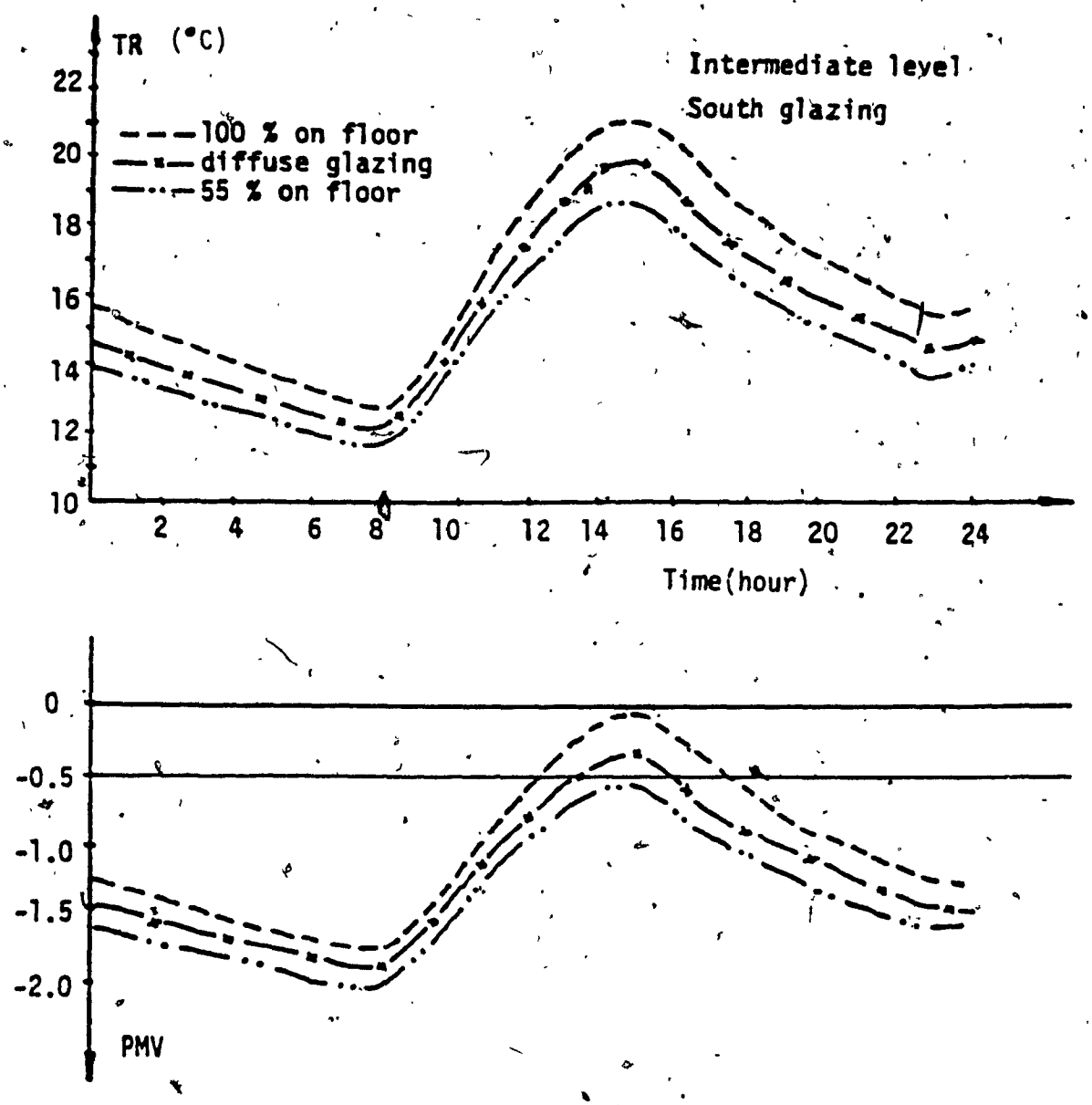

Fig. 3.16 Variation of the room air temperature TR and the thermal comfort index PMV in terms of the distribution of solar radiation on interior surfaces.

When the diffuse glazing is assumed, the comfort conditions are not obtained in the room. When the solar radiation is concentrated only on the floor, the thermal comfort is expected to be obtained between 12:00 and 6:00 p.m.

Gadgil et al. [62] analyzed the effect of solar radiation distribution on the floor, using a detailed computer program which simulates the convective processes within rooms. The results indicate that the convective heat transfer from the floor to the air is double for the case where the solar radiation is concentrated over one-fourth of the floor, than for the case of uniform distribution.

3.4 HEAT TRANSFER THROUGH WINDOWS.

The heat is transfered through windows as a result of two factors:

- solar radiation
- temperature difference between outdoor and indoor

3.4.a Solar Radiation Through Glazing.

The solar radiation penetrating through a sunlit glazing is expressed by the following relation:

$$ITP = (IDNC \cos\theta \tau SR + Id\ 0.75)\ SC\ SG \qquad (3.129)$$

For the case of shaded glazing:

$$ITP = 0.75\ (Id + IRBLD)\ SC\ SG \qquad (3.130)$$

The user has, also, the option to use the hourly variation of the solar radiation IT on the exterior surfaces, calculated by other solar models or obtained from experiments. In this case, the solar radiation penetrating through glazing is:

$$ITP = 0.75\ IT\ SC\ SG \tag{3.131}$$

The CBS-MASS program contains default values of the glass transmissivity in terms of the incidence angle θ, for single and double glazing (Fig. 3.17) [69]. If the user wishes to use another type of window, he has to provide the required information about the glass transmissivity.

3.4.b Heat Gain/Loss Due to the Temperature Difference.

The following heat balance equation is used for glazing:

$$U^* (TDB - TG) + IT\ \alpha = (TG - TR)\ h_{cvg} + (TG - TMRT)\ h_{Rg} \tag{3.132}$$

Since the absorptivity coefficient α of the conventional glazing has a value of about 0.05 [46], the increase of the glass temperature due to the solar radiation is neglected. The following relation is obtained:

$$TG\ (U^* + h_{cvg} + h_{Rg}) - h_{cvg}\ TR = U^*\ TDB + h_{Rg}\ TMRT \tag{3.133}$$

where

$$U^* = \frac{1}{\frac{1}{U_g\ RWN} - 0.125} \tag{3.134}$$

RWN is the ratio between the U value of glazing at night and by day, and 0.125 is the inside film coefficient. U_g is the overall heat transfer coefficient between inside and outside.

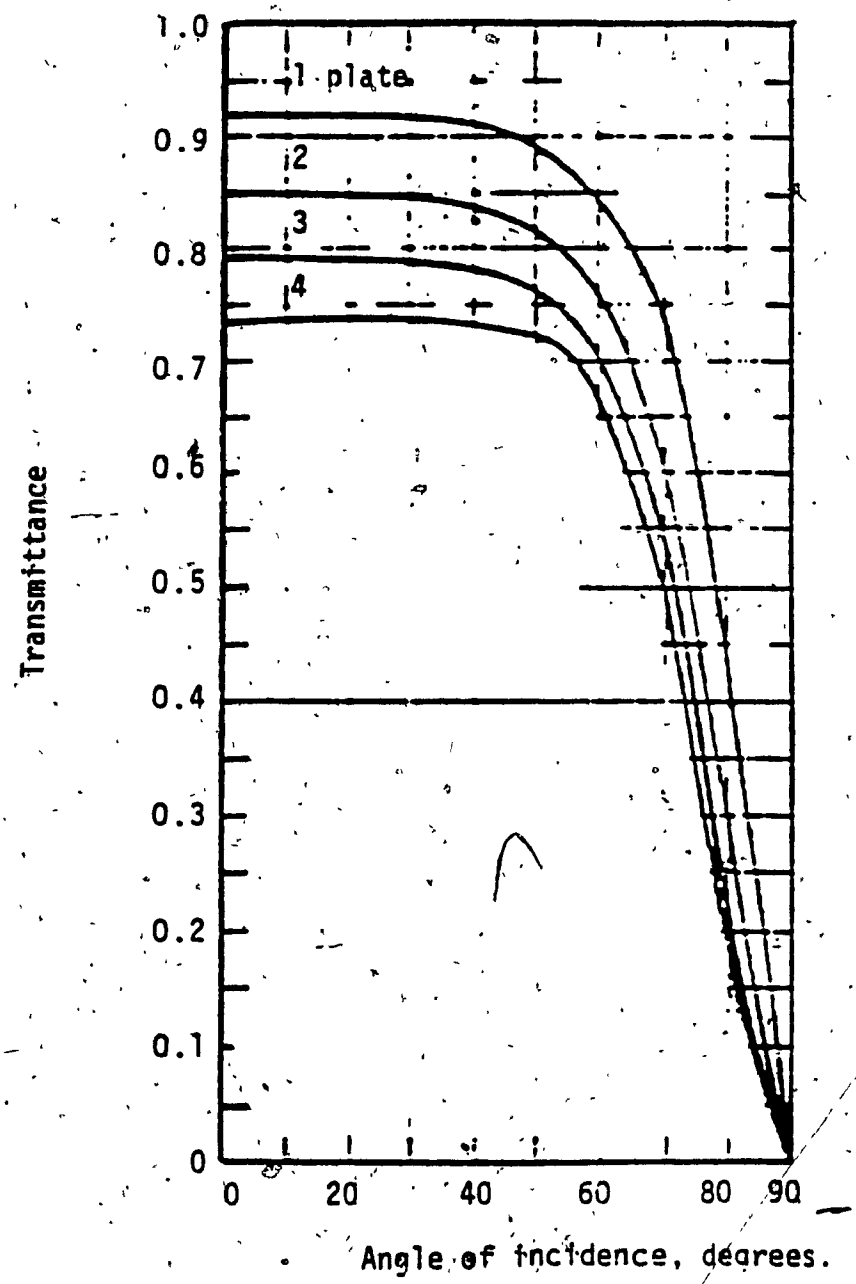

Fig. 3.17 Transmittance of a system of glass plates[69]

3.4.c Shading Calculations.

The existing energy analysis programs incorporate the shading calculations, which increase the computing time.

In the CBS-MASS program another approach is used, where the user has to provide the hourly variation of the sunlit area on each window or wall. To help him to do that, a microcomputer program called SOL [70, 71] was developed on IBM-PC/AT during this research for calculating these data.

Manual or graphic procedures already exist [46, 72], but their use is reduced due to the great amount of required computation to calculate the shading over several hours and seasons. A code for a programmable calculator HP-41C was developed [73], using an exact method but it is relatively slow and it has small storage space which limits the cases for which it can be effectively used.

The detailed computer programs use two types of algorithms for calculating the shaded and sunlit areas of glazing produced by external shading devices. The DOE and ESP programs use the so called Direct Element Analysis, which divides the glazing surface into a matrix of small elements. If the center of each element lies within the shade, defined by the vertices of the shadows cast, then the whole element is considered shaded. This procedure can be used for any type of external shading surfaces, but for an acceptable level of accuracy, the computation time is high and a large core memory is required. The accuracy of

procedure depends on the number of elements into which the glazing surface is divided. The NBSLD, BLAST and TARP programs calculate the shaded area as a sum of plane polygons, using the vertices of the shadows cast.

A mathematical model was developed [70, 71] (Appendix 1) during the present study, for most commonly used exterior shading devices such as: single or multiple overhangs, two or multiple side fins, and overhang-side fins combination (Fig. 3.18). They are assumed to be centered over the symmetry axis of the window and having negligeable thickness. The window is rectangular and the shading devices are parallel to the window edges.

The shape of the shaded area on the window can take one of the three shapes shown in Figure 3.19, depending on the location of point A. Consequently, the coordinates of point A are first defined in respect to origin O on the overhang edge (Fig. 3.20).

$$AB = d \left(\frac{\tan\beta 1}{\cos\gamma} \cos\alpha 1 + \sin\alpha 1\right) \qquad (3.135)$$

$$BO = d \tan\gamma \qquad (3.136)$$

where

$\beta 1$ = solar altitude angle minus inclination of the window

$\alpha 1$ = inclination of overhang

γ = absolute difference between the solar azimuth angle ϕ and the wall azimuth angle ψ

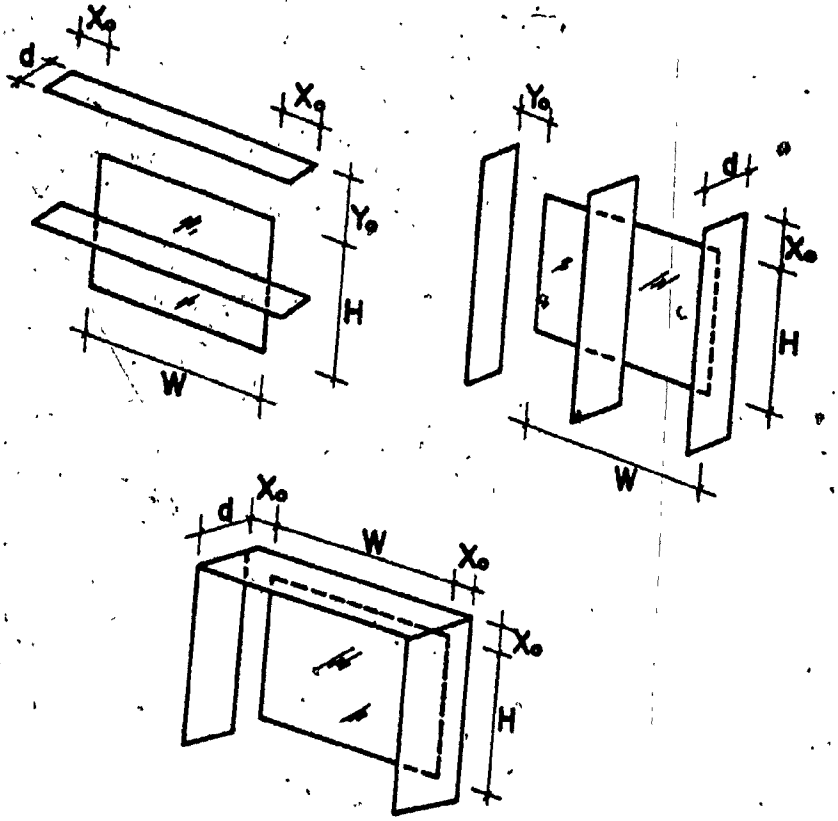

Fig. 3.18 Exterior shading devices.

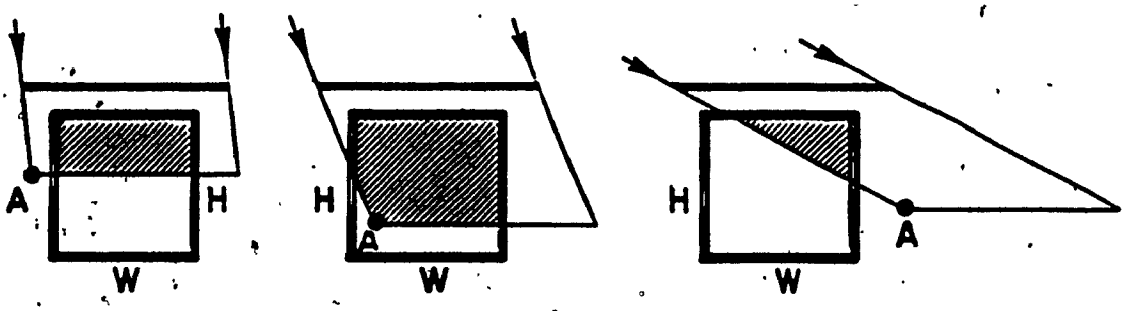

Fig. 3.19 Shape of shaded area created by exterior shading devices.

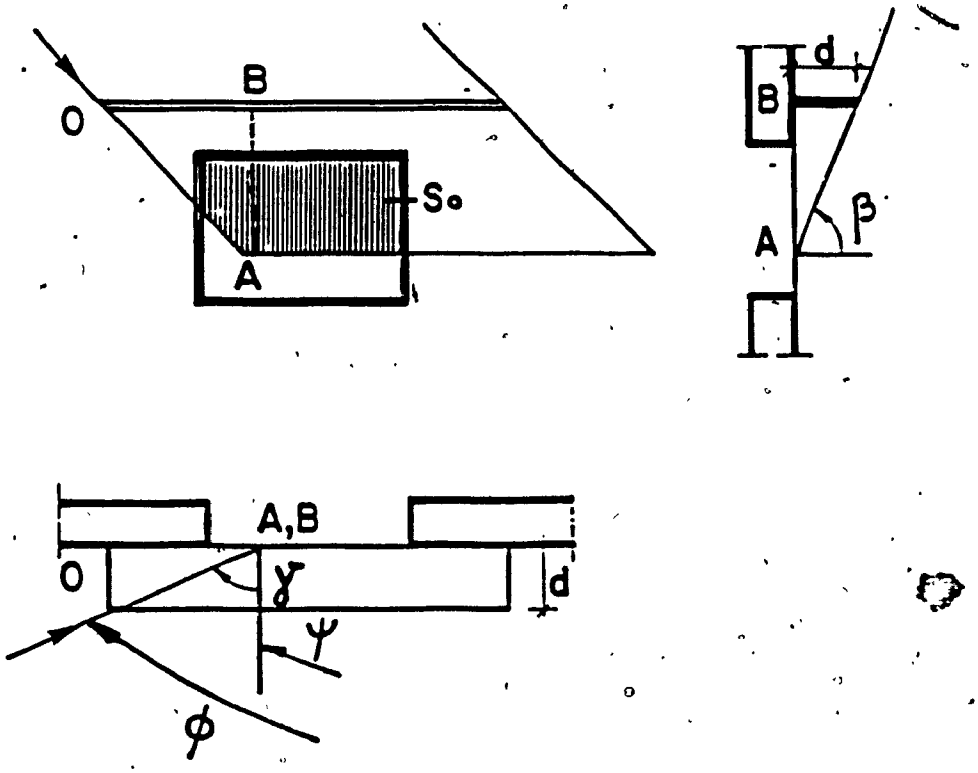

Fig. 3.20 Coordinates of point A which define the shape of shade

Secondly, the shaded area So is computed, using specific relations developed for all possible locations of point A. Since the overhang and the side fins produce shades of similar forms, common relations are used for both cases. For example, the following relation is used to compute the window shaded area for cases presented in Figure 3.21.

$$So = (R + X_0 - \frac{T}{2}) V - X_0^2 \frac{P}{2} \qquad (3.137)$$

The correspondence between variables is given in Table 3.1. Finally, the sunlit ratio is computed:

$$SR = 1 - \frac{So}{HW} \qquad (3.138)$$

The graphical presentation on colour screen of the window configuration is used instead of the question-answer approach, to facilitate the input data task (Fig. 3.22 - 3.24).

An example of the results displayed on screen is presented in Figure 3.25, when overhang and side fins are used for South facing, vertical window.

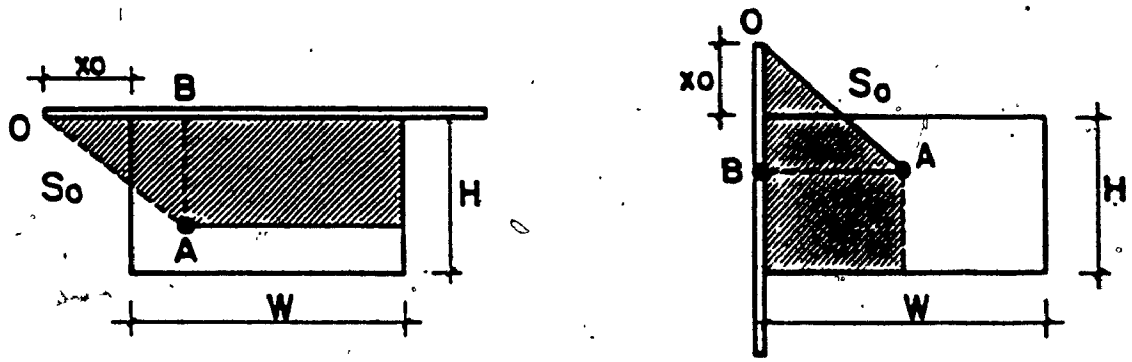

Fig. 3.21 Similar shape of shaded area created by overhang and side-fins.

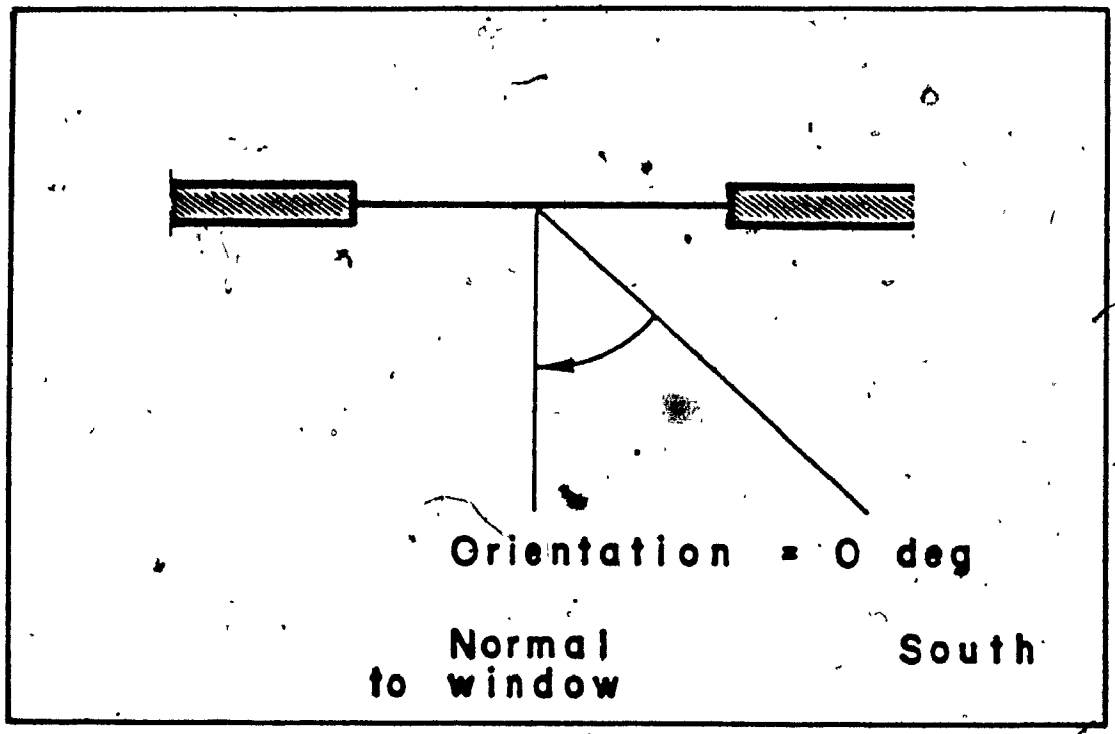

Fig. 3.22 Example of input data for SOL program. Orientation of window.

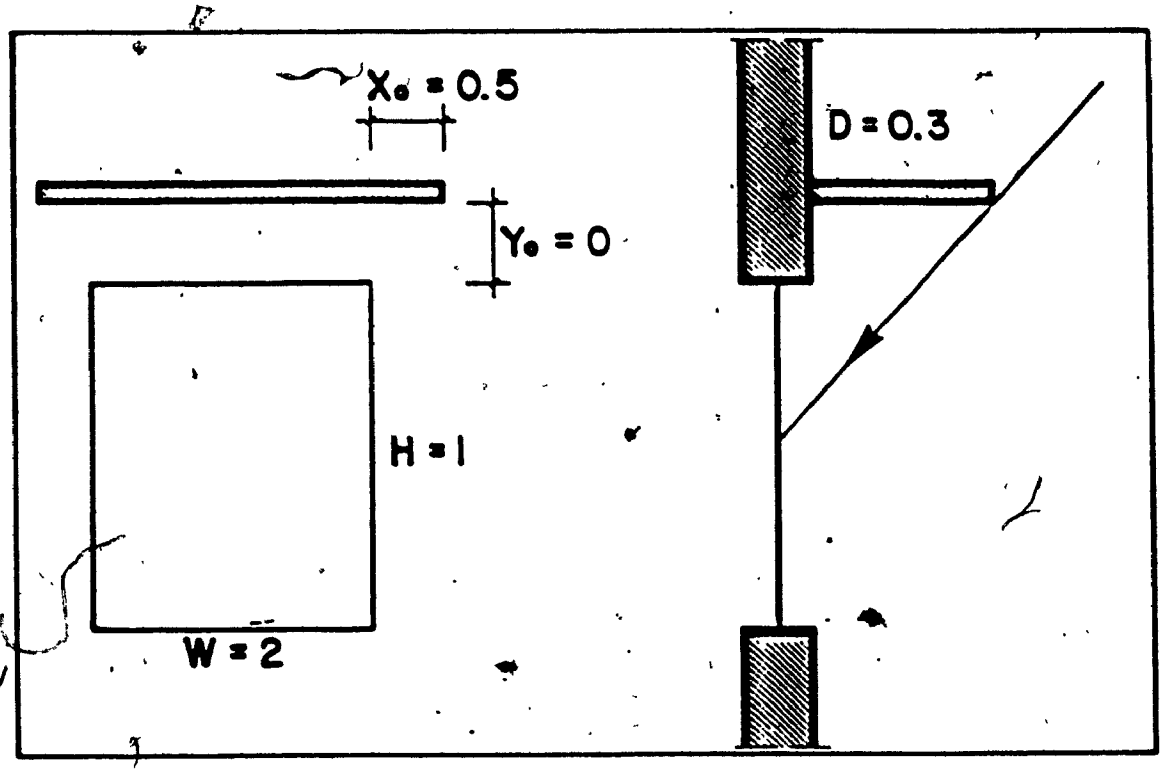

Fig. 3.23 Example of input data for SOL program. Window and overhang sizes.

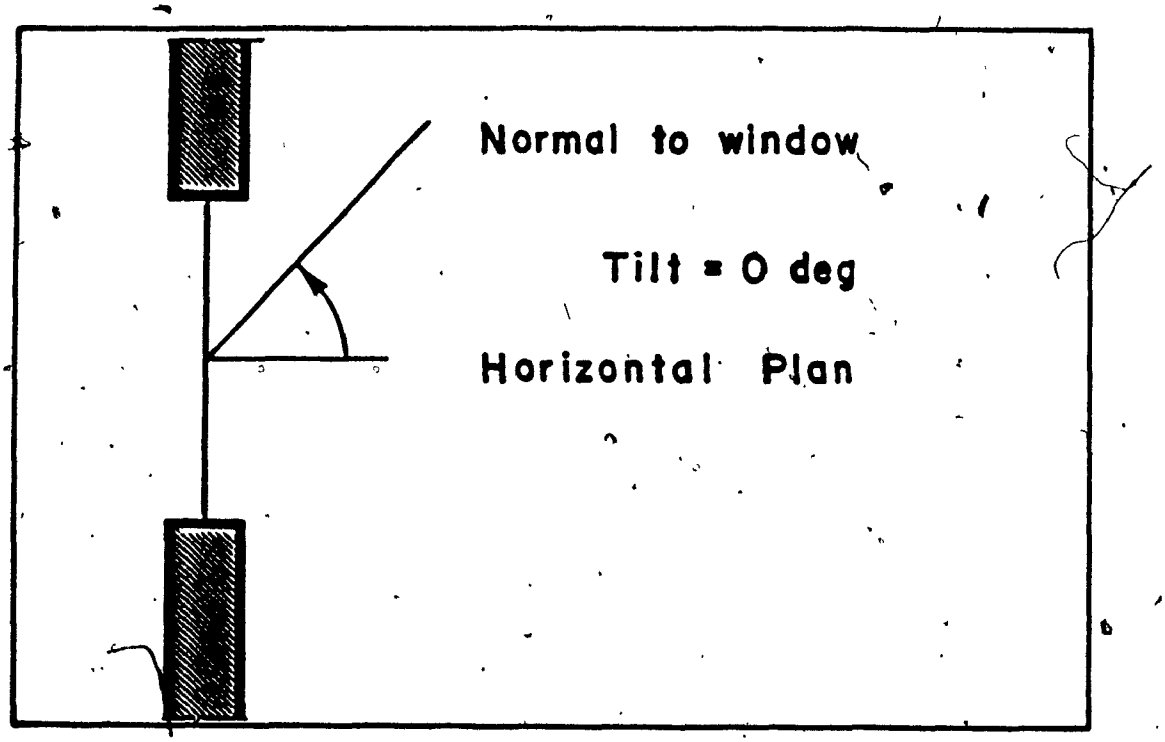

Fig. 3.24 Example of input data for SOL program. Inclination of window.

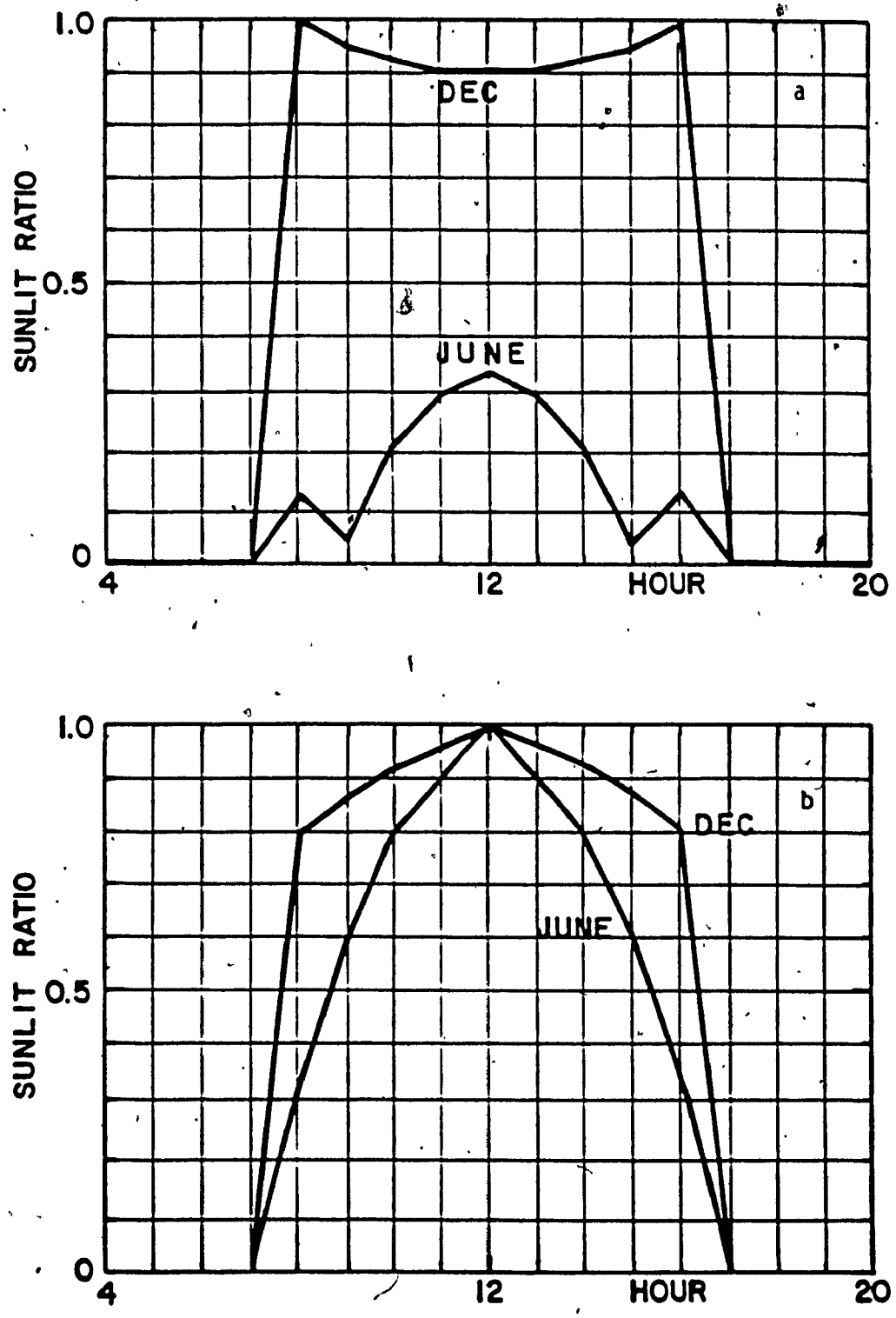

Fig. 3.25 Example of graphical output from SOL program. Sunlit ratio for overhang (a) and for side-fins (b).

TABLE 3.1

Correspondance between variables used in common relation for overhang or side fin

VARIABLE	CORRESPONDING DIMENSION FOR	
	OVERHANG	SIDE FIN
R	W	H
T	BO	AB
V	AB	BO
P	$\tan\beta 1/\sin\gamma \cos\alpha 1 + \sin\alpha 1$	$1/(\tan\beta 1/\sin\gamma \cos\alpha 1 + \sin\alpha 1)$

3.5 AIR INFILTRATION

The air infiltration accounts for about 30 percent of the building energy consumption and consequently a good simulation of this phenomenon is required. However, the air movement through the building envelope is the most difficult to be accurately modeled, for the following reasons:

i) The sizes of the gaps in the building envelope are subjected to large variations and uncertainties. Hence, they are not available to the user. Usually, equivalent values obtained by measurements in similar building types are used in computations.

ii) The air movement in building is influenced by the pressurization created by the HVAC system, the resistance to air flow between spaces, the type of activity and the sources of convective heat.

iii) The wind speed as measured at the local weather station, usually near an airport, is modified by the built environment. Hence, the real pressure on the exterior walls is unknown.

Thus, the air infiltration is usually simulated in building energy analysis programs by simple and approximate models. Even for these models, the input data are not always available, and other approximations are used.

BLAST program requires that the infiltration peak value IMAX (m^3/s) and a schedule be defined by the user. An additional option use a set of coefficients to estimate the actual infiltration from the peak value, taking into account the outdoor temperature and the windspeed. Practically, the program uses only the infiltration value provided by the user and does not simulate this process. There are no explanations about the wind speed and the way to define the necessary coefficients. DOE program uses three models of air infiltration: air change, crack method and residential.

The implementation of new modules into the building energy analysis programs, for simulating the air movement around the building, as effected by the built environment, and the air flow through building envelope will create a huge program, difficult to be used in the current practice.

Hence, the air change method is incorporated in CBS-MASS program. The user can provide the required information based on:

- published average values for similar buildings,
- experimental results,
- simulation results using sophisticated programs for modeling the air flow between environment and building.

3.6 INTERNAL HEAT GAINS

The CBS-MASS program takes into consideration the schedules for occupancy and lighting, the user providing the hourly variation of the total heat gains.

The heat from people is considered as convective heat gain and is used in the heat balance equation of the room.

The heat from lighting Q_L is split into convective (50%) and radiative (50%) portions. The former acts in the heat balance of room, while the later is uniformly distributed over the interior surfaces

$$Q = \frac{0.5}{\sum S_i - S_{ceiling}} \cdot Q_L = a\, Q_L \qquad (3.139)$$

and is used to define the boundary conditions of interior surfaces.

3.7 THERMAL COMFORT

Ideally, a building should satisfy all the functional requirements of the user at a minimum total cost (investment and operation).

Consequently, the correlation between the building structure, the indoor comfort, the weather conditions, the activity and the building services must be taken into consideration in the early stage of the design.

A comfortable interior environment is one in which there is freedom from annoyance and distraction, so that working or pleasure tasks can be carried out unhindered physically or mentally. Not only the thermal or air quality parameters play an important role, but also the psycho-sociological factors such as attitudes of people around us, organization of space or colours. Since the comfort sensation is obtained as a result of the correlation between these factors, a deficiency in one of them can spoil the balance of the environment.

The interior environment has a strong influence on the arousal level of people, and then it can increase or decrease their productivity (Fig. 3.26) [74]. For example, poorly ventilated areas which are stuffy can induce lassitude, while the use of air conditioning systems may increase the productivity between 2 to 54 percent. The noisy climates can make people feel tense and anxious. The heat, light and sound can distract people. The optimum arousal level could be different for different tasks.

Although human beings are very adaptable, adaptation in itself may be more of philosophical acceptance of conditions rather than a purely physiological acceptance to them. Some researches have shown that only certain types of people express their complaints.

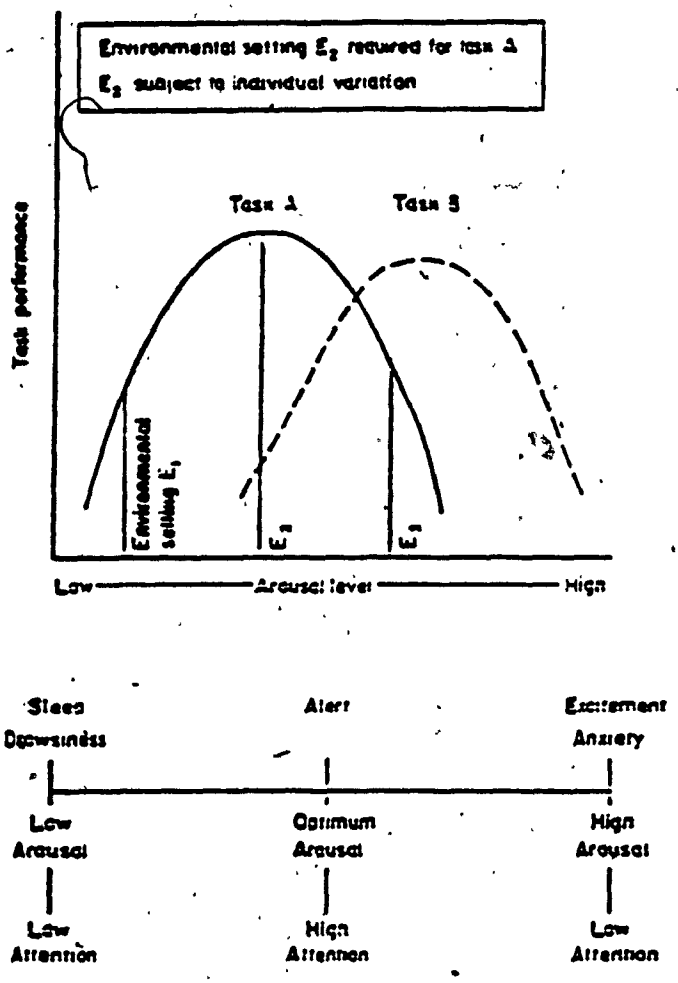

Fig. 3.26 Arousal level concept[74].

Each person has his own range of comfort in different situations. The task of the building designer is to create environments which are acceptable to most people living inside the building, and this is difficult when large groups of different people are involved.

A dynamic comfort, where changes are accepted within certain limits to assure the brain that the body is working properly, is a better solution than a static comfort, with neutral and constant conditions.

3.7.a Thermal Comfort Factors

The following factors can be controlled by the building design and by the design and operation of the mechanical systems.

i) Room air temperature. A room should be as cool as is compatible with comfort. Some works established that a 2.5°C fall in temperature during summer, or 1.8°C in winter with respect to the design conditions, increased the freshness sensation [74]. An investigation in a school has shown that the children performances were significantly deteriorated at an air temperature of 27°C, as opposed to 20°C. Investigations in Swiss offices served by ceiling heating and by radiators have shown that people found the air temperature in the range 20 to 22°C pleasant. An investigation on thermal comfort in office buildings in France has shown that most people prefered the "neutral-warm" zone.

The actual design values of comfort parameters may be quite different depending on the climate of the country, as it is presented in Figure 3.27, where the comfort vote against the mean globe temperature is represented for different countries. Many subjects voted in the band "neutral-comfortable warm" rather than "neutral-comfortable cool".

ii) Mean radiant temperature of surrounding surfaces.

The average temperature of the surrounding surfaces should preferably be higher than the air temperature in winter. Some works suggested that the environments where the wall temperature is about 1-2°C above the air temperature are more pleasant than the converse case or when the temperatures are equal [74].

iii) Temperature distribution in space.

Various parts of the body respond to the surrounding air temperature differently (e.g., the forehead surface temperature varies little with air temperature, whereas the foot is very sensative to temperature changes- Fig. 3.28).

The air at head level should not be distinctly warmer than that near the floor. This gradient should not exceed 2-3°C. The heads of occupants should not be exposed to excessive radiant heat. Irradiation of the skin by long-wave infra-red, which requires a relatively low intensity to rise the warmth sensation level, can cause difficulty in breathing and a sense of stuffiness. This helps to explain why some people find the heat from

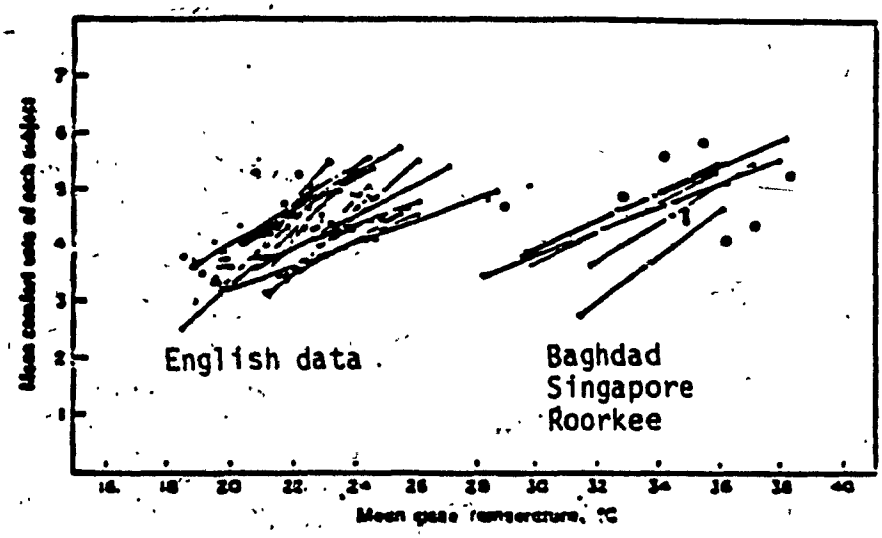

Fig. 3.27 Comfort vote against mean globe temperature for different countries[74].

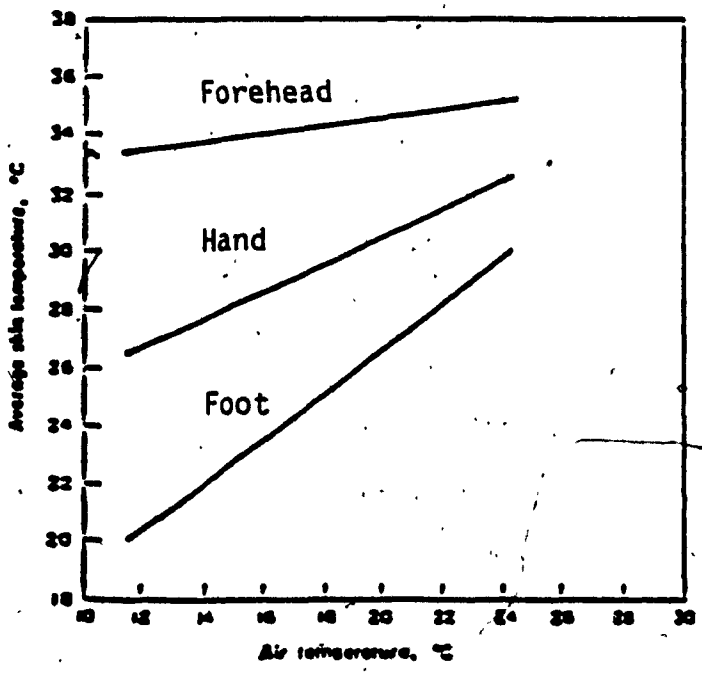

Fig. 3.28 Sensitivity of human body to changes in air temperature [74].

electric equipment oppressive, while that from coal fires is acceptable.

iv) Temperature swing.

Researches have indicated [74] that the subjective tolerance of temperature swings can be much greater than has been supposed. The largest swings are tolerated when the rate of temperature change is high. In addition, wider changes in air temperature were observed to be tolerated when subjects were performing mental work than when resting.

v) Relative humidity

A relative humidity between 30-70% is recommended for comfort, but usually in winter lower values are recommended to reduce the energy consumption of the HVAC systems.

vi) Air velocity

Too much air movements causes draughts, and too little contributes to producing a stuffy atmosphere. The back of the neck and the ankles are very draught sensitive, while air currents across the forehead are welcome. A range of air velocities recommended for thermal comfort is shown in Figure 3.29 for people wearing average indoor clothing, sitting with air movement incident on the front of the body.

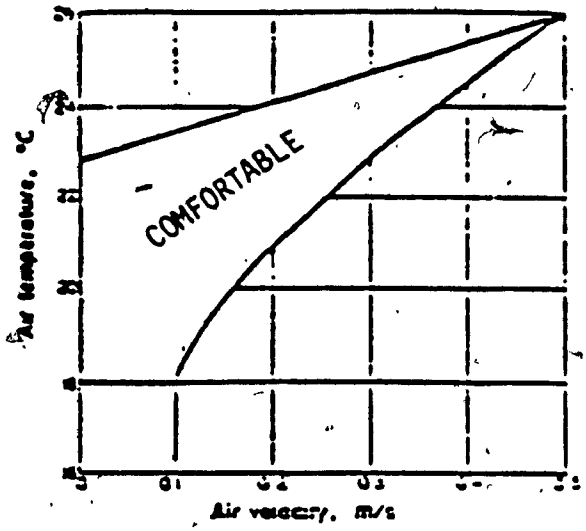

Fig. 3.29 Recommended air velocity for comfort vs. air temperature[74]

3.7.b Comfort Estimation

The physical and psychological effects cannot be dissociated when the human comfort in buildings is analyzed. However, there are no procedures for estimating the general comfort and most developments have concerned only the estimation of the thermal comfort.

Sometimes the theoretical scales, involving mixtures of several factors such as dry-bulb and wet-bulb temperature, air velocity or mean radiant temperature, are unrealistic because they permit many combinations, some of which would be uncomfortable, to produce a thermal comfort value.

More adequate are those methods which are based on analytical developments related to experiments on people in the environmental chambers. Fanger [75] has established the Predicted Mean Vote Index as a function of activity level, clothing type, air and mean radiant temperature, air velocity and vapour pressure.

The internal temperature of the human body, about 37°C, can be kept constant only if there is a balance between the heat produced by the body and the heat lost to the environment.

$$M \pm W_1 - E - RES = \pm K = \pm R \pm C \qquad (3.140)$$

where

E = heat exchange by evaporation

M = metabolism (Table 3.2)

W_1 = external work

RES = heat exchange by respiration

R = heat exchange by radiation

C = heat exchange by convection

K = heat conduction through clothing

Based on heat balance of the human body, Fanger has obtained the Predicted Mean Vote Index (PMV):

TABLE 3.2

Example of metabolic rate M for various practical activities

ACTIVITY	met	W/m^2
Lying down	0.8	47
Seated, quietly	1.0	58
Sedentary activity (office, home, laboratory, school)	1.2	70
Standing, relaxed	1.2	70
Light activity, standing (shopping, laboratory, light industry)	1.6	93
Medium activity, standing (shop assistant, domestic work, machine work	2.0	117
High activity (heavy machine work, garage work)	3.0	175

$$PMV = (0.303e^{-0.036M} + 0.028)\,[(M-W_1)$$

$$- 3.05\,10^{-3}\,\{5733 - 6.99(M-W_1) - pa\} - 0.42\,\{(M-W_1) - 58.15\}$$

$$- 1.7\,10^{-5}\,M(5867 - pa) - 0.0014\,M(34 - TR)$$

$$- 3.96\,10^{-8}\,f_{cl}\,\{(T_{cl} + 273)^4 - (TMRT + 273)^4\} - f_{cl}\,h_c(T_{cl} - TR)] \qquad (3.141)$$

where

$$T_{cl} = 35.7 - 0.028\,(M-W_1) - 0.155\,I_{cl}\,[3.96\,10^{-8}\,f_{cl}\,\{(T_{cl} + 273)^4$$

$$- (TMRT + 273)^4\} + f_{cl}h_{cl}(T_{cl} - TR)] \qquad (3.142)$$

$$h_{cl} = \begin{cases} 2.38(T_{cl}-TR)^{0.25} & \text{for } 2.38\,(T_{cl}-TR)^{0.25} > 12.1\sqrt{v} \\ 12.1\sqrt{v} & \text{for } 2.38\,(T_{cl}-TR)^{0.25} < 12.1\sqrt{v} \end{cases} \qquad (3.143)$$

$$f_{cl} = \begin{cases} 1.00 + 0.2\,I_{cl} & \text{for } I_{cl} < 0.5 \text{ clo} \\ 1.05 + 0.1\,I_{cl} & \text{for } I_{cl} \geq 0.5 \text{ clo} \end{cases} \qquad (3.144)$$

where

PMV = Predicted Mean Vote

I_{cl} = thermal resistance of clothing (1 clo = 0.155 m^2°C/W)

f_{cl} = ratio of the surface area of the clothed body to the surface area of the nude body.

TR = room air temperature (°C)

TMRT = mean radiant temperature (°C)

v = air velocity (m/s)

p_a = water vapour pressure (Pa)

T_{cl} = surface temperature of clothing (°C)

From experiments, using 1300 Danish and North American subjects in a climatic room, Fanger has correlated physical data with subjective thermal sensation votes, and developed a seven-point scale (Table 3.3). Acceptable thermal comfort environment is expected for:

$$-0.5 < PMV < +0.5$$

In order to consider the heating effect of the incident solar radiation I on human body, the metabolism in Equation 3.141 is modified in the CBS-MASS program as follows:

$$M = M + \frac{\alpha I}{58.15} \qquad (3.145)$$

Most computer programs such as BLAST, DOE, ESP or TARP do not provide estimations of the thermal comfort. The CBS-MASS program, uses the Fanger's model to estimate the thermal comfort within a room.

TABLE 3.3

Fanger's seven-point scale of the thermal comfort

PMV	SENSATION
3	hot
2	warm
1	slightly warm
0	neutral
-1	slightly cool
-2	cool
-3	cold

The room air temperature TR and the mean radiant temperature of surrounding surfaces TMRT are hourly calculated by the CBS-MASS program, and then become input data for CONFORT module. The metabolism M and the thermal resistance of clothing I_{cl} (Table 3.4) are supplied by user in terms of activity, season and room air temperature control. It is assumed a good design of the HVAC system, and consequently the air velocity is assessed at 0.15 m/s.

The water vapour pressure, pa is calculated as:

$$pa = ps\ \phi \qquad (3.146)$$

where,

ps = saturated water vapour pressure [46]:

$$\ln ps = -\frac{5800.22}{TR+273} + 1.3915 - 0.04864\ (TR+273) +$$

$$+ 0.47765\ 10^{-4}\ (TR+273)^2 - 0.144521\ 10^{-7}\ (TR+273)^3 +$$

$$+ 6.54597\ \ln\ (TR+273) \qquad (3.147)$$

ϕ = relative humidity of the room air

Since the program calculates the space sensible loads, a default relative humidity of 50 percent in summer and of 30 percent in winter are used.

TABLE 3.4

Examples of values I_{cl} for various practical combinations of clothing

CLOTHES	IcL	
	clo	m^2K/W
Shorts	0.1	0.016
Typical tropical clothing outfit Briefs (underpants), shorts, open-neck shirt with short sleeves, light socks, and sandals	0.3	0.047
Light summer clothing Briefs, long light-weight trousers, open-neck shirt with short sleeves, light socks, and shoes	0.5	0.078
Working clothes Underwear, cotton working shirt with long sleeves, working trousers, woollen socks, and shoes	0.8	0.124
Typical indoor winter clothing combination Underwear, shirt with long sleeves, trousers, sweater with long sleeves, heavy socks, and shoes	1.0	0.155
Heavy traditional European business suit Cotton underwear with long legs and sleeves, shirt, suit comprising trousers, jacket and waistcoat (US vest), woollen socks, and heavy shoes	1.5	0.233

3.8 SOLUTION OF THE SIMULTANEOUS EQUATIONS SYSTEM

When the equations developed for each element of the space (exterior and interior walls, glazing and room air), are connected together a set of simultaneous linear equations is obtained.

$$[A][T] = [B] \qquad (3.148)$$

Figure 3.30 presents the form of the matrix A, for a room with two exterior walls, one floor and one window, for calculations required by STEP 1, i.e., the room air temperature is calculated with no constraints imposed by user. Figure 3.31 presents the form of matrix A, for the same room, for the calculations required by STEP 2, i.e., the rom air temperature is imposed equal to the lower or upper limit and the space loads are calculated. In this case, the inside surface temperature of glazing is separately calculated, and the number of equations is reduced.

In actual version of CBS-MASS program, there is a module containing the Gauss-Seidel iterative method to solve this set of simultaneous equations (block SOLUT).

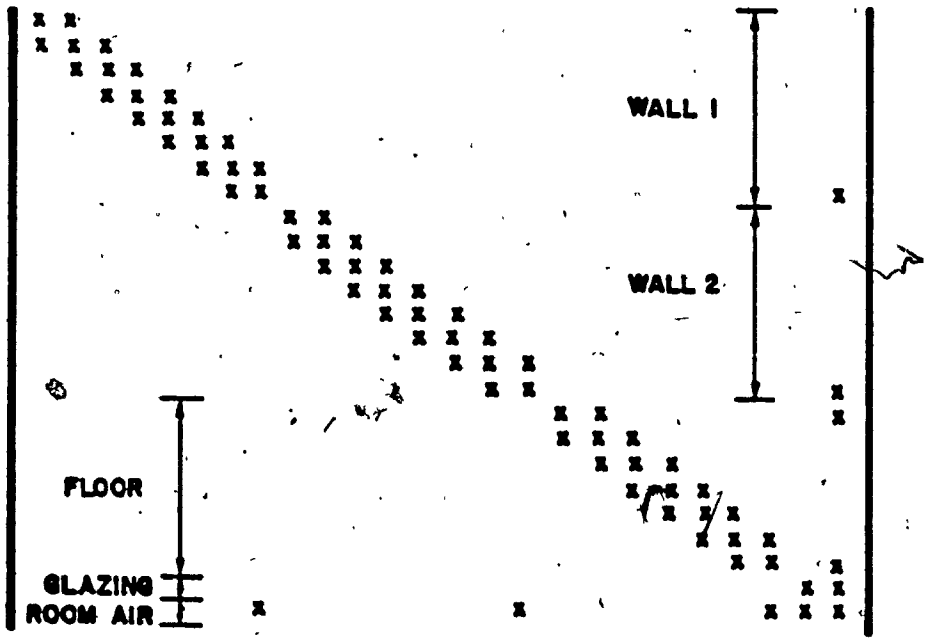

Fig. 3.30 Matrix A of the system of simultaneous equations describing the thermal behavior of the building, for STEP 1.

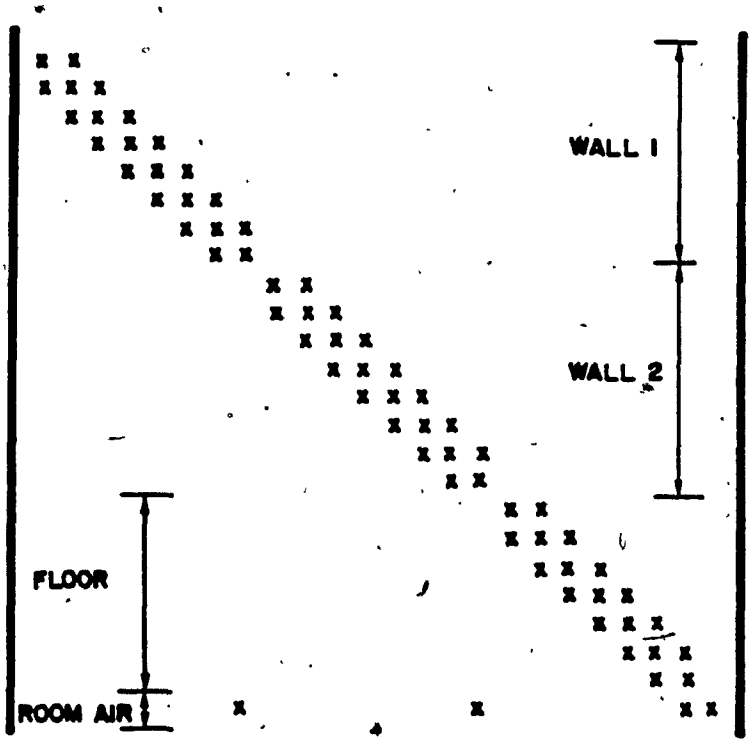

Fig. 3.31 Matrix A of the system of simultaneous equations describing the thermal behavior of the building, for STEP 2.

CHAPTER 4

ANALYTICAL AND FUNCTIONAL VALIDATION OF CBS-MASS PROGRAM

CHAPTER 4

ANALYTICAL AND FUNCTIONAL VALIDATION OF CBS-MASS PROGRAM

4.1 VALIDATION OF EXISTING PROGRAMS

The authors of the building energy analysis programs usually emphasize the capabilities of their programs, but provide little information about their limitations and no information about their accuracy.

Generally, the users assume that each program is validated by its author before it is released. However, this is not the case. Moreover, there is no standardized validation procedure for energy analysis programs and each author has his own understanding of this procedure. Usually, some work is done by researchers, independent of authors, after the programs are released to find out the limitations and the accuracy of results.

The aim of these computer programs was to provide quantitative energy and cost comparisons among design alternatives, and not accurate prediction of utility bills, due to the large number of uncontrolled and unknown factors [46]. However, the most utilized approach to validate the building energy analysis programs is to compare the estimations of the energy consumption, the indoor air temperature or the cooling/heating loads against the measured values. Another method to test the performances of energy analysis programs is to compare the results from several programs with similar capabilities.

Yuill [76] verified the performance of BLAST program in simulating a single-family house located in Edmonton, by comparing the measurements against the program predictions of the space temperature and power consumption. The overall agreement between the measured data and the BLAST predictions of energy consumption and temperature indicates that the program predicts well the energy flows. The comparisons on hourly and daily basis indicate that the heat balance algorithms model correctly the major energy flows. Some differences between predictions and measurements are caused by the infiltration model, especially by its lack of sensitivity to wind direction. Another source of error was the modeling of the basement heat loss.

Bauman et al. [77] compared the estimations of BLAST program with the air temperature measurements of a solar-dominated test cell. The maximum temperature difference is about 1.8°C in September and more than 2.0°C in December. The BLAST temperature predictions were sensitive to the infiltration rate, shifting by up to 4.0°C in response to a 50 percent change. The average temperature difference between the predictions and the measured values rises from 0.4°C to 1.31°C in September, and from 0.8°C to 2.8°C in December. That is caused by the absence of detailed information on construction tightness and microclimatic effects. When the BLAST predictions were compared against the measurements of a thermally massive structure, the quality of agreement was generally good, but with observable discrepancies. The predictions of interior air temperature were higher than the measured values by about 2.0°C.

Yuill and Phillips [78] compared the predictions of the energy consumption provided by BLAST program with the utility bills of two office buildings in Canada. For the first building the differences were 13 percent (electricity), 8 percent (steam) and 15 percent (chilled water), while for the second building the differences were about 10 percent (electricity) and 20 percent (gas). However, the energy consumption for July and August were not considered in the analysis, since the authors believed the bills for these months were suspected high.

Colborne et al. [79] compared the predictions of DOE program with measured energy consumption from single-family dwellings. The differences between annual values for a single-storey house with basement and for a single-storey house on a slab are between 1 and 5 percent. They compared, also, the hourly variation of energy consumption and space temperature, for an unoccupied house with electric heating and the results indicate 12 percent difference between predictions and measurements.

Diamond and Hunn [80] compared the predictions of DOE program with the monthly utility metered data of seven commercial buildings (restaurant, single-floor office building, retail store, hospital, multi-floor office building, school and solar-heated and cooled building). For the set of seven building tested, there is a standard deviation of

7.9 percent and a maximum difference of 12 percent between predicted and measured data for annual total energy use. The range of differences for annual gas/fuel, oil and electric energy use is between 1 and 19 percent. The composite standard deviation for the set of seven buildings, on a monthly basis, is 16.7 percent for total energy use, 26.3 percent for gas/fuel oil use, and 18.7 percent for electric energy use. The range of differences is between 9 and 35 percent in terms of building type.

Arumi-Noe [51] found differences less than 5 percent or about 4°C, when compared the room temperature predictions of the DEROB/PASOLE program with the measurements in seven passive test rooms. He also found, the thermal properties of the test houses were not accurately modeled, which produces a phase difference between the measured and the predicted room air temperature.

Alereza and Hovander [81] compared the estimations of the energy consumption provided by the ADM-2 microcomputer program with the utility bills of three buildings (office, restaurant, retail). The annual difference is between 1.2 and 2 percent and the maximum monthly difference is 26 percent (office) and 42 percent (restaurant).

Kusuda et al. [49] compared the measured sensible cooling loads with the predictions of BLAST, NBSLD and DOE programs for a test house. They found daily differences of 3.1 percent (NBSLD), 20.3 percent (DOE) and 12.3 percent (BLAST).

Fazio and Zmeureanu [82] compared the DOE-2.1B predictions with the utility bills of two buildings in Montreal, and obtained a difference of about 6 percent for building #1 (Fig. 4.1). For the second building the difference was 2.6 percent when the utility bills for 1980-1981 were used and 10.6 percent for 1979-1980 (Fig. 4.2).

Another method to test the performances of energy analysis programs is to compare the results from several programs with similar capabilities.

Carroll [48] compared the annual heating and cooling requirements for a residential model provided by NBSLD, DOE 2.1 (SWF and CWF) and BLAST programs. For a summer design day, the peak loads values are in good agreement for NBSLD and DOE (SWF and CWF), while BLAST is 6 percent less. For intermediate loads, the DOE (CWF) predictions agree better with NBSLD and BLAST results than those of DOE (SWF). The DOE (SWF) daily total is about 25 percent higher than BLAST and NBSLD. The DOE (CWF) results agree better (7 percent higher). For a winter design day the peak heating loads predicted by BLAST, DOE (SWF) and DOE (CWF) agree well, both in value and time of occurrence. The NBSLD peak load is about 12 percent higher. For daily total loads, NBSLD results are 15 percent higher than BLAST predictions, while DOE (SWF) gives estimations 13 percent smaller.

These validations provide usefull information about the level of accuracy and the capabilities of these programs. Also, the conclusions from validation increase the confidence of software's user, and

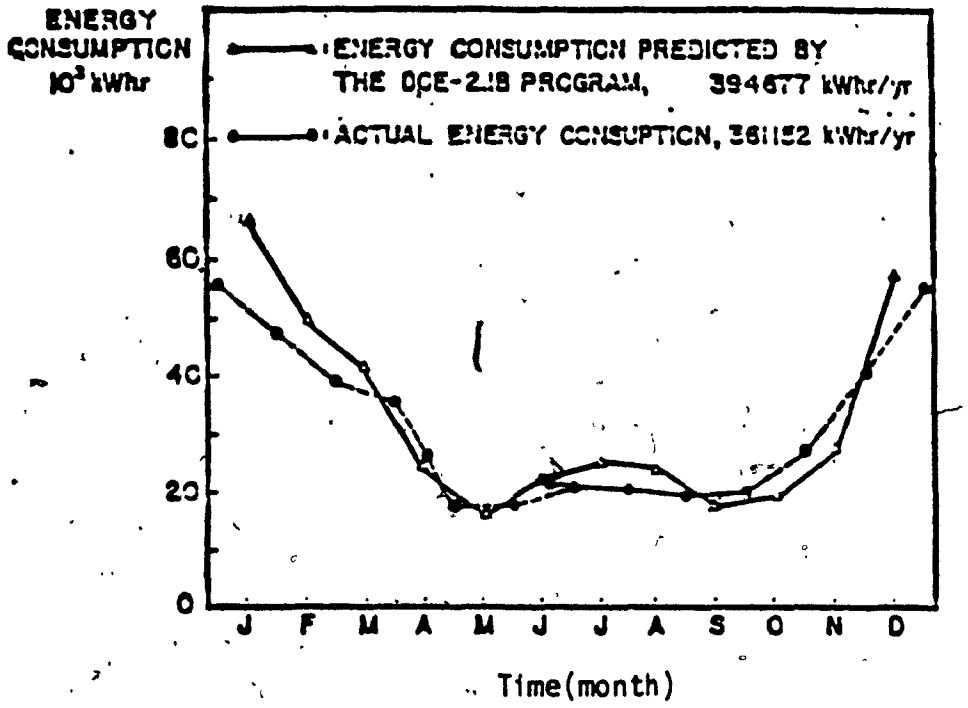

Fig. 4.1 Hardware store Rona - Montreal. Comparison between the measured and predicted energy consumption

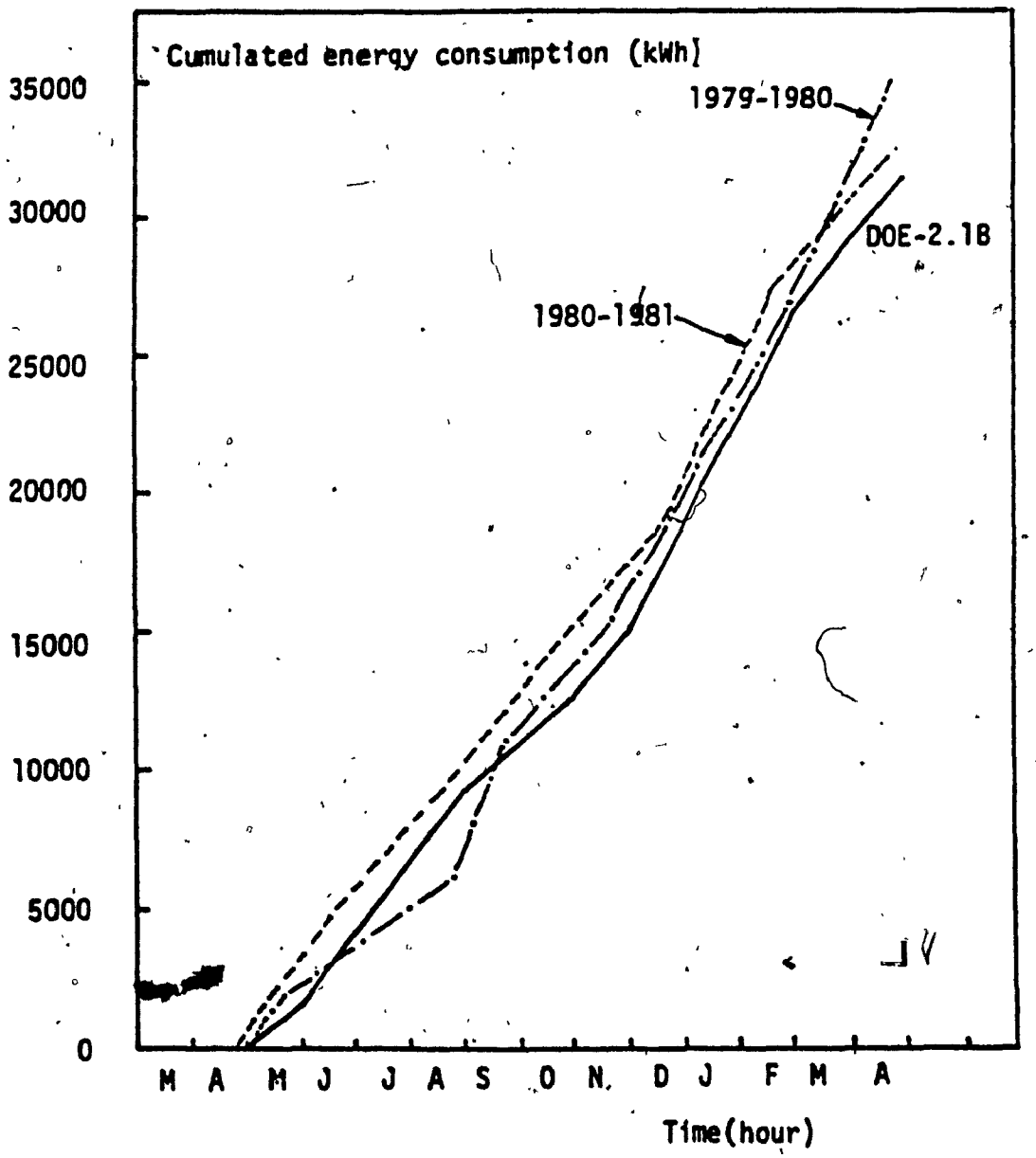

Fig. 4.2 Commercial building-Montreal.
Comparison between the measured and the predicted energy consumption.

consequently increase the application of computer simulation in building energy analysis.

However, these approaches have a number of disadvantages:

i) Large number of different buildings and systems should be evaluated to generalize the results.

ii) Since a complete monitoring is too expensive, the values of some input parameters are not measured, but chosen. Hence, the program provides an approximation for the energy consumption of the building as defined by the user, rather than that of a real building. Colborne and al. [79] mentioned some parameters with high uncertainty to be defined:

- ground temperatures,
- soil conductivity,
- snow cover and moisture content of soil,
- occupant-related effects,
- seasonal efficiency of heating and cooling systems,
- air infiltration.

Fazio and Zmeureanu [54, 82] observed that the uncertainties of specifying input data which were related to people habits (thermostat settings, window and door openings, use of appliances) or to as built thermal performance of buildings have an important effect on the estimation of energy consumption. Since the assignment of such factors involves subjective estimations,

it becomes relatively easy to fit the utility bills by iterative runs, without a high accuracy in simulation of other phenomena such as air infiltration or heat storage in building mass. Wagner [83] found variations 40:1 due to occupant effects, and he concluded that the availability of accurate and sufficiently complete input data, especially on the occupant behavior, limits the ability of the detailed models to accurately predict the energy use. Judkoff [84] found errors of about 60 percent in auxiliary load prediction, due to the difference between standard and as-built thermal properties of walls.

iii) A good agreement between the estimated and measured energy consumption can cover weaknesses at algorithm level, which have not been discovered during the validation. Judkoff et al. [85] compared SUNCAT, DEROB, DOE and BLAST programs and discovered that DEROB, which was already validated [51], is insensitive to the building mass due to errors within the iterative process. Fazio and Zmeureanu [54] found that the SHADOW subroutine of NBSLD program predicts a negative sunlit ratio on window with exterior shading devices involving overhang and side fins with different widths (Fig. 4.3), while it can only take values between 0 and 1.

Comparisons between different computer programs can lead to useful information, provided that similar conditions are used. This implies a detailed understanding of algorithms, and

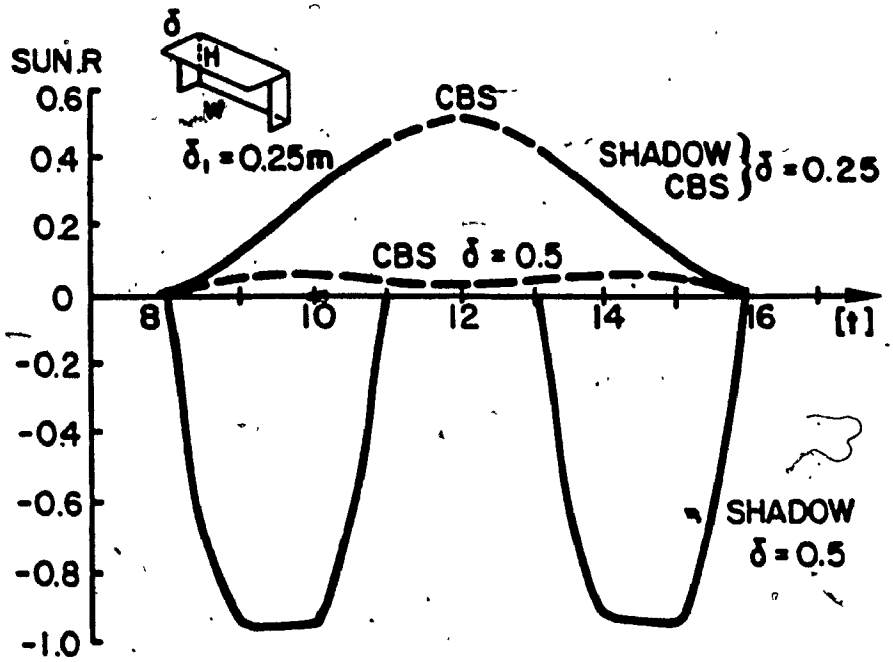

Fig. 4.3 Errors in shading simulation in the NBSLD program.

eventually their modification to become comparable to those utilized by other programs.

Under the auspices of the International Energy Agency, twenty-three computer programs were used for estimating the daily energy consumption of an hypothetical 12 storey building [86]. The degree of sophistication of the thermal analysis of buildings varied from simplified techniques to the finite difference and the response factor technique. The substantial differences between programs are due to the way the programs handle dynamic effects such as internal radiation transfer and thermal storage. Other differences are due to the way the programs split the radiative and convective portions of the internal heat gains and of the indoor surface coefficients.

Less utilized is the theoretical validation, where the computer program predictions are compared with the analytical solutions of the heat transfer processes occurring in buildings. Although the analytical models are available only for a small number of cases, this comparison provides useful information about the accuracy of the algorithms which are tested.

The British Research Establishment BRE group analyzed the accuracy of the building energy analysis programs using a wide range of input excitations, such as sinusoidal variations with a 24 hour period or step-function change [87].

Wortman et al. [88] compared the results from DOE, DEROB and SUNCAT 2.4 programs against analytical solutions. They found that the response of a building to step changes in ambient temperature was very close to the analytical solution for high mass building. For low mass building, DEROB program provides higher estimations.

Little [89] compared the results from ESP, SUNCODE and SPIEL programs with the analytical solutions, when the ambient temperature suddenly rises from 0°C to 10°C. The results indicate maximum difference of about 1°C, and consequently the conclusion was these programs provide good estimation of the dynamic heat loss.

4.2 ANALYTICAL VALIDATION OF CBS-MASS PROGRAM

As stated by Beizer [90], it is not possible to develop a testing procedure which gives 100 percent confidence. However, the goal should be to provide sufficient testing to assure that the probability of failure is sufficiently low to be acceptable.

The monitoring of existing buildings becomes prohibitively expansive, if a detailed thermal comparison is required. This implies at least the hourly measurement of:

- room air temperature in different points,
- temperature distribution in walls,
- coefficient of inside and outside surfaces,

- solar radiation on interior surfaces,
- weather data (dry bulb temperature, global radiation on horizontal plane, total cloud amount, solar radiation on exterior surfaces, wind speed and direction).

Other measurements will include the thermal properties of building elements, schedules of equipment and occupancy.

The analytical validation is applied for defining the accuracy of CBS-MASS program in simulating the thermal processes within a room.

An intermediate level room 6.0 x 6.0 x 3.6 m with four exterior walls is considered, and the following parameters are compared:

i) Distribution of the wall temperature due to steady heat flow.

ii) Variation of the inside surface temperature of a cavity wall due to step-function change of outdoor air temperature.

iii) Variation of the room air temperature for step-function change of outdoor air temperature.

iv) Radiant heat exchange between interior surfaces.

4.3 DISTRIBUTION OF THE WALL TEMPERATURE DUE TO STEADY HEAT FLOW

The distribution of wall temperature is calculated under steady state heat flow, when the room air temperature is kept at 20°C and the outdoor temperature is 0°C. There are no air infiltration, solar radiation, internal mass and internal heat gains.

The steady state temperature distribution in multilayers wall is obtained from Equation 4.1, where equilibrium between "heat flow in" and "heat flow out" is assumed for each layer, as well as for the whole wall (Fig. 4.4).

$$q = U\,(TR - TDB) = \frac{1}{\frac{1}{h_o}}\,(T_1 - TDB) = \frac{1}{\frac{1}{h_o} + \frac{\delta 1}{k_1}}\,(T_3 - TDB) =$$

$$= \frac{1}{\frac{1}{h_o} + \frac{\delta 1}{k_1} + \frac{1}{h_{ac}}}\,(T_4 - TDB) = \frac{1}{\frac{1}{h_o} + \frac{\delta 1}{k_1} + \frac{1}{h_{ac}} + \frac{\delta 2}{k_2}}\,(T_6 - TDB) =$$

$$= \frac{1}{\frac{1}{h_o} + \frac{\delta 1}{k_1} + \frac{1}{h_{ac}} + \frac{\delta 2}{k_2} + \frac{\delta 3}{k_3}}\,(T_8 - TDB) = \frac{1}{\frac{1}{h_i}}\,(TR - T_8) \qquad (4.1)$$

where T_1 = TOS and T_8 = TIS

One obtains:

$$T_1 = TDB + \frac{U}{h_o}\,(TR - TDB) \qquad (4.2)$$

$$T_3 = TDB + \frac{\sum R_t}{R_T}\,(TR - TDB) \qquad (4.3)$$

$$T_4 = TDB + \frac{\sum R_t}{R_T}\,(TR - TDB) \qquad (4.4)$$

$$T_6 = TDB + \frac{\sum R_t}{R_T}\,(TR - TDB) \qquad (4.5)$$

$$T_8 = TDB + \frac{\sum R_t}{R_T}\,(TR - TDB) \qquad (4.6)$$

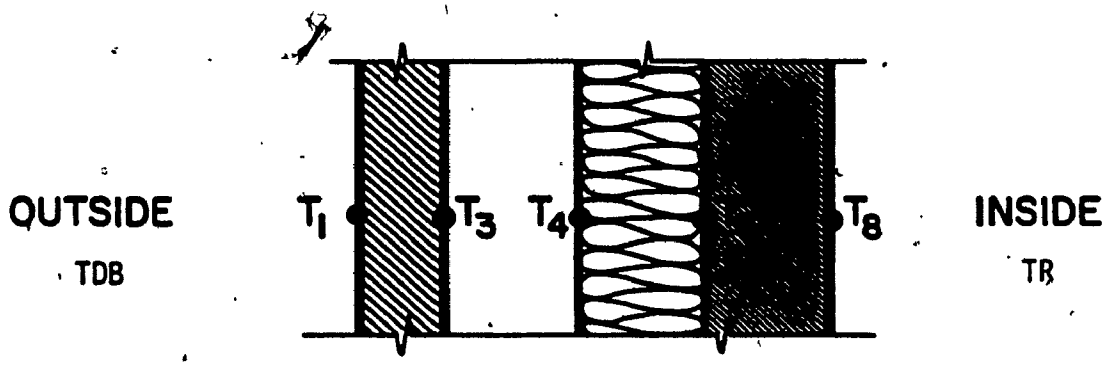

Fig. 4.4 Schema of air cavity wall.

or

$$T_8 = TR - \frac{U}{h_i} (TR - TDB) \qquad (4.7)$$

The comparison between theoretical model and CBS-MASS predictions, after a long time run to reach the steady state, are presented in Tables 4.1 - 4.3 for three wall types, and indicates good agreement.

The theoretical model assumes that the mean radiant temperature of interior surfaces TMRT equals the room air temperature TR, and consequently:

$$q = q_R + q_{cv} = h_R (TMRT - TIS) + h_{cv} (TR - TIS) =$$

$$= (h_R + h_{cv}) (TR - TIS) = h_i (TR - TIS) \qquad (4.8)$$

TABLE 4.1

Comparison between the analytical solution for steady-state and the CBS-MASS program results for wall A

	Denomination	Thick (m)	k W/m°C	R_t m²°C/W	Temperature (°C)		
						Analytic	CBS-MASS
1	Outside air			0.0294	T_1	0.35	0.35
2	Concrete	0.05	1.73	0.0289	T_3	0.70	0.70
3	Air cavity			0.167	T_4	2.70	2.72
4	Insulation	0.05	0.04	1.25	T_6	15.67	15.73
5	Gypsum	0.02	0.43	0.0465	T_8	18.28	18.36
6	Inside air			0.125			

$R_T = 1.647$ m²°C/W

TABLE 4.2

Comparison between the analytical solution for steady-state and the CBS-MASS program results for wall B

	Denomination	Thick (m)	k W/m°C	R_t m^2 °C/W	Temperature (°C)		
						Analytic	CBS-MASS
1	Outside air			0.0294	T_1	1.49	1.46
2	Concrete	0.05	1.73	0.0289	T_3	2.95	2.89
3	Air cavity			0.167	T_4	11.39	11.18
4	Concrete	0.05	1.73	0.0289	T_6	12.86	12.55
5	Concrete	0.02	1.73	0.0116	T_8	13.47	13.16
6	Inside air			0.125			

R_T = 0.391 m^2 °C/W

TABLE 4.3

Comparison between the analytical solution for steady-state and the CBS-MASS program results for wall C

	Denomination	Thick (m)	k W/m°C	R_t m^2 °C/W	Temperature (°C)		
						Analytic	CBS-MASS
1	Outside air			0.0294	T_1	0.83	0.81
2	Brick	0.14	0.73	0.192	T_3	6.20	6.10
3	Air cavity			0.167	T_4	10.89	10.68
4	Brick	0.07	0.73	0.096	T_6	13.59	13.53
5	Brick	0.07	0.73	0.096	T_8	16.29	16.15
6	Inside air			0.125			

R_T = 0.705 m^2 °C/W

When the predictions of the computer program, using hourly calculations of the mean radiant temperature and the room air temperature, are compared with the analytical solution, differences of about 2°C on the inside surface temperature are obtained for wall A (Table 4.4), and 4.3°C for wall B (Table 4.5).

TABLE 4.4

Effect of the assumption TMRT=TR on the comparison between the analytical solution for steady-state and the CBS-MASS program results for wall A

		T_1(°C)	T_3(°C)	T_4(°C)	T_6(°C)	T_8(°C)
TMRT ≠ TR	CBS-MASS	0.31	0.62	2.39	15.67	16.30
	Analytic	0.35	0.70	2.70	17.73	18.28
TMRT = TR	CBS-MASS	0.35	0.70	2.72	17.76	18.36
	Analytic	0.35	0.70	2.70	17.73	18.28

TABLE 4.5

Effect of the assumption TMRT=TR on the comparison between the analytical solution for steady-state and the CBS-MASS program results for wall B

		T_1(°C)	T_3(°C)	T_4(°C)	T_6(°C)	T_8(°C)
TMRT ≠ TR	CBS-MASS	1.01	2.00	7.72	8.68	9.15
	Analytic	1.49	2.95	11.39	12.86	13.47
TMRT = TR	CBS-MASS	1.46	2.89	11.18	12.55	13.16
	Analytic	1.49	2.95	11.39	12.86	13.47

The CBS-MASS program was then modified to include the basic assumption of the model (TMRT=TR), and under this condition good agreement was obtained between results.

4.4 NUMBER OF IDENTICAL DAYS TO BE USED FOR OBTAINING A STABILIZED SOLUTION

A stabilized solution is assumed to be obtained when the difference from the final solution ($t \to \infty$) is less than 0.5°C.

i) Initially, the temperatures of walls and room air are assumed 20°C. Then, the room and outdoor air temperatures drop suddenly to a given value (10°C, 0°C, -20°C). The variation of the wall temperature toward a stabilized solution is analyzed. No solar radiation was considered, and glazing-to-wall ratio was equal to 0.01. When the room air temperature is kept within a narrow range; and no internal heat gains occur in space, a stabilized solution is obtained after 24 hours, that is, the results for the second identical day can be considered as final solution (Fig. 4.5 - 4.7).

ii) Initially, the temperatures of walls and room air are equal to 20°C. Then, the room air temperature is kept at 20 ± 0.2°C, and the outdoor conditions correspond to December 21, 1979, in Montreal [53]. The results indicate that a stabilized solution is obtained after 2 identical days (Table 4.6) for glazing-to-wall ratio between 0.01 and 0.5 .

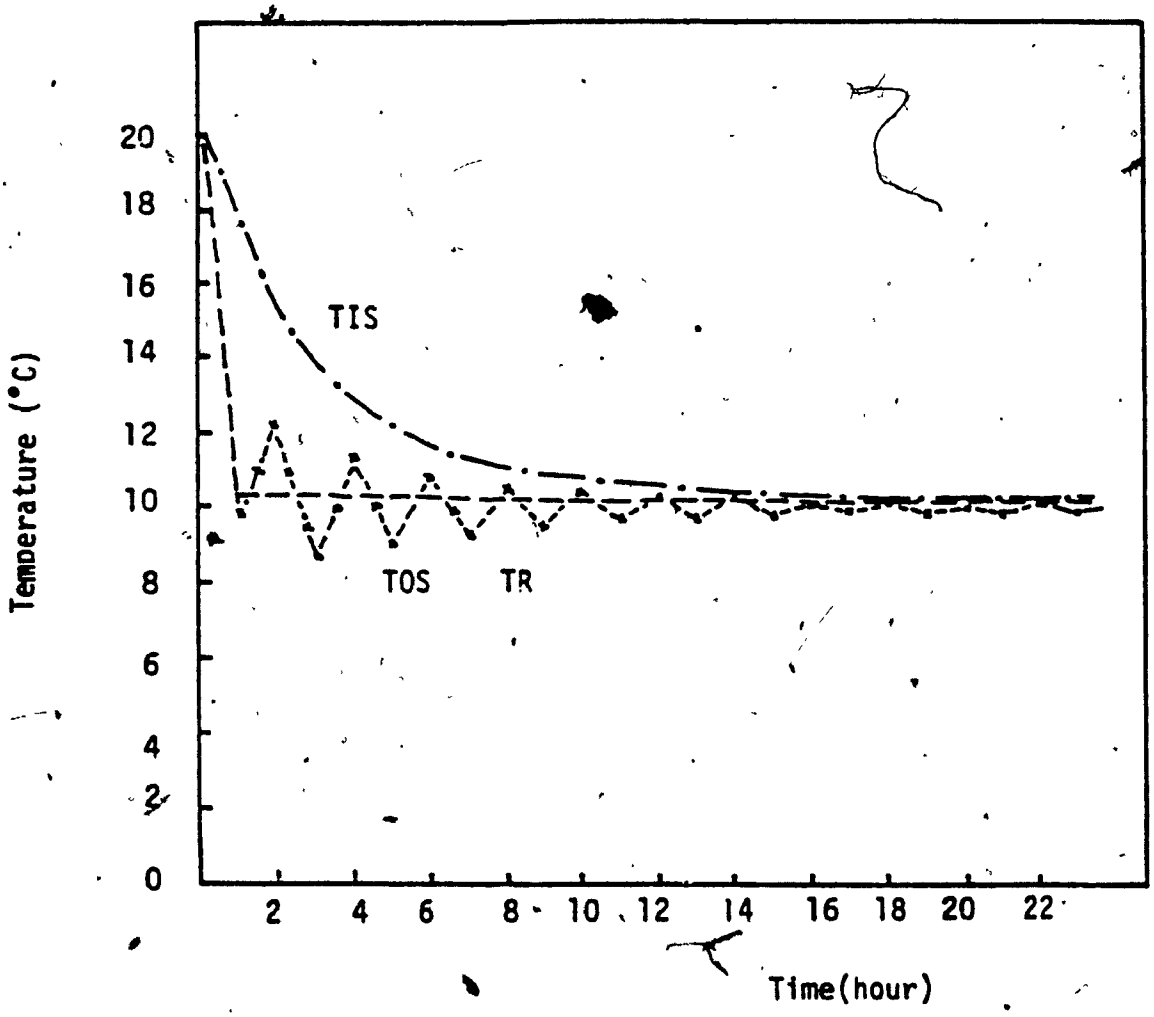

Fig. 4.5 Temperature variation toward a stabilized solution (T= 10°C).

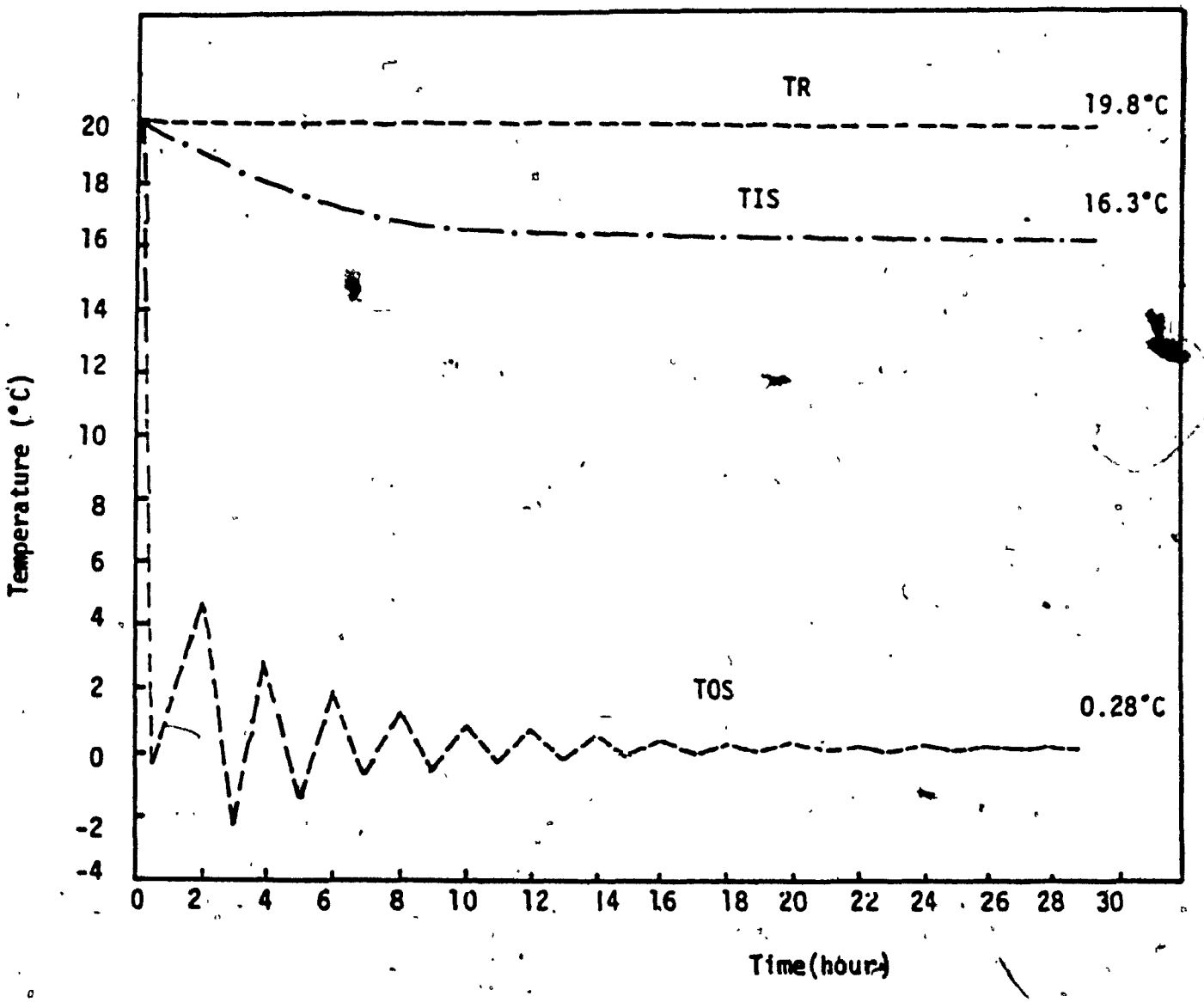

Fig. 4.6 Temperature variation toward a stabilized solution (T= 0°C).

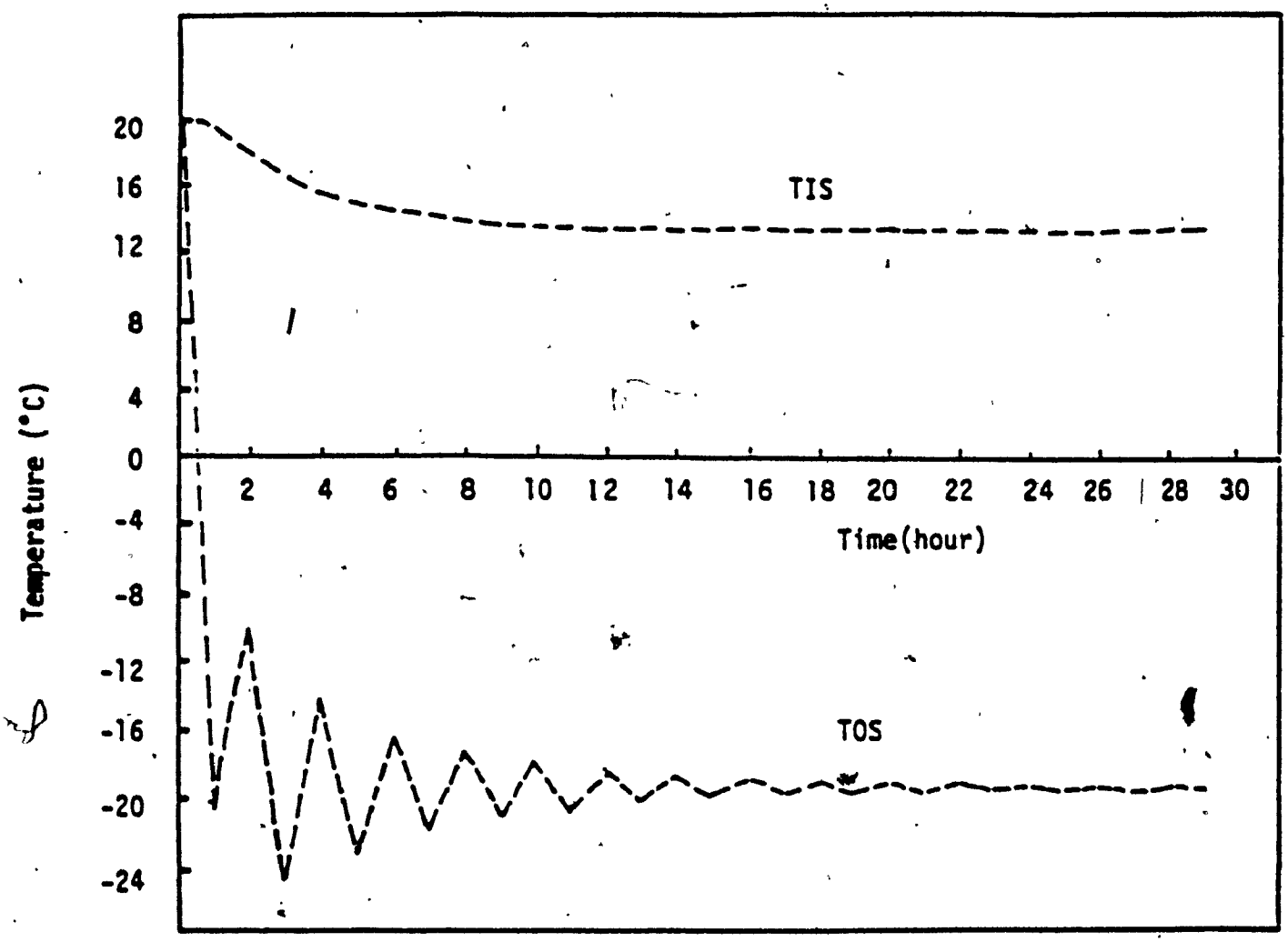

Fig. 4.7 Temperature variation toward a stabilized solution (T_s=-20°C).

iii) When the room air temperature can fluctuate without limitations, the results of simulation for December 21, and July 30, 1979, in Montreal indicate that 4-5 days are required to obtain a stabilized solution (Tables 4.7-4.8).

Hence, the number of identical days to be simulated depends on the control of room air temperature, and varies for these particular cases from one day (room air temperature within narrow limits) to five days (no control). The application of standard number of identical days, to obtain a stabilized solution as recommended by I.E.A. or used by BLAST/ NBSLD program, can be overestimated (controlled room air temperature) or can be underestimated. The user of building energy analysis programs should have the option to define the number of identical days to obtain a stabilized solution, to optimize the computing time.

TABLE 4.6 Variation of the inside and outside surface temperature (°C) toward a stabilized solution, for outdoor conditions December 21, 1979, in Montreal and room air temperature 20 ± 0.2°C

DAY	TOS				TIS			
	6:00 am	12:00 am	6:00 pm	12 pm	6:00 am	12:00 am	6:00 pm	12:00 pm
1	- 0.91	1.88	2.74	- 4.12	16.45	16.56	16.90	16.19
2	- 2.91	1.22	2.51	- 4.21	15.82	16.46	16.87	16.21
3	- 2.95	1.21	2.50	- 4.22	15.82	16.46	16.87	16.21
4	- 2.95	1.21	2.50	- 4.22	15.82	16.46	16.87	16.21
5	- 2.95	1.21	2.50	- 4.22	15.82	16.46	16.87	16.21
6	- 2.95	1.21	2.50	- 4.22	15.82	16.46	16.87	16.21
7	- 2.95	1.21	2.50	- 4.22	15.82	16.46	16.87	16.21
8	- 2.95	1.21	2.50	- 4.22	15.82	16.46	16.87	16.21
9	- 2.95	1.21	2.50	- 4.22	15.82	16.46	16.87	16.21
10	- 2.95	1.21	2.50	- 4.22	15.82	16.46	16.87	16.21

TABLE 4.7

Variation of the inside and outside surface temperature (°C) toward a stabilized solution for outdoor conditions December 21, 1979, in Montreal and room temperature with no control

DAY	TOS				TIS			
	6:00 am	12:00 am	6:00 am	12:00 am	6:00 am	12:00 am	6:00 pm	12:00 pm
1	- 11.90	4.81	- 14.25	- 11.05	13.56	9.57	6.62	1.14
2	- 14.13	3.98	- 14.61	- 11.25	- 1.21	- 1.15	- 1.48	- 4.55
3	- 14.26	3.89	- 14.67	- 11.28	- 5.81	- 4.72	- 4.16	- 6.40
4	- 14.29	3.87	- 14.69	- 11.29	- 7.29	- 5.87	- 5.02	- 7.06
5	- 14.30	3.86	- 14.70	- 11.29	- 7.82	- 6.27	- 5.32	- 7.31
6	- 14.31	3.86	- 14.70	- 11.29	- 8.02	- 6.43	- 5.44	- 7.41
7	- 14.31	3.86	- 14.70	- 11.29	- 8.10	- 6.49	- 5.48	- 7.45
8	- 14.31	3.86	- 14.70	- 11.29	- 8.13	- 6.51	- 5.50	- 7.46
9	- 14.31	3.86	- 14.70	- 11.29	- 8.14	- 6.52	- 5.51	- 7.47
10	- 14.31	3.86	- 14.70	- 11.29	- 8.14	- 6.53	- 5.51	- 7.47

TABLE 4.8

Variation of the inside and outside surface temperature (°C) toward a stabilized solution, for outdoor conditions July 30, 1979, in Montreal and room temperature with no control

DAY	TOS				TIS			
	6:00 am	12:00 am	6:00 pm	12:00 am	6:00 am	12:00 am	6:00 pm	12:00 pm
1	17.62	39.79	28.92	18.60	19.67	22.68	27.25	26.46
2	17.55	39.86	29.01	18.68	25.38	27.04	30.46	29.05
3	17.62	39.91	29.05	18.71	27.59	28.74	31.74	30.09
4	17.64	39.93	29.07	18.72	28.44	29.39	32.23	30.48
5	17.65	39.94	29.07	18.72	28.71	29.60	32.39	30.61
6	17.65	39.94	29.08	18.72	28.82	29.68	32.45	30.66
7	17.65	39.94	29.08	18.73	28.86	29.72	32.48	30.68
8	17.65	39.94	29.08	18.73	28.88	29.73	32.49	30.69
9	17.65	39.94	29.08	18.73	28.89	29.74	32.50	30.70
10	17.65	39.94	29.08	18.73	28.89	29.74	32.50	30.70

4.5 VARIATION OF THE INSIDE SURFACE TEMPERATURE OF A CAVITY WALL DUE TO STEP-FUNCTION CHANGE OF OUTDOOR AIR TEMPERATURE.

Initially, the temperatures of wall and air are equal to 20°C. Then, while the room air temperature is kept constant at 20°C, the outdoor air temperature drops suddenly to 0°C (ΔT_o = 20°C). Equation 4.9 presents the analytical solution of the variation of inside surface temperature under these conditions, as developed by Pratt [67]:

$$TIS\ (t) = \frac{R_{1,2}}{R_T}\ TR + 2\ a_o\ a_1\ \Delta T_o \sum \frac{\exp[-\alpha_n^2 t]}{\beta\ (\alpha_n)} \qquad (4.9)$$

CBS-MASS program was modified to use identical assumptions as the analytical model such as:

- mean radiant temperature of interior surfaces equals room air temperature (TMRT=TR),
- constant inside surface coefficient h_i = 8 W/(m²°C)
- no air infiltration,
- no internal mass.
- no solar radiation.

The results of comparison between the analytical solution and the predictions of the CBS-MASS program for two concrete cavity walls (Fig. 4.8 - 4.9) and one brick cavity wall (Fig. 4.10) indicate good agreement, with differences less than 5 percent.

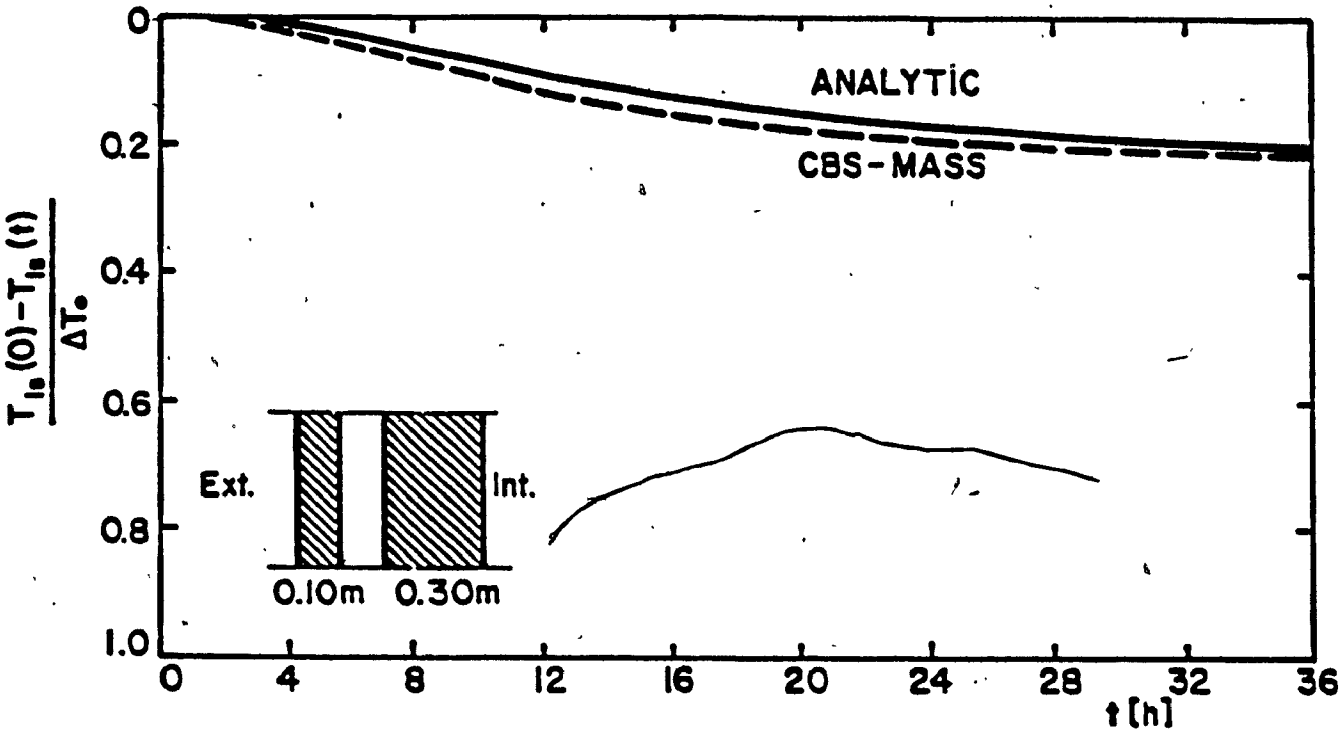

Fig. 4.8 Variation of the inside surface temperature of a 0.40 m concrete wall due to step-function change in outdoor air temperature

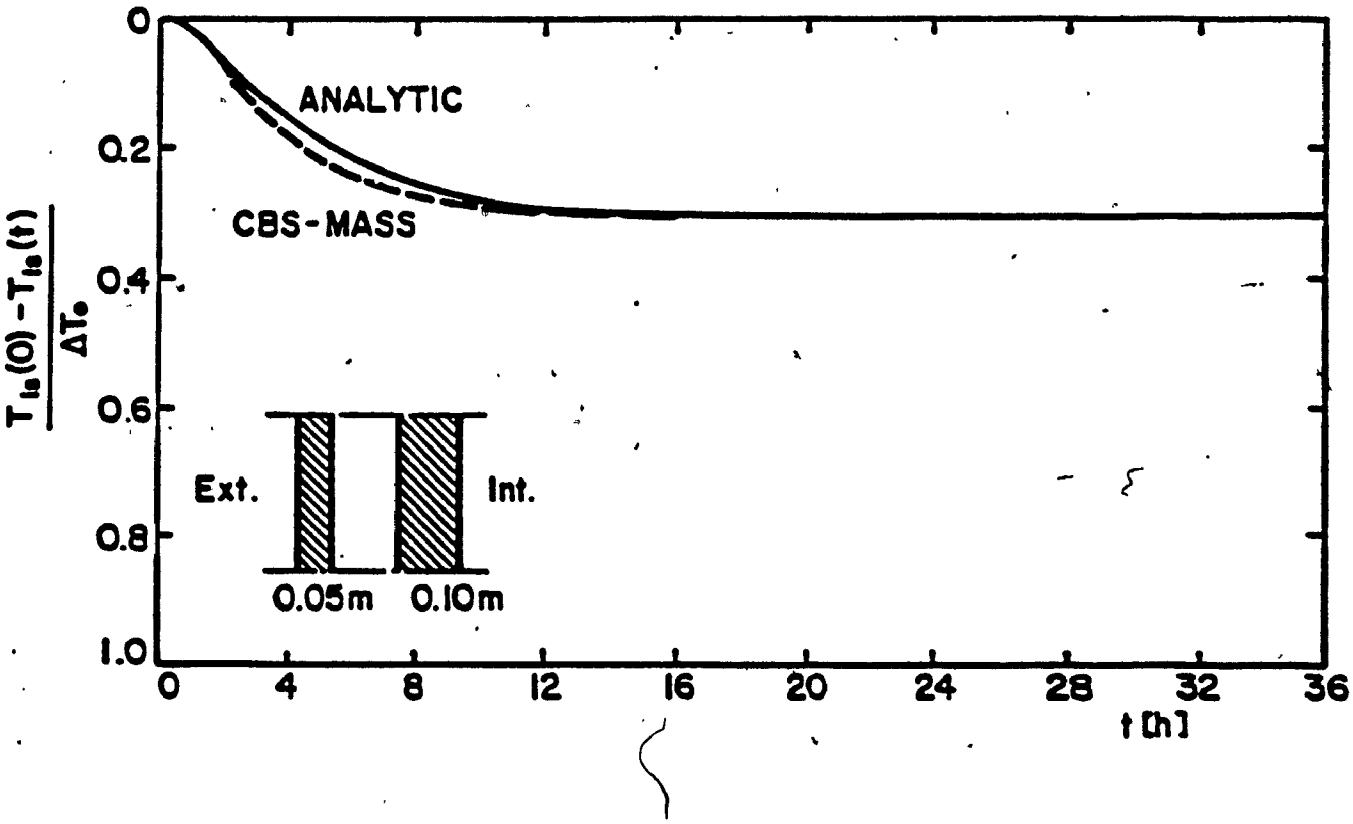

Fig. 4.9 Variation of the inside surface temperature of a 0.15 m concrete wall due to step-function change in outdoor air temperature

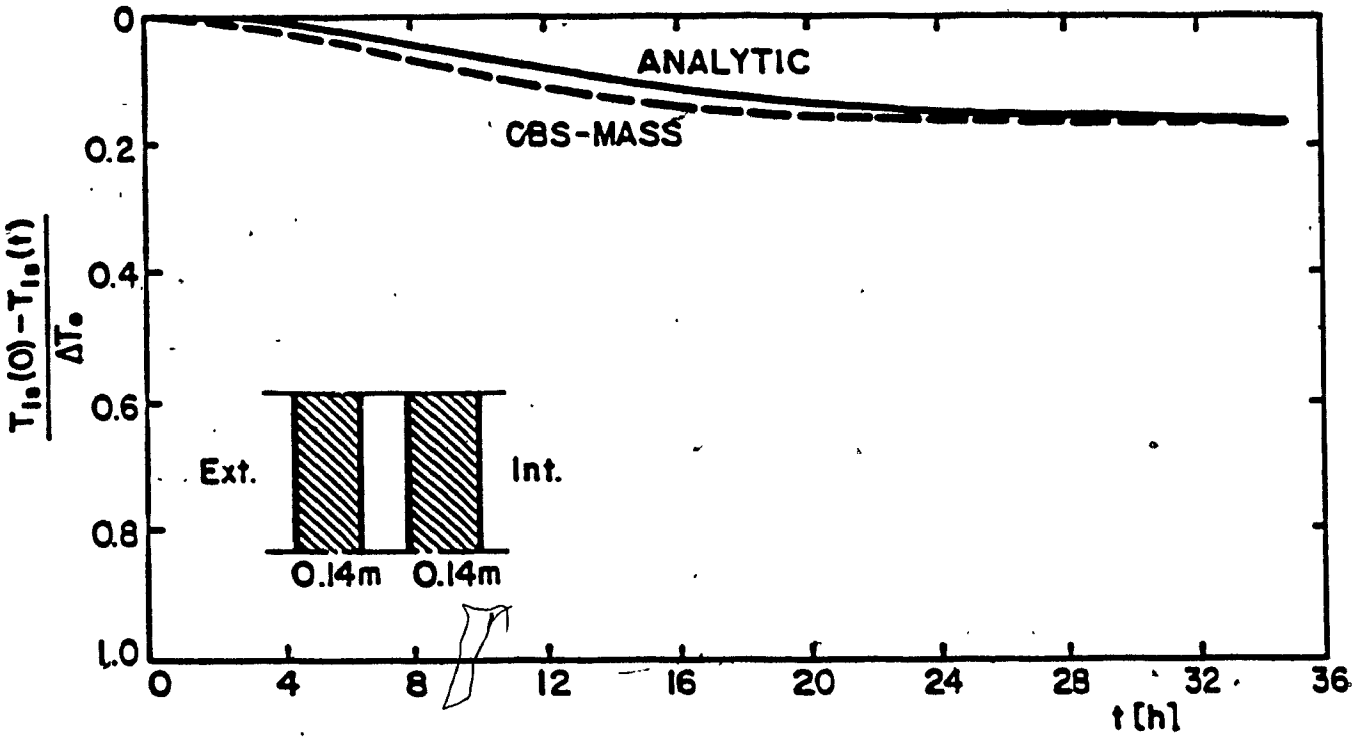

Fig. 4.10 Variation of the inside surface temperature of a 0.28 m brick wall due to step-function change in outdoor air temperature.

When the assumption of room air temperature equal mean radiant temperature (TR = TMRT) is used, the obtained inside surface temperature is greater than that when the mean radiant temperature is calculated hourly (Fig. 4.11 - 4.12). The results emphasize the need for using identical assumptions for the analytical model and for the computer program.

4.6 VARIATION OF THE ROOM AIR TEMPERATURE FOR STEP-FUNCTION CHANGE OF OUTDOOR AIR.

Initially, the temperatures of wall and air are equal to 20°C. The variation in time of the room air temperature, subjected to a sudden drop of outdoor air temperature to 0°C (ΔT_o = 20°C) is analyzed.

Equation 4.10 presents the analytical solution of the variation of room air temperature, as developed by Pratt [67].

$$\frac{TR(0) - TR(t)}{\Delta T_o} = 1 - \frac{(B_s - C[\alpha_1^2])[\alpha_2^2]}{B_s(1+VA)([\alpha_2^2]-[\alpha_1^2])}$$

$$X \left\{1 + \frac{VB_f(B_s - C[\alpha_1^2])(\cos[\alpha_1] + (B_o/[\alpha_1])\sin(\alpha_1])}{CB_o(B_f+B_s+V)(\beta - [\alpha_1^2])}\right\}$$

$$X \exp(-[\alpha_1^2]t) + \frac{(B_s - C[\alpha_2^2])[\alpha_1^2]}{B_s(1+VA)([\alpha_2^2]-[\alpha_1^2])}$$

$$X \left\{1 + \frac{VB_f(B_s - C[\alpha_2^2])(\cos[\alpha_2] + (B_o/[\alpha_2])\sin[\alpha_2])}{CB_o(B_f+B_s+V)(\beta - [\alpha_2^2])}\right\}$$

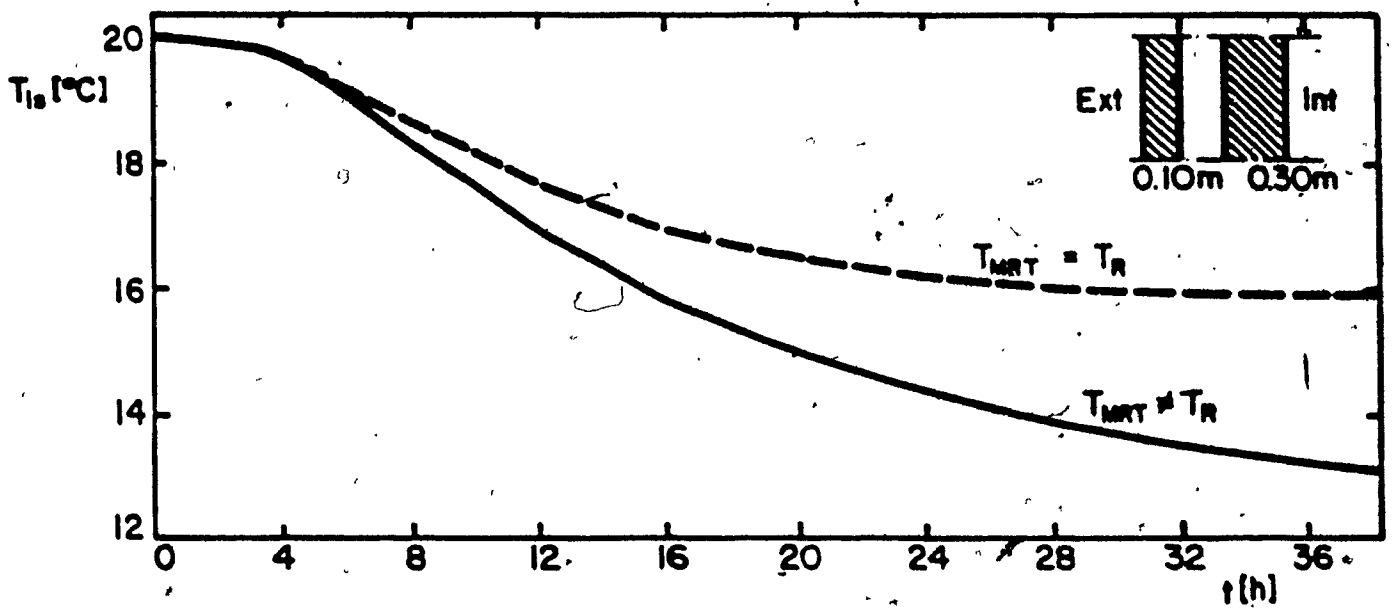

Fig. 4.11 Effect of assumption TMRT=TR on the estimation of inside surface temperature of 0.40 m concrete wall, subjected to a step-function change in outdoor air temperature.

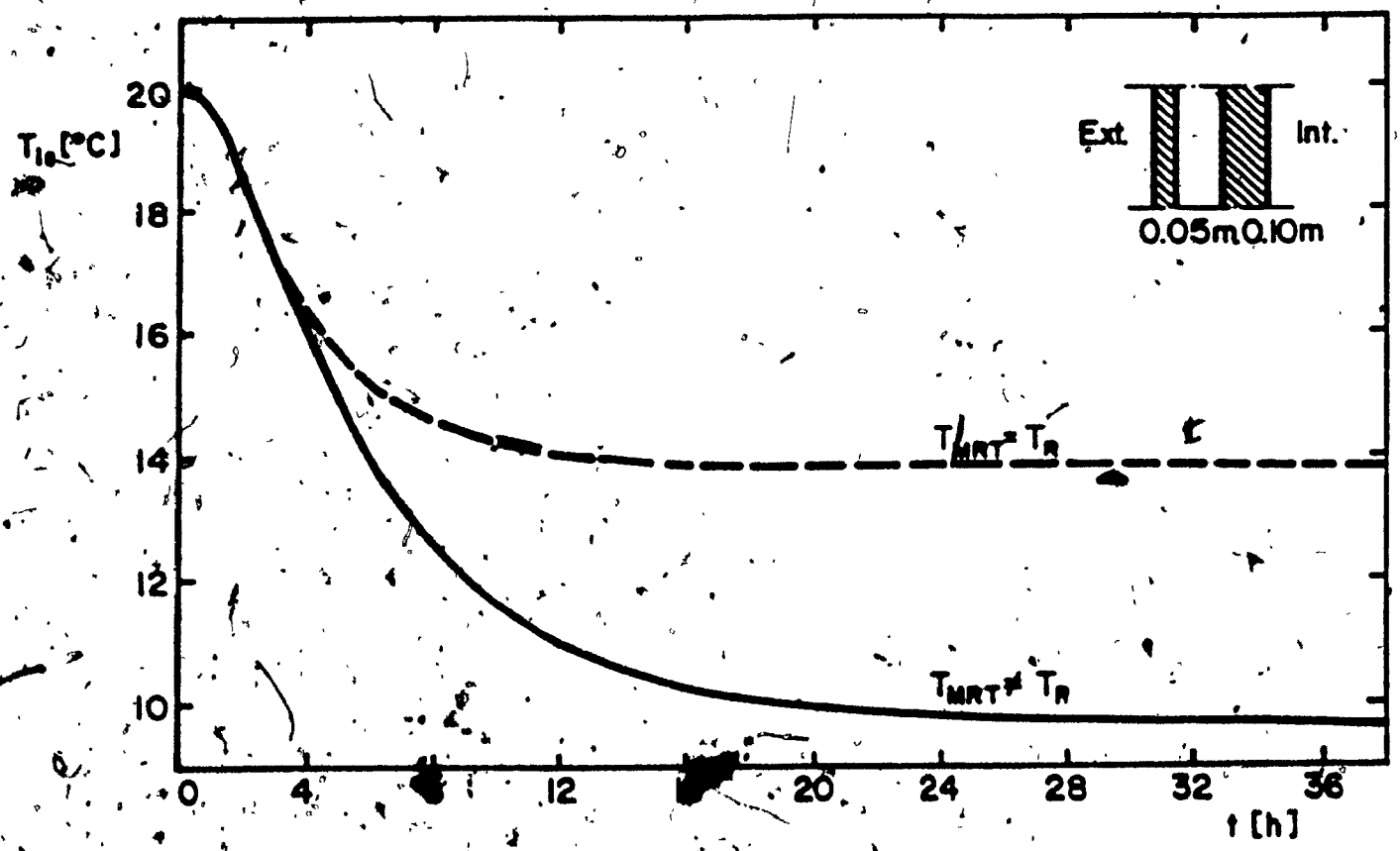

Fig. 4.12 Effect of assumption TMRT = TR on the estimation of inside surface temperature of 0.15 m concrete wall, subjected to a step-function change in outdoor air temperature.

$$X \exp\left(-[\alpha_2^2]t\right) - \frac{VB_s^2}{C_\beta (B_i+B_s+V)^2}$$

$$X \left\{1 + \frac{B_i (B_s-C_\beta)^2 (B_i+B_s+V)\left[\cos\sqrt{\beta}+(B_0/\sqrt{\beta})\sin\sqrt{\beta}\right]}{B_0 B_s^3 (1+VA)(1-\beta/[\alpha_1^2])(1-\beta/[\alpha_2^2])}\right\}$$

$$X \exp(-\beta t) \qquad (4.10)$$

The CBS-MASS program was modified to use the same assumptions as the analytical model such:

- mean radiant temperature equals room air temperature,
- constant inside surface coefficient $h_i = 8/(W/m^2\,°C)$.

A room with 0.28 m brick wall was analyzed under the conditions presented in Table 4.9, to take into account the effect of internal mass and air infiltration.

CASE 1. The difference between analytical solution and program predictions for the case with no internal mass and no air infiltration are less than 3 percent, which indicates good agreement (Fig. 4.13).

CASE 2. The analytical model considers the temperature of internal mass either equal with the room air temperature or constant. The program predictions, which takes into account the temperature gradient in internal walls, are situated between the two analytical solutions (Fig. 4.14).

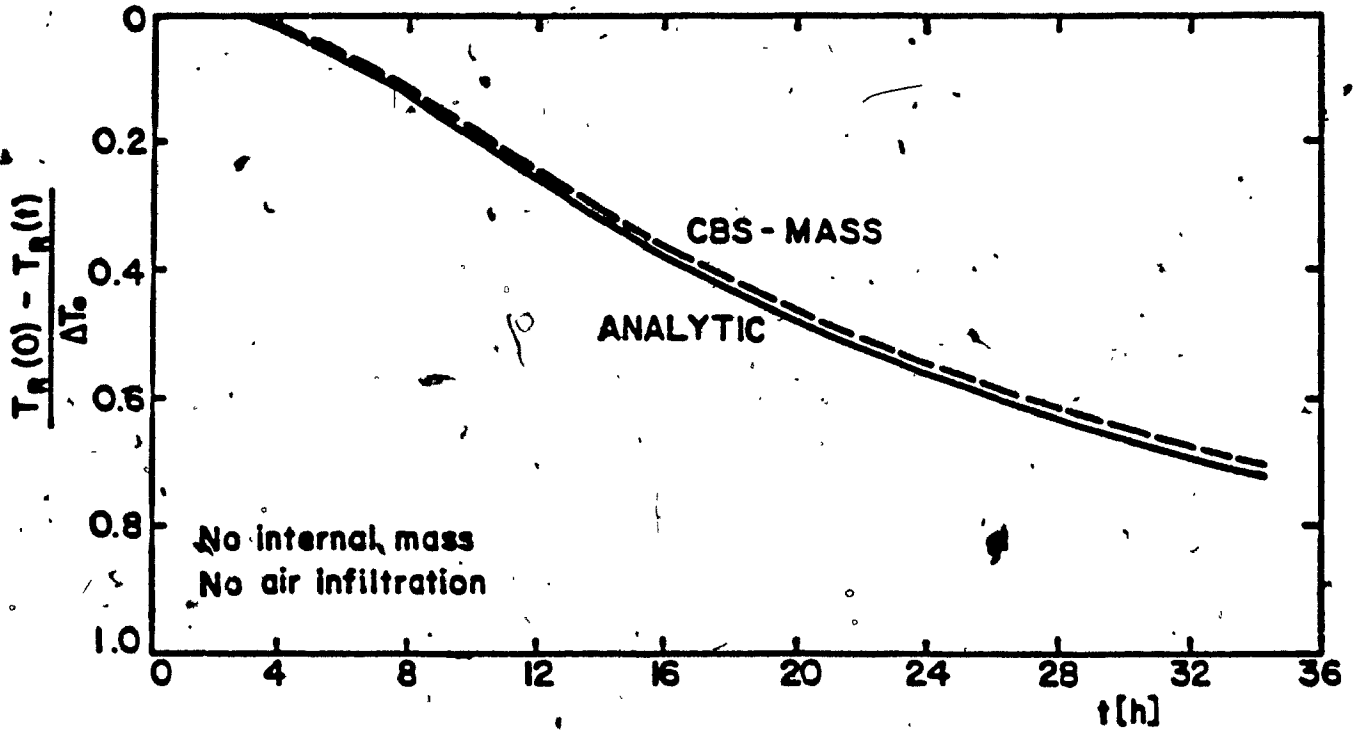

Fig. 4.13 Variation of the room air temperature due to step-function change in outdoor air temperature. No internal mass and no air infiltration.

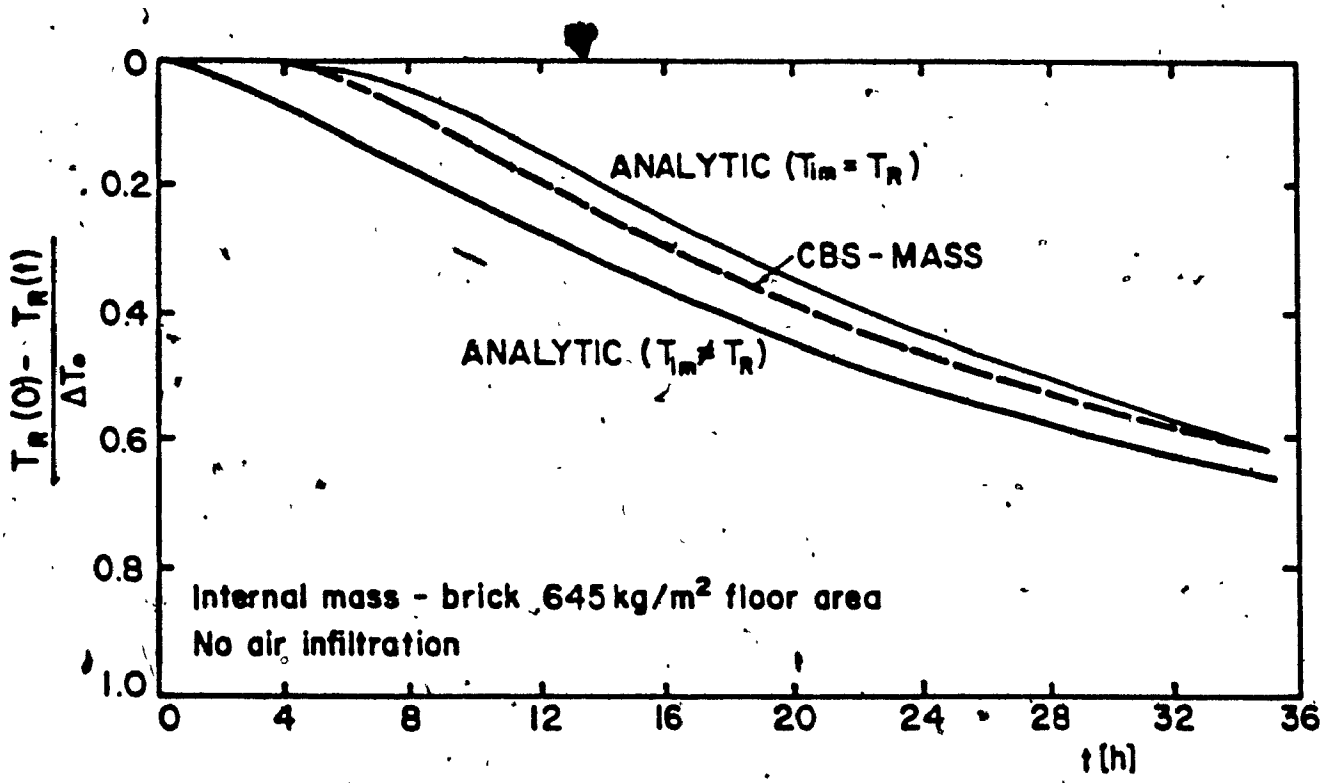

Fig. 4.14 Variation of the room air temperature due to step-function change in outdoor air temperature. Internal mass and no air infiltration.

CASE 3. The results indicate good agreement between predictions and analytical solutions for the case with no internal mass and with air infiltration, except the first hours where a perturbation of analytical solution occurs (Fig. 4.15).

CASE 4. The program predictions for the case with air infiltration and internal mass are close to the analytical solutions which assume the temperature of the interior mass is not equal with the room air temperature (Fig. 4.16).

TABLE 4.9

List of cases used in the comparison between the analytical solution of room temperature and the CBS-MASS results

Case	Interior mass	Air infiltration	Figure
1	N	N	4.13
2	Brick, 645 kg/m^2	N	4.14
3	N	1 ach	4.15
4	Brick, 645 kg/m^2	1 ach	4.16

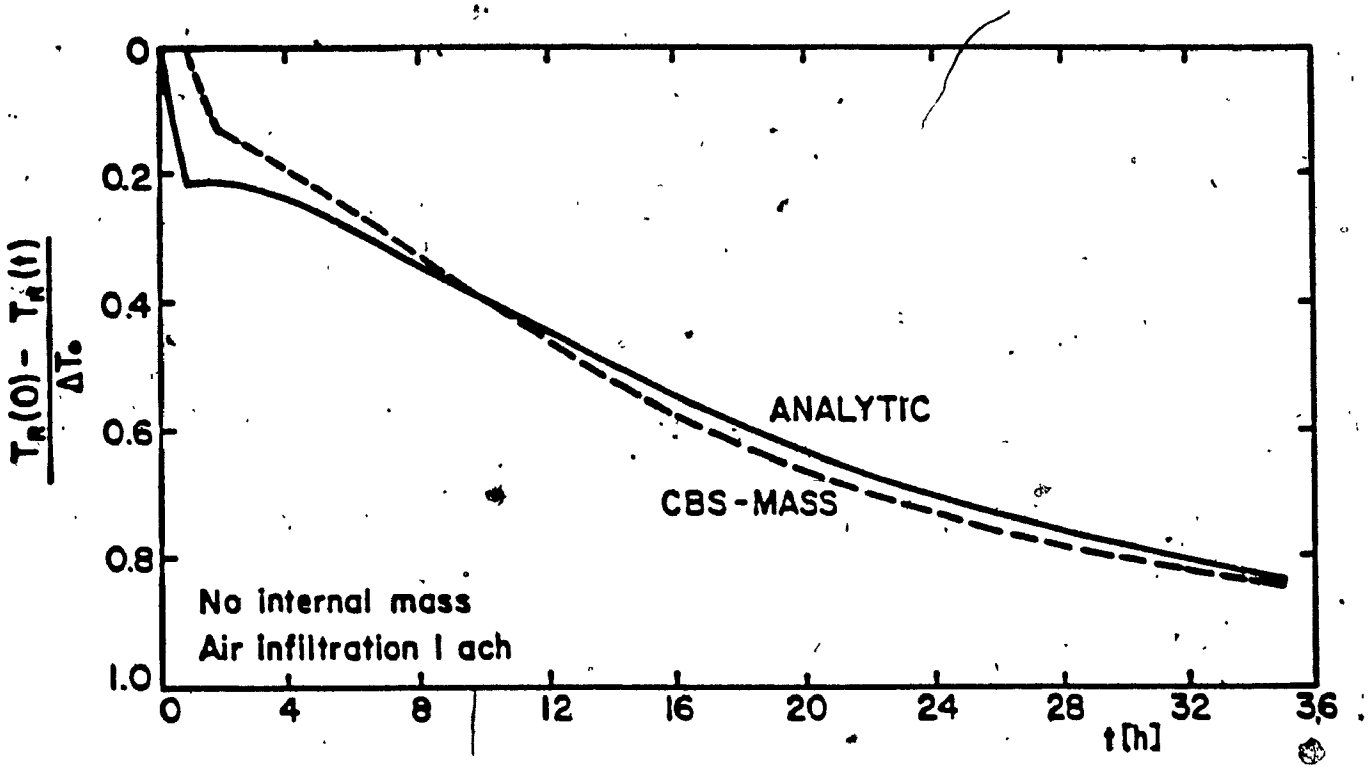

Fig. 4.15 Variation of the room air temperature due to step-function change in outdoor air temperature. No internal mass and air infiltration.

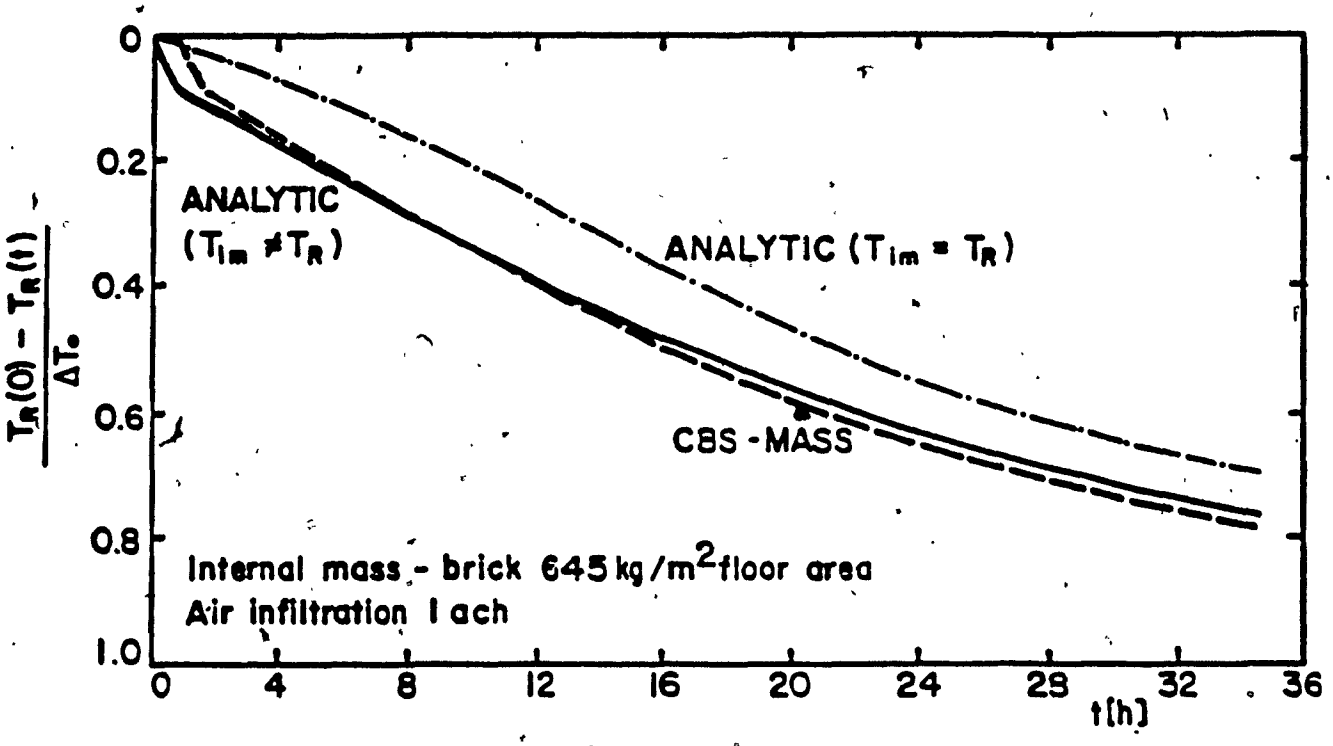

Fig. 4.16 Variation of the room air temperature due to step-function change in outdoor air temperature. Internal mass and air infiltration.

4.7 RADIANT HEAT EXCHANGE BETWEEN INTERIOR SURFACES

The proposed model for radiant heat exchange between interior surfaces (Eq. 3.107-3.111) was compared with the non-linear model (Eq. 3.87), for a cube-shaped space (3.0 x 3.0 x 3.0 m) with occupancy between 9:00 a.m. and 5:00 p.m. The weather data for June 21, 1979, in Montreal was used for the simulation with CBS-MASS program.

The results indicate good agreement with differences less than 10 percent for the following cases:

a. No glazing, internal gains and air infiltration. Five exterior walls and one floor (Table 4.10). Figure 4.17 presents the variation of room air temperature and the temperature of inside surfaces.

b. No glazing, internal gains and air infiltration. One exterior wall, three interior walls and two floors (Table 4.11).

c. No glazing. Five exterior walls and one floor (Table 4.12).

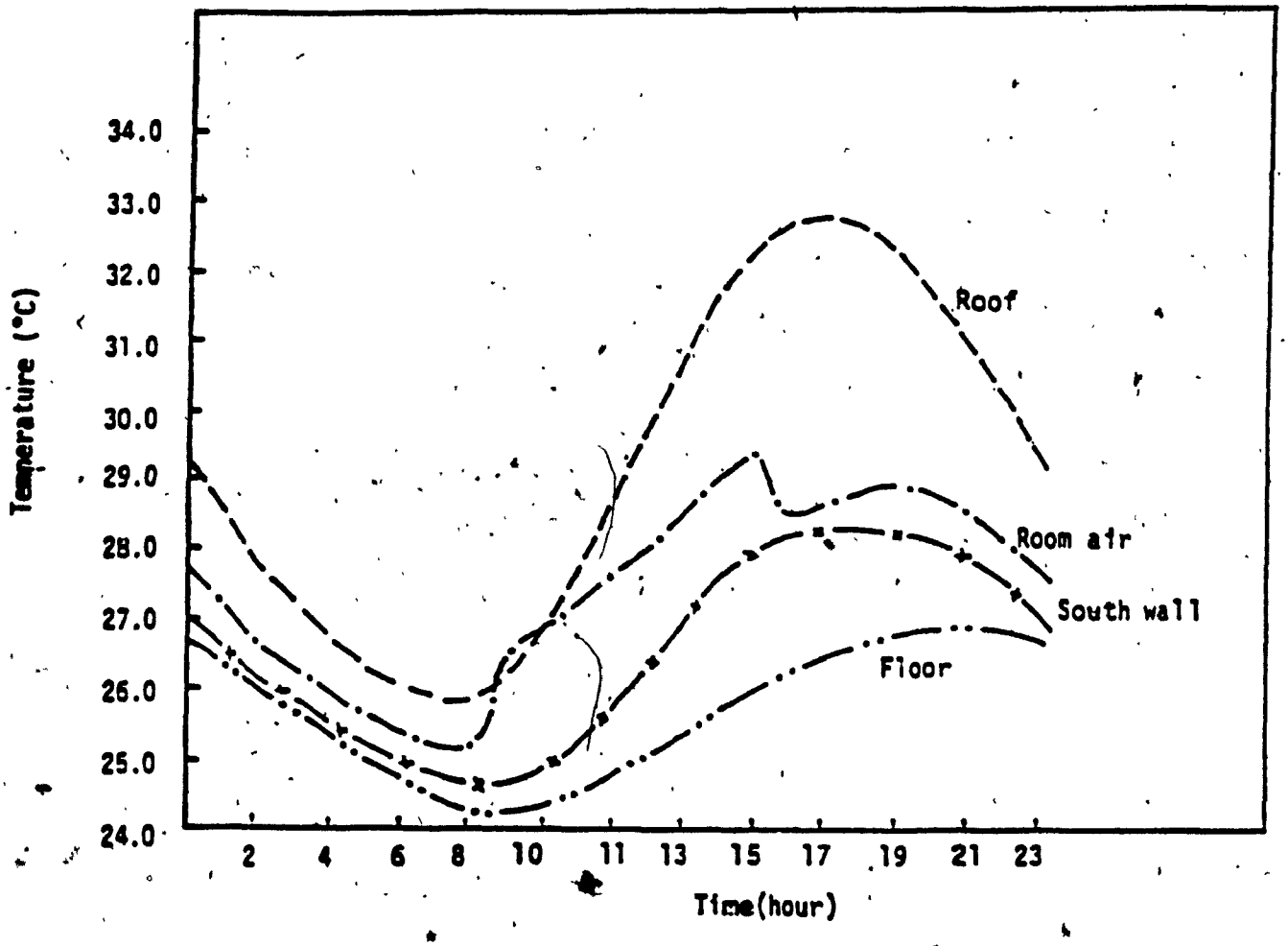

Fig. 4.17 Variation of room air temperature and inside surfaces temperature vs. time.

TABLE 4.10

Radiant heat flow (W/m^2).
No glazing, no internal loads, no infiltration
Five exterior walls and floor

TIME	SOUTH WALL		NORTH WALL		ROOF		FLOOR	
	Proposed	N-L	Proposed	N-L	Proposed	N-L	Proposed	N-L
1	4.58	4.25	1.59	1.49	- 7.83	- 7.30	6.79	6.27
2	4.27	3.95	1.12	1.06	- 6.45	- 6.00	5.50	5.08
3	3.92	3.62	0.67	0.64	- 5.43	- 5.05	4.87	4.50
4	3.57	3.31	0.25	0.25	- 4.65	- 4.33	4.65	4.30
5	3.27	3.02	-0.12	-0.11	- 4.06	- 3.78	4.67	4.31
6	3.10	2.87	-0.52	-0.48	- 3.58	- 3.32	4.92	4.54
7	3.29	3.05	-0.92	-0.84	- 3.25	- 3.01	5.57	5.14
8	3.98	3.68	-1.05	-0.96	- 3.35	- 3.11	6.67	6.15
9	5.03	4.65	-0.54	-0.48	- 4.32	- 4.00	8.07	7.43
10	5.95	5.51	0.69	0.69	- 6.39	- 5.92	9.60	8.84
11	6.25	5.81	2.34	2.22	- 9.44	- 8.79	11.20	10.31
12	5.71	5.33	3.97	3.74	-13.2	-12.33	12.79	11.76
13	4.50	4.24	5.35	5.02	-17.23	-16.18	14.17	13.02
14	3.06	2.93	6.44	6.03	-21.05	-19.85	15.17	13.94
15	1.95	1.92	7.38	6.90	-24.11	-22.82	15.90	14.60
16	1.57	1.58	8.18	7.64	-26.05	-24.70	16.59	15.22
17	2.05	2.03	8.74	8.15	-26.66	-25.30	17.23	15.80
18	3.17	3.06	8.77	8.19	-25.92	-24.56	17.68	16.20
19	4.49	4.27	8.06	7.53	-23.88	-22.57	17.65	16.17
20	5.47	5.15	6.68	6.26	-20.88	-19.67	16.91	15.50
21	5.79	5.43	5.09	4.78	-17.54	-16.47	15.43	14.15
22	5.60	5.23	3.75	3.52	-14.44	-13.52	13.37	12.28
23	5.23	4.86	2.78	2.62	-11.81	-11.04	11.04	10.16
24	4.88	4.53	2.11	1.98	-9.61	- 8.97	8.73	8.05

TABLE 4.11

Radiant heat flow (W/m^2)
No glazing, no internal gains, no infiltration
One exterior wall and five interior walls

TIME	SOUTH WALL		NORTH WALL		CEILING		FLOOR	
	Proposed	N-L	Proposed	N-L	Proposed	N-L	Proposed	N-L
1	-17.09	-16.16	3.44	3.23	3.44	3.23	3.44	3.23
2	-16.28	-15.37	3.28	3.07	3.28	3.07	3.28	3.07
3	-15.87	-14.98	3.19	3.00	3.19	3.00	3.19	3.00
4	-15.71	-14.82	3.16	2.96	3.16	2.96	3.16	2.96
5	-15.65	-14.77	3.15	2.95	3.15	2.95	3.15	2.95
6	-15.65	-14.77	3.15	2.95	3.15	2.95	3.15	2.95
7	-15.69	-14.80	3.16	2.96	3.16	2.96	3.16	2.96
8	-15.70	-14.82	3.16	2.96	3.16	2.96	3.16	2.96
9	-15.75	-14.86	3.17	2.97	3.17	2.97	3.17	2.97
10	-16.04	-15.14	3.23	3.03	3.23	3.03	3.23	3.03
11	-16.89	-15.96	3.40	3.20	3.40	3.20	3.40	3.20
12	-18.41	-17.43	3.71	3.49	3.71	3.49	3.71	3.49
13	-20.33	-19.29	4.10	3.86	4.10	3.86	4.10	3.86
14	-22.21	-21.12	4.49	4.22	4.49	4.22	4.49	4.22
15	-23.74	-22.61	4.80	4.52	4.80	4.52	4.80	4.52
16	-24.73	-23.58	5.00	4.72	5.00	4.72	5.00	4.72
17	-25.10	-23.95	5.08	4.79	5.08	4.79	5.08	4.79
18	-24.85	-23.70	5.03	4.74	5.03	4.74	5.03	4.74
19	-24.1	-23.00	4.88	4.60	4.88	4.60	4.88	4.60
20	-23.21	-22.09	4.69	4.42	4.69	4.42	4.69	4.42
21	-22.16	-21.07	4.47	4.47	4.21	4.21	4.47	4.21
22	-21.02	-19.96	4.24	3.99	4.24	3.99	4.24	3.99
23	-19.74	-18.71	3.98	3.74	3.98	3.74	3.98	3.74
24	-18.37	-17.38	3.70	3.48	3.70	3.48	3.70	3.48

TABLE 4.12

Radiant heat flow (W/m^2)
No glazing
Five exterior walls and floor

TIME	SOUTH WALL		NORTH WALL		ROOF		FLOOR	
	Proposed	N-L	Proposed	N-L	Proposed	N-L	Proposed	N-L
1	4.74	4.39	1.65	1.55	- 7.73	- 7.20	6.33	5.85
2	4.40	4.07	1.17	1.09	- 6.37	- 5.93	5.12	4.74
3	4.03	3.73	0.71	0.67	- 5.36	- 4.98	4.55	4.21
4	3.67	3.40	0.29	0.28	- 4.60	- 4.28	4.38	4.05
5	3.35	3.10	-0.1	-0.09	- 4.01	- 3.73	4.44	4.11
6	3.18	2.94	-0.5	-0.46	- 3.54	- 3.28	4.73	4.37
7	3.35	3.11	-0.9	-0,83	- 3.28	- 2.98	5.41	4.99
8	4.03	3.74	-1.04	-0.95	- 3.33	- 3.08	6.54	6.03
9	5.07	4.70	-0.54	-0.48	- 4.16	- 3.85	7.86	7.24
10	6.03	5.59	0.71	0.69	- 6.23	- 5.78	9.38	8.64
11	6.38	5.92	2.4	2.27	- 9.26	- 8.61	10.78	9.93
12	5.92	5.53	4.09	3.85	-12.97	-12.12	12.09	11.12
13	4.76	4.47	5.51	5.16	-17.0	-15.96	13.28	12.22
14	3.36	3.21	6.64	6.21	-20.8	-19.63	14.11	12.98
15	2.29	2.23	7.61	7.1	-23.9	-22.6	14.7	13.51
16	1.97	1.94	8.45	7.88	-25.8	-24.45	15.23	14.0
17	2.49	2.43	9.03	8.40	-26.5	-25.1	15.85	14.56
18	3.63	3.47	9.07	8.44	-25.7	-24.35	16.20	14.88
19	4.93	4.66	8.32	7.78	-23.68	-22.40	16.29	14.96
20	5.84	5.49	6.88	6.44	-20.7	-19.5	15.80	14.51
21	6.12	5.72	5.26	4.93	-17.4	-16.32	14.48	13.30
22	5.88	5.48	3.87	3.64	-14.3	-13.39	12.57	11.56
23	5.46	5.08	2.88	2.71	-11.67	-10.91	10.36	9.54
24	5.08	4.71	2.19	2.05	-9.50	- 8.86	8.17	7.54

4.8 COMPARISON BETWEEN CBS-MASS PROGRAM AND TNODE PROGRAM PREDICTIONS

The variation of the room air temperature for a step-function change of outdoor air temperature was analyzed using CBS-MASS and TNODE-4.0 programs. The room and the thermal conditions are presented in Chapter 4.5, case 1.

TNODE-4.0 program is a thermal network microcomputer program developed by the Energy Group at Georgia Technical Institute [91], and uses up to 20 nodes.

Figure 4.18 presents the comparison between the predictions of CBS-MASS and TNODE programs, and the analytical solution, which indicates good agreement between different models, with differences less than 10 percent.

4.9 FUNCTIONAL VALIDATION OF CBS-MASS PROGRAM

The functional validation deals with comparison between the estimations of the space thermal loads provided by the CBS-MASS program against the predictions of two well-known programs (BLAST and TARP) used in the thermal analysis of buildings. These two programs use similar algorithms to calculate the transient heat transfer through walls, based on the conduction transfer functions technique, while the CBS-MASS program uses numerical procedures to solve the heat transfer equation.

The comparison is performed on winter design day (December 21) for an intermediate level office space 30 x 30 x 3.6m, with four exterior

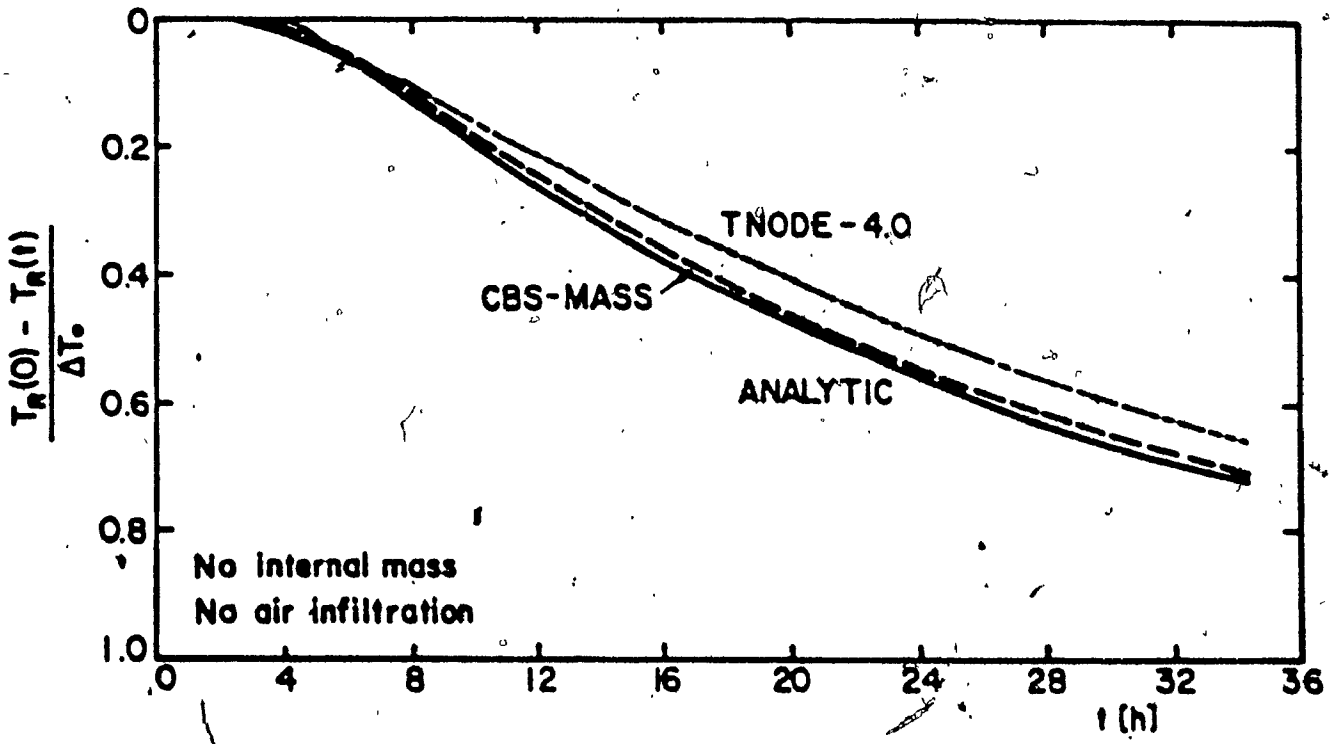

Fig. 4.18 Variation of the room air temperature due to step-function change in outdoor air temperature. Comparison between the analytical solution and the predictions of the CBS-MASS and TNODE programs.

walls (Table 4.13). The air temperature of the adjacent rooms is assumed to be either equal to the air temperature of the analyzed room (case 1) or equal to 19°C (case 2).

The weather data (outdoor dry bulb temperature and horizontal solar radiation) for December 21 in Montreal, used by the CBS-MASS, BLAST and TARP programs, are presented in Table 4.14.

The comparison for the first case (TRE=TR) shows that the BLAST and CBS-MASS programs provide close estimations of the peak heating load, with a difference of 1.65kW (2.8%), while the estimations of the TARP program are smaller than those provided by the BLAST program by 4.69kW (7.9%). (Fig. 4.19). The difference between the BLAST and CBS-MASS programs in estimating the daily total heating load is 5.6%, while the difference between the BLAST and TARP programs is 4.6%.

The comparison for the second case (TRE=19°C) shows differences in estimating the peak heating load of 0.5% between the BLAST and CBS-MASS programs, and of 7.8% between the BLAST and TARP programs (Fig. 4.20). The difference between the BLAST and CBS-MASS programs in estimating the daily total heating load is 1.9%, while the difference between the BLAST and TARP programs is 6.3%.

It is interesting to note that the differences between the estimations of the peak heating load provided by the BLAST and TARP programs, which use similar algorithms, are higher than the differences between the CBS-MASS and BLAST programs.

TABLE 4.13

Main Characteristics of the Intermediate Level Space

Exterior wall	0.10 m concrete 0.025 m air cavity 0.10 m insulation 0.02 m gypsum board glazing-to-wall ratio = 0.5 double glazing U = 2.8 $W/m^2 \cdot C$
Interior wall	0.01 m gypsum board 0.02 m insulation 0.01 m gypsum board
Air infiltration	1 ach
Occupancy	9:00 a.m. to 5:00 p.m.
Internal heat gains	people = 10 W/m^2 lights = 20 W/m^2
Room air temperature	20 ± 1°C

Continuous operation of HVAC system

TABLE 4.14

Weather Data for Design Day (December 21) in Montreal

Hour	Outdoor temperature (°C)	Horizontal solar radiation (W/m^2)	Direct normal radiation (W/m^2)
1	-18.05	-	-
2	-18.80	-	-
3	-19.40	-	-
4	-19.85	-	-
5	-20.00	-	-
6	-19.70	-	-
7	-18.95	-	-
8	-17.60	-	-
9	-15.65	73.1	398.1
10	-13.40	206.0	685.9
11	-10.85	303.1	794.5
12	-8.45	351.3	833.7
13	-6.65	346.3	830.0
14	-5.45	288.7	781.2
15	-5.00	183.6	652.7
16	-5.45	47.9	301.9
17	-6.50	-	-
18	-8.15	-	-
19	-10.10	-	-
20	-12.05	-	-
21	-13.70	-	-
22	-15.20	-	-
23	-16.40	-	-
24	-17.30	-	-
TOTAL (Wh/m^2)		1800.0	5278.0

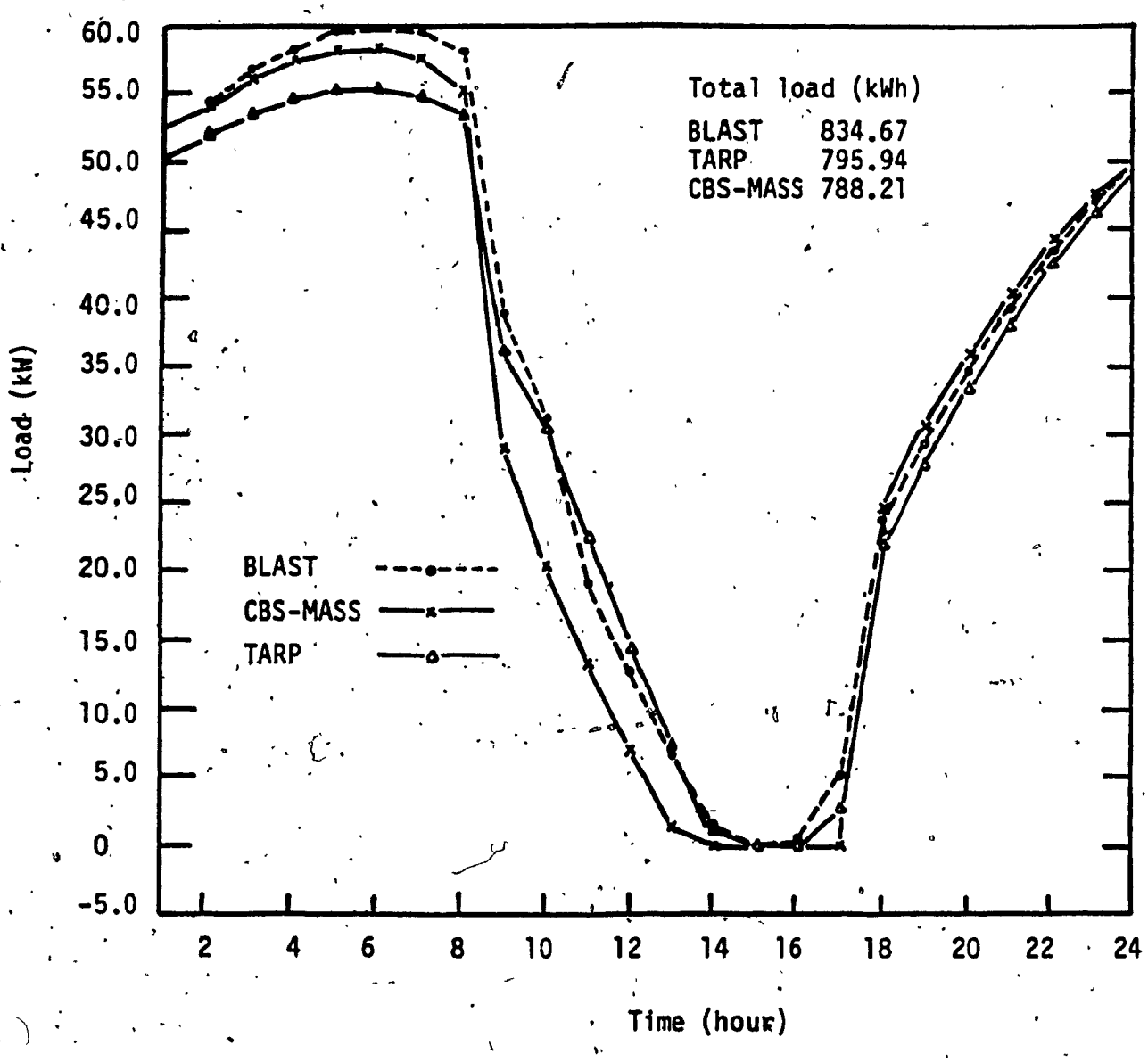

Fig. 4.19 Comparison between the predictions of CBS-MASS, BLAST and TARP programs. Case 1 (TRE = TR).

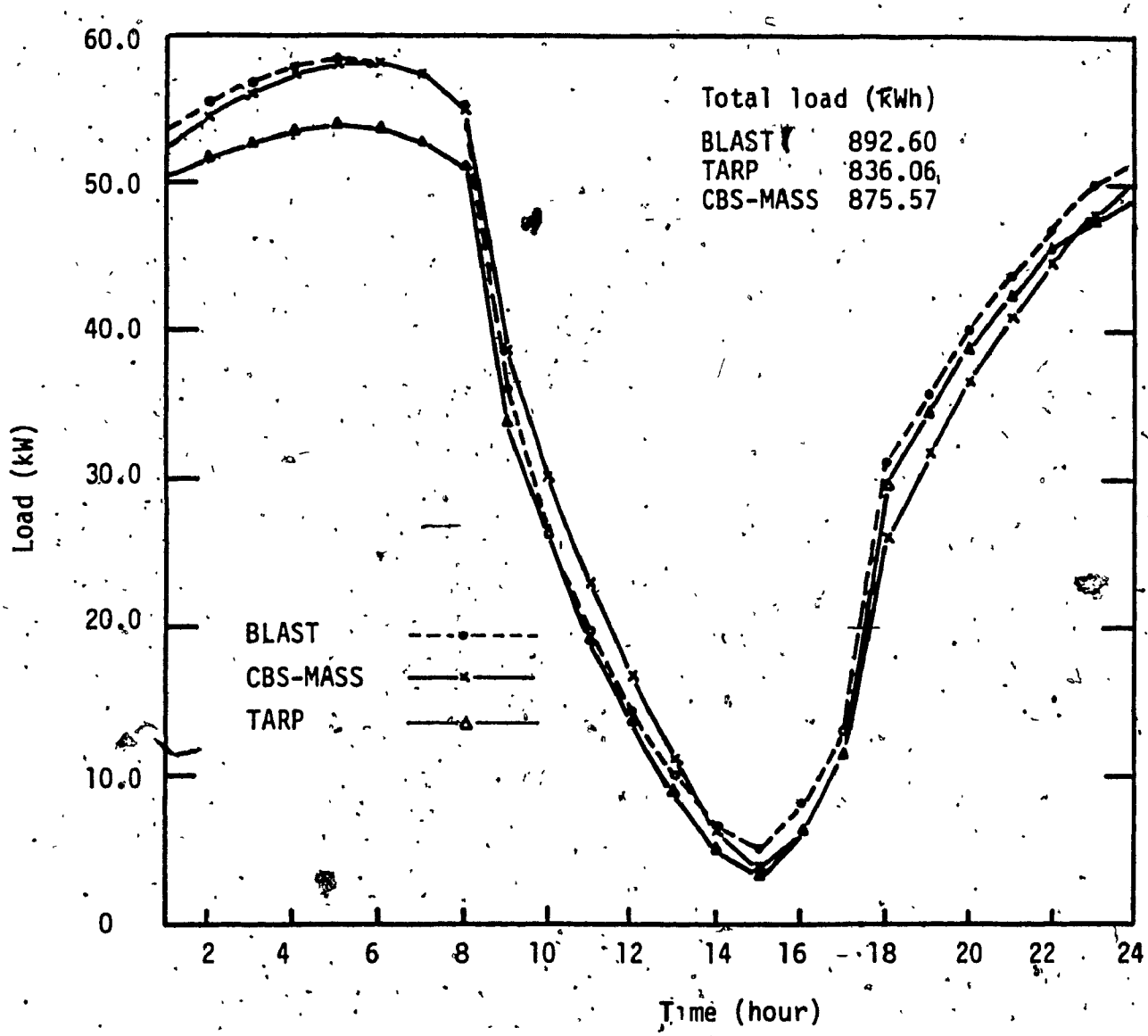

Fig. 4.20 Comparison between the predictions of CBS-MASS, BLAST and TARP programs. Case 2 (TRE = 19°C).

This functional validation shows that the CBS-MASS program provides estimations of the thermal behavior of rooms, which are very close to those of well-known and already validated programs such as BLAST and TARP.

4.10 CONCLUSIONS

From the analytical and functional validation of the CBS-MASS program the following conclusions have been drawn:

i) The heat transfer processes occurring in buildings are well simulated by the CBS-MASS program, since good agreement has been obtained between the analytical solutions and the results of the program

ii) When the comparison is carried out against analytical solutions, the computer programs should be modified to use the same assumptions as the analytical model.

iii) The comparison between the CBS-MASS, BLAST and TARP programs shows good agreement between the predictions of these programs. Hence the program developed during this research provides as good estimation of the thermal behavior of buildings as BLAST and TARP programs do.

CHAPTER 5

THERMAL ANALYSIS OF DESIGN ALTERNATIVES USING HOLLOW CORE SLABS

CHAPTER 5

THERMAL ANALYSIS OF DESIGN ALTERNATIVES USING HOLLOW CORE SLABS

The thermal performances of the design alternatives using the Hollow Core Slabs (HCS) on summer for reducing the cooling loads was carried out for an office building in Montreal.

The outdoor air is circulated through the Hollow Core Slab before it is introduced in the room (Fig. 5.1). At night the concrete slab is cooled, and by day it will act as a heat sink, reducing the cooling load of the room. Moreover, the concrete slab will act as a heat exchanger, reducing the temperature of the outdoor air to be introduced in the room.

Due to the modular structure of the CBS-MASS program, it is possible to compare three design alternatives under the same general conditions:

a) Hollow Core Slab design, where the outdoor air is circulated through the HCS before it is introduced in the room. No mechanical cooling system is used to keep the room under comfortable conditions.

b) Conventional design, where the outdoor air is directly introduced in the room. No mechanical cooling system is used.

c) Mechanical cooling design, where the HVAC system controls the room air temperature within given limits.

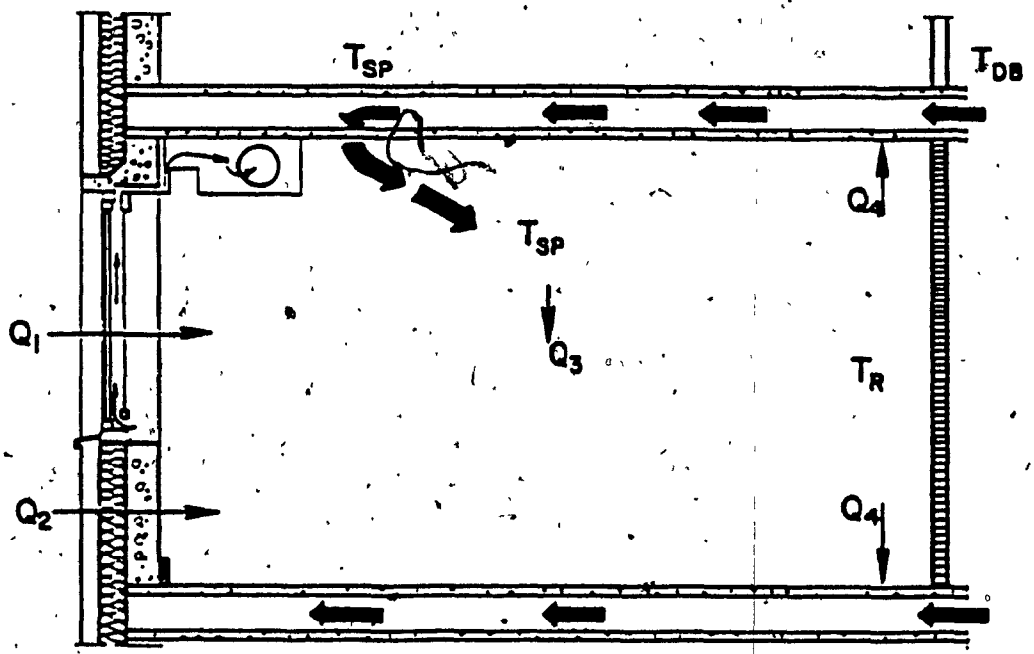

Fig. 5.1 Design alternative using Hollow Core Slab

Comparing the design alternatives a and b, the cooling effect of the Hollow Core Slab is obtained. The HVAC system is simulated for providing the room air temperature within the same limits as the hollow core design. The cooling load calculated for the design alternatives "c" represents the energy savings obtained by the Hollow Core Slab design.

The ventilation rate corresponds to four air changes per hour during occupation. The simulations were performed by the CBS-MASS program for Montreal on July 22, 1979 (Table 5.1), which was a sunny and warm day, with a daily temperature difference of 15°C.

A space at intermediate level in an office building is considered (Table 5.2). The Hollow Core Slab is approximated by two concrete plates of 0.15 m thickness, which bound an air space of 0.05 m.

5.1 CASE 1: OFFICE SPACE 6.0 x 6.0 x 3.6 m, SOUTH FACING (FIG. 5.2)

The building block approach is used to isolate the orientation effect, by considering an office space with an exterior wall facing South and three interior walls.

The air ventilation rate is increased twelve times between 11:00 p.m. and 7:00 a.m., for cooling the building structure.

TABLE 5.1

Weather data in Montreal, July 22, 1979

Hour	Dry bulb temperature (°C)	Total cloud amount	Solar radiation on horizontal plane (W/m^2)
1	18.3	0.2	-
2	18.3	0.1	-
3	17.2	0.1	-
4	16.1	0.2	-
5	15.0	0.2	-
6	17.2	0.2	115.0
7	18.3	0.2	272.2
8	20.6	0.1	422.2
9	23.9	0.1	581.4
10	25.6	0.1	706.9
11	26.7	0.2	805.8
12	28.3	0.2	858.1
13	28.9	0.2	810.6
14	29.4	0.2	803.6
15	30.0	0.5	727.8
16	29.4	0.4	605.8
17	28.3	0.4	426.7
18	27.2	0.7	283.6
19	26.7	0.9	50.0
20	24.4	0.6	2.2
21	21.7	0.3	-
22	23.3	1.0	-
23	22.8	1.0	-
24	18.3	0.3	-

TABLE 5.2

Main characteristics of office space where the Hollow Core Slab design is applied

Exterior wall	0.10 m concrete air cavity 0.10 m insulation 0.01 m gypsum board glazing-to-wall ratio 0.5 shading coefficient 0.5 window U-value 2.8 W/(m^2 °C)
Interior wall	0.01 m gypsum board 0.02 insulation 0.01 m gypsum board
Air infiltration	1 ach
Occupancy	9:00 a.m. to 5:00 p.m.
Internal heat gains	people 10 W/m^2 light 20 W/m^2

Air flow rate during the occupied hours corresponds to 4 ach.

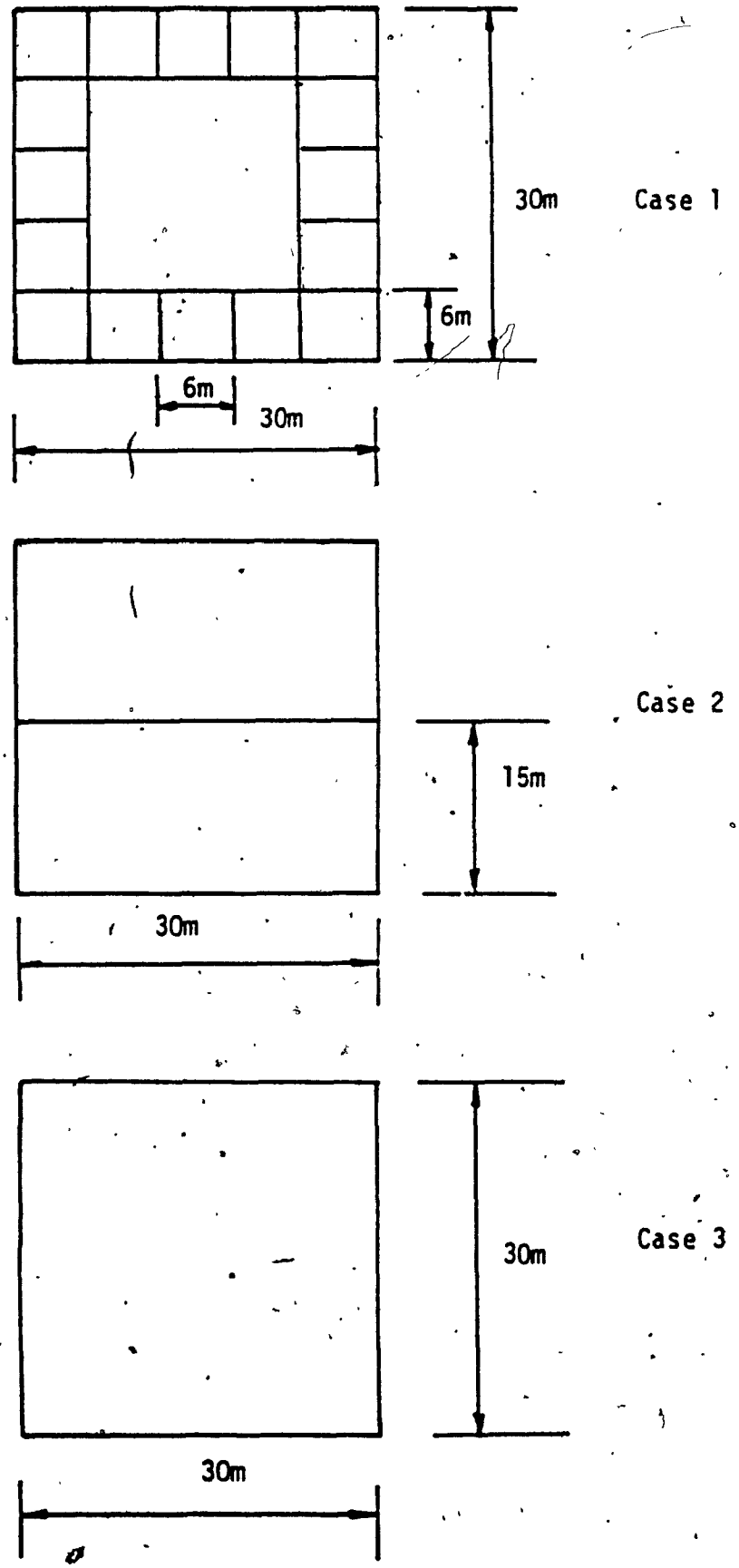

Fig. 5.2 Schema of office spaces used in the thermal analysis of the Hollow Core Slab design.

Figure 5.3 shows the room air temperature for the Hollow Core Slab design is lower, by about 3°C during the occupation, than for the conventional design. This is due to the following factors (Fig. 5.4-5.5):

- the floor and ceiling temperature is lower by about 2°C for the Hollow Core Slab design than for the conventional design,
- the supply air is cooler by 5-6°C than the outdoor air.

The thermal confort index (Fig. 5.6) indicates that during the occupation the people feel well ($-0.5 < PMV < 0.1$), when the Hollow Core Slab design is applied, while the conventional design will create too warm indoor conditions.

The Hollow Core Slab acts as a heat exchanger, cooling by day or heating at night the air which is circulated through it. The higher ventilation rate at night, the greater air temperature drop by day is obtained (Fig. 5.7). The maximum temperature difference between the air entering and the air leaving the Hollow Core Slab is betwen 3°C (ventilation rate is not increased at night) and 7°C (ventilation rate is increased at night 18 times). If the ventilation rate is increased, no significant increase in the temperature drop is obtained.

The heat storage capacity of the Hollow Core Slab is proportional with the daily temperature swing of the concrete plate. When the ventilation rate is not increased at night, the temperature swing is 2.5°C, for an average temperature of 25.3°C (Fig. 5.8). The increase of the ventilation rate at night by 6 to 18 times produces a

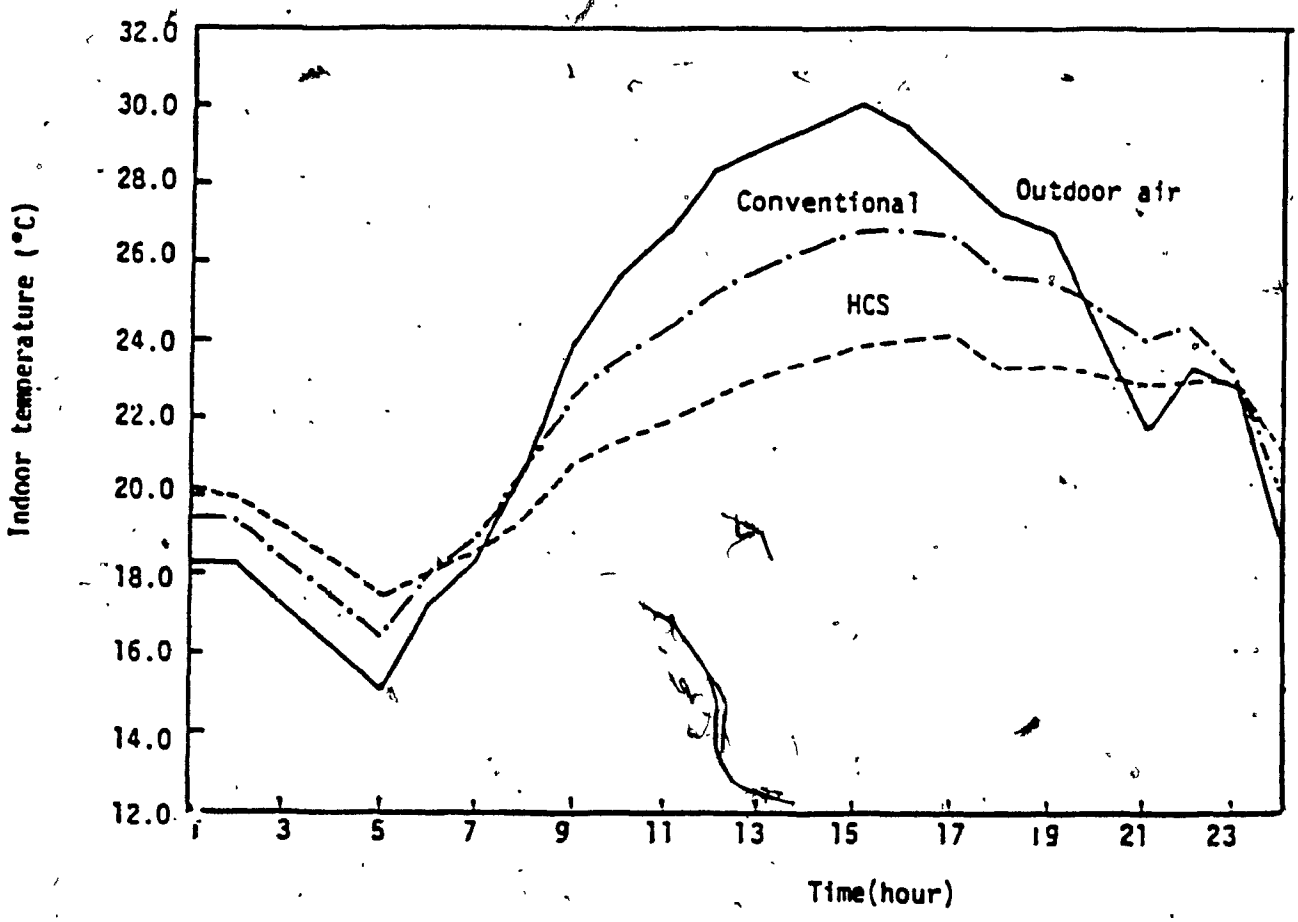

Fig. 5.3 Comparison between the Hollow Core Slab and the conventional design. Case 1.

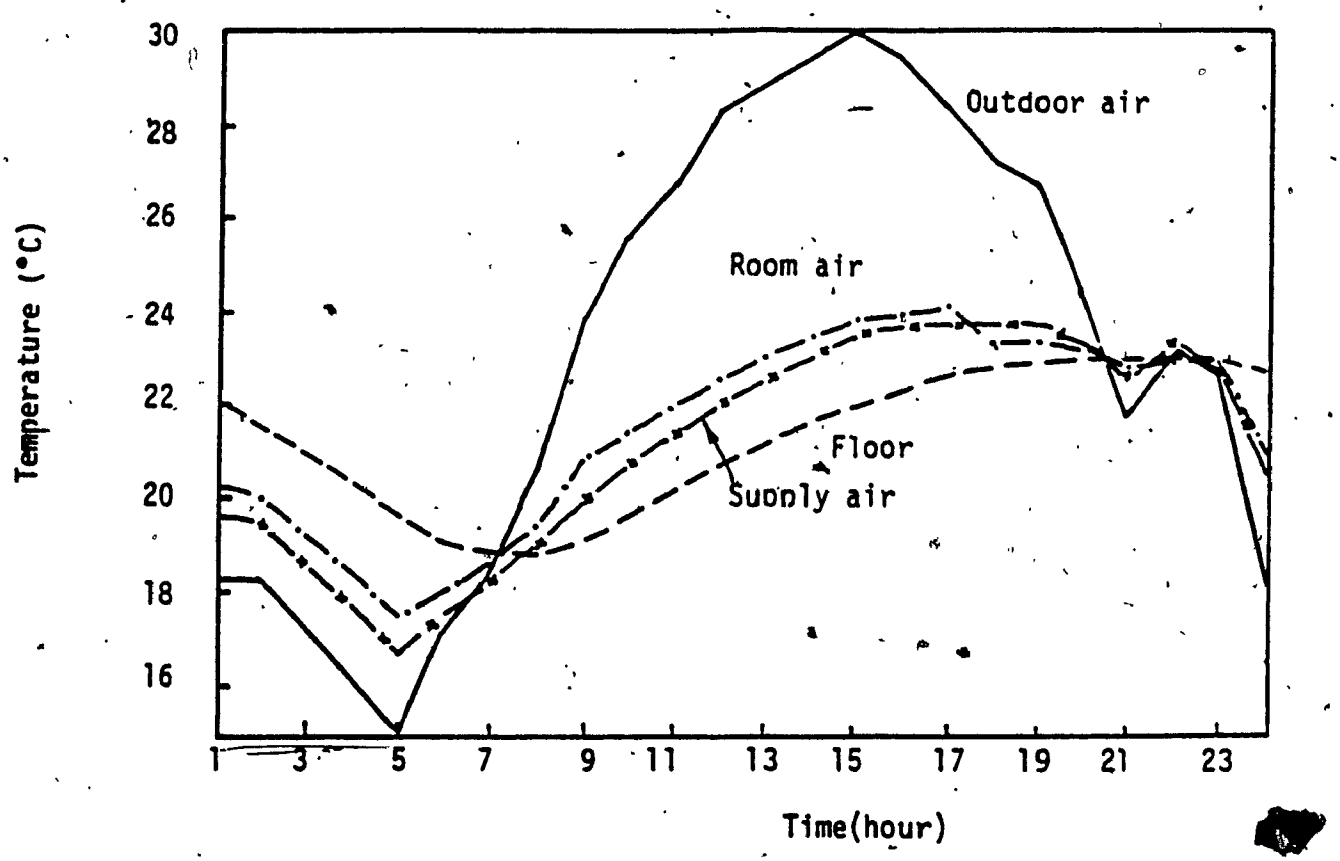

Fig. 5.4 Thermal behavior of the Hollow Core Slab design. Case 1.

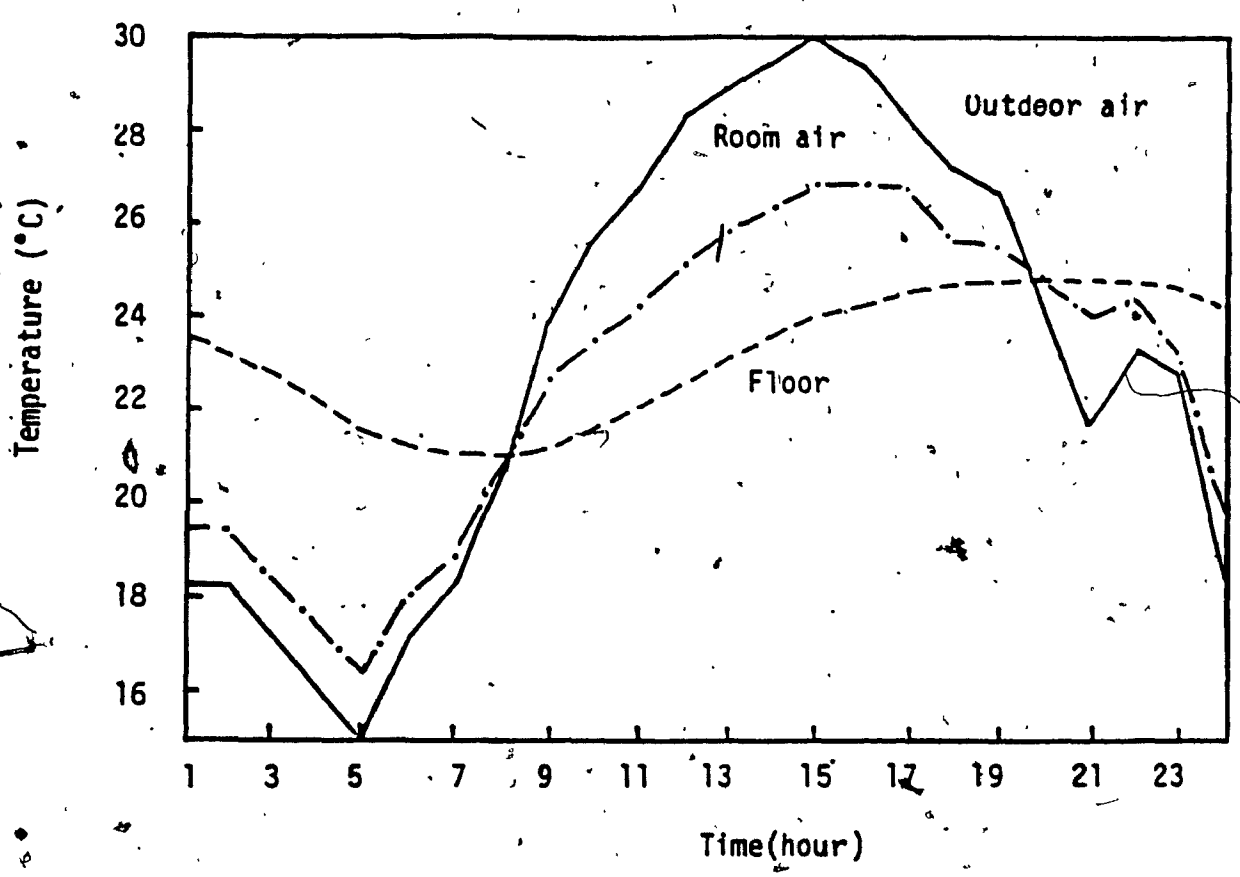

Fig. 5.5 Thermal behavior of the conventional design. Case 1.

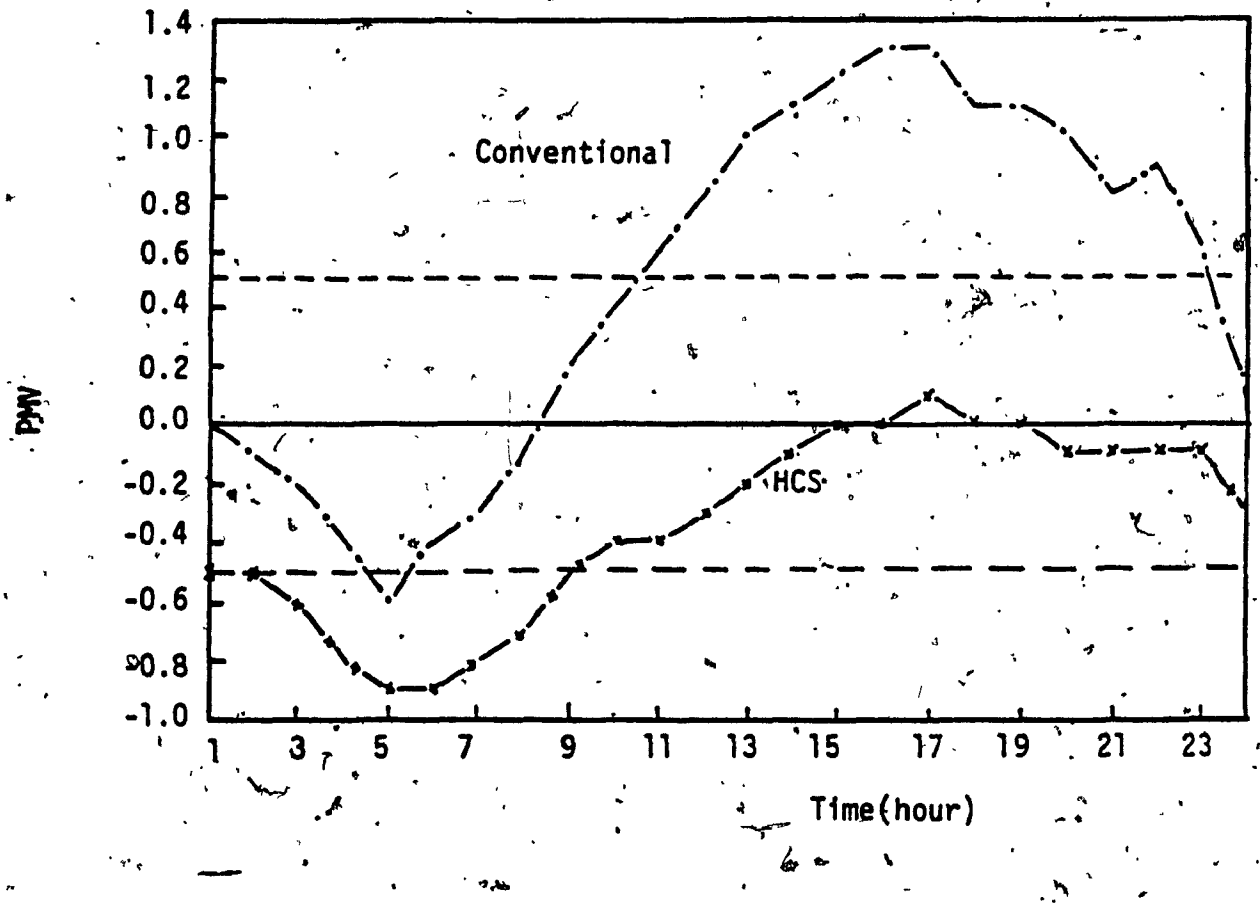

Fig. 5.6 Thermal comfort index. Case 1.

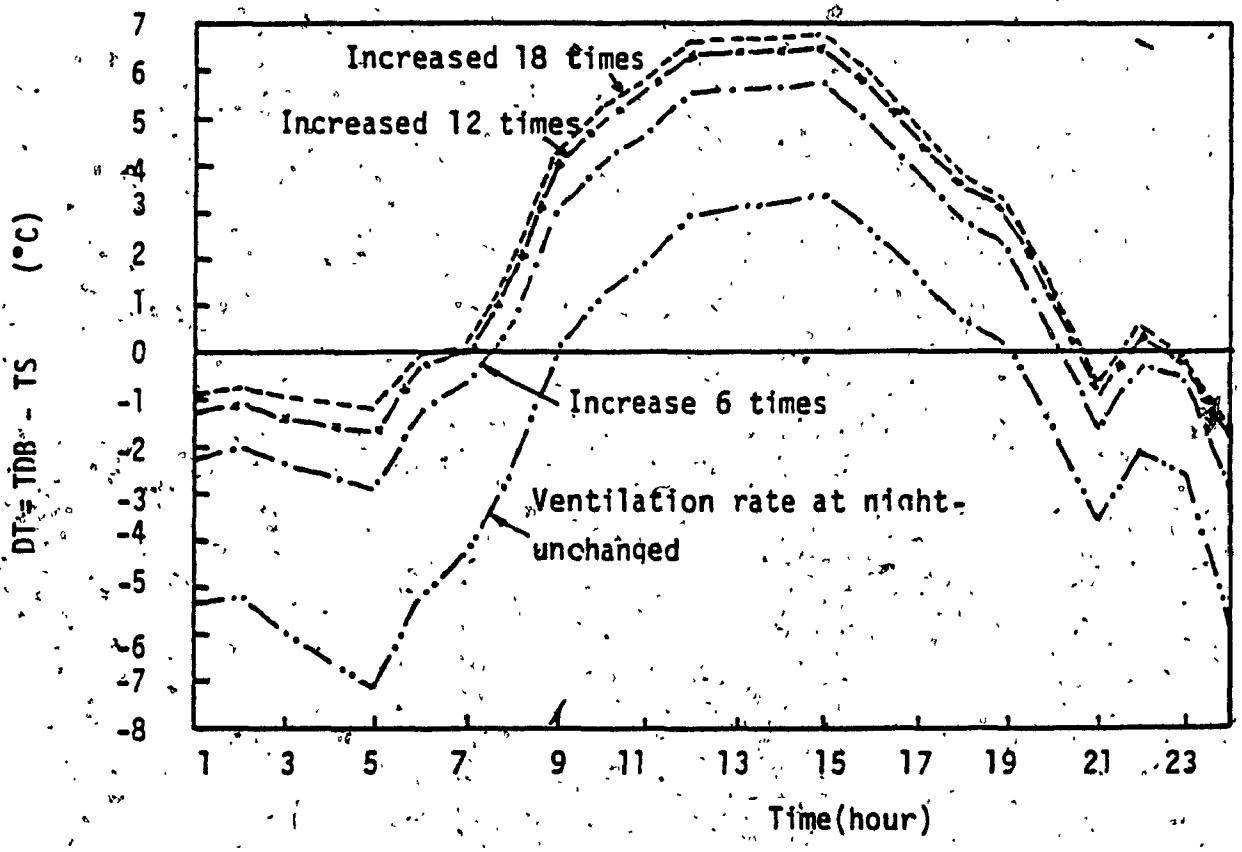

Fig. 5.7 Air temperature drop DT within the hollow core slab, as difference between the entering temperature TDB and the leaving temperature TS. Case 1.

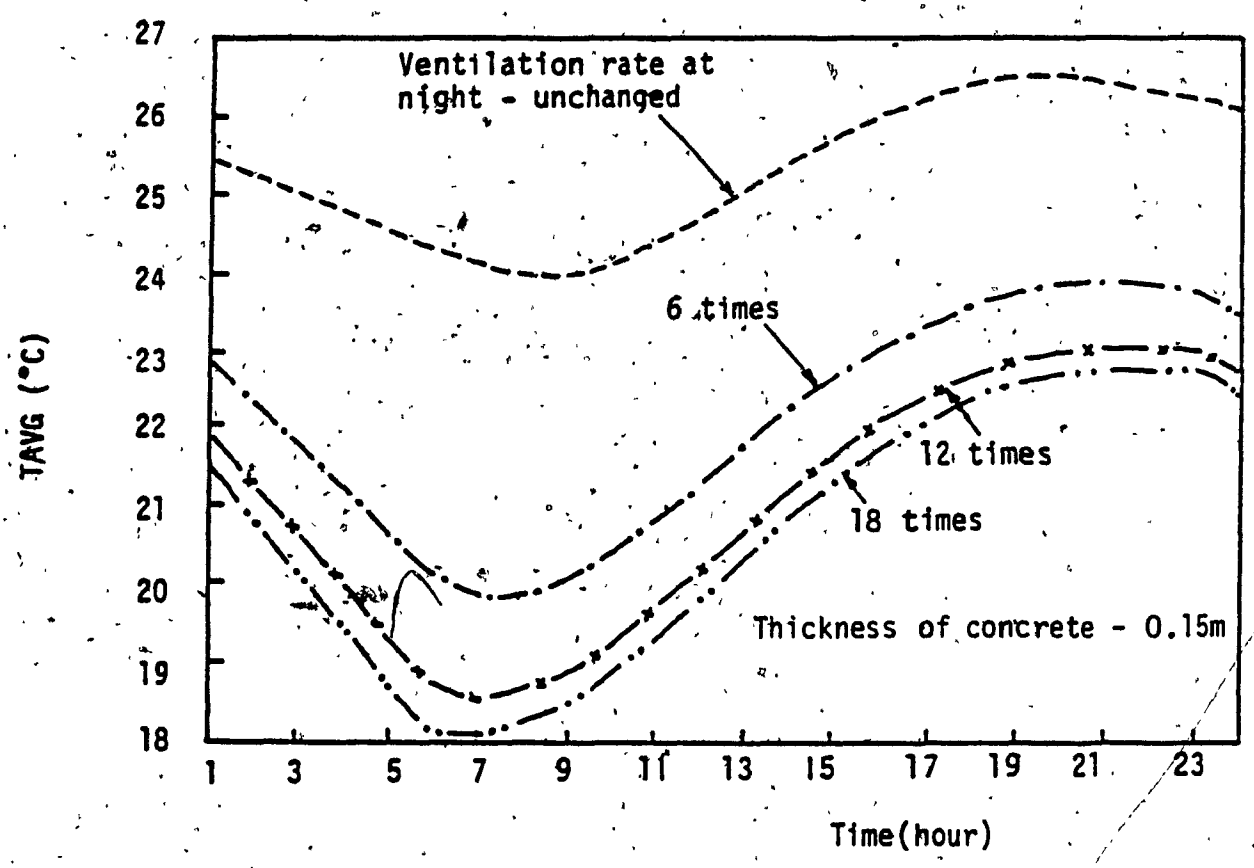

Fig. 5.8 Variation of HCS temperature vs. ventilation rate. Case 1.

temperature swing of 4 - 4.7°C, for an average temperature of 20.7 to 22.1°C. Hence, the heat storage capacity of the Hollow Core Slab is increased by about 100 percent when the ventilation rate is increased at night.

The increase of the concrete plate thickness from 0.10 to 0.25 m reduces the daily temperature swing from 6°C to 3°C, while the average temperature is almost unchanged (21 - 21.2°C) (Fig. 5.9).

The cooling effect of the Hollow Core Slab design is obtained as a difference between the cooling loads of the design alternatives "a" and "b", to keep the room air temperature at a reference value (TREF):

$$Q_{HCS} = \frac{1}{(t_2-t_1)S} \sum_{t_1}^{t_2} [\dot{m}\, c\, (TR^{CONV} - TREF) - \dot{m}\, c\, (TR^{HCS} - TREF)] =$$

$$\frac{1}{(t_2-t_1)S} \sum_{t_1}^{t_2} \dot{m}\, c\, (TR^{CONV} - TR^{HCS}) \qquad (5.1)$$

where

Q_{HCS} - is the cooling effect of the Hollow Core Slab design (W/m^2),

t_2-t_1 is the occupancy duration,

$S = S_{floor} + S_{ceiling}$, and

$\dot{m}$ - is the air flow rate during the occupation

The variation of the cooling effect versus the ventilation rate and the thickness of the concrete plate is presented in Figure 5.10.

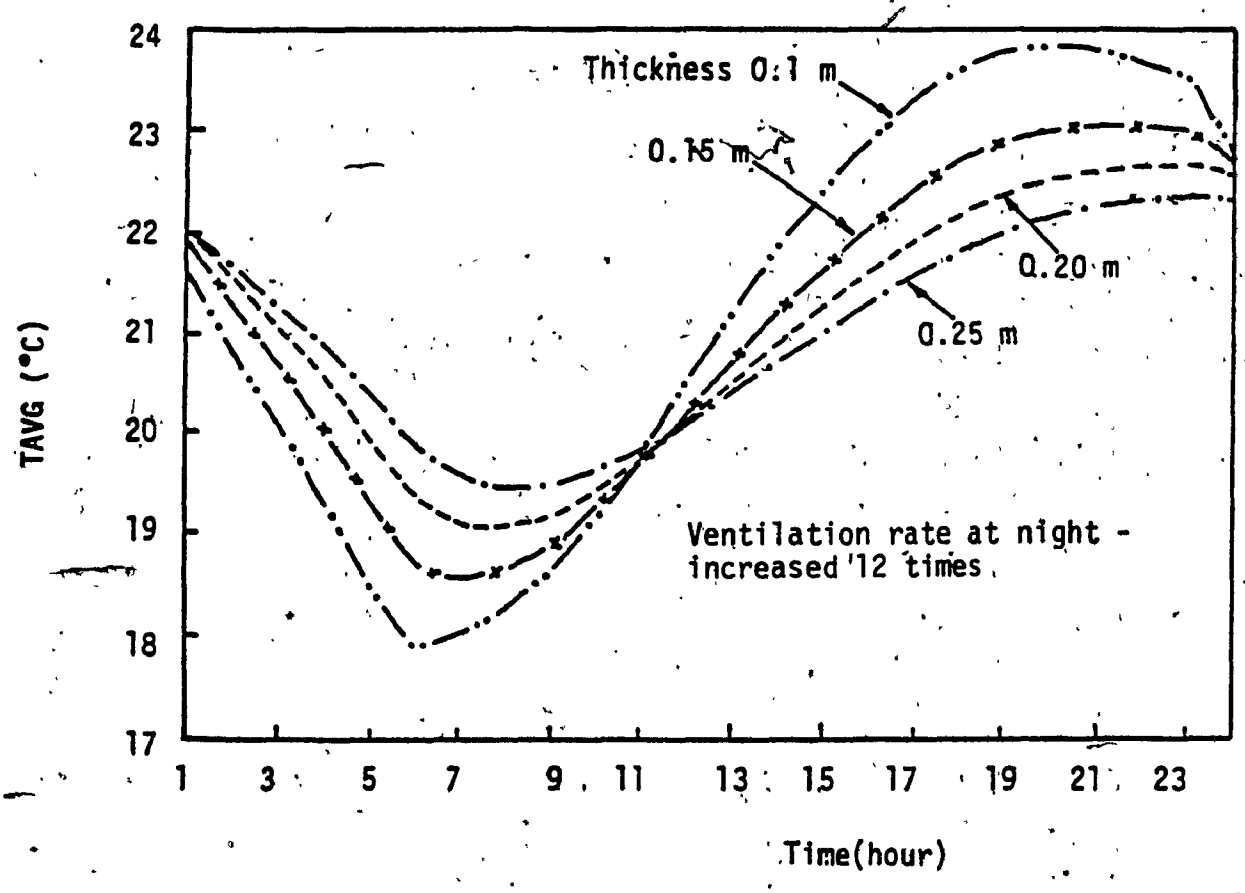

Fig. 5.9 Variation of HCS temperature vs. concrete thickness. -- Case 1.

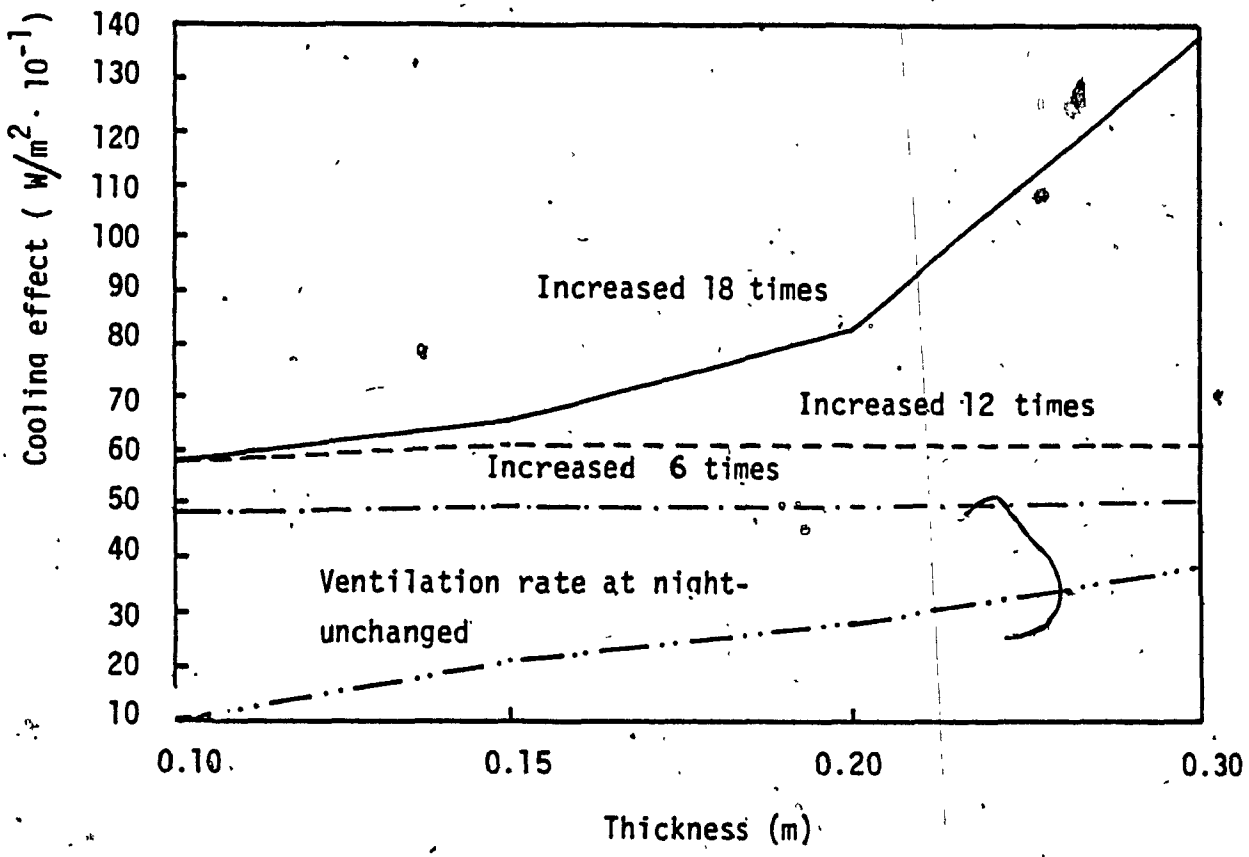

Fig. 5.10 Cooling effect of HCS design vs. conventional design. Case 1.

When the ventilation rate is increased at night by 6 to 12 times, the thickness does not influence the cooling effect. For light structures (< 0.15 m) the increase of the ventilation rate more than 12 times does not affect the cooling effect, while for heavy structures (0.20-0.30 m) the same increase will modify the cooling effect by 260 percent, from 3.8 W/m^2 to 13.7 W/m^2.

The index PMV which defines the thermal behavior of the Hollow Core Slab design is presented in Table 5.3 in terms of the ventilation rate at night and the thickness of the concrete plate. The temperature swing of the room air over 24 hours varies between 3.8 to 7.9°C, while the variation over the occupation is between 1.6 to 4.3°C. The temperature swing of the Hollow Core Slab over 24 hours varies between 1.47 and 6,26°C. Considering the people wear typical office suits (thermal resistance of clothing is 1.0 clo), the highest ventilation rate will create discomfort during the first hours of occupation.

TABLE 5.3

Temperature variation (°C) and thermal comfort index, PMV, for HCS design. Case 1

Ventilation rate at night	Thickness (m)			
	0.1	0.15	0.2	0.3
x 1				
DT room occup	2.9	2.5	2.3	2.1
DT room day	4.4	4.1	3.9	3.8
DT HCS	3.24	2.54	2.07	1.47
PMV (Icl = 0.7)	-0.1,..,0.5	-0.2,..,0.4	-0.2,..,0.3	-0.3,..,0.1
x 6				
DT room occup	3.9	3.1	2.6	2.3
DT room day	6.6	5.9	5.5	5.2
DT HCS	5.33	4.06	3.23	2.15
PMV (Icl = 0.7)	-0.1,..,-1.0	-0.2,..,-0.9	-0.3,..,-0.8	-0.3,..,-0.8
PMV (Icl = 1.0)	-0.4,..,0.3	-0.3,..,0.2	-0.3,..,0.2	-0.3,..,0.1
x 12				
DT room occup	4.2	3.3	2.8	2.4
DT room day	7.5	6.6	6.3	6.1
DT HCS	5.95	4.5	3.62	2.42
PMV (Icl = 0.7)	-0.3,..,-1.2	-0.4,..,-1.1	-0.5,..,-1.1	-0.5,..,-1.0
PMV (Icl = 1.0)	-0.6,..,0.2	-0.5,..,0.1	-0.5,..,0	-0.4,..,0
x 18				
DT room occup	4.3	3.4	2.7	1.6
DT room day	7.9	7	6	4.9
DT HCS	6.26	4.74	3.54	1.72
PMV (Icl = 0.7)	-0.4,..,-1.3	-0.5,..,-1.2	-0.8,..,-1.3	-1.4,..,-1.7
PMV (Icl = 1.0)	-0.7,..,0.1	-0.6,..,0	-0.6,..,0	-0.5,..,-0.1

DT room - maximum variation of the room air temperature
DT HCS - maximum variation of the hollow core slab temperature
I_{cl} - thermal resistance of clothing

From the thermal comfort point of view, the ventilation rate can be increased at night up to 12 times, for thickness of concrete plate greater than 0.15 m.

The heat storage capacity of the hollow core slab is given by the following relation:

$$Q_{ST} = \frac{m\ c\ DT_{SW}}{S} = \rho\ \delta_1\ cp\ DT_{sw} \qquad (5.2)$$

where

Q_{ST} - storage capacity (kJ/m^2)

DT_{SW} - temperature swing of the concrete plate (°C)

δ_1 - thickness of the concrete plate (m)

ρ, cp - density (kg/m^3) and specific heat (kJ/kg°C) of the concrete plate

Table 5.4 presents the heat storage capacity of the Hollow Core Slab, for this particular case, in terms of the ventilation rate at night and the thickness of the concrete plate. The values are between 490 and 1090 kJ/m^2, comparing with the general value of 1200 kJ/m^2 indicated by Svenberg [23].

The analysis of the HVAC system shows cooling loads between 29.2 W/m^2 (for 24 hours operation) and 24.4 W/m^2 (for 9 hours operation and 15 hours natural convective cooling). Hence, the Hollow Core Slab system provides savings of about 20 - 30 W/m^2.

TABLE 5.4

Heat storage capacity of HCS (kJ/m^2). Case 1

$\dot{m}$ \ δ_1	0.10 m	0.15 m	0.20 m	0.30 m
x 1	487	572	622	662
x 6	801	915	970	969
x 12	894	1014	1087	1091
x 18	940	1068	1063	775

5.2 CASE 2. OFFICE SPACE 30.0 x 15.0 x 3.6 m. SOUTH FACING (FIG. 5.2)

The air ventilation rate is increased three times between 23:00 p.m. and 7:00 a.m. for cooling the building structure.

Figure 5.11 shows the variation of the room air temperature for the design alternative "a" (HCS) and "b" (conventional design). Due to large glazing surfaces, the Hollow Core Slab has smaller effect than in the previous case, the maximum room air temperature being now 27°C, while for the case #1 was about 24°C. However, the room air temperature for the hollow core slab design is lower by about 3°C than for the conventional design. The floor and ceiling temperature is lower by about 2°C for the Hollow Core Slab design than for the conventional design (Fig. 5.12 - 5.13).

The thermal comfort index (Fig. 5.14) shows that during the occupation, the people feel well ($-0.5 < PMV < 0.3$) because of application of the Hollow Core Slab.

The maximum temperature drop of the air circulating through the hollow core slab is between 3°C (ventilation rate is not increased at night) and 7°C (ventilation rate is increased six times at night) (Fig. 5.15).

Figure 5.16 shows the cooling effect of the Hollow Core Slab based on the comparison between the HCS design and the conventional design.

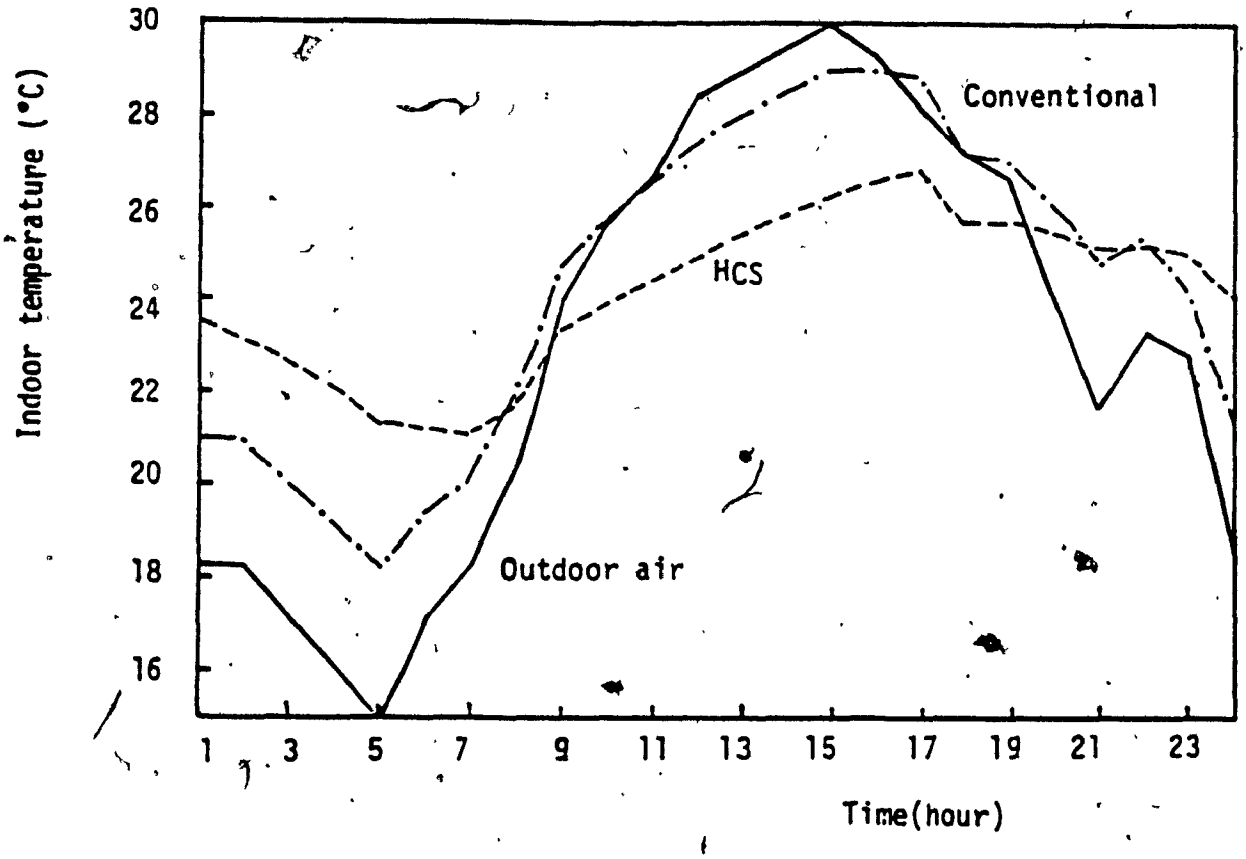

Fig. 5.11 Comparison between the hollow core slab and the conventional design. Case 2.

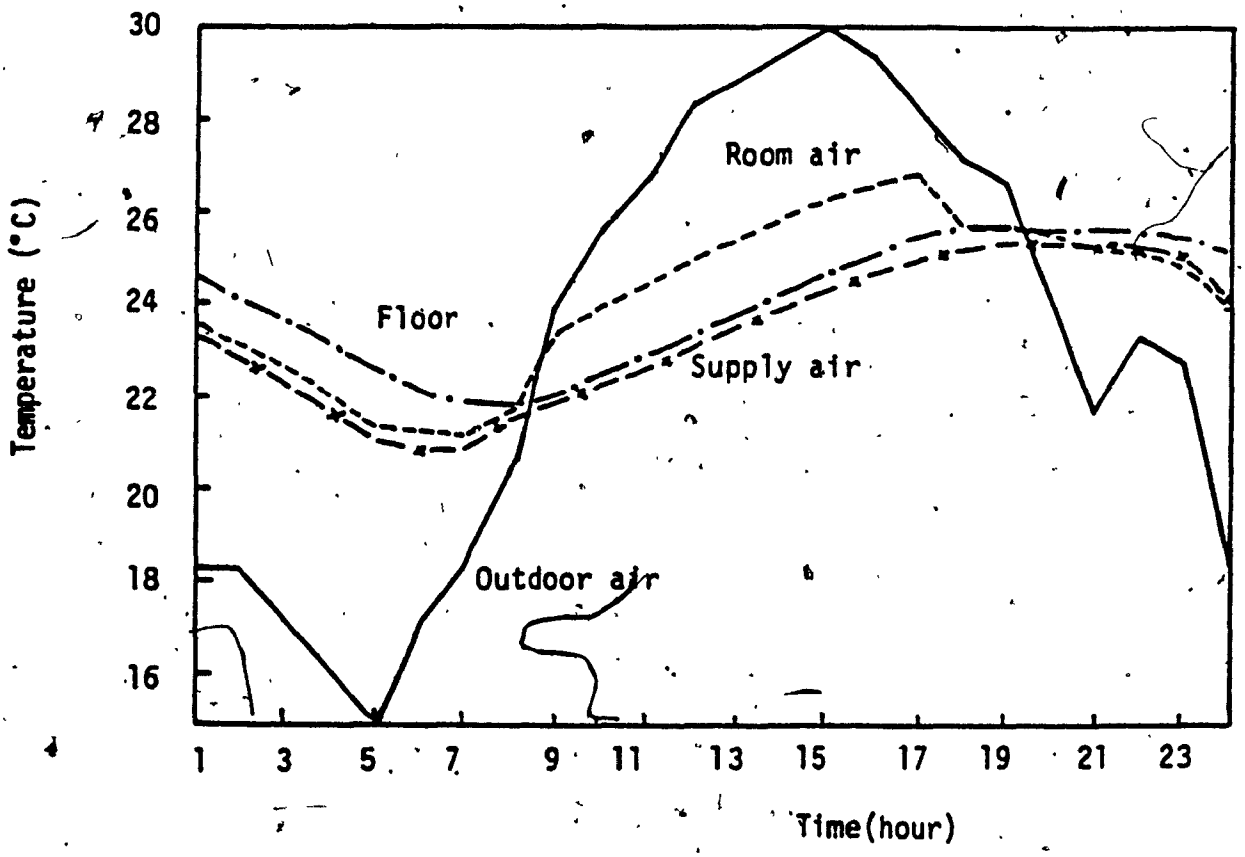

Fig. 5.12 Thermal behavior of the hollow core slab design. Case 2.

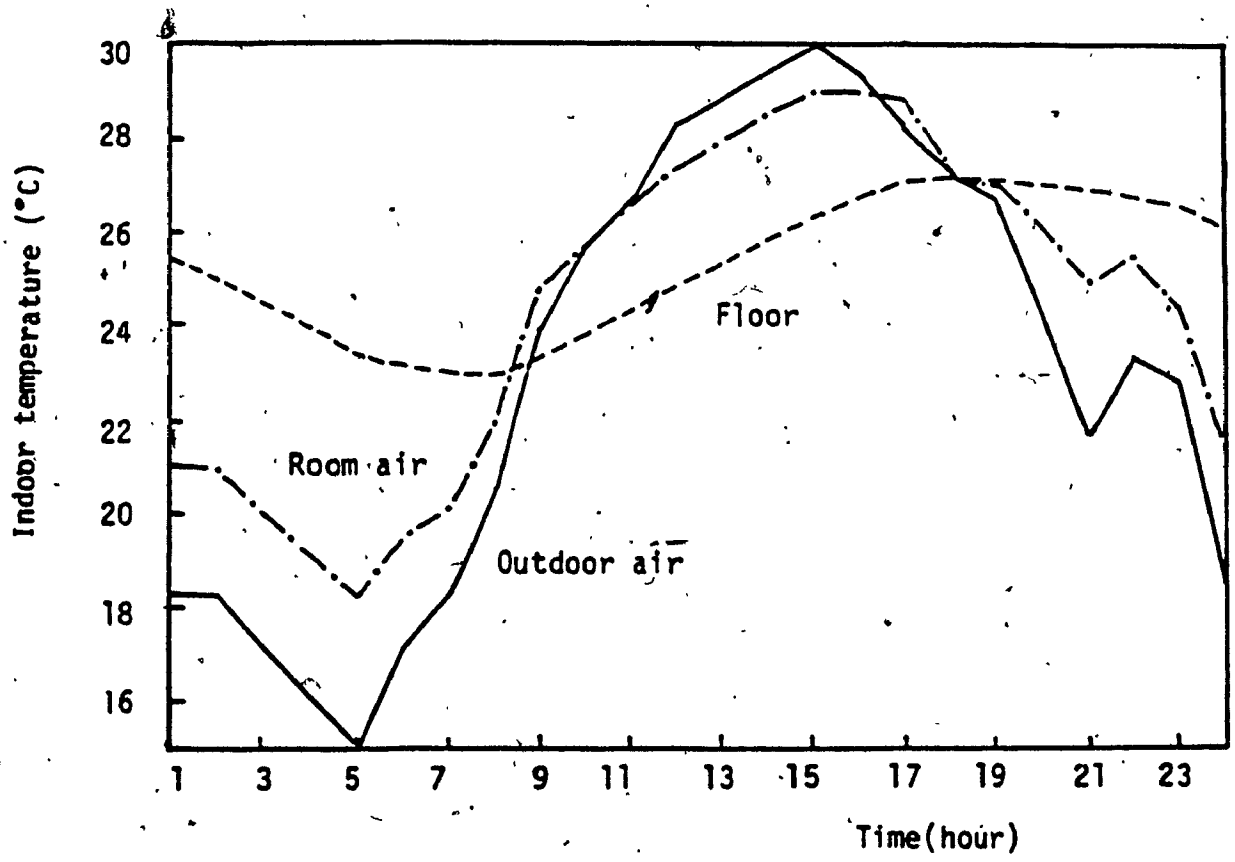

Fig. 5.13 Thermal behavior of the conventional design. Case 2.

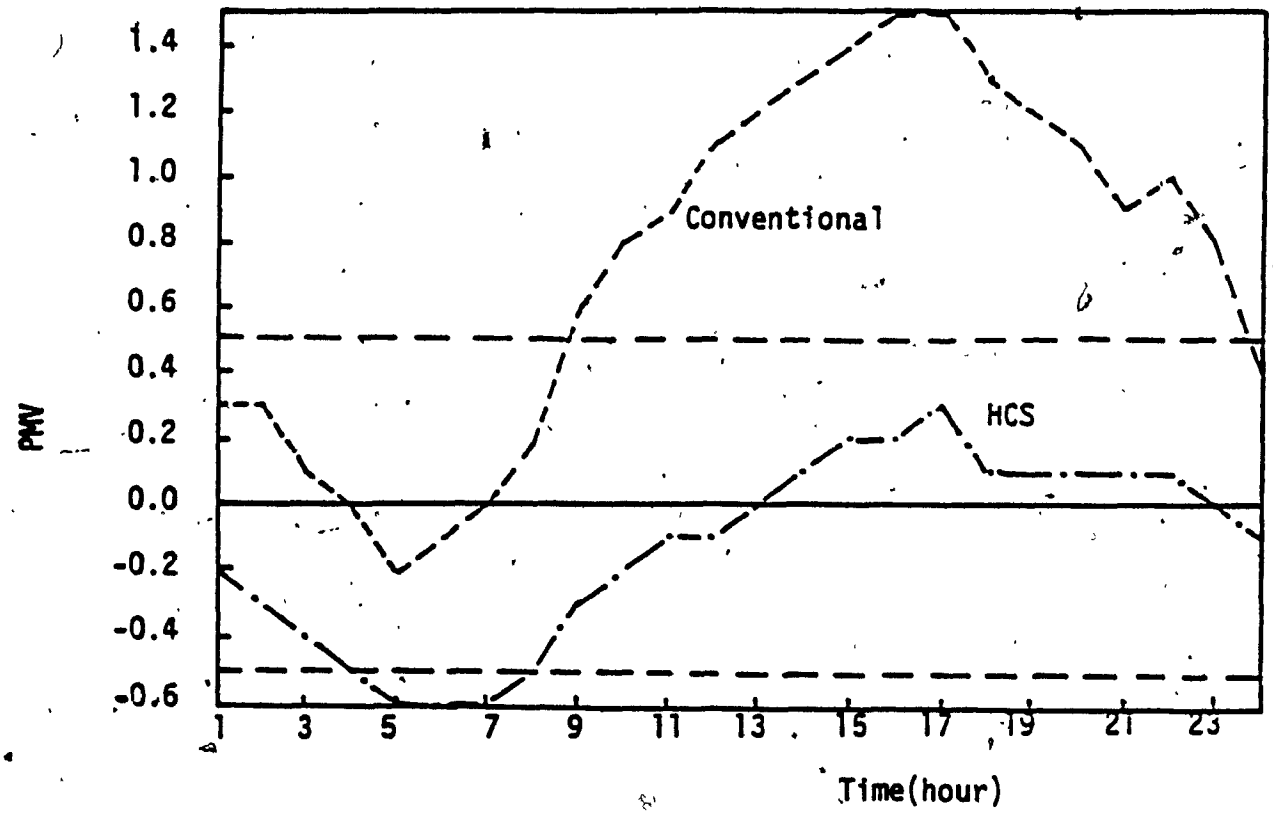

Fig. 5.14 Thermal comfort index. Case 2.

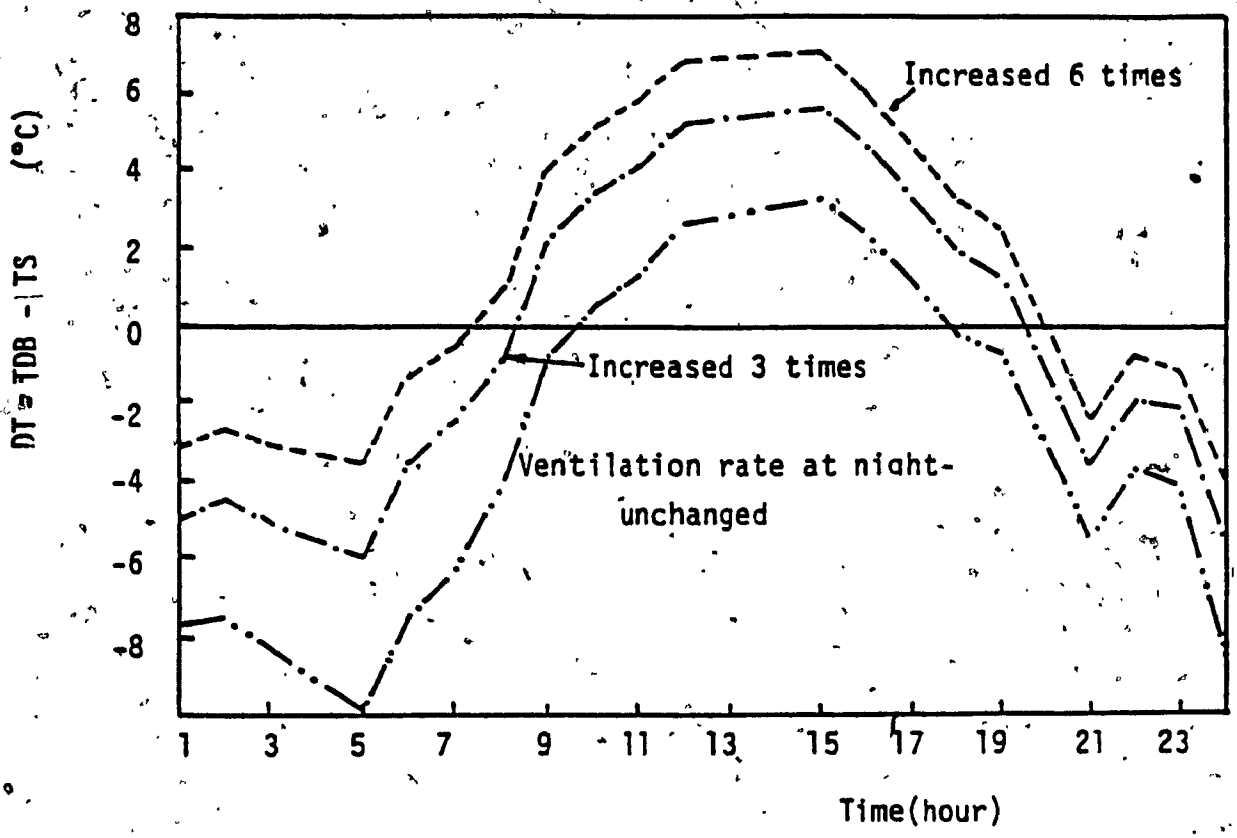

Fig. 5.15 Air temperature drop DT within the hollow core slab, as difference between the entering temperature TDB and the leaving temperature TS. Case 2.

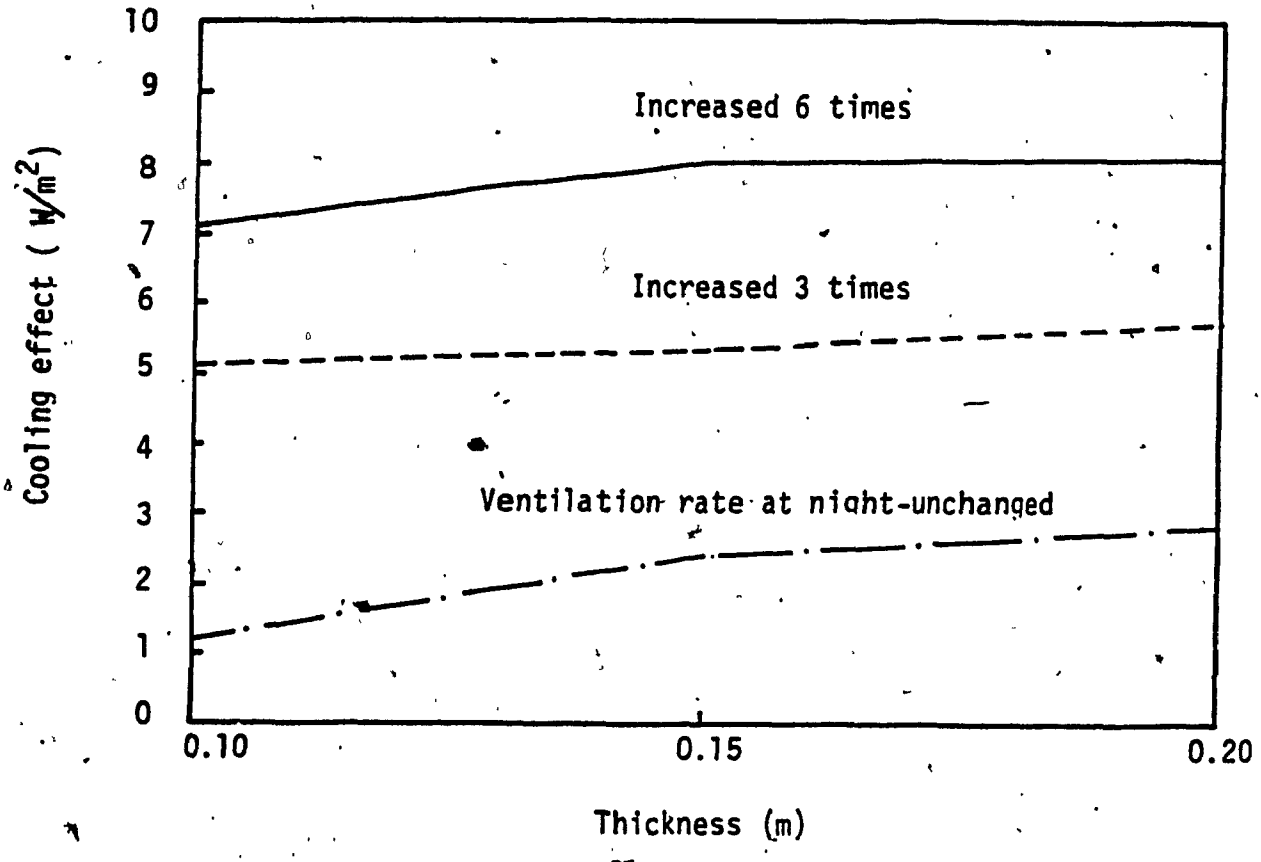

Fig. 5.16 Cooling effect of HCS design vs. conventional design. Case 2.

The modification of the thickness of concrete plate has a small effect, while the increase of the ventilation rate at night by six times changes the cooling effect from 2 W/m^2 to 8 W/m^2.

The parameters defining the thermal behavior of the Hollow Core Slab design are presented in Table 5.5 in terms of the ventilation rate, the thickness of the concrete plate and the shading coefficient of glazing. The temperature swing of the room air over the occupation varies between 2.3°C and 5.4°C, while the temperature swing of the concrete plate over 24 hours varies between 2.25°C and 7.28°C. The analysis of the thermal comfort index shows:

- People feel warm when the ventilation rate is not increased at night (PMV > 0.5)
- When the ventilation rate is increased three times at night, comfortable indoor conditions are obtained in the space for the shading coefficients 0.5 and 0.75, except for the case of thin concrete plate (0.10 m) and SC=0.75. For this case, the storage capacity of the Hollow Core Slab is not sufficient to cool the room by day.
- When the ventilation rate is increased six times at night, comfortable indoor conditions are obtained using concrete plate of 0.20 m (SC=0.5) and 0.15 m (SC=0.75).

TABLE 5.5

Temperature variation (°C) and thermal comfort index, PMV, for HCS design. Case 2

Ventilation rate at night	Tickness (m)		
	0.1	0.15	0.2
x 1			
SC = 0.5			
DT room occup	3.4	2.7	2.3
DT HCS	3.76	2.8	2.25
PMV (Icl = 1.0)	0.1,..,0.8	0.2,..,0.6	0.1,..,0.6
x 3			
SC = 0.5			
DT room occup	4.5	3.4	2.7
DT HCS	5.83	4.21	3.29
PMV (Icl = 1.0)	-0.4,..,0.4	-0.3,..,0.3	-0.3,..,0.2
SC = 0.75			
DT room occup	4.9	3.6	3
DT HCS	6.4	4.57	3.55
PMV (Icl = 1.0)	-0.3,..,0.6	-0.2,..,0.4	-0.2,..,0.3
x 6			
SC = 0.5			
DT room occup	5.1	3.8	3.1
DT HCS	6.86	5.05	3.92
PMV (Icl = 1.0)	-0.7,..,0.2	-0.6,..,0.1	-0.5,..,0
SC = 0.75			
DT room occup	5.4	4.2	3.3
DT HCS	7.28	5.53	4.24
PMV (Icl = 1.0)	-0.6,..,0.3	-0.5,..,0.2	-0.5,..,0.1

DT room - maximum variation of the room air temperature
DT HCS - maximum variation of the hollow core slab temperature
I_{cl} - thermal resistance of clothing
SC - shading coefficient

Table 5.6 presents the heat storage capacity of the Hollow Core Slab in terms of the ventilation rate at night and the thickness of the concrete plate. The values are between 560 and 1270 kJ/m^2, comparing with the general value of 1200 kJ/m^2 indicated by Svenberg [23].

The comparison between the Hollow Core Slab design and the HVAC design shows that the HCS system provides savings of about 49 W/m^2.

5.3 CASE 3: OFFICE SPACE 30.0 x 30.0 x 3.6 m (FIG. 5.2)

The air ventilation rate is increased three times at night, between 23:00 p.m. and 7:00 a.m. Figure 5.17 shows the variation of the room air temperature for the Hollow Core Slab design and the conventional design. The room air is warmer by about 0.5°C during the occupation, than in the previous case. The floor and ceiling temperature is lower by about 2°C for the Hollow Core Slab design than for the conventional design (Fig. 5.18 - 5.19).

The thermal comfort index (Fig. 5.20) shows that during occupation, the people feel well ($-0.4 < PMV < 0.4$), because of application of the Hollow Core Slab.

Comparing the design alternatives "a" (HCS) and "b" (conventional design) it obtains a cooling effect of 4.9 W/m^2, and the comparison between the design alternatives "a" (HCS) and "c" (HVAC) shows energy savings of 42 W/m^2.

TABLE 5.6

Heat storage capacity of HCS (kJ/m^2). Case 2

$\dot{m}$ \ δ	0.10 m	0.15 m	0.20 m
x 1 SC=0.5	565	631	676
x 3 SC=0.5	876	949	988
SC=0.75	961	1030	1066
x 6 SC=0.5	1030	1138	1178
SC=0.75	1093	1246	1274

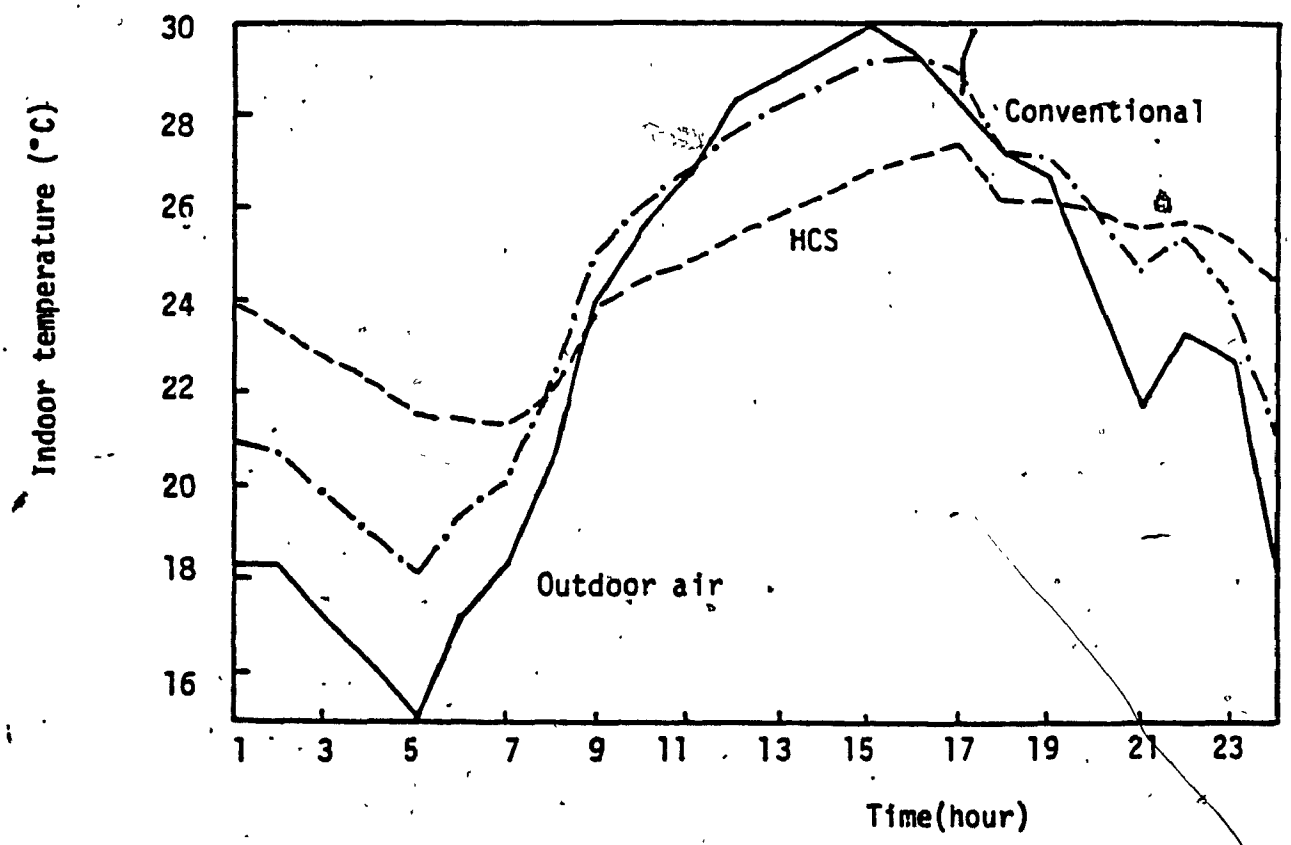

Fig. 5.17 Comparison between the hollow core slab and the conventional design. Case 3.

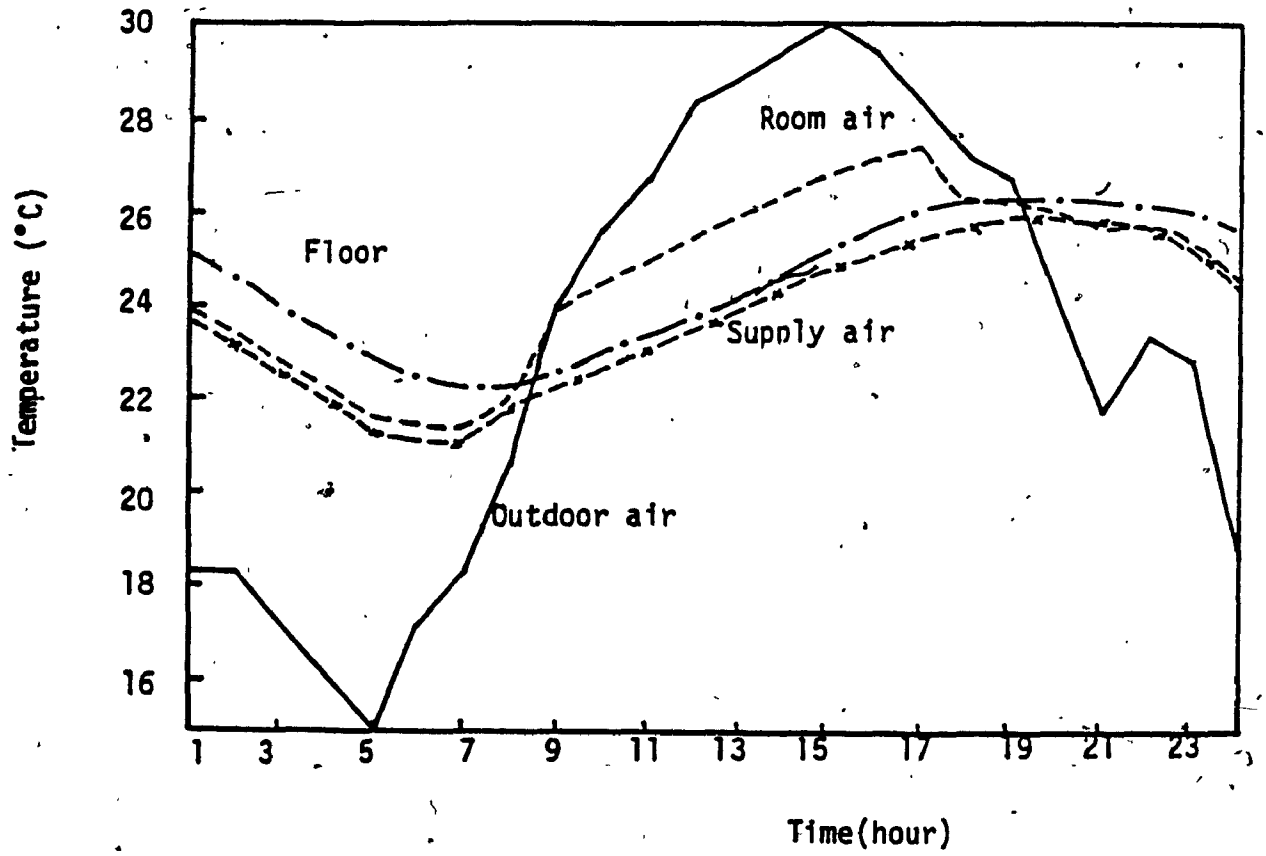

Fig. 5.18 Thermal behavior of the hollow core slab design. Case 3.

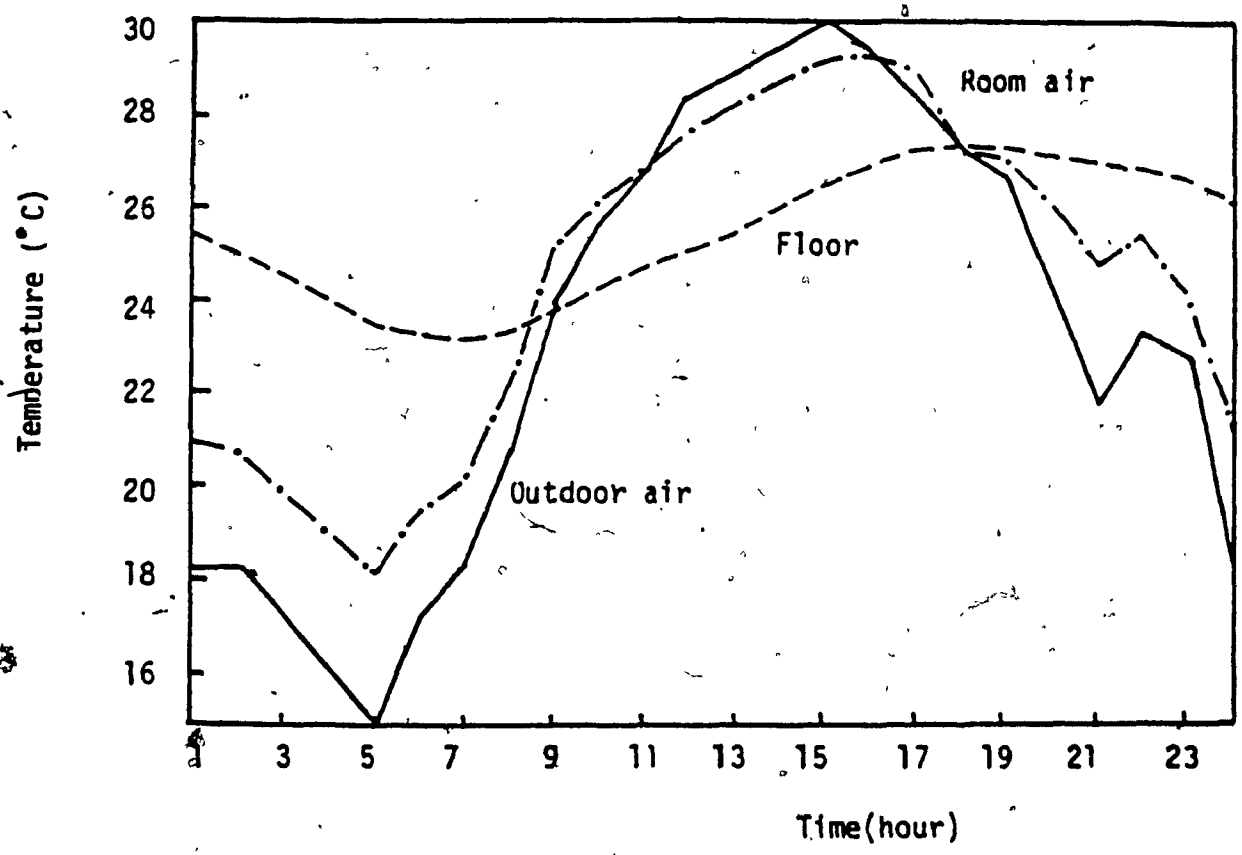

Fig. 5.19 Thermal behavior of the conventional design. Case 3.

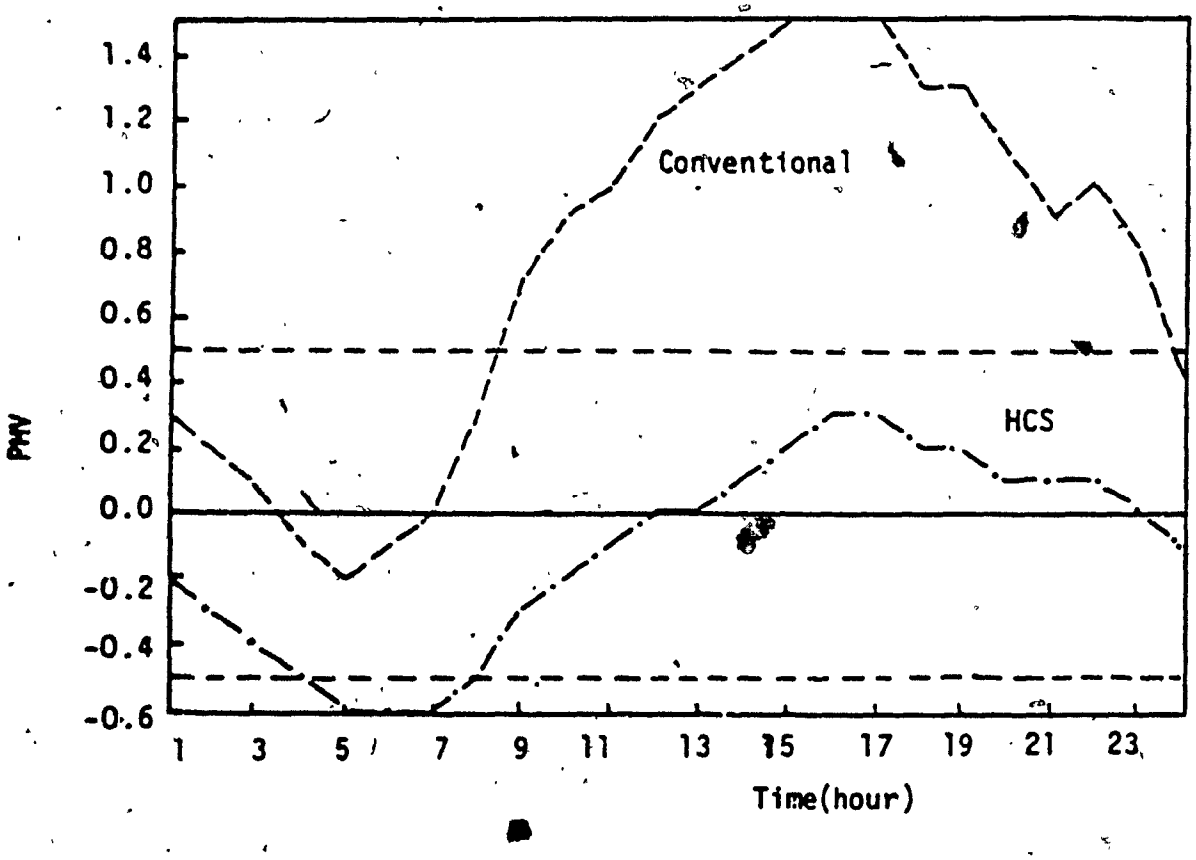

Fig. 5.20 Thermal comfort index. Case 3.

5.4 CONCLUSIONS

The analysis of these cases for that particular sunny and warm day in Montreal shows:

- The Hollow Core Slab design provides thermal comfort during the occupancy. The ventilation rate should be increased only three times at night, to cool the structure sufficiently to reduce the cooling loads by day.
- The energy savings obtained by using the Hollow Core Slab system are between 20 and 50 W/m^2, with respect to an HVAC system which keeps the room air temperature within the same limits.
- The cooling effect of the Hollow Core Slab with respect to the conventional design is between 2 and 7 W/m^2, for a thickness of the concrete plate of 0.15 m.
- The maximum temperature difference between the air entering and the air leaving the HCS is between 3 and 7 °C, during the occupation. Hence, the temperature of the supply air does not produce uncomfortable indoor conditions.
- The Hollow Core Slab system should be integrated with a predictive control system, to assess the ventilation rate at night based on the forecasting for the next day.

CHAPTER 6

THERMAL ANALYSIS OF DESIGN ALTERNATIVES USING SOLARIA

CHAPTER 6

THERMAL ANALYSIS OF DESIGN ALTERNATIVES USING SOLARIA

6.1 ATTACHED UNHEATED SOLARIUM

The analysis is performed for intermediate level room 6.0 x 6.0 x 3.6 m (Table 6.1) in a large office building in Montreal on December 25, 1979, which was a sunny and cold day (Table 6.2). An unheated attached solarium is considered (Fig. 6.1). The office space is kept at 21 $\pm$ 0.2°C by an HVAC system.

The variation of the air temperature in the solarium is analyzed, and then the reduction of the heating load of the office space is calculated.

Figure 6.2 shows the variation of the air temperature for the South facing solarium, when the common wall between the solar space and the office is either 0.30 m brick or 0.10 m lightweight concrete.

When the night insulating shutters are not used ($U_{DAY} = U_{NIGHT}$), the thicker wall which has a higher storage capacity will increase the air temperature at night by 2-3°C, while by day will reduce the peak temperature by 2°C. The use of night insulating shutters, reducing the U-value of glazing by 90 percent (as an extreme case), has an important effect on the temperature in solarium. The effect of the heat storage in the common wall is more evident. The 0.30 m brick wall increases the air temperature by 3-5°C by day and by 5-7°C at night.

TABLE 6.1

Base case for the analysis of unheated attached solarium

Intermediate level room	6 x 6 x 3.6 m
Exterior wall	South
	0.10 m concrete, air cavity, 0.10 m insulation, 0.02 m gypsum board
	glazing to wall ratio = 50%
	shading coefficient = 1
	window U-value = 2.6 W/(m^2°C)
	night insulating shutters
Interior walls	0.10 m brick
Floors	0.15 m concrete
Air infiltration	1.0 ach
Room air temperature	21 + 0.2°C
Adjacent rooms temperature	21°C
Occupancy	9:00 a.m. to 6:00 p.m.
Internal heat gains	people = 10 W/m^2
	lights = 20 W/m^2
HVAC system on continuous operation	

TABLE 6.2

Weather data in Montreal, 25 December 1979*

Hour	Dry bulb temperature (C)	Total cloud amount	Solar radiation on horizontal plane (W/m^2)
1	- 8.9	0.8	-
2	-10.6	0.7	-
3	-11.7	0.6	-
4	-12.2	0.4	-
5	-12.2	0.4	-
6	-12.8	0.3	-
7	-13.3	0.3	-
8	-13.9	0.2	5.8
9	-13.3	0.2	82.5
10	-13.3	0.1	212.8
11	-13.3	0.2	306.9
12	-12.8	0.1	375.6
13	-12.2	0.3	370.8
14	-12.2	0.2	320.8
15	-12.2	0.2	210.6
16	-13.3	0.3	87.2
17	-13.3	0.3	5.8
18	-13.3	0.3	-
19	-12.8	0.5	-
20	-12.2	1.0	-
21	-11.7	1.0	-
22	-11.7	1.0	-
23	-11.1	1.0	-
24	- 5.6	1.0	-

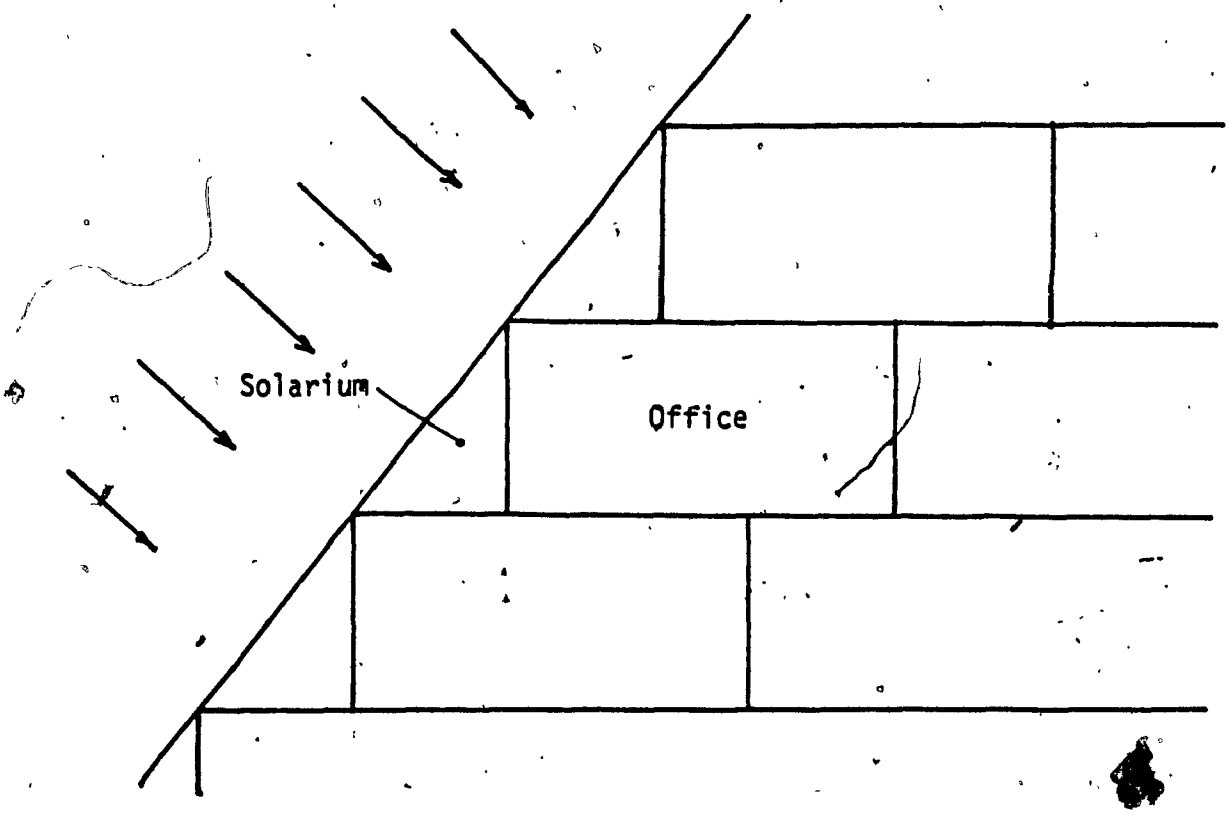

Fig. 6.1 Schema of the attached solarium.

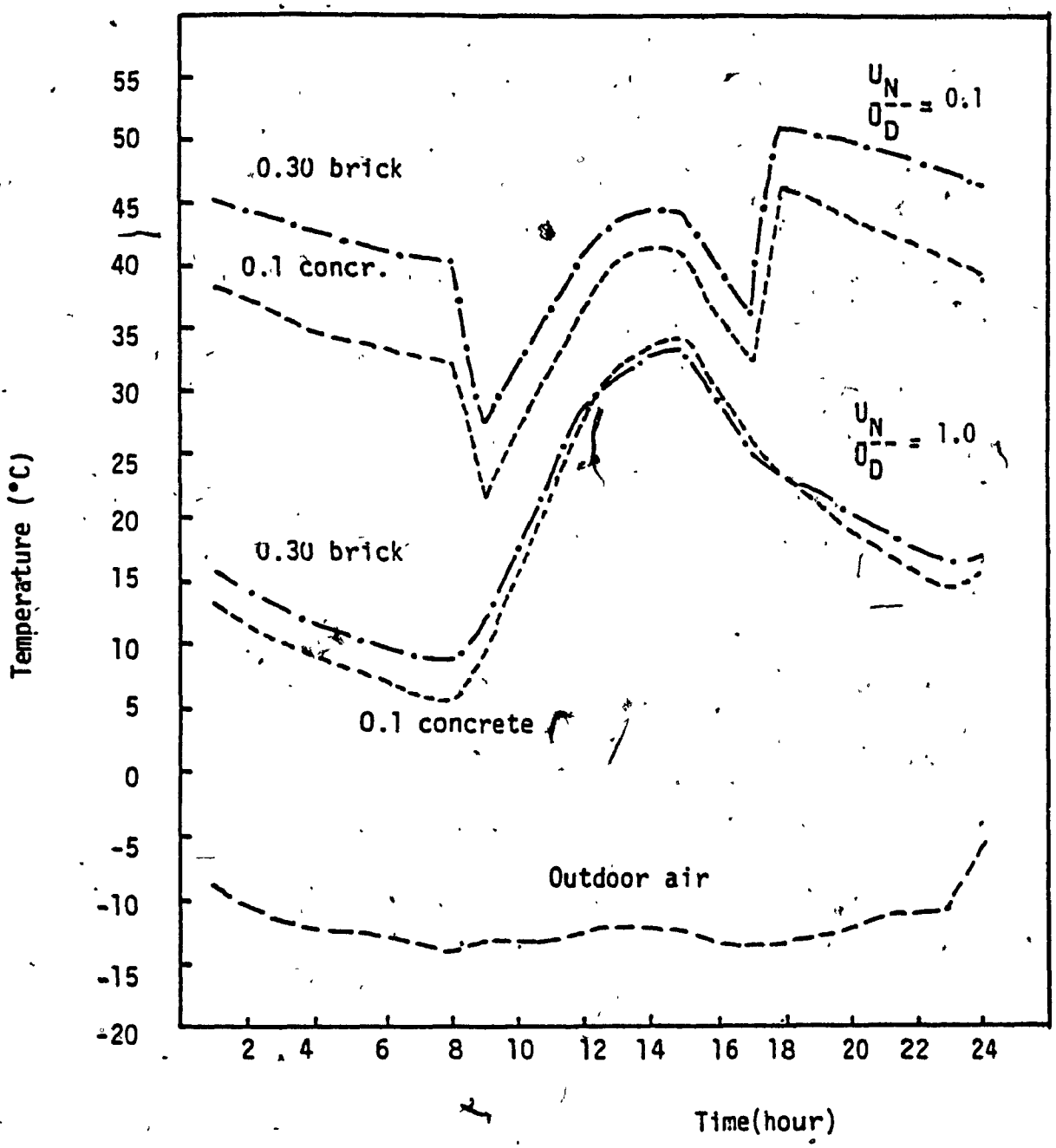

Fig. 6.2 Variation of the air temperature of South facing solarium.

Figure 6.3 shows the effect of the solarium orientation and of the night insulating shutters on the air temperature for a common wall of 0.30 m brick. As expected, the highest effect is obtained for South orientation with a maximum difference of about 55°C between the solarium temperature and the outdoor air temperature. The smallest effect is for North orientation with a maximum difference of 15°C.

The use of an unheated solarium attached on the exterior wall of the office room reduces the heating load of the HVAC system, for this particular day, by 60 (North) to 100 percent (South) (Table 6.3). Moreover, the South facing office requires cooling.

Figures 6.4 - 6.6 show the variation of the heating load of the office room, for cases without and with unheated attached solarium on South, East and North walls.

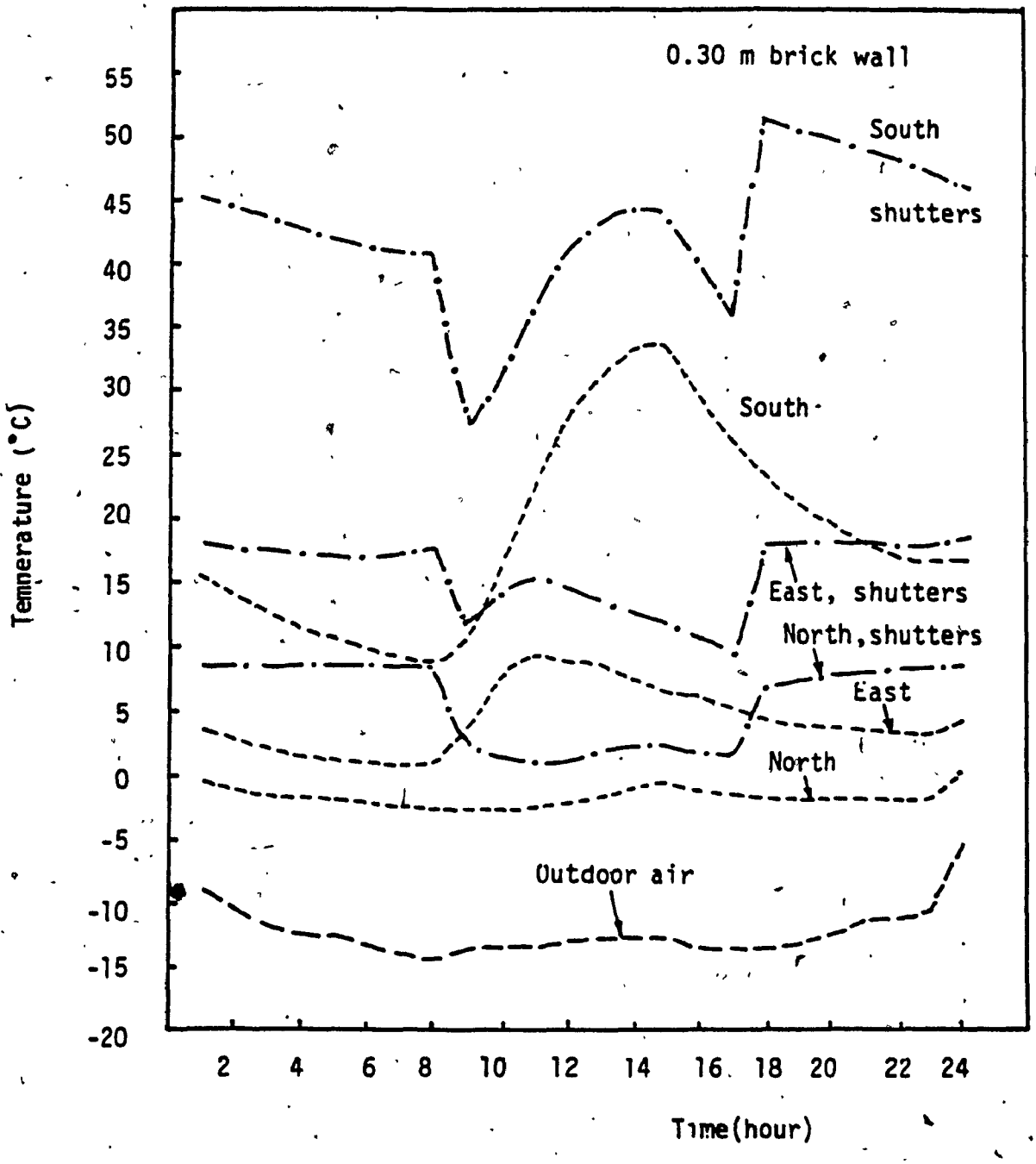

Fig. 6.3 Effect of the orientation and of the night insulating shutters.

TABLE 6.3

Effect of solarium orientation on the daily total heating load (kWh)

	SOUTH	EAST	NORTH	WEST
With Solarium	-101.16	6.74	44.30	12.96
Without Solarium	85.0	103.1	107.88	103.99
Difference	85.0	93.36	63.58	91.03
Savings %	100	93.5	58.9	87.5

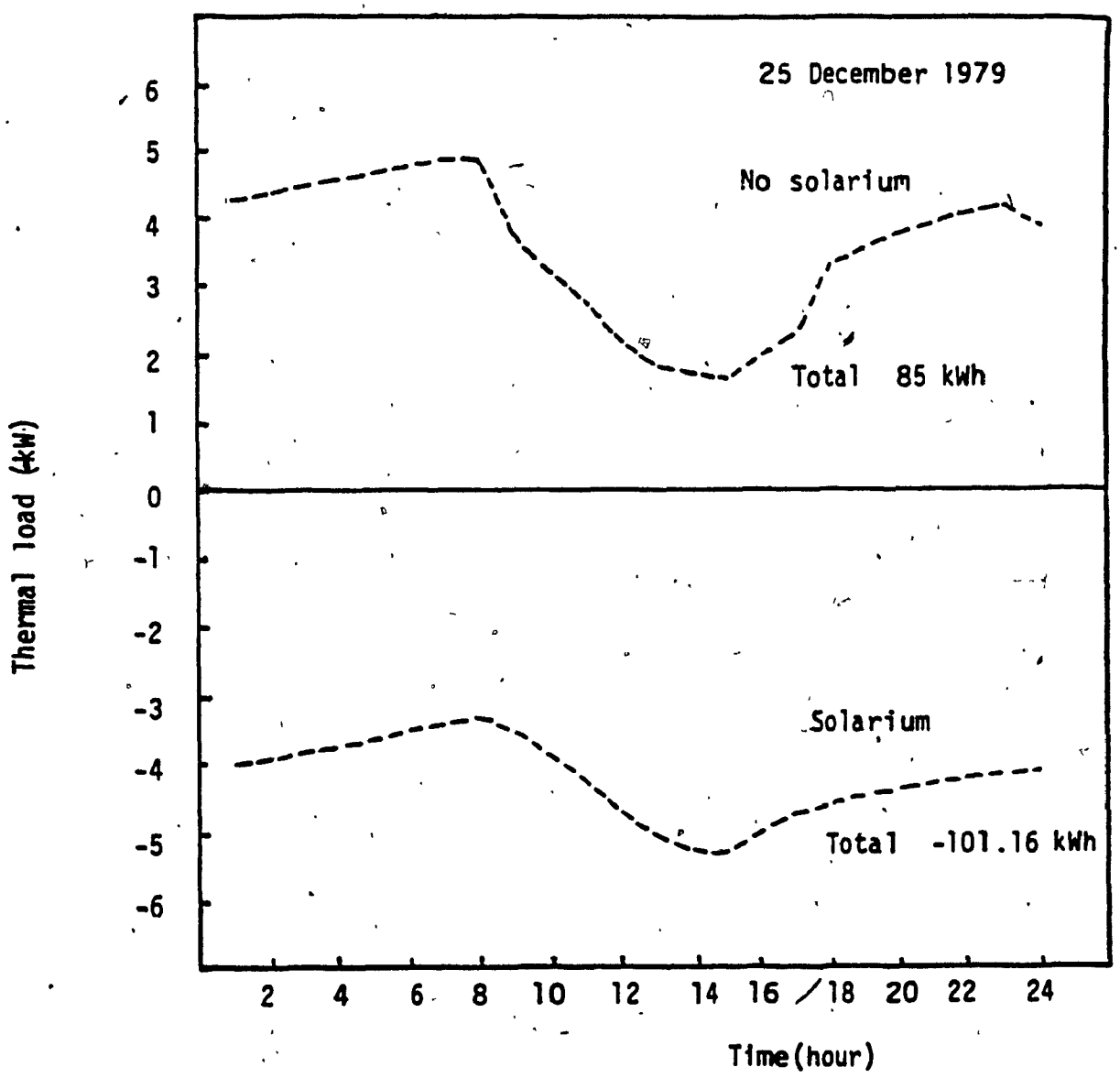

Fig. 6.4 Heating load of office space with South solarium.

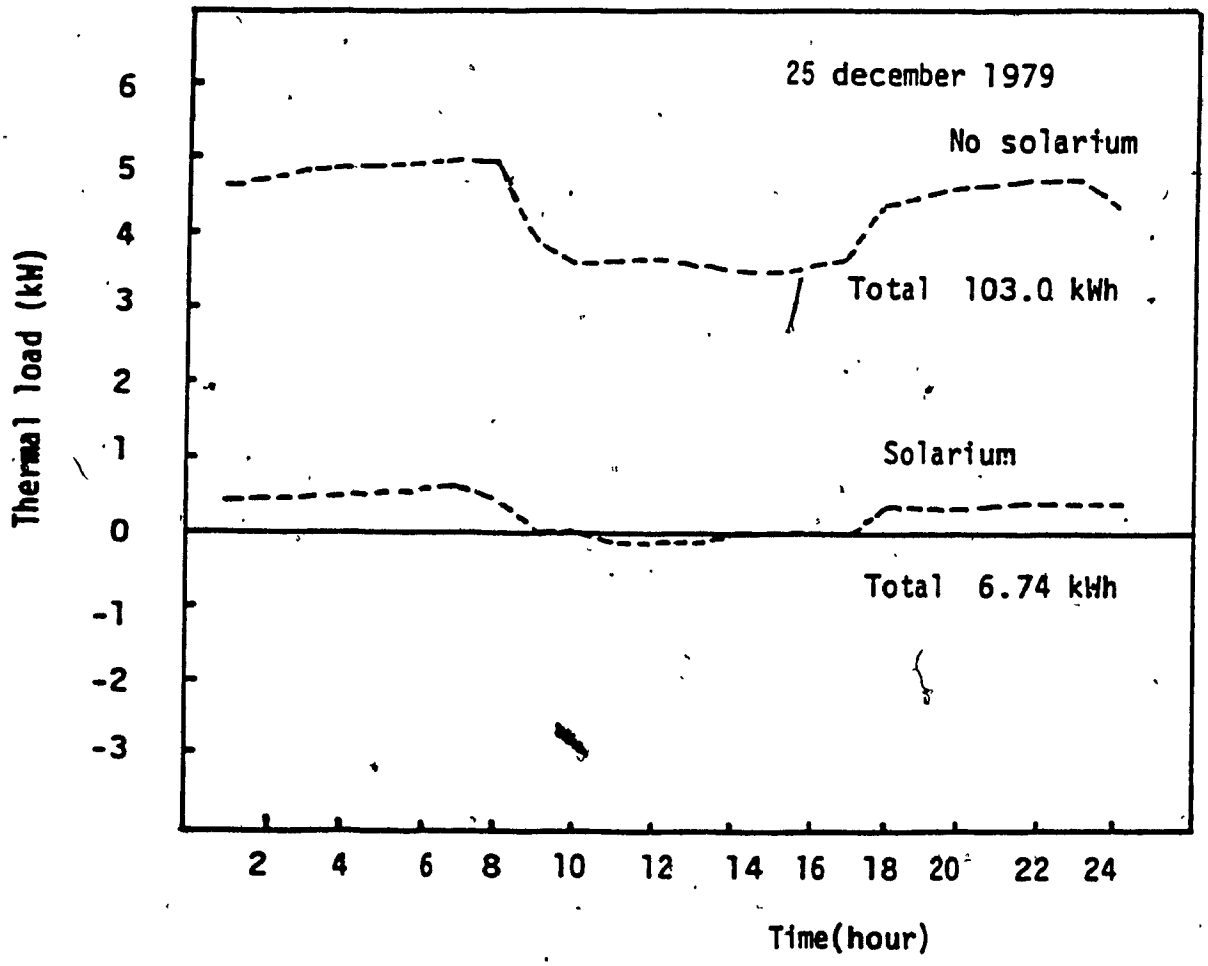

Fig. 6.5 Heating load of office space with East solarium.

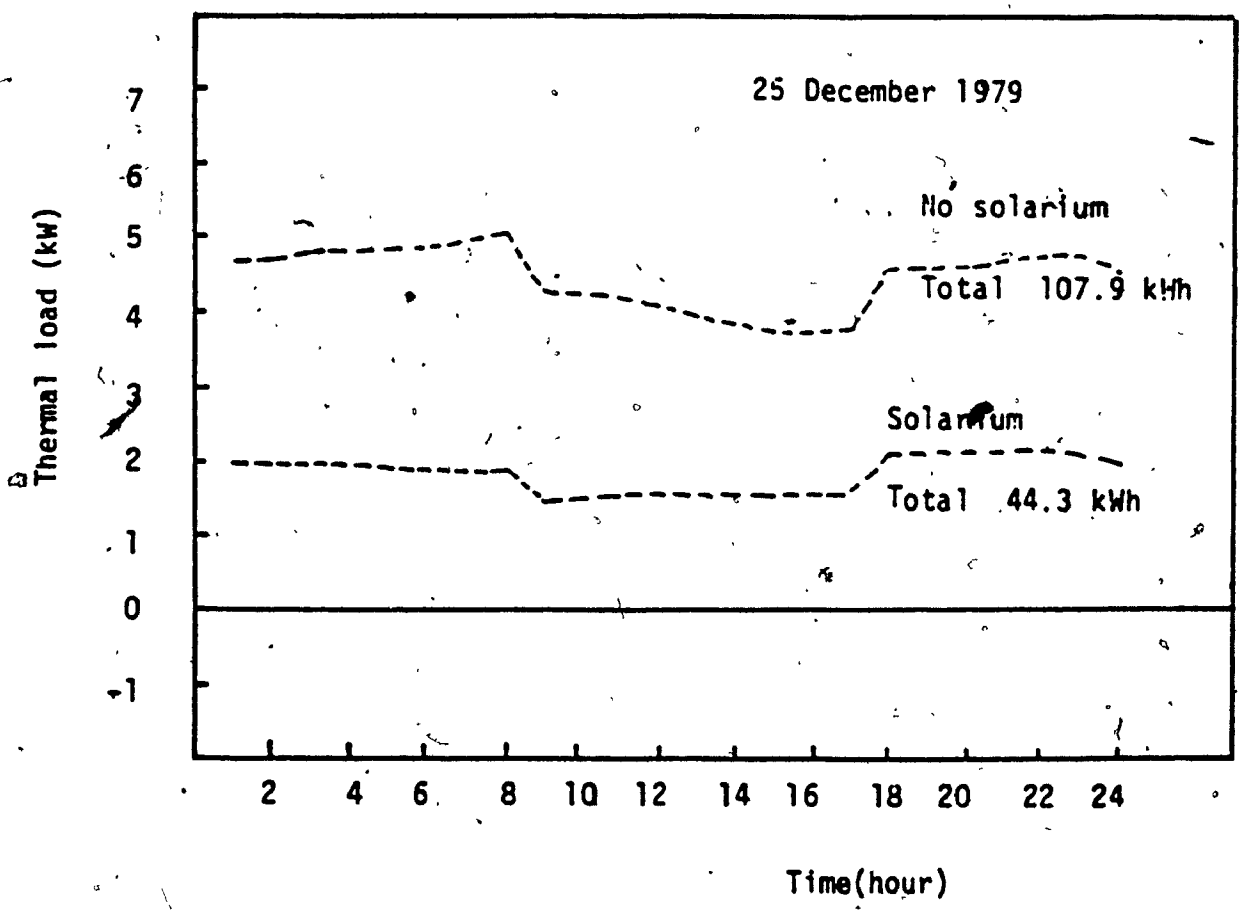

Fig. 6.6 Heating load of office space with North solarium

6.2 CONCLUSIONS

The results of the thermal analysis show:

- The unheated solarium attached to an office room performs well on a sunny and cold day in Montreal, reducing the heating load by 60 (North) to 100 percent (South).
- The heat storage effect in the common wall increases when night insulating shutters are used, which reduces the heat losses through glazing.

CHAPTER 7

UTILIZATION OF DECISION MODELS UNDER UNCERTAINTY FOR THE ANALYSIS OF THERMAL BEHAVIOR OF BUILDINGS

CHAPTER 7

UTILIZATION OF DECISION MODELS UNDER UNCERTAINTY FOR THE ANALYSIS OF THERMAL BEHAVIOR OF BUILDINGS

7.1 DECISION MODELS UNDER UNCERTAINTY

Usually, the building energy analysis programs use the weather data for a reference year or for an average design day to estimate the building thermal loads, which implies a deterministic relationship between the weather data and the building loads. The high computing time and cost of the use of the detailed energy analysis programs constrain the user to limit his analysis to only one year, which could be the average, the worst or the best year with respect to the weather conditions. Hence, the effect of different weather conditions are not taken into consideration.

As an alternative to the deterministic procedure, some statistical methods have been developed to predict the expected behavior of the thermal systems under random conditions.

Lameiro and Duff [90] employed a Markov chain to model the weather conditions (ambient temperature and solar radiation) and the long-term performance of a solar heating system. Anand et al. [93] developed an algorithm to predict the performance of a solar cooling system, using a synthetic weather data developed on probabilistic manner.

Tanthapanichakoon et al. [94] employed the Monte-Carlo simulation method to characterize the stochastic response of a solar heated and cooled house. The deterministic model is transformed into a stochastic model by using a random variable as a parameter. Haghighat et al. [95, 96] developed a stochastic method to handle uncertainty in the thermal analysis of buildings. Randomness is modeled as a Gaussian white noise which provides the mean and standard deviation of variables. Based on this information, the designer can select the size of HVAC systems with different levels of confidence.

A probabilistic approach is used in this research to analyze the results from the computer simulation of the thermal behavior of buildings, taking into consideration the uncertainties in predicting the climate.

The use of the weather data for a typical year does not take into account in appropriate manner the complex effect of combination of the weather factors such as ambient temperature and solar radiation, which both have a random hourly variation, on the building thermal loads. The building configuration and operation can act also as a filter reducing the variation of the thermal loads under the random climate, some of the design alternatives being more sensitive to the weather variation.

The evaluation method should compare and select, among a set of design alternatives, that one which performs better in terms of energy consumption, under all possible weather conditions.

The use of models of decision theory [97,98,99] provides an adequate frame for comparing the design alternatives of buildings, in order to decide which one is the best in terms of energy consumption when different weather conditions are expected to occur.

Since meteorological stations provide hourly weather data from previous measurements, usually over a long period of time, the designer can define the probability of occurrence of a particular weather condition by analyzing these long records. Then, the selection of the best design alternative is carried out by using decision models under risk, which assume that the possible futures are uncertain, but their probability of occurrence is known.

When the weather data are available from measurements over a short period of time or when sensible modification in climate has been observed in the past few years or is expected to occur, the designer should be able to compare the effect of uncertain futures with unknown probability of occurrence. This approach has been used in this reseach.

A decision model under uncertainty includes the following components:

i) Design alternatives, which are assumed to be mutually exclusive, feasible and represent the total set of alternatives the decision maker can consider.

ii) Possible states of nature or possible futures, which correspond to the weather conditions. It is assumed they are mutually exclusive, the occurrence of a state is not influenced by the alternative selected and the occurrence of a state is not known

with certainty by the decision maker. In this research the weather conditions for several individual days in Montreal as provided by the meteorological services [53], are considered as possible futures.

iii) Consequences or outcomes of the design alternatives under various states of nature, which in this research are the daily total thermal load L or the energy savings E, and the thermal comfort index PMV. The consequences of all design alternatives are obtained by computer simulation, using the CBS-MASS program. The interactions between design alternatives, possible states of nature and consequences are displayed in the payoff matrix (Table 7.1).

TABLE 7.1

Payoff matrix of the decision models

ALTERNATIVES	STATES OF NATURE			
	N_1	N_2	----	N_m
A_1	$L_{1,1}$ $PMV_{1,1}$	$L_{1,2}$ $PMV_{1,2}$	----	$L_{1,m}$ $PMV_{1,m}$
A_2	$L_{2,1}$ $PMV_{2,1}$	$L_{2,2}$ $PMV_{2,2}$	----	$L_{2,m}$ $PMV_{2,m}$
A_n	$L_{n,1}$ $PMV_{n,1}$	$L_{n,1}$ $PMV_{n,2}$		$L_{n,m}$ $PMV_{n,m}$

iv) Objectives, which define the criteria to be used for selecting the best design alterative. In this research the following objectives are considered:

- minimum heating/cooling loads L,
- maximum energy savings E,
- thermal comfort within acceptable limits.

v) Systematic evaluation of all the alternatives toward the assumed objectives. In this research the evaluation is performed in a two-step process:

v.1) The aspiration level criterion [97] is used to eliminate those alternatives providing thermal discomfort (PMV $>$ 0.5 or PMV $<$ -0.5) or increasing the energy consumption.

v.2) The Hurwicz criterion [97] is applied to the remaining alternatives, and the best alternative design will respect the following condition:

$$\min_i \{(1 - \Omega) \max_j L_{ij} + \Omega \min_j L_{ij}\} \qquad (7.1)$$

when the best solution must minimize the thermal load, or

$$\max_i \{\Omega \max_j E_{ij} + (1 - \Omega) \min_j E_{ij}\} \qquad (7.2)$$

when the best solution must maximize the energy savings,

where

Ω is index of optimism
i - index of design alternative
j - index of possible future
L_{ij} - space load in the case of alternative i, under future j
E_{ij} - energy savings in the case of alternative i, under future j

The Hurwicz criterion considers that the degree of optimism of the decision maker varies between the extreme pessimism and the extreme optimism. In the case of the extreme pessimism, the user assumes the worst consequences (maximum thermal loads or minimum energy savings) are obtained, and he selects that alternative which provides the most advantageous outcome, that is the minimum thermal load among maximum values (minimax principle) or the maximum energy savings among the minimum values (maximin principle). In the case of the extreme optimism, the user assumes the best consequences are obtained, and he selects the most advantageous alternative, that is, the minimum thermal load among the minimum values (minimin principle) or the maximum energy savings among the maximum values (maximax principle).

Any degree of optimism of the decision maker is incorporated into the evaluation process by defining an index of optimism Ω, which takes values between 0 and 1. A value of $\Omega = 0$ denotes extreme pessimism and the worst consequences are expected to occur, while a value of $\Omega = 1$ denotes extreme optimism, that is, the best outcomes are expected. For a chosen index Ω the best design alternative should respect Equation 7.1 or 7.2.

All possible consequences for each alternative are in a range bounded by the most optimistic and the most pessimistic outcomes. The width of this range expresses the sensitivity of the design alternatives to the random weather conditions.

In this research, decision models under uncertainty are used to analyze the effectiveness of the implementation of passive design alternatives to office buildings in Montreal.

Those design alternatives providing outcomes within 10 percent from the absolute minimum, in the case of thermal loads, or from absolute maximum, in the case of energy savings, are selected as the best solutions.

7.2 UTILIZATION OF DECISION MODELS UNDER UNCERTAINTY FOR THE ANALYSIS OF SOLARIA

The analysis is performed for South facing, intermediate level room in a large office building in Montreal [100].

The 100 percent elimination parametrics procedure [101] is used to identify those parameters with a significant effect on thermal loads, and then to establish the most appropriate design alternatives. The daily thermal load is computed for a base case (Table 6.1) on December 25, 1979, to be 0.44 kwh/(m^2 day). Then, this thermal load is compared to that of cases where a building parameter is eliminated (Table 7.2). Since the solar radiation has an important effect on the thermal load, providing a variation of about 160 percent, several design alternatives are considered such as increase in the window size, increase in the building mass, larger room temperature swing, better insulation of windows or use of an attached unheated solarium.

The following parameters are considered in the analysis, for the two main categories of design alternatives:

a. Conventional design

Windows - glazing to wall ratio: 0.5, 0.8, 0.99

- U-value: 1.3, 2.6 W/(m^2°C)

- night insulating shutters reducing U-value by 50 percent.

Interior mass - medium (380 kg/m^2 floor area) and heavy (510 kg/m^2 floor area)

Office air temperature - 21 ± 0.2°C, 21 ± 1°C, 21 ± 2°C, 22 ± 2°C

b. Attached unheated solarium

Windows - U-value: 2:6, 6.2 W/(m^2°C)

- night insulating shutters reducing U-value by 50 percent

Interior mass - heavy (570 kg/m^2 floor area) and very heavy (1000 kg/m^2)

Office air temperature: 21 ± 0.2°C

TABLE 7.2

100% Elimination parametrics

	Daily load (kWh/m^2 day)	Difference (%)
Base case	0.44	--
No internal gain	0.7	67.2
No solar radiation through windows	1.15	164.3
No conduction through glazing	0.15	65.0
No conduction through walls	0.31	29.2
No air infiltration	-0.72	263.7

The weather conditions for seventeen individual days in December 1979 in Montreal [53] are considered as possible futures with unknown probability of occurrence. As shown in Figure 7.1, among those possible futures are sunny and cold days (December 22 and 25), cloudy and warm days (December 21 and 24) or a cloudy and cold day (December 30).

The initial set of design alternatives is reduced, by eliminating those providing thermal discomfort, and the remaining twenty alternatives are presented in Table 7.3. The daily total heating load for these design alternatives, under all possible futures, are presented in Table 7.4.

Then, the expected heating load for each alternative is calculated, considering five levels of optimism (Ω = 0, 0.25, 0.50, 0.75, 1.0) (Table 7.5).

For optimism between 0 and 0.75 the best design alternative is the attached unheated solarium (A19), which reduces the heating load by 35 to 49 percent with respect to the best conventional design (A1-A17).

For the most pessimistic conditions (Ω = 0), this best conventional design has smallest and well insulated windows. For Ω = 0.25 to 0.75, the solution requires large well insulated windows.

For the most optimistic conditions (Ω = 1), several solutions provide small heating load (less than 2 kWh/day), but the attached solarium increases the cooling load.

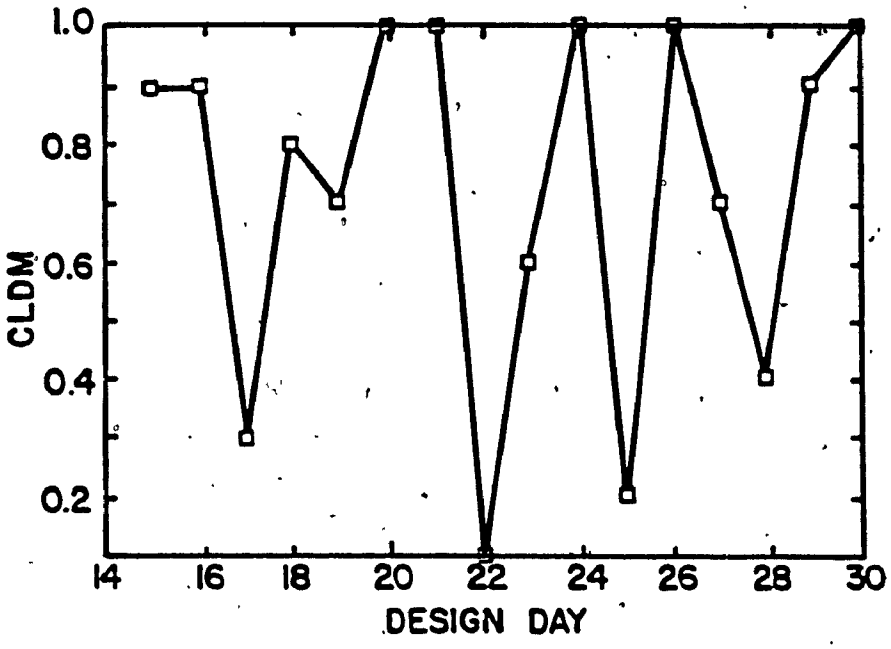

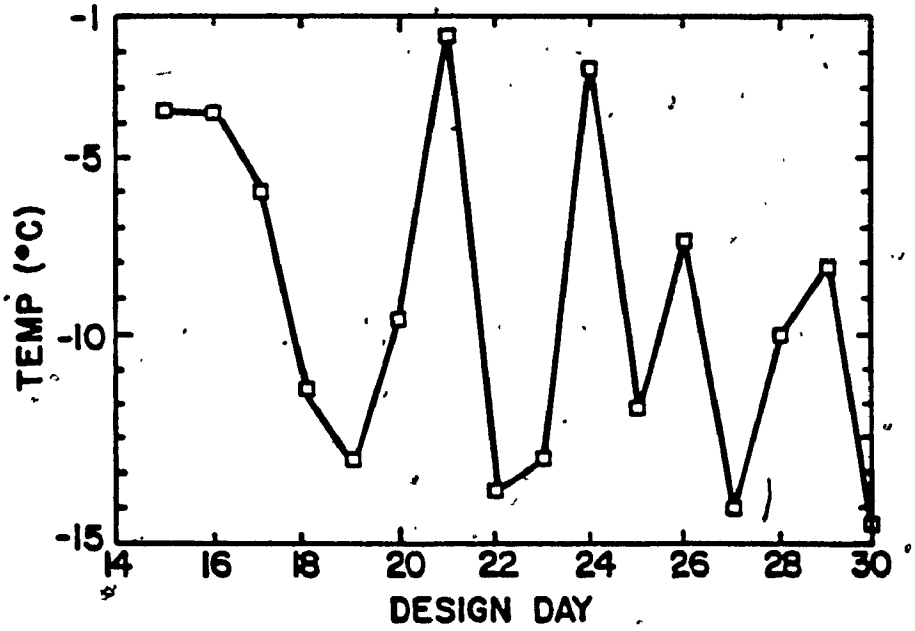

Fig. 7.1 Weather data - Montreal, December 1979.

TABLE 7.3

Design alternatives

	OFFICE AIR TEMP (C)	U-glazing ($W/m^2°C$)	Night shutter	Window Wall	Interior mass
	Conventional design				
1	21 + 0.2	2.60	N	0.50	Medium
2	21 ∓ 0.2	2.60	Y	0.50	Medium
3	21 ∓ 0.2	2.60	Y	0.80	Medium
4	21 ∓ 1	2.60	Y	0.80	Medium
5	21 ∓ 1	2.60	Y	0.80	Heavy
6	22 ∓ 2	2.60	Y	0.80	Heavy
7	22 ∓ 2	2.60	Y	0.50	Medium
8	21 ∓ 1	2.60	Y	0.50	Medium
9	21 ∓ 1	2.60	Y	0.50	Heavy
10	22 ∓ 2	2.60	Y	0.50	Heavy
11	21 ∓ 0.2	2.60	Y	0.50	Heavy
12	21 ∓ 0.2	2.60	Y	0.80	Heavy
13	21 ∓ 1	1.30	N	0.80	Heavy
14	21 ∓ 1	1.30	N	0.50	Heavy
15	22 ∓ 2	1.30	N	0.50	Heavy
16	22 ∓ 2	1.30	N	0.80	Heavy
17	22 ∓ 2	2.60	Y	0.99	Heavy
	Attached sunspace				
18	21 + 0.2	2.60	N	0.80	Heavy
19	21 ∓ 0.2	2.60	Y	0.80	Heavy
20	21 ∓ 0.2	2.60	Y	0.80	Very heavy

TABLE 7.4

Daily total heating load (kWh)

ALTERNATIVE	DAY				
	14	15	16	17	18
A1	29.5	29.54	15.71	13.81	40.72
A2	25.79	27.03	13.57	9.29	36.82
A3	25.84	29.45	14.23	4.27	37.38
A4	19.52	23.35	10.54	9.01	31.8
A5	20.56	23.96	10.61	4.53	30.22
A6	20.56	23.96	10.61	0.58	30.22
A7	19.44	21.06	10.09	7.55	31.18
A8	19.44	21.06	10,09	7.05	31.18
A9	20.35	21.58	10.16	8.36	29.67
A10	20.35	21.58	10.16	8.36	29.67
A11	25.09	26.18	13.8	10.62	34.05
A12	25.18	28.5	14.51	1.82	34.81
A13	17.78	21.05	10.03	7.92	26.53
A14	18.57	19.89	9.75	6.52	27.40
A15	18.57	19.89	9.75	7.63	27.40
A16	17.78	21.05	10.03	3.48	26.53
A17	20.44	25.41	10.89	6.56	30.41
A18	10.7	13.22	5.7	7.83	16.66
A19	6.9	10.65	4.5	16.29	12.16
A20	8.35	14.27	6.15	17.22	15.07

TABLE 7.4 (continued)

ALTERNATIVE	DAY				
	19	20	21	22	23
A1	42.64	41.07	26.25	21.61	40.52
A2	38.81	37.3	22.65	16.57	36.37
A3	38.49	40.38	24.64	1.17	34.1
A4	33.01	34.17	18.58	5.36	25.74
A5	30.99	33.38	19.66	4.0	27.62
A6	30.99	33.38	19.66	0.11	27.62
A7	33.37	31.25	16.93	14.55	30.95
A8	33.37	31.25	16.93	14.55	30.95
A9	31.08	30.5	17.98	14.4	28.95
A10	31.08	30.5	17.98	14.4	28.95
A11	35.76	35.3	22.75	16.24	33.59
A12	35.77	38.38	24.61	0.37	32.08
A13	27.18	29.76	17.65	8.15	24.53
A14	28.71	28.27	16.78	11.98	26.59
A15	28.71	28.27	16.78	12.73	26.59
A16	27.18	29.76	17.65	3.12	24.53
A17	30.66	35.27	20.66	7.96	26.79
A18	17.09	20.19	10.94	9.07	8.48
A19	12.0	17.21	8.28	21.89	1.82
A20	15.2	21.7	10.93	21.81	2.77

TABLE 7.4 (continued)

ALTERNATIVE	DAY						
	24	25	26	27	28	29	30
A1	25.58	20.52	36.95	44.91	22.04	33.76	51.7
A2	25.42	15.72	33.59	40.71	17.61	29.89	47.93
A3	27.27	0.06	36.39	40.81	2.98	29.92	51.6
A4	22.27	4.98	30.74	35.26	1.87	24.19	45.8
A5	21.51	1.72	29.98	33.75	0.74	23.7	42.69
A6	21.51	1.37	29.98	33.76	2.75	23.7	42.69
A7	20.14	12.24	27.85	35.49	13.18	24.92	41.97
A8	20.14	12.24	27.85	35.49	13.18	24.92	41.97
A9	19.78	13.67	27.39	33.62	14.02	23.58	39.96
A10	19.78	13.67	27.39	33.62	14.02	23.58	39.96
A11	23.88	15.53	31.82	37.95	16.19	27.78	43.94
A12	25.92	0.77	34.48	38.27	3.08	27.86	47.45
A13	19.65	6.46	26.78	29.36	4.04	21.41	38.93
A14	18.75	11.59	25.49	30.95	11.19	22.16	37.19
A15	18.75	12.15	25.49	30.95	12.52	22.16	37.19
A16	19.65	2.26	26.78	29.36	1.56	21.41	38.93
A17	22.53	5.91	31.61	33.86	4.49	23.62	44.8
A18	12.66	7.25	17.59	18.83	5.33	12.19	26.73
A19	10.26	18.24	14.76	13.37	13.97	7.55	23.16
A20	13.65	18.51	18.91	15.74	28.43	45.44	56.31

TABLE 7.5

Heating load (kWh) vs. index of optimism

DESIGN ALTERNATIVE	INDEX OF OPTIMISM				
	0	0.25	0.50	0.75	1.0
A1	51.70	42.23	32.76	23.28	13.81
A2	47.93	38.27	28.61	18.95	9.29
A3	51.60	38.71	25.83	12.95	0.06
A4	45.80	34.82	23.84	12.85	1.87
A5	42.69	32.20	21.72	11.23	0.74
A6	42.69	32.04	21.40	10.76	0.11
A7	41.97	33.37	24.76	16.16	7.55
A8	41.97	33.24	24.51	15.78	7.05
A9	39.96	32.06	24.16	16.26	8.36
A10	39.96	32.06	24.16	16.26	8.36
A11	43.94	35.61	27.28	18.95	10.62
A12	47.45	35.68	23.91	12.14	0.37
A13	38.93	30.21	21.49	12.76	4.04
A14	37.19	29.52	21.86	14.19	6.52
A15	37.19	29.80	22.41	15.02	7.63
A16	38.93	29.59	20.25	10.90	1.56
A17	44.80	34.72	24.65	14.57	4.49
A18	26.73	21.38	16.03	10.68	5.33
A19	23.16	17.82	12.49	7.15	1.82
A20	56.31	42.93	29.54	16.16	2.77

The sensitivity of the design alternatives to the random weather conditions is expressed as the difference between the heating loads for the extreme pessimism ($\Omega = 0$) and for the extreme optimism ($\Omega = 1$).

The design alternatives A18 and A19, using the attached unheated solarium, are less sensitive (variation of about 21 kWh) than the conventional design alteratives A1 to A17, where the heating loads vary by 30 to 51 kWh.

Consequently, the best design alternative is the attached unheated solarium (A19) which not only requires less energy for heating, but also is less sensitive to the weather variations.

7.3 UTILIZATION OF DECISION MODELS UNDER UNCERTAINTY FOR THE THERMAL ANALYSIS OF HOLLOW CORE SLABS

The analysis is performed for intermediate level space in a large office building in Montreal (Fig. 5.2, case 3 and Table 5.2).

The following parameters are considered in the analysis:

i) Thickness of the concrete plate - 0.10, 0.15, 0.20 m with an air space of 0.05 m.

ii) Ventilation rate at night - unchanged, increased twice, four times and eight times.

iii) Schedule for night operation: 1:00 - 5:00 a.m.
1:00 - 7:00 a.m.

The corresponding design alternatives are presented in Table 7.6.

The weather conditions for several individual days in July 1979 in Montreal [53] are selected as possible futures with unknown probability of occurrence. As shown in Table 7.7, among the possible futures are sunny days with large temperature swing of 13-15°C (July 26 and 22), and cloudy days with small temperature swing of 8.5-9.4°C (July 1 and 9). The maximum outdoor air temperature of the selected days is between 27 and 31°C.

TABLE 7.6

Design alternatives

ALTERNATIVE		Thick (m)	Ventilation rate	Night operation
AA1	A1 A2 A3 A4	0.1	X 1 X 2 X 4 X 8	1:00 - 5:00 a.m.
AA2	A5 A6 A7 A8	0.15	X 1 X 2 X 4 X 8	1:00 - 5:00 a.m.
AA3	A9 A10 A11 A12	0.20	X 1 X 2 X 4 X 8	1:00 - 5:00 a.m.
AA4	A13 A14 A15 A16	0.10	X 1 X 2 X 4 X 8	1:00 - 7:00 a.m.
AA5	A17 A18 A19 A20	0.15	X 1 X 2 X 4 X 8	1:00 - 7:00 a.m.
AA5	A21 A22 A23 A24	0.20	X 1 X 2 X 4 X 8	1:00 - 7:00 a.m.

TABLE 7.7

Weather conditions for the selected days in July 1979

DAY	TMAX (°C)	TMIN (°C)	DT (°C)	CLDM
July 1	27.80	23.30	4.50	0.80
July 5	28.90	15.60	13.30	0.80
July 7	27.20	17.80	9.30	0.40
July 9	28.30	18.90	9.40	0.60
July 22	30.00	15.00	15.00	0.30
July 23	30.00	20.00	10.00	0.60
July 26	31.10	17.80	13.30	0.30

In the first step, for each design alternative AA is selected that alternative A which provides thermal comfort in room ($-0.5 < PMV < 0.5$) at minimum ventilation rate at night (Table 7.8).

In the second step, an HVAC system is considered to maintain the room air temperature during the day at 25 $\pm$ 1°C, with no hollow core slab. During the night, the mechanical cooling system is shutoff and the outdoor air is circulated through the space, to cool the building. The estimation of the electrical energy consumption of the meachanical cooling system is based on the daily total cooling load, as provided by the CBS-MASS program, and for a Coefficient of Performance (COP) equal to three (Table 7.9). This represents the energy saving which is obtained by using the hollow core slab system instead of the HVAC system, to keep the room within comfortable conditions. However, the electrical consumption for fan, which is proportional with the pressure loss through the hollow core slab, should be reduced from this value to obtain the net saving (Tables 7.9 - 7.10).

The design alternative AA1 is dropped from the payoff matrix (Table 7.9) since for one possible future (July 23) an increase of the energy consumption is obtained rather than savings (aspiration level criterion). In this case, a high ventilation rate at night was required, since the minimum outdoor temperature was not low enough to cool the building structure. This increases the electrical consumption for fan, which becomes greater than the energy savings due to the application of the Hollow Core Slab system.

TABLE 7.8 Thermal comfort index (PMV) vs. design alternatives

ALTERNATIVE		JULY						
		1	5	7	9	22	23	26
AA1	A1	0.2,..,0.5	-0.1,..,0.4	-0.2,..,-0.3	0.2,..,0.7	0.1,..,0.7	0.3,..,0.8	0.2,..,0.8
	A2	0.2,..,0.5			0.1,..,0.6	-0.1,..,0.5	0,..,0.8	0,..,0.7
	A3				-0.1,..,0.5		0,..,0.6	-0.2,..,0.5
	A4						-0.2,..,0.5	
AA2	A5	0.2,..,0.5	-0.1,..,0.4	-0.2,..,0.2	0.2,..,0.6	0.1,..,0.6	0.3,..,0.7	0.3,..,0.8
	A6				0.1,..,0.5	-0.1,..,0.4	0.2,..,0.6	0,..,0.6
	A7						0,..,0.5	-0.1,..,0.4
	A8							
AA3	A9	0.2,..,0.4	-0.1,..,0.3	-0.2,..,0.1	0.2,..,0.5	0.1,..,0.5	0.3,..,0.6	0.2,..,0.6
	A10		-0.1,..,0.3	-0.3,..,0.1	0.1,..,0.5	-0.1,..,0.4	0.2,..,0.6	0,..,0.5
	A11						0.1,..,0.5	
	A12							
AA4	A13	0.2,..,0.5	-0.1,..,0.4	-0.2,..,0.3	0.2,..,0.7	0.1,..,0.7	0.3,..,0.8	0.2,..,0.8
	A14				0,..,0.6	-0.2,..,0.5	0.1,..,0.7	0,..,0.6
	A15				-0.2,..,0.5		-0.1,..,0.5	-0.3,..,0.5
	A16							
AA5	A17	0.2,..,0.5	-0.1,..,0.4	-0.2,..,0.2	0.2,..,0.6	0.1..0.6	0.3..0.7	0.3,..,0.8
	A18				0,..,0.5	-0.2..0.4	0.1..0.6	0,..,0.5
	A19						0..0.5	
	A20							
AA6	A21	0.2,..,0.4	-0.1,..,0.3	-0.2,..,0.1	0.2,..,0.5	0.1,..,0.5	0.3,..,0.6	0.2,..,0.6
	A22						0.1,..,0.5	0,..,0.4
	A23							
	A24							

TABLE 7.9

Energy savings (kWh)

ALTERNATIVE	JULY						
	1	5	7	9	22	23	26
AA1							
Elec	214.6	200.5	198.9	209	189.5	210.2	195.1
Fan	0.6	0.6	0.6	45.8	6.2	460.4	45.8
Save	214.0	199.9	198.3	163.2	183.7	-250.2	149.3
AA2							
Elec	226.8	198.9	205.0	226.4	185.2	222.5	182.0
Fan	0.6	0.6	0.6	6.2	6.2	45.8	45.8
Save	226.2	198.3	204.4	220.2	179.0	176.7	136.2
AA3							
Elec	225.9	195.2	203.4	235.0	228.2	218.4	219.1
Fan	0.6	0.6	0.6	0.6	0.6	45.8	6.2
Save	225.3	194.6	202.8	234.4	227.6	172.6	212.9
AA4							
Elec	195.4	185.4	177.7	191.9	180.7	199.7	177.2
Fan	0.8	0.8	0.8	64.1	8.7	64.1	64.1
Save	194.6	184.6	176.9	127.8	172.0	135.6	113.1
AA5							
Elec	205.5	183.9	181.7	204.4	174.8	196.5	196.6
Fan	0.8	0.8	0.8	8.7	8.7	64.1	8.7
Save	204.7	183.1	180.9	195.7	166.1	132.4	187.9
AA6							
Elec	202.9	171.9	176.3	212.6	202.0	205.7	191.1
Fan	0.8	0.8	0.8	0.8	0.8	8.7	8.7
Save	202.1	171.1	175.5	211.8	201.2	197.0	182.4

TABLE 7.10

Fan electrical consumption

	Ventilation rate at night			
	x1	x2	x4	x8
Air flow (m^3/s)	3.70	7.30	14.70	29.30
Velocity (m/s)	1.2	2.5	4.9	9.8
Pressure loss (Pa)	15.00	75.00	255.00	1200.00
Roughness coeff	1.50	1.62	1.75	1.87
Corrected pressure loss (Pa)	22.50	121.50	446.30	2244.00
Electrical consumption (kWh)				
t=5 h	0.6	6.20	45.80	460.40
t=7 h	0.8	8.70	64.10	644.60

TABLE 7.11

Energy savings (kWh) vs. index of optimism

DESIGN ALTERNATIVE	INDEX OF OPTIMISM				
	0	0.25	0.5	0.75	1
AA2	136.20	158.70	181.20	203.70	226.20
AA3	172.60	188.00	203.50	219.00	234.50
AA4	113.10	133.50	153.90	174.30	194.60
AA5	132.40	150.50	168.60	186.70	204.70
AA6	171.10	181.40	191.50	201.70	211.80

Then, the energy savings for each design alternative AA are calculated, considering five levels of optimism Ω = 0. 0.25, 0.50, 0.75 and 1.0.

For optimism between 0.0 and 0.25, the best design alternatives use thick concrete plates of 0.20 m (AA3 and AA6). The duration of night operation has small effect on energy savings, of about 10 percent. For optimism between 0.50 and 1.0, the best design alternatives use concrete plates of 0.15 - 0.20 m, for night operation of five hours (AA2 and AA3), and concrete plate of 0.20 m for night operation of seven hours (AA6).

The difference between the energy savings for extreme optimism (Ω = 1) and extreme pessimism (Ω = 0) shows that the design alternative AA6 is less sensitive (variation of about 40 kWh in energy savings) than the alternatives AA2 and AA3 (variation between 61 and 81 kWh), to the climate variations.

7.4 CONCLUSIONS

The analysis of the thermal behavior of attached solaria and holow core slabs in a large office building in Montreal, under different weather conditions with unknown probability of occurrence shows:

1) The attached unheated solarium with South orientation reduces the heating load of the space by 35 to 40 percent, with respect to the best conventional design.

ii) The thick hollow core slab provides the largest energy savings with respect to HVAC systems, for optimism between 0 and 0.50. The night operation of only five hours can cool the building structure to keep the space within comfortable conditions without HVAC system. If the best weather conditions are expected, the design alternatives can use thinner core slabs for night operation of five hours.

CHAPTER 8

SUMMARY OF ORIGINAL CONTRIBUTIONS

CHAPTER 8

SUMMARY OF ORIGINAL CONTRIBUTIONS

The original contributions can be summarized as follows:

i) The modification of the existing software or the implementation of new algorithms, as required by this research is very difficult, if not impossible task, due to the internal structure of these programs. Hence, a research oriented program with modular structure was developed, which allows the researcher to build a code for a particular problem, using the available modules from library and by adding new modules. Due to this structure, different design alternatives were analyzed by incorporating the corresponding modules into the library (Chapter 3).

ii) The CBS-MASS computer program allows the researcher to assess the link between the thermal behavior of buildings and the thermal comfort, which is not possible with other programs (Chapter 3).

iii) New mathematical models were developed and incorporated into the program to simulate (Chapter 3):

- heat transfer through hollow core slabs, air cavity walls and interior walls
- exterior shading devices.

iv) The authors of the building energy analysis programs usually emphasize the capabilities of their programs, but provide no information about their accuracy. Moreover, there is no standardized validation procedure for energy analysis programs and each

author has his own understanding of this process. In this research, the validation of the CBS-MASS computer program was performed against analytical solutions for particular heat transfer problems and by comparing the results of CBS-MASS, BLAST and TARP programs. The results indicate that the basic heat transfer phenomena occurring in buildings are well simulated by CBS-MASS program (Chapter 4).

iv) The thermal analysis of the design alternatives which use a "dynamic approach" of the heat storage in the building mass (hollow core slab in summer for reducing the cooling loads, and attached solaria in winter for reducing the heating loads) was performed for large office buildings in Montreal, and shows important energy savings can be obtained by using these design solutions (Chapter 5 and 6).

vi) Usually, the building energy analysis programs use the weather data for a reference year to estimate the building thermal loads. Instead of using the deterministic relationship between the weather data and the building load, as implicitly defined by this procedure, a probabilistic approach was used in this research, to take into consideration the uncertainties in predicting the climate (Chapter 7).

vii) The research contributes to the advance in the knowledge of the design of energy-responsive buildings and enable professionals (architects and engineers) to provide better design solutions which reduce the energy consumption, using the heat storage effect in the building mass.

CHAPTER 9

RECOMMENDATIONS FOR FURTHER RESEARCH

CHAPTER 9

RECOMMENDATIONS FOR FURTHER RESEARCH

Further research into the following directions are of interest:

i) Transfer of the CBS-MASS program from Perkin-Elmer minicomputer to IBM-AT microcomputer. Development of a user-friendly pre-processor, using the OMNI-SCREEN software, to aid users in defining the building and in selecting the appropriate modules from the library. Development of a post-processor, using the META-WINDOW software, to display the simulation results.

ii) Development of new modules to be incorporated in library such as:
- solar calculations, which allow the user to analyze the effect of different mathematical models,
- solution of the system of simultaneous linear equations,
- heat transfer through wall using the Conduction Transfer Functions, which will allow to compare the results provided by this method against the numerical solution,
- non-diffuse glazing,
- phase change materials.

iii) Modification of the program to analyze a succession of several different days.

iv) Analysis of the thermal behavior of buildings taking into consideration the uncertainties in estimating the thermal properties of existing walls and the accuracy of mathematical models.

REFERENCES

REFERENCES

1. "Canada inefficient in energy use, agency says", The Gazette, Montreal, June 17, 1985.

2. Bourassa, G.F., Latta, J.K., Thompson, A.J., Housch, S., and Monteyne, R., "Energy budgets for office buildings", Building Research and Practice, Volume 9, Number 4, July/August 1981.

3. Yellot, J.I., "Energy Supplies for the Buildings of the Future", Proceedings of the International Congress Povoa de Varzim, Portugal, May 1980.

4. Faucher, G., "Illumination of building interior through lumiducts", Proceedings of the International Congress Povoa de Varzim, Portugal, May 1980.

5. Elmahdy, A.H., "Low-energy office buildings", Proceedings of the W67 Symposium held at the Division of Building Research, National Research Council of Canada, Ottawa, 16 May 1984.

6. Wilson, A.G., "Overview of the office and medium to high-rise residential sectors", Proceedings of the Conference on Building Science and Technology, Waterloo, Ontario, November 10-11, 1983.

7. Piette, M.A., Wall, L.W., and Gardiner, B.L., "Measured performance", ASHRAE Journal, January 1986.

8. "NRC's Solar Energy Program Identifies Passive R & D as Highest Priority", SOL 44, May 1984.

9. "IEA to study use of passive solar in commercial buildings, SOL 50, September - October 1985.

10. Catani, M.J., "Insulation and the M-factor", ASHRAE Transactions, vol. 84, 1978.

11. Recknagel-Sprenger, "Heizung, Luftung and Klimatechnik", Oldenbourg, Verlag, Munchen - Wien, 1972.

12. Howard, B.D., "Advances in thermal mass assessment data", Proceedings of the Third North American Masonry Conference, June 3-5, 1985, University of Texas at Arlington, Texas.

13. Romanko, K.J., and Rudoy, W., "Some effects of thermal mass in multifamily dwellings. Effects on heating and cooling loads", ASHRAE Transactions, 1981.

14. Mitalas, G.P., "Effect of building mass on annual heating energy requirements", Proceedings of CIB'79 Energy Conservation in Built Environment, Copenhagen, 1979.

15. Mackie, E.I., "The effect of building heat storage on HVAC systems", Third International Symposium on the Use of Computers for Environmental Engineering related to Buildings, Banff, Alberta, May 1978.

16. Givoni, B., "Options and Applications of Passive Cooling", Energy and Buildings, No. 7, 1984.

17. Hoffman, M.E., Gideon, M., Muller, K., and Katz, Y., "Ventilation as a Means of Air-conditioning Power Saving in Reinforced Concrete Telephone-exchange Buildings - Analysis and Directions for Design", Energy and Buildings, No. 7, 1984.

18. Monette, M., "Use of a composite concrete and steel floor system as a combination air storage medium/plenum for enhanced passive solar utilization", Proceedings of SESCI '84, Calgary, August 1984.

19. Allen, G., Kani, M., and Carpenter, St., "Mechanically enhanced passive solar thermal storage", Proceedings of SESCI '84, Calgary, August 1984.

20. Seppane, O., "Cost effective energy conservation in an office building", Proceedings of the International Congress Povoa de Varzim, Portugal, May 1980.

21. Croome, D.J., and Robert, B.M., "Air Conditioning and Ventilation of Buildings", 2nd Edition, Vol. 1, Pergamon Press, 1981.

22. Barnaby, Ch.S., Nall, D.H., and Dean, Ed., "Structural mass cooling in a commercial building using hollow core concrete plank", Proceedings of the National Solar Conference, Amherst, Mass, 1980.

23. Svenberg, S.A., "The viability of thermal storage", Energy Technology, Sweden, No. 1, 1982.

24. Block, D.A., and Hodges, L., "Use of concrete cored slab for passive cooling in an Iowa residence", Proceedings of the 4th National Passive Solar Conference, Kansas City, October 1979.

25. Tamblyn, R.T., "Toward zero energy in buildings", Proceedings of the International Congress Povoa de Varzim, Portugal, May 1980.

26. Birrer, W.A., "Structural storage as a part of a total system for energy efficient office buildings: two examples", Proceedings of the First E.C., Conference on Solar Heating, Amsterdam, April 30-May 4, 1984.

27. "Winning low energy building designs", Public Works Canada and Energy, Mines and Resources Canada, Ottawa, 1980.

28. Jones, L., "Solar Energy Program. Review of the potential of passive solar strategies for office buildings", National Research Council Canada, August 1983.

29. Sodha, M.S., Nayak, J.K., Bansal, N.K., and Geyal, I.C., "Thermal Performance of a Solarium with Removable Insulation", Building and Environment, No. 2, 1983.

30. Kusuda, T., "A comparison of Energy Calculation Procedures", ASHRAE Journal, August 1981.

31. Kusuda, T., "NBSLD, the Computer Program for Heating and Cooling Loads in Buildings", U.S. Department of Commerce, July 1976.

32. Hittle, D.C., "BLAST, the building load analysis and system thermodynamics program", Vol. 1: User's manual, U.S. Army Construction Engineering Research Laboratory, Champaign, Illinois, December 1977.

33. Herron, D., Walton, G., and Lawrie, L., "BLAST program user's manual", Vol. 1, Supplement, Version 3.0, U.S. Army Construction Engineering Research Laboratory, Champaign, Illinois, March 1981.

34. Hittle, D.C., "The building loads analysis and systems thermodynamics (BLAST) program", Proceedings of the third international symposium on the use of computers for environmental engineering related to building, Banff, Alberta, May 10-12, 1978.

35. Stephenson, D.G., and Mitalas, G.P., "Calculation of Heat Conduction Transfer Functions for Multi-Layer Slabs", ASHRAE Transactions, Vol. 77, 1971.

36. Kusuda, T., "Thermal Response Factors for Multi-Layer Structures of Various Heat Conduction Systems", ASHRAE Transactions, 1969.

37. Mitalas, G.P., and Arseneault, J.G., "Fortran IV Program to Calculate Heat Flux Response Factors for Multi-Layer Slabs", DBR Computer Program No. 23, National Research Council of Canada.

38. Sowell, E.F., and Walton, G.N., "Efficient Computation of Zone Loads", ASHRAE TRANSACTIONS, 1980.

39. Walton, G.N., "Thermal Analysis Research Program", Proceedings of CIB '83 Stockholm, 1983.

40. Carroll, J.A., "A comparison of radiant interchange algorithms", Solar Engineering, Reno, Nevada, April 27 - May 1, 1981.

41. "DOE-2 Engineers Manual", Version 2.1A, Lawrence Berkeley Laboratory, November 1982.

42. Lokmanhekim, M., Buhl, F.W., Curtis, R.B., Gates, S.G., Hirsch, J.J., Jaeger, S.P., Rosenfeld, A.H., Winkelman, F.C., Hunn, B.D., Roschke, M.A., Leighton, G.S., and Ross, H.D., "DOE-2: a new state-of-the-art computer program for the energy analysis of buildings", Proceedings of the third international symposium on the use of computers for environmental engineering related to buildings, Banff, Alberta, May 10-12, 1978.

43. Mitalas, G.P., and Stephensen, D.G., "Room thermal response factors", ASHRAE Transactions, Vol. 73, 1967.

44. Stephensen, D.G., and Mitalas, G.P., "Cooling load calculations by thermal response factor method", ASHRAE Transactions, Vol. 73, 1967.

45. "DOE-2 Reference Manual", Version 2.1, Lawrence Berkeley Laboratory and Los Alamos National Laboratory, May 1980.

46. American Society of Heating, Refrigerating and Air Conditioning Engineers, Handbook of Fundamentals, 1981.

47. Cumali, Z.O., Sezgen, A.O., Sullivan, R., and Kammerud, R.C., "Extension of methods used for analyzing passive solar systems", Passive Solar Conference, Kansas City, October, 1979.

48. Carroll, W.L., "Annual heating and cooling requirements and design day performance for a residential model in six climates: a comparison of NBSLD, BLAST-2 and DOE-2.1", Proceedings of the ASHRAE/DOE/ORNL Conference, Thermal Performance of the Exterior Envelope of Buildings, Florida, December, 1979.

49. Kusuda, T., Pierce, E. Th., and Bean, J.W., "Comparison of calculated hourly cooling load and attic temperature with measured data for a Houston test house", ASHRAE Transactions, Vol. 87, 1981.

50. McFarland, R.D., "PASOLE a general simulation program for passive solar energy", National Energy Software Center, Argonne National Laboratory, 1975.

51. Arumi-Noe, F., "Field validation of the DEROB/PASOLE System", The 3rd National Passive Solar Conference, San Jose, January 11-13, 1979.

52. Fazio, P., and Zmeureanu, R., "Research oriented software in building energy analysis", Proceedings of the Canadian Conference on Industrial Computer Systems, Montreal, May 28-30, 1986.

53. "Documentation of the digital archive of Canadian climatological data (surface) identified by element", Atmospheric Environment Service, Canadian Climate Centre, Data Management Division, Ontario, April, 1985.

54. Fazio, P., and Zmeureanu, R., "Meeting the researcher's needs in building energy simulation", Proceedings of the International Building Energy Simulation Conference, Seattle, August 21-22, 1985.

55. Hirsch, J.J., "Plan for the development of the next-generation building energy analysis computer software", Proceedings of the International Building Energy Simulation Conference", Seattle, August 21-22, 1985.

56. American Society of Heating, Refrigerating and Air Conditioning Engineers, Handbook of Fundamentals, 1977

57. Standaert, P., "Thermal bridges: a two-dimensional and three-dimensional analysis", Proceedings of the ASHRAE/DOE/BTECC Conference, Thermal Performance of the Exterior Envelope of Buildings III, December 2-5, 1985, Clearwater Beach, Florida.

58. Ames, W.F., "Numerical methods for partial differential equations", Thomas Nelson and Sons Ltd., London, 1969.

59. Clarke, J.A., "Computer simulation of energy exchanges in buildings", Proceedings of CIB'79, Copenhagen, 1979.

60. Emery, A.F., Kippenhan, C.J., Heerwagen, D.R., and Varey, G.B., "The simulation of building heat transfer for passive solar systems", Energy and Buildings, No. 3, 1981.

61. Burghardt, M.D., "Engineering thermodynamics with applications", Harper & Row, Publishers, New York, 1982.

62. Gadgil, A., Goldstein, D., Kammerud, R., and Mass, J., "Residential building simulation model comparison using several building analysis programs", The 3rd National Passive Solar Conference, San Jose, January, 11-13, 1979.

63. Carroll, J.A., "A comparison of radiant interchanges algorithms", Solar Engineering 1981, Nevada, April 1981.

64. Walton, G.N., "A new algorithm for radiant interchange in room loads calculation", ASHRAE Transactions, Part 2, 1980.

65. Walton, G.N., "Developments in the heat balance method for simulating room thermal response", Proceedings of the Workshop on HVAC Controls, Modeling and Simulation, Georgia Institute of Technology, February 1984.

66. Sullivan, R., Nozaki, N., and Cumali, O., "Thermal load and computer simulation run-time comparisons using a research version of DOE-2", ASHRAE Transactions, 1982.

67. Pratt, A.W., "Heat transmission in buildings", John Wiley and Sons Ltd., 1981.

68. Achterbosch, G.G.J., deJong, P.P.G., Krist-Spit, C.E., van der Meulen, S.F., and Verberne, J., "The development of a convenient thermal dynamic building model", Energy and Buildings, No. 8, 1985.

69. Kreith, F., and Kreider, J.F., "Principles of Solar Engineering", Hemisphere, Washington, D.C., 1978.

70. Fazio, P., and Zmeureanu, R., "Micro-Computer Software for Solar Window Design", Proceedings of the First Canadian Conference on Computer Applications in Civil Engineering, McMaster University, Hamilton, May 20-23, 1986.

71. Fazio, P., and Zmeureanu, R., "Programme de simulation de l'ombrage sur micro-ordinateur", 53e Congrès de l'Association Canadienne-Française pour l'Avancement des Science (ACFAS), Université du Québec a Chicoutimi, 20-24 Mai 1985.

72. Mazria, E., "The Passive Solar Energy Book", Rodale Press, Emmaus, Pa., 1979.

73. Nawrocki, A.D., and Kammerud, R., "Description of an exact, recursive method to simplify shading calculations", Solar Engineering 1981, Reno, Nevada, April 27 - May 1, 1981.

74. Croome, D.J., and Roberts, B.M., Air Conditioning and Ventilation of Buildings", 2nd edition, vol. 1, Pergamon Press, 1981.

75. Fanger, P.O., "Thermal Comfort", McGraw-Hill Book Company, New York, 1973.

76. Yuill, G.K., "The BLAST verification", ASHRAE Journal, January 1985.

77. Bauman, F., Anderson, B., Carroll, W.L., Kammerud, R., and Friedman, N.E., "Verification of BLAST by comparison with measurements of a solar-dominated test cell and a thermally massive building", Solar Engineering 1981, Reno, Nevada, April 27-May 1, 1981.

78. Yuill, G.K., and Phillips, E.G., "Comparison of BLAST program predictions with the energy consumptions of two buildings", ASHRAE Transactions, vol. 87, 1981.

79. Colborne, W.G., Hall, J.D., and Wilson, N.W., "The validation of DOE-2.1 for application to single family dwellings", ASHRAE Transactions, 1984.

80. Diamond, S.C., and Hunn, B.D., "Comparison of DOE-2 computer program simulations to metered data for seven commercial buildings", ASHRAE Transactions, Vol. 87, 1981.

81. Alereza, T., and Hovander, L., "A micro evaluation", ASHRAE Journal, December 1985.

82. Fazio, P., Zmeureanu, R. and Guité, P., "Validation du logiciel T.I.E.", Contract No. 02SO.23216-3-6110, Centre for Building Studies, Concordia University, Montral, May 1985.

83. Wagner, B., "Comparison of predicted and measured energy use in occupied buildings", ASHRAE Transactions, Vol. 90, 1984.

84. Judkoff, R., "Empirical validation using data from the SERI Class A Validation House", Proceedings of Annual Meeting of American Section of ISES, Minneapolis, Vol. 6, 1983.

85. Judkoff, R., Wortman, D., Christensen, C., O'Doherty, B., Simms, D., and Hannifan, M, "A comparative study of four passive building energy simulations: DOE-2.1, BLAST, SUNCAT-2.4, DEROB-111", Proceedings of the 5th National Passive Solar Conference, University of Massachusetts, October 19-26, 1980.

86. Irving, S.J., "Energy program validation: conclusions of IEA Annex 1", Computer Aided Design, Vol. 14, No. 1, January 1982.

87. Allen, E., Bloomfield, D., Bowman, N., Lomas, K., Allen, J., Whittle, J., and Irving, A., "Analytical and empirical validation of dynamic thermal building models", Proceedings of the International Building Energy Simulation Conference, Seattle, August 21-22, 1985.

88. Wortman, D., O'Doherty, B., and Judkoff, R., "The implementation of an analytical verification technique on three building energy analysis codes: SUNCAT-2.4, DOE-2.1, and DEROB 111", Solar Engineering 1981, Reno, Nevada, April 27 - May 1, 1981.

89. Little, J.G.K., "Comparison of passive solar design methods", Proceedings of the Second International PLEA Conference, Passive and Low Energy Architecture, Crete, Greece, 28 June-1 July 1983.

90. Beizer, B., "Software Testing Techniques", Van Nostrand Reinhold Company, 1983.

91. "TNODE - a thermal network analysis program for the IBM-PC. Version 4.0", The Energy Group, Architecture Georgia Technical Institute, August 1984.

92. Lameiro, G.F., and Duff, W.S., "A Markov Model of Solar Energy Space and Hot Water Heating Systems", Solar Energy, Vol. 22, 1979.

93. Anand, O.K., Deif, I.N., Bazques, E.D., and Allen, R.W., "Stochastic Prediction of Solar Cooling Systems Performance", Journal of Solar Energy Engineering, Vol. 102, 1980.

94. Tanthapnichakoon, W., and Himmelblan, D.M., "A Stochastic Analysis of a Solar Heated and Cooled House", Journal of Solar Energy Engineering, Vol. 103, 1981.

95. Haghighat, F., Unny, T.E., and Chandrashekar, M., "Stochastic Modeling of Transient Heat Flow Through Walls", Journal of Solar Energy Engineering, Vol. 107, 1985.

96. Haghighat, F., Chandrashekar, M., ad Unny, T.E., "Thermal behavior of buildings under random conditions", submitted to the Applied Mathematical Modelling Journal, 1986.

97. Szonyi, A.J., Fenton, R.G., White, J.A., Agee, M.H., Case, K.E., "Principles of engineering economic analysis", John Wiley & Sons Canada Limited, Toronto, 1982.

98. Bradley, J.V., "Probability; decision; statistics", Prentice-Hall, Inc., New Jersey, 1976.

99. Harnett, D.L., "Statistical Methods", Addison-Wesley Publishing Company, Inc., 1982.

100. Fazio, P., and Zmeureanu, R., "Utilization of decision models under uncertainty for the analysis of building energy simulation results", Proceedings of the 10th CIB'86 Congres, Washington, 21-26 September, 1986.

101. Ternoey, St., Bickle, L., Robbins, R., Busch, R, and McCord, K., "The design of energy-responsive commercial buildings", John Wiley & Sons, New York, 1985.

102. Institution of Heating and Ventilating Engineers (IHVE), Guide Book A, London, 1970.

APPENDIX 1

MATHEMATICAL MODEL OF EXTERIOR SHADING DEVICES

The shape of the shaded area on the window depends on the location of point A (Fig. 1).

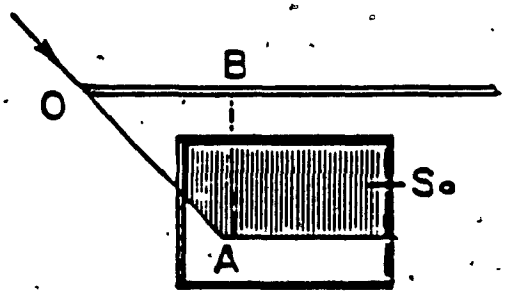

Fig. 1 Coordinates of point A

The coordinates of point A are defined as follows (Fig. 2).

$$AC = MC \tan \beta \quad (1)$$

$$MC = d \cos \alpha 1 \quad (2)$$

then $$AC = d \tan \beta \cos \alpha 1 \quad (3)$$

The projection on the plane normal to the window gives;

$$AC = \frac{d \tan \beta 1 \cos \alpha 1}{\cos \gamma} \quad (4)$$

$$BC = d \sin \alpha 1 \quad (5)$$

then

$$AB = d \left(\frac{\tan \beta 1}{\cos \gamma} \cos \alpha 1 + \sin \alpha 1\right) \quad (6)$$

On horizontal plane:

$$BO = d \tan \gamma \quad (7)$$

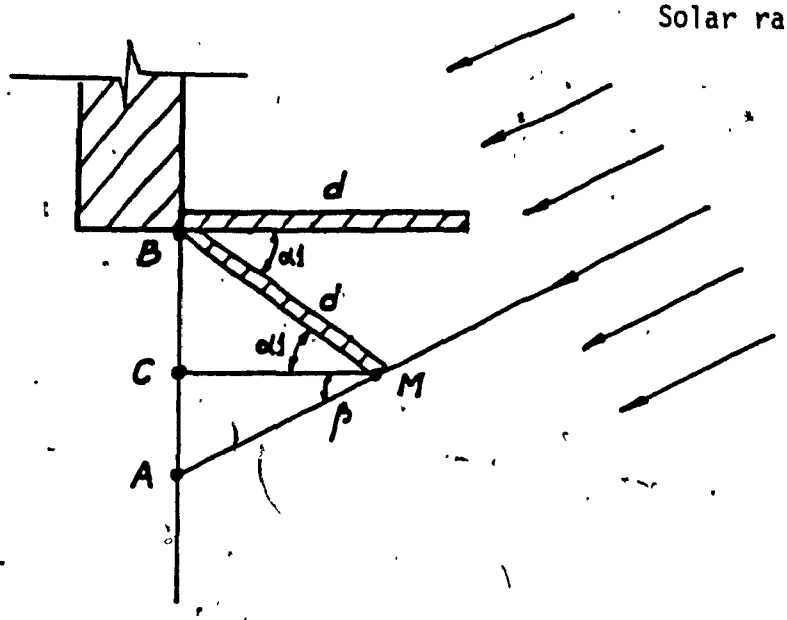

Fig. 2 Vertical section through window